

**Oklahoma Water Resources Research Institute
Annual Technical Report
FY 2012**

Introduction

During 2012 the Oklahoma Water Resources Research Institute (OWRRI) continued its integration in to the Division of Agricultural Sciences and Natural Resources at Oklahoma State University (OSU). Together with the Water Research and Extension Center (WREC) these units form the Oklahoma Water Resources Center. 2012 brought a new emphasis on outreach and extension for the OWRRI (see Information Transfer section below).

This report summarizes some of our accomplishments in 2012. Highlights are presented below.

1. We awarded three research grants of \$50,000 each to researchers at both OSU and the Northeastern State University (Tahlequah, OK) to conduct studies of the impact of wastewater treatment facility effluent on microbial genotypes and nitrogen cycling, climate variability and land surface change on streamflow, and identifying nutrient pathways to streams, including subsurface flows and bank erosion. Funding for these projects was provided by the USGS WRI Program and the Oklahoma Water Resources Board.
2. Research activities continued on our two 104G projects. In 2010 an OSU and University of Arkansas research team won a \$200,000, two-year grant to investigate the subsurface flow of phosphorus through preferential flow channels in the alluvium of streams in eastern Oklahoma and western Arkansas. In 2009, a team based at OSU and OU, received a \$225,000, three-year grant to investigate the impact of eastern red cedar encroachment on groundwater.
3. We co-sponsored and co-hosted the 10th annual Water Research Symposium and 33th annual Governor's Water Conference in Tulsa, which was attended by more than 450. The keynote speakers were Dayton Duncan, principal writer of documentary *The Dust Bowl* and Cynthia Barnett author of *The Blue Revolution*.
4. We electronically published two issues of our newsletter the *Aquahoman*, conducted seminars for Extension staff on water policy and hydraulic fracturing.

Research Program Introduction

In 2012, OWRRI revised its annual grants competition (for 2013 awards) to begin with the submission of one-page preproposals. These preproposals are reviewed by our 22-member Water Research Advisory Board (WRAB) and five to ten selected to continue in the competition by submitting full proposals. After peer reviews, the WRAB chooses three projects for funding.

Preproposals were solicited from all comprehensive universities in Oklahoma. Twenty nine preproposals were received from four institutions: Oklahoma State University, East Central University, the University of Tulsa, and the University of Oklahoma. Eight were selected to be submitted as full proposals, and from these, three projects were selected for funding for one year each. (Note: due to budget cuts by the USGS only two of these projects were funded with federal funds.)

- Comparison of Grain Sorghum and Corn Productivity under Limited Irrigation with Subsurface Drip (Dr. Jason Warren, OSU) will investigate the production advantage of grain sorghum over corn when irrigation is significantly limited. This project will also serve as a demonstration for the use of subsurface irrigation for sorghum.
- Remote Sensing of Water Quality and Harmful Algae in Oklahoma's Lakes (Dr. David Hambright, OU) will use satellite imagery and handheld devices to test the efficacy of remote sensing to detect potential harmful algae blooms. This is a proof-of-concept project.
- Developing the Groundwater Monitoring Potential of the Oklahoma Mesonet. (Dr. Tyson Ochsner, OSU) builds on this team's previous two projects sponsored by OWRRI that developed plant available moisture capabilities for the Oklahoma Mesonet to produce data regarding groundwater recharge from the same instrumentation.

Eastern redcedar encroachment and water cycle in tallgrass prairie

Basic Information

Title:	Eastern redcedar encroachment and water cycle in tallgrass prairie
Project Number:	2009OK141G
Start Date:	9/1/2009
End Date:	9/30/2012
Funding Source:	104G
Congressional District:	3
Research Category:	Climate and Hydrologic Processes
Focus Category:	Groundwater, Hydrology, Ecology
Descriptors:	baseflow, evapotranspiration, grassland, precipitation interception, sapflow, soil water dynamic, streamflow, water budget and water cycle
Principal Investigators:	Chris Zou, Dave Engle, Sam Fuhlendorf, Don Turton, Rodney Will, Kim Winton

Publications

1. Zou Chris, Peter Folliott, Michael Wine. 2010. Streamflow responses to vegetation manipulations along a gradient of precipitation in the Colorado River Basin. *Forest Ecology and Management* 259:1268-1276.
2. Zou Chris, Shujun Chen. 2009. Eastern redcedar encroachment and alternations of ecohydrological properties in tallgrass prairie. *IUFRO Forest and Water*. Raleigh, NC, USA.
3. Zou Chris, Don Turton, Rod Will, Sam Fuhlendorf, David Engle, Kim Winton. 2009. Eastern Redcedar Encroachment and the Water Cycle in Mesic Great Plains Grasslands. *The Oklahoma Water Research Symposium*. Oklahoma City.
4. Zou Chris, Don Turton, Rod Will, Sam Fuhlendorf, David Engle, Jenny Hung. 2010. Estimating watershed level evapotranspiration using water budget method. *ESA 95th Annual Meeting*.
5. Zou Chris, Peter Folliott, Michael Wine. 2010. Streamflow responses to vegetation manipulations along a gradient of precipitation in the Colorado River Basin. *Forest Ecology and Management* 259:1268-1276.
6. Zou Chris, Shujun Chen. 2009. Eastern redcedar encroachment and alternations of ecohydrological properties in tallgrass prairie. *IUFRO Forest and Water*. Raleigh, NC, USA.
7. Zou Chris, Don Turton, Rod Will, Sam Fuhlendorf, David Engle, Kim Winton. 2009. Eastern Redcedar Encroachment and the Water Cycle in Mesic Great Plains Grasslands. *The Oklahoma Water Research Symposium*. Oklahoma City.
8. Zou Chris, Don Turton, Rod Will, Sam Fuhlendorf, David Engle, Jenny Hung. 2010. Estimating watershed level evapotranspiration using water budget method. *ESA 95th Annual Meeting*.
9. Zou, CB, Turton D, Engle D. 2010. How eastern redcedar encroachment affects the water cycle of Oklahoma rangelands. NREM-2888. *Oklahoma Coop. Ext. Serv. Oklahoma State University, Stillwater*.
10. Stebler E, Turton D, Zou C. 2011. Impact of eastern redcedar (*Juniperus virginiana*) encroachment on streamflow in Oklahoma grassland watersheds. Poster presentation at Oklahoma Clean Lakes and Watershed Association Conference, Edmond OK, April 7 - 8, 2011. (Poster, Abstract)

Eastern redcedar encroachment and water cycle in tallgrass prairie

11. Stebler E, Turton D, Zou C. 2010. Rainfall interception by eastern redcedar (*Juniperus virginiana*) and its implications for water balance in Oklahoma grassland watersheds. Governor's Water Conference and OWRRI Water Research Symposium. 2010. Norman, Oklahoma. (Poster, Abstract)
12. Hung J, Zou CB, Engle D, Turton, Will R, Fuhlendorf S, Winton K. 2010. Temporal dynamics of soil-water content and soil-water depth in mesic tallgrass prairie and eastern redcedar woodland. Governor's Water Conference and OWRRI Water Research Symposium. 2010. Norman, Oklahoma (Poster, Abstract)
13. Zou CB. Climatic change and ecohydrology. Special session. 2010. The 95th ESA Annual Meeting, Pittsburgh, PA. (Oral presentation, Abstract)
14. Zou CB, Turton D, Will R, Fuhlendorf S, Engle D, Hung J. 2010. Estimating watershed level evapotranspiration using water budget method. The 95th ESA Annual Meeting, Pittsburgh, PA (Poster, Abstract).
15. Wine ML, Zou CB. 2012. Long-term streamflow relations with riparian gallery forest expansion into tallgrass prairie in the Southern Great Plains, USA. *Forest Ecology and Management* 266: 170–179.
16. Zou CB, Turton D, Engle D, Will R, Fuhlendorf S, Winton K. 2011. Eastern Redcedar Encroachment and Water: Update of 2010 Research. Water Research and Extension Center. WREC-101. Oklahoma Coop. Ext. Serv. Oklahoma State University, Stillwater
17. Zou C, Will R, Turton D, Acharya B, West A. Encroachment of redcedar into grassland - change in soil water and carbon. AAAS SWARM April 7, 2012, Tulsa, OK
18. Hung J, Zou CB, Will RE, Engle DM, Fuhlendorf SD. 2011. Interactive effects of vegetation and soil types on soil water dynamics in woody-encroached grasslands. The 94th Ecological Society of America Annual Meeting, August 7–12, 2011, Austin, TX.
19. Turton D, Zou C, Will R, Stebler E. 2012. Watershed research on the effects of redcedar encroachment on water quantity: Initial results. AAAS SWARM April 7, 2012, Tulsa, OK
20. Caternia G, Will R, Turton D, Zou C, 2012. Water use of individual redcedar trees; How much, how variable, and what factors affect it. AAAS SWARM April 7, 2012, Tulsa, OK

Interim Report 2012

Title: Eastern redcedar encroachment and water cycle in tallgrass prairie

Start Date: 09/01/09

End Date: 12/31/14

Congressional District: Oklahoma Congressional District 3

Focus Category: ECL, FL, GW, HYDROL, INV, SW, WS, WU

Descriptors: baseflow, evapotranspiration, grassland, precipitation interception, sapflow, soil water dynamic, streamflow, water budget and water cycle

Principal Investigators:

Chris Zou, Don Turton, Rod Will, Samuel Fuhlendorf, David Engle at Oklahoma State University and Kim Winton at Oklahoma Water Science Center

Supported Students:

Student Status	Number	Disciplines
Undergraduate	1	Engineering
M.S.	2	Natural Resource Ecology and Management
Ph.D.	1	Natural Resource Ecology and Management
Post Doc	0	
Total	3	

Problem and Research Objectives:

The overall objectives are to develop an improved understanding of the effects of eastern redcedar encroachment in tallgrass prairie on ecohydrological processes and potential effect on water supplies.

The specific objectives for this reporting period include:

- Data analysis of redcedar canopy interception
- Data analysis of redcedar transpiration
- Data collection and analysis of streamflows of grassland watersheds and grassland heavily encroached by redcedar

Summary of research program progress and research findings:

1. *Redcedar canopy interception*

- We measured throughfall, and stemflow, and analyzed which factors control them. We sampled redcedar trees of different diameters (from 6 to 47 cm DBH) and from different growth types (closed and open grown). We also accounted for environmental factors that could influence canopy interception and stemflow variation, as well as rainfall amount, intensity and duration, daily average wind speed, daily maximum wind gust, and daily potential evapotranspiration.
- Throughfall ranged from 0% to 80% of the precipitation depending on the size of rainfall events.
- Rainfall amount, intensity and duration were the factors that significantly explained ratio of throughfall to total rainfall (throughfall percentage). Throughfall percentage increased with increasing rainfall amount, intensity and decreased with rainfall duration. Throughfall was not significantly correlated to tree diameter or growth type.
- Stemflow was generated in 34 rainfall events, representing an average of 7% of rainfall when generated. Stemflow was positively related to event rainfall intensity, and negatively related to tree diameter.
- Redcedar average canopy interception was 37% of the total rainfall that occurred during 47 events.

2. *Redcedar water use*

- We used the thermal dissipation technique to quantify redcedar daily water use of 19 trees of different size from low and high density stands. The technique was calibrated to increase accuracy by comparing actual water use of cut trees to probe-based measurements.
- Redcedar trees used water year-round reaching a peak in late May and exhibiting reduced water use in summer time when conditions were dry. Overall daily average water use was 27 liters (± 5.5 liters s.e.). Large trees transpired greater amounts of water than smaller trees, ranging from a daily maximum of 4 liters (2cm diameter at breast height) to 150 liters (31cm diameter at breast height).
- Trees from low density stands used more water than trees with similar diameters from denser stands. However, there was no difference in water use between the two types of locations on a canopy area basis.
- Approximately two-thirds of the day-to-day variation in water use could be explained using a functional equation that included daily potential evapotranspiration, vapor pressure deficit, maximum temperature, solar radiation, and volumetric soil water content between 0-10 cm. When scaled to a hectare basis, redcedar trees used most of the effective precipitation, indicating potential for encroachment to reduce water yield such as streamflow and groundwater recharge.

3. *Streamflow responses*

- To understand the effect of woody plant encroachment on hydrological function of mesic grasslands, we quantified streamflow responses of a grassland watershed and a watershed heavily encroached by redcedar.

- During the three years from May 2008 to April 2011, the annual runoff coefficients for the encroached watershed ranged from 1.61% to 4.76%, in contrast to 14.15% to 15.75% for the grassland watershed.
- The annual streamflow duration ranged from 80 to 250 hours for the encroached site, substantially reduced from the 600 to 800 hours for the grassland watershed, due mainly to diminishing subsurface flow.

Publications

Master Thesis

1. Caternia Giulia, *Juniperus Virginiana* encroachment into mesic grasslands: rainfall interception and tree water use. 2012. Master Thesis. Department of Natural Resource Ecology and Management, Oklahoma State University, Stillwater, Oklahoma, 107 Pages.

Abstract in conference proceedings

1. Zou CB, Turton D, Stebler E, Will R, Engle D. 2013. Streamflow responses after juniper (*Juniperus virginiana*) encroachment in previously cultivated mesic grasslands. Society of Range Management Annual Meeting, Feb. 2-8, 2013, Oklahoma City, OK.
2. Zou CB, Turton DJ, Stebler E, Will RE, Winton K, Fuhlendorf S, Engle D. 2012. Effects of redcedar encroachment on water quantity: watershed infiltration, soil water dynamics, and streamflow. OWRRI Symposium. November 13 – 14, Tulsa.
3. Caterina GL, Will RE, Zou CB, Turton DJ. 2012. Effects of redcedar encroachment on water quantity: water use of individual redcedar trees. OWRRI Symposium. November 13 – 14, Tulsa.
4. Turton DJ, Caterina GL, Zou CB, Stebler E, Will RE. 2012. Effects of redcedar encroachment on water quantity: introduction and throughfall, interception and stemflow results. OWRRI Symposium. November 13 – 14, Tulsa
5. Zou CB, Will R, Acharya B, Guidotti V. 2012. Redistribution and potential loss of soil carbon at watershed after redcedar encroachment in a mesic grassland. The 97th Ecological Society of America Annual Meeting, August 5 -10, 2012, Portland, OR.
6. Caterina G, Will R, Turton D, Zou CB. 2012. Water use of individual *Juniperus virginiana* trees; How much, how variable, and what factors affect it. The 97th Ecological Society of America Annual Meeting, August 5 -10, 2012, Portland, OR.

Drought monitoring: a system for tracking plant available soil moisture based on the Oklahoma Mesonet

Drought monitoring: a system for tracking plant available soil moisture based on the Oklahoma Mesonet

Basic Information

Title:	Drought monitoring: a system for tracking plant available soil moisture based on the Oklahoma Mesonet
Project Number:	2010OK184B
Start Date:	3/1/2011
End Date:	6/30/2012
Funding Source:	104B
Congressional District:	3
Research Category:	Climate and Hydrologic Processes
Focus Category:	Drought, Agriculture, Water Quantity
Descriptors:	None
Principal Investigators:	Tyson Ochsner, Jeffrey Basara, Chris Fiebrich, Bradley Illston, Albert Sutherland

Publications

1. Ochsner, T.E., B.L. Scott, J. Basara, B. Illston, A. Sutherland, and C. Fiebrich. 2010. Drought monitoring: A system for tracking plant available water based on the Oklahoma Mesonet. Oklahoma Water Resources Research Symposium. Norman, OK. Oct. 26, 2010.
2. Scott, B.L., T.E. Ochsner, J.B. Basara, and B.G. Illston. 2011. Developing a soil physical property database for the Oklahoma mesonet. ASA-CSSA-SSSA International Annual Meetings. San Antonio, TX. Oct. 16-19, 2011.
3. Scott, B.L., T.E. Ochsner, B.G. Illston, C.A. Fiebrich, J.B. Basara and A.J. Sutherland. in review. New soil property database improves Oklahoma Mesonet soil moisture estimates. J. Atmos. Ocean. Tech.

Final Technical Report 2012

Project Title:

Drought monitoring: a system for tracking plant available soil moisture based on the Oklahoma Mesonet

Authors' Names and Affiliations:

Tyson Ochsner
Asst. Professor, Soil Physics
Plant and Soil Sciences
Oklahoma State University
368 Agricultural Hall
Stillwater, OK 74078
tyson.ochsner@okstate.edu
405-744-3627

Jeff Basara
Director of Research
Oklahoma Climatological Survey
120 David L. Boren Blvd., Suite 2900
Norman, OK 73072
jbasara@ou.edu
405-325-2541

Brad Illston
Research Associate
Oklahoma Climatological Survey
illston@ou.edu
405-325-5445

Chris Fiebrich
Associate Director for Mesonet
Oklahoma Climatological Survey
120 David L. Boren Blvd., Suite 2900
Norman, OK 73072
chris@mesonet.org
405-325-6877

Albert Sutherland
OSU Mesonet Agricultural Coordinator
Biosystems and Agricultural Engineering
Oklahoma State University
120 David L. Boren Blvd., Suite 2900
Norman, OK 73072

albert.sutherland@okstate.edu
405-325-3463

Start Date: March 1, 2011

End Date: June 30, 2012

Congressional District: Oklahoma's 3rd Congressional District

Focus Category: AG, CP, DROU, ECL, HYDROL, M&P, WQN

Descriptors: drought, soil moisture, Oklahoma Mesonet

Principal Investigators:

same as authors

Publications:

Ochsner, T.E., B.L. Scott and B.G. Illston. 2012. Soil-moisture based drought monitoring in Oklahoma. AGU Fall Meeting. San Francisco, California.

Scott, B.L., T.E. Ochsner, J.B. Basara, and B.G. Illston. 2011. Developing a soil physical property database for the Oklahoma mesonet. ASA-CSSA-SSSA International Annual Meetings. San Antonio, TX. Oct. 16-19, 2011.

Scott, B.L., T.E. Ochsner, B.G. Illston, C.A. Fiebrich, J.B. Basara and A.J. Sutherland. in review. New soil property database improves Oklahoma Mesonet soil moisture estimates. J. Atmos. Ocean. Tech.

Problem and Research Objectives:

Real-time drought monitoring is essential for early detection and adaptive management to mitigate the negative impacts of drought on the people, economy, and ecosystems of Oklahoma, and improved drought monitoring is a key need identified in the 1995 Update of the Oklahoma Comprehensive Water Plan. Drought impacts can be severe in Oklahoma. For example, the 2006 drought cost the state's economy over \$500 million from lost crop production alone. While drought monitoring is critical to Oklahoma's resource managers, it is hampered by a lack of data on a crucial drought indicator: plant available water. Crop yield losses and, by extension, the economic impacts of drought, are strongly linked to plant available water. Plant available water (PAW) is the amount of soil moisture currently in the profile which is available for plant uptake. Some water is held so strongly by the soil that it is not available to plants.

The *long term goal* of the team of collaborators representing Oklahoma State University, the Oklahoma Mesonet, the Oklahoma Climatological Survey, and the University of Oklahoma is to develop the Mesonet as an innovative tool for understanding and managing the water resources of Oklahoma. The *objective of this proposal* is to bring to completion a first-

generation drought monitoring system for Oklahoma based on PAW. The rationale for the proposed research is that providing resource managers with daily data on PAW will enable them to adopt management strategies to mitigate drought impacts. The proposal team is well prepared to succeed with this project due to the extensive expertise and strong achievement records in soil moisture related research, leadership in managing the Oklahoma Mesonet, and experience in the development of online products through the popular websites www.mesonet.org and www.agweather.mesonet.org. The following specific aims are proposed as part of the project:

Specific aim #1: Develop a scientifically-sound procedure for interpolating plant available water between Mesonet sites. Existing meteorological and geostatistical interpolation schemes will be tested for PAW and optimized to create a first-generation method suitable for mapping large-scale patterns in PAW.

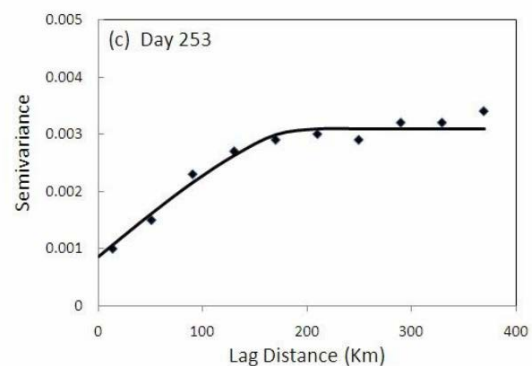
Specific aim #2: Create and release a new daily plant available water map for drought monitoring in Oklahoma. The measured soil properties, the real-time Mesonet sensor data, and the chosen interpolation scheme will be combined to create operational PAW maps on the Mesonet and Agweather websites.

Specific aim #3: Discover the similarities and differences between plant available water and other significant drought indicators (preliminary work only). A statewide PAW database will be created using archived Mesonet data from 1997-2010. Spatial and temporal patterns of PAW will be compared to those of other drought indicators. The goal is to generate preliminary data to leverage future funding opportunities.

Methodology:

Specific aim #1: Develop a scientifically-sound procedure for interpolating plant available water between Mesonet sites. We will develop a scientifically-sound procedure for interpolating PAW between Mesonet sites and for estimating the uncertainty of the interpolation. We will test two candidate methods: the meteorologically-derived Barnes objective analysis and a geostatistical approach called ordinary kriging.

The Barnes objective analysis was selected as a candidate method because it is widely accepted in meteorology and is currently used for interpolating many of the above- and below-ground variables measured by the Mesonet. The Barnes scheme was originally developed for interpolating sea-level pressure across the US. It is an inverse distance weighting approach in which the influence of a given observation drops off exponentially as the distance from the observation increases. Multiple "passes" or iterations of the interpolation are performed and compared to the observation set with the accuracy of the interpolation improving upon each pass. Three or four passes are recommended for optimal performance (Barnes, 1994). Barnes objective analysis requires only about 10% as much computing time as ordinary kriging (Su and Stensland, 1988), and in some cases the Barnes scheme can be as accurate as ordinary kriging (Dirks et al., 1998). We will evaluate the effectiveness of a four pass Barnes scheme for interpolating PAW. In the testing phase, the scheme will be implemented using the "barnes.m" function (Pierce, 2010) in Matlab (Mathworks, Inc. Natick, MA).



The second method evaluated will be ordinary kriging (Matheron, 1971). This method is built on the semivariogram, which shows how the spatial variance increases with the separation distance (lag) between the points. Ordinary kriging was selected as a candidate method in part because it has been successfully applied in a recent study of the Mesonet soil moisture data (Lakhankar et al., 2010). Figure 1 is reproduced from that study and shows an empirical and a fitted theoretical semivariogram of soil moisture in Oklahoma. The lag distance at which the semivariogram approaches the maximum value (or "sill") is called the "range", and that value defines how far spatial dependence extends. In this example, the range is ~175 km. The positive y-intercept in Fig. 1 is called the "nugget" and arises from small-scale spatial variability primarily due to variability in processes and properties at the land surface scale. Based on Fig. 1, these scales and processes accounted for about 33% of the total spatial variance in soil moisture (ratio of nugget to sill).

Fig. 1. Empirical (symbols) and theoretical (line) semivariograms for Mesonet soil moisture, 9/10/03.

Ordinary kriging offers some distinct advantages. In some cases it significantly outperforms inverse distance weighted methods like the Barnes objective analysis (Engel, 1999; Zimmerman et al., 1999). It will also result in semivariogram parameters for PAW which will be of tremendous scientific value for tasks like distributed hydrologic modeling, remote sensing validation, or designing future PAW monitoring networks. And, significantly, ordinary kriging can produce uncertainty maps for the interpolated PAW. Thus, it provides a built in indicator of the interpolation quality. But, as we have mentioned, the ordinary kriging is more complex than the Barnes objective analysis. For our application it is possible that the semivariogram parameters will have to be recalculated for each day of data. And, ordinary kriging assumes that the variable of interest is stationary, i.e. has the same mean value everywhere in the domain. Fortunately, it has been demonstrated that using localized search neighborhoods makes ordinary kriging fairly robust to nonstationary data (Journel and Rossi, 1989; Yost et al., 1982). We will evaluate the effectiveness of ordinary kriging for interpolating PAW. We will use the Geostatistical Analyst extension in ArcGIS (ESRI, Redlands, CA) to accomplish the ordinary kriging during the testing phase.

To evaluate the performance of the two interpolation methods, a set of 15 Mesonet stations will be left out and not used when optimizing the parameters of the interpolation schemes. The 15 omitted stations then provide independent validation data. The value of PAW on selected days as predicted by interpolation at those 15 locations will be compared to the measured values from the Mesonet sensors. Standard statistics such as bias, RMSE, and coefficients of determination will be calculated to determine the accuracy of the interpolation. These validation statistics will be key in quantifying the uncertainty associated with the interpolated PAW values. A similar validation procedure has already been successfully applied for evaluating the interpolation of Mesonet soil moisture data (Lakhankar et al., 2010). We hypothesize that ordinary kriging will lead to greater interpolation accuracy but at the cost of higher computational requirements. We will consider both of these factors in selecting the interpolation method for creating the operational PAW maps.

Specific aim #2: Create and release a new daily plant available water map for drought monitoring in Oklahoma. The measured soil properties, the real-time Mesonet sensor data, and the selected interpolation scheme will be combined to create these first-generation maps.

Operational PAW maps will be added to the Mesonet and Agweather websites and disseminated to a broad range of end users.

Software developers from the Oklahoma Climatological Survey will integrate the formulas for plant available water calculation and interpolation into the C++ based, derived-variable calculation engine for the Mesonet's WeatherScope visualization software. The plant available water formulas will be made available to customers in version 1.9 of WeatherScope. This code will also be incorporated into the WeatherMapper software for server-side generation of map images, and WeatherWriter software for text product generation. Finally, the formulas will be incorporated into PHP-based software that produces vector graphs in HTML for display in web browsers.

We will incorporate new versions of these software packages into the Mesonet's operational data processing system, and configure that system to produce map and graph products for plant available water. The new products will be incorporated into the Mesonet and Agweather web sites and made available to the public. The maps will include an indication of the uncertainty of the interpolation. If the Barnes method is chosen, then we will provide a single uncertainty value applicable to the entire PAW map, e.g. reported values are accurate to within +/- XX mm. If the kriging method is chosen, we will be able to provide uncertainty values for any point in the State.

Specific aim #3: Discover the similarities and differences between plant available water and other significant drought indicators (preliminary work only). Multiple techniques have been developed to provide qualitative and quantitative assessments of the magnitude and spatial extent of drought conditions. Quiring (2009) provides a thorough overview of drought monitoring analyses and notes that each methodology has relative strengths and weaknesses. In particular, the use of real-time soil moisture conditions is drastically limited in operational drought monitoring. As noted previously, Illston and Basara (2003) discovered that soil moisture anomalies in Oklahoma were often displaced from regions identified as experiencing drought conditions via the PSDI and the SPI.

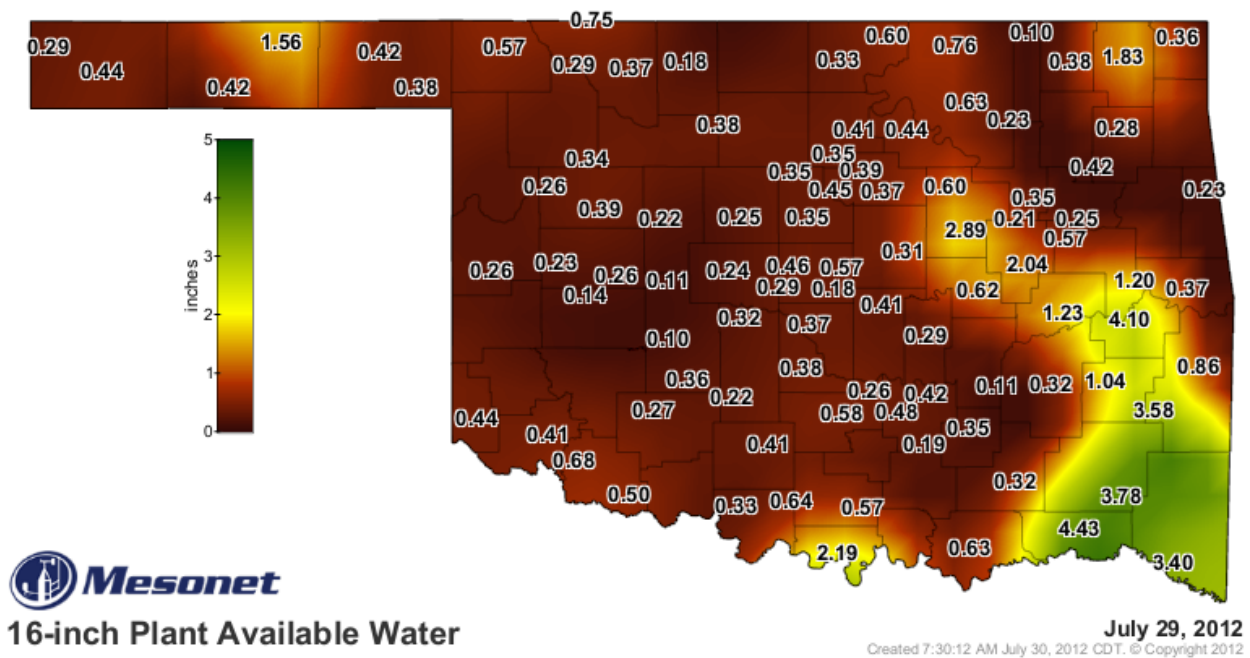
Preliminary analysis of PAW estimates utilizing Oklahoma Mesonet data demonstrate that the values provide enhanced insight regarding the spatial and temporal variability of water within the near-surface soil column. In regards to drought monitoring, a great challenge is identifying when meteorological drought conditions impact agricultural and hydrological drought conditions both during the onset and at the conclusion of drought. Because PAW provides an integrated value of soil moisture in the soil column, it captures longer-term trends associated with wetting and drying of the soil useful for monitoring drought. Further, PAW can be monitored in near real-time using Oklahoma Mesonet data.

To quantify the utility of PAW as a drought monitoring tool, a 14-year, statewide, PAW database will be created using archived Mesonet data from 1997-2010. Spatial and temporal analyses of PAW will be compared to other drought indicators including PSDI, SPI, the effective drought index (Byun and Wilhite, 1999), percent normal values, and deciles/percentiles (Gibbs and Maher, 1967). In addition, analyses from the U. S. Drought Monitor (<http://drought.unl.edu/dm/monitor.html>), available beginning in 2000, will also be compared with PAW. This work will enable us to begin to discover and document the connections between PAW and other accepted indicators of drought. The goal is to generate quantifiable

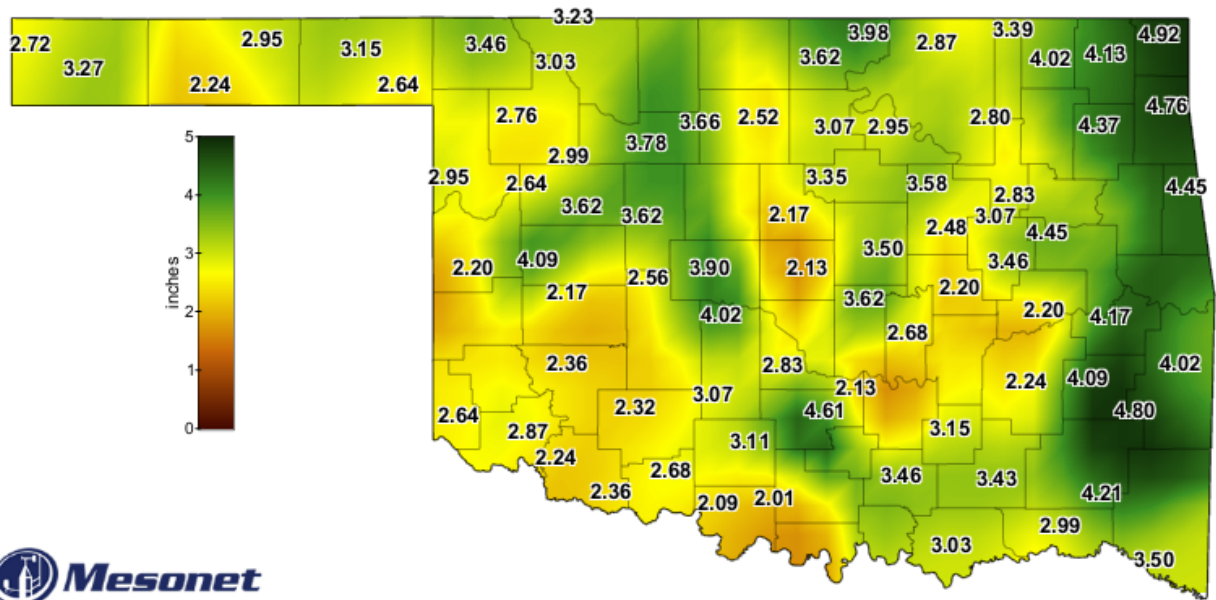
results demonstrating the utility of real-time drought monitoring in Oklahoma using PAW that can be used to leverage future funding opportunities.

Principal Findings and Significance:

We completed the development of a system for tracking PAW based on mesoscale observations from the Oklahoma Mesonet. We have developed and released to the public statewide daily PAW maps for the 0-4 inch, 0-16 inch, and 0-32 inch soil layers as described in specific aims #1 and #2 (Fig. 2). We have opted to use the Barnes objective analysis for interpolation of PAW data at present because we have no evidence yet that ordinary kriging will produce more accurate maps and the Barnes approach is simpler. This is an area that needs further research.



We have also created and released publicly via www.mesonet.org user-selectable, historical maps of statewide PAW as described in specific aim #3 (Fig. 3).



Average Plant Available Water in Top 16 inches

April 2000-2011

Created 11:58:42 AM May 1, 2012 CDT. © Copyright 2012

Student Status	Number	Disciplines
Undergraduate	2	Environmental Sci.
M.S.	1	Plant and Soil Sciences
Total	3	

Scale Dependent Phosphorus Leaching in Alluvial Floodplains

Basic Information

Title:	Scale Dependent Phosphorus Leaching in Alluvial Floodplains
Project Number:	2010OK192G
Start Date:	9/1/2010
End Date:	8/30/2012
Funding Source:	104G
Congressional District:	3
Research Category:	Water Quality
Focus Category:	Nutrients, Groundwater, Water Quality
Descriptors:	None
Principal Investigators:	Garey Fox, Brian E. Haggard, Todd Halihan, Phil D Hays, Chad Penn, Andrew Sharpley, Daniel E. Storm

Publications

1. Storm, P.Q. and G.A. Fox. 2013. Plot-scale leaching of phosphorus in an alluvial floodplain in the Ozark ecoregion. Oklahoma State University Undergraduate Journal of Research (provisionally accepted).
2. Heeren, D.M., G.A. Fox, and D.E. Storm. 2013. Technical Note: A berm infiltration method for conducting leaching tests at various spatial scales. Journal of Hydrologic Engineering (In Press, Accepted February 6, 2013), DOI: 10.1061/(ASCE)HE.1943-5584.0000802.
3. Heeren, D.M., G.A. Fox, and D.E. Storm. 2013. Scale analysis of infiltration measurements in heterogeneous soils. Proceedings of the World Environmental and Water Resources Congress, ASCE, Cincinnati, OH.

Third Annual Progress Report

**SCALE-DEPENDENT
PHOSPHORUS LEACHING IN
ALLUVIAL FLOODPLAINS**

USGS Award No. G10AP00137

*Garey Fox, Todd Halihan, Chad Penn, and Daniel Storm
Oklahoma State University*

*Brian Haggard, Andrew Sharpley, and Phil Hayes
University of Arkansas and USGS*

This report is the second of two annual progress reports for this two-year project.

Because it is concise, no executive summary is provided.

SCALE-DEPENDENT PHOSPHORUS LEACHING IN ALLUVIAL FLOODPLAINS

USGS AWARD NO. G10AP00137

Principal Investigators:

Garey Fox, Todd Halihan, Chad Penn, and Daniel Storm
Oklahoma State University

Brian Haggard and Andrew Sharpley
University of Arkansas

Phil Hayes
University of Arkansas and Arkansas USGS

Start Date: 9/1/2010

End Date: 8/31/2013

Congressional District: 2nd and 3rd in Oklahoma; 3rd in Arkansas

Focus Category: AG, GEOMOR, GW, HYDROL, NPP, NU, ST, SW, WQL

(1) Problem and Research Objectives

This research hypothesizes that macropores and gravel outcrops in alluvial floodplains have a significant, scale-dependent impact on contaminant leaching through soils; therefore, both soil matrix and macropore infiltration must be accounted for in an analysis of nutrient transport. However, quantifying the impact and spatial variability of macropores and gravel outcrops in the subsurface is difficult, if not impossible, without innovative field studies. This research proposes an innovative plot design that combines these and other methods in order to characterize water and phosphorus movement through alluvial soils.

The specific objectives of this research are twofold. The first objective is to quantify the phosphorus (P) transport capacity of heterogeneous, gravel soils common in the Ozark ecoregion. Two characteristics of the soil are expected to promote greater infiltration and contaminant transport than initially expected: (1) macropores or large openings (greater than 1-mm) in the soil (Thomas and Phillips, 1979; Akay et al., 2008; Najm et al., 2010) and (2) gravel outcrops at the soil surface (Heeren et al., 2010). This research will estimate P concentration and P load of water entering the gravelly subsoil from the soil surface for various topsoil depths, storm sizes, and initial P concentrations. Second, the impact of experimental scale on results from P leaching studies will be evaluated. If a material property is measured for identical samples except at various sample sizes, a representative element volume (REV) curve can be generated showing large variability below the REV. This provides a helpful framework for evaluating scales in P leaching. What minimum land area is necessary to adequately measure P leaching? It is hypothesized that measured P leaching ($\text{kg m}^{-2} \text{s}^{-1}$) will generally increase as the scale increases from point (10^{-3} m^2) to plot (10^2 m^2) scales. This will be evaluated by measuring P leaching at the point scale in the laboratory and at plot scales with bermed infiltration experiments for three plot sizes (approximately 10^0 , 10^1 , and 10^2 m^2).

If subsurface transport of P to alluvial groundwater is significant, these data will be critical for identifying appropriate conservation practices based on topsoil thickness. Riparian buffers are primarily aimed at reducing surface runoff contributions of P; however, their effectiveness within floodplains may be significantly reduced when considering heterogeneous subsurface pathways.

Methodology and Principal Findings/Significance

The three selected riparian floodplain sites are located in the Ozark region of northeastern Oklahoma and western Arkansas. The Ozark ecoregion of Missouri, Arkansas, and Oklahoma is characterized by karst topography, including caves, springs, sink holes, and losing streams. The erosion of carbonate bedrock (primarily limestone) by slightly acidic water has left a large residuum of chert gravel in Ozark soils, with floodplains generally consisting of coarse chert gravel overlain by a mantle of gravelly loam or silt loam (Figure 1). The three floodplain sites are located adjacent to the Barren Fork Creek, Pumpkin Hollow and Clear Creek (Figure 2).



Figure 1. Floodplains in the Ozark ecoregion generally consist of coarse chert gravel overlain by a mantle (1-300 cm) of topsoil.



Figure 2. Location of riparian floodplain sites in the Ozark ecoregion of Oklahoma and Arkansas.

Barren Fork Creek Site (Oklahoma)

The Barren Fork Creek site, five miles east of Tahlequah, Oklahoma, in Cherokee county (latitude: 35.90°, longitude: -94.85°), is located just downstream of the Eldon U.S. Geological Survey (USGS) gage station (07197000). A tributary of the Illinois River, the Barren Fork Creek has a median daily flow of 3.6 m³ s⁻¹ and an estimated watershed size of 845 km² at the study site. Historical aerial photographs of the site demonstrate the recent geomorphic activity including an abandoned stream channel that historically flowed in a more westerly direction than its current southwestern flow path (Figure 3).

Fuchs et al. (2009) described some of the soil and hydraulic characteristics of the Barren Fork Creek floodplain site. The floodplain consists of alluvial gravel deposits underlying 0.5 to 1.0 m of topsoil (Razort gravelly loam). Topsoil infiltration rates are reported to range between 1 and 4 m/d based on USDA soil surveys. The gravel subsoil, classified as coarse gravel, consists of approximately 80% (by mass) of particle diameters greater than 2.0 mm, with an average particle size (d₅₀) of 13 mm. Estimates of hydraulic conductivity for the gravel subsoil range between 140 and 230 m d⁻¹ based on falling-head trench tests (Fuchs et al., 2009). Soil particles less than 2.0 mm in the gravelly subsoil consist of secondary minerals, such as kaolinite and noncrystalline Al and Fe oxyhydroxides. Ammonium oxalate extractions on this finer material estimated initial phosphorus saturation levels of 4.2% to 8.4% (Fuchs et al., 2009).



Figure 3. Aerial photos for 2003 (left) and 2008 (right) show the southward migration of the stream toward the bluff and the large deposits of gravel in the current and abandoned stream channels. The study site is the hay field in the south-central portion of each photo (red arrow).

The floodplain site is a hay field with occasional trees (Figure 4). The field has a Soil Test Phosphorus (STP) of 33 mg/kg (59 lb/ac) and has not received fertilizer for several years. The southern border of the floodplain is a bedrock bluff that rises approximately 5 to 10 m above the floodplain elevation and limits channel migration to the south. The floodplain width at the study site is 20 to 100 m from the streambank (based on the 100 year floodplain); however, water was observed 200 m from the streambank (to the bluff) during a 6 year recurrence interval flow event (Figure 4).



Figure 4. The Barren Fork site is a hay field (left). The site becomes completely inundated during large flow events (right).

Pumpkin Hollow Site (Oklahoma)

The Pumpkin Hollow site, 12 miles northeast of Tahlequah, Oklahoma, in Cherokee County (Figure 5, latitude: 36.02°, longitude: -94.81°) has an estimated watershed area of 15 km². A small tributary of the Illinois River, Pumpkin Hollow is an ephemeral stream in its upper

reaches. The Pumpkin Hollow site is pasture for cattle (Figure 6). The entire floodplain is 120 to 130 m across. Soils in the study area include Razort gravelly loam and Elsayh very gravelly loam.



Figure 5. Pumpkin Hollow is a narrow valley ascending from the Illinois River to the plateau.



Figure 6. The Pumpkin Hollow site in spring (left) and winter (right). The site includes soils with shallow layers of topsoil and gravel.

Clear Creek Site (Arkansas)

The Clear Creek site is 5 miles northwest of Fayetteville, Arkansas, in Washington County (Figure 7, latitude: 36.125°, longitude: -94.235°). Clear Creek is a fourth order stream, and is a tributary to the Illinois River. Streamflow during baseflow conditions is estimated to be around 0.5 cms. The Clear Creek site is also pasture for cattle (Figure 8). The floodplain is

approximately 300 to 400 m across. The soils included intermixed layers of gravel and silt loam (Figure 8).



Figure 7. Clear Creek and an overflow channel at the Clear Creek floodplain site.



Figure 8. The Clear Creek site is pasture (left). Soils are composed of gravel and silt loam alluvial deposits (right).

Electrical Resistivity Imaging

Electrical Resistivity Imaging (ERI) is a geophysical method commonly used for near-surface investigations which measures the resistance of earth materials to the flow of DC current between two source electrodes. The method is popular because it is efficient and relatively unaffected by many environmental factors that confound other geophysical methods. According to Archie's Law (Archie, 1942), earth materials offer differing resistance to current depending on grain size, surface electrical properties, pore saturation, and the ionic content of pore fluids.

Normalizing the measured resistance by the area of the subsurface through which the current passes and the distance between the source electrodes produces resistivity, reported in ohmmeters (Ω -m), a property of the subsurface material (McNeill, 1980). Mathematical inversion of the measured voltages produces a two-dimensional profile of the subsurface showing areas of differing resistivity (Loke and Dahlin, 2002, Halihan et al., 2005).

ERI data were collected using a SuperSting R8/IP Earth Resistivity Meter (Advanced GeoSciences Inc., Austin, TX) with a 56-electrode array. Fourteen lines were collected at the Barren Fork Creek site, three at the Pumpkin Hollow site, and eight lines at the Clear Creek site. One line at the Barren Fork Creek site and all of the lines at Pumpkin Hollow were “roll-along” lines that consisted of sequential ERI images with one-quarter overlap of electrodes. The profiles at the Barren Fork Creek site employed electrode spacing of 0.5, 1.0, 1.5, 2.0 and 2.5 m with associated depths of investigation of approximately 7.5, 15.0, 17.0, 22.5 and 25.0 m, respectively. All other sites utilized a 1.0-m spacing. The area of interest in each study site was less than 3 m below the ground surface and thus well within the ERI window. The resistivity sampling and subsequent inversion utilized a proprietary routine devised by Halihan et al. (2005), which produced higher resolution images than conventional techniques.

The OhmMapper (Geometrics, San Jose, CA), a capacitively-coupled dipole-dipole array, was effectively deployed at the relatively open Barren Fork Creek site for large scale mapping. The system used a 40 m array (five 5 m transmitter dipoles and one 5 m receiver dipole with a 10 m separation) that was pulled behind an ATV. Two data readings per second were collected to create long and data-dense vertical profiles. The depth of investigation was limited to 3 to 5 m. Positioning data for the ERI and OhmMapper were collected with a TopCon HyperLite Plus GPS with base station. Points were accurate to within 1 cm.

Barren Fork Creek

Resistivity at the Barren Fork Creek site appeared to conform generally to surface topography with higher elevations having higher resistivity, although the net relief was minor (~1 m). This was most evident in the OhmMapper resistivity profiles which covered most of the floodplain and which revealed a pattern of high and low resistivity that trended SW to NE (Figure 9). More precise imaging with reduced spatial coverage was obtained with the ERI. A composite ERI line collected from the site is shown in Figure 10. The line, which is approximately parallel to the stream, begins only 5 m from the stream. Gravel outcrops are indicated by gray colors reaching closer to the surface and will be the location for induced leaching experiments at different spatial scales at this site.

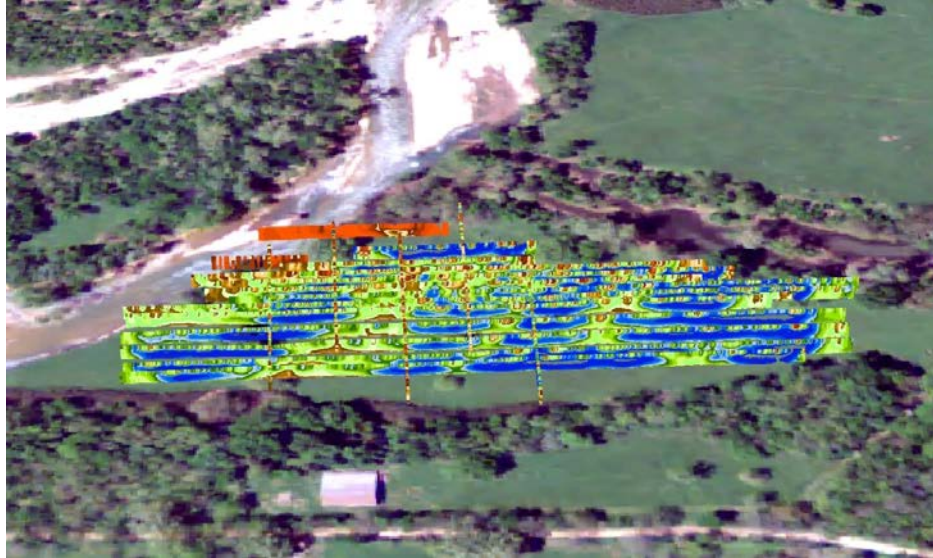


Figure 9. OhmMapper coverage of the Barren Fork Creek alluvial floodplain showing SW to NE trends of low (blue) and high (orange) resistivity. View is to the North and subsurface resistivity profiles are displayed above the aerial image for visualization purposes. Modified from Heeren et al. (2010).

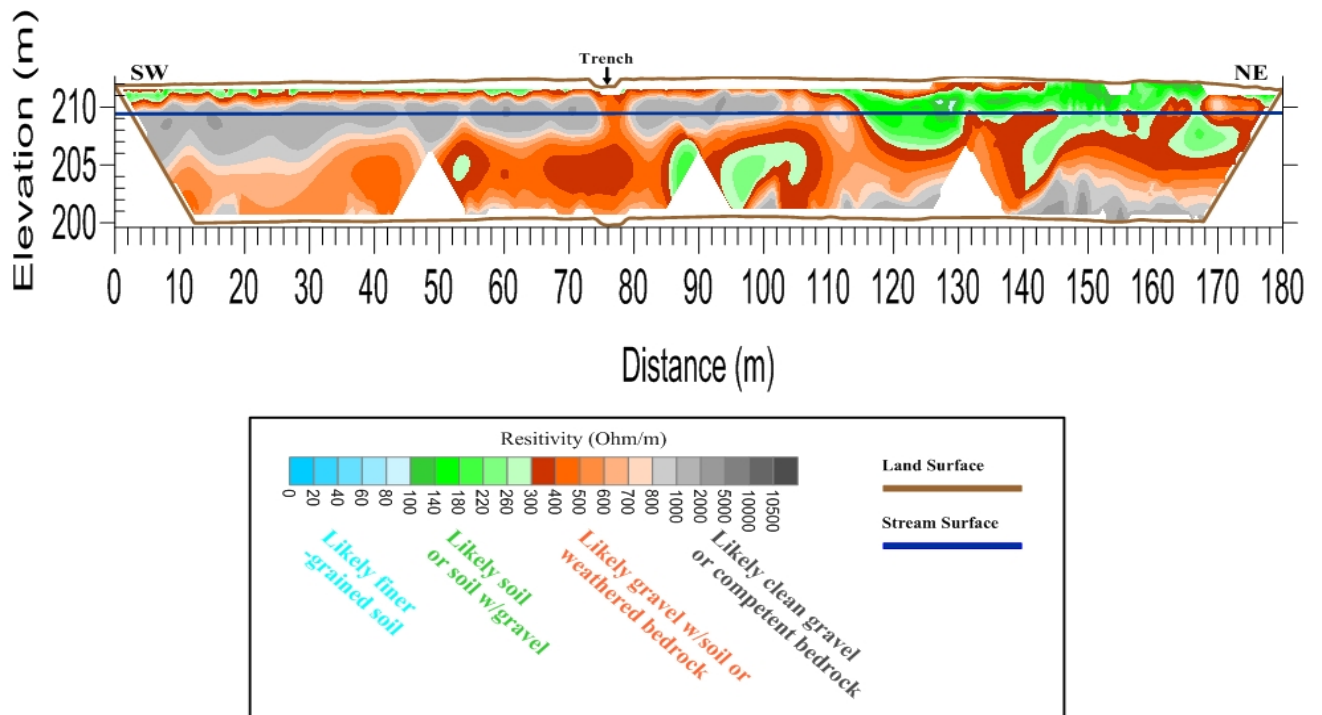


Figure 10. Composite SuperSting image, showing mapped electrical resistance ($\Omega\text{-m}$), running southwest to northeast along a trench installed for studying subsurface phosphorus transport in the gravel subsoils by Fuchs et al. (2009). The x-axis represents the horizontal distance along the ground; the y-axis is elevation above mean sea level. Source: Heeren et al. (2010).

Pumpkin Hollow

Pumpkin Hollow differed from the other streams because it was a headwater stream with a smaller watershed area. The valley at the study site was approximately 200 m wide and the roll-along lines spanned nearly the entire valley width, crossing Pumpkin Hollow Creek at about the midpoint of the line. The ERI survey at Pumpkin Hollow consisted of three lines oriented W-E with 1 m electrode spacing, 12.5 m depth, and 97 m (lines 1-2 and 3-4) or 139 m (line 5-6-7) length (Figure 11).

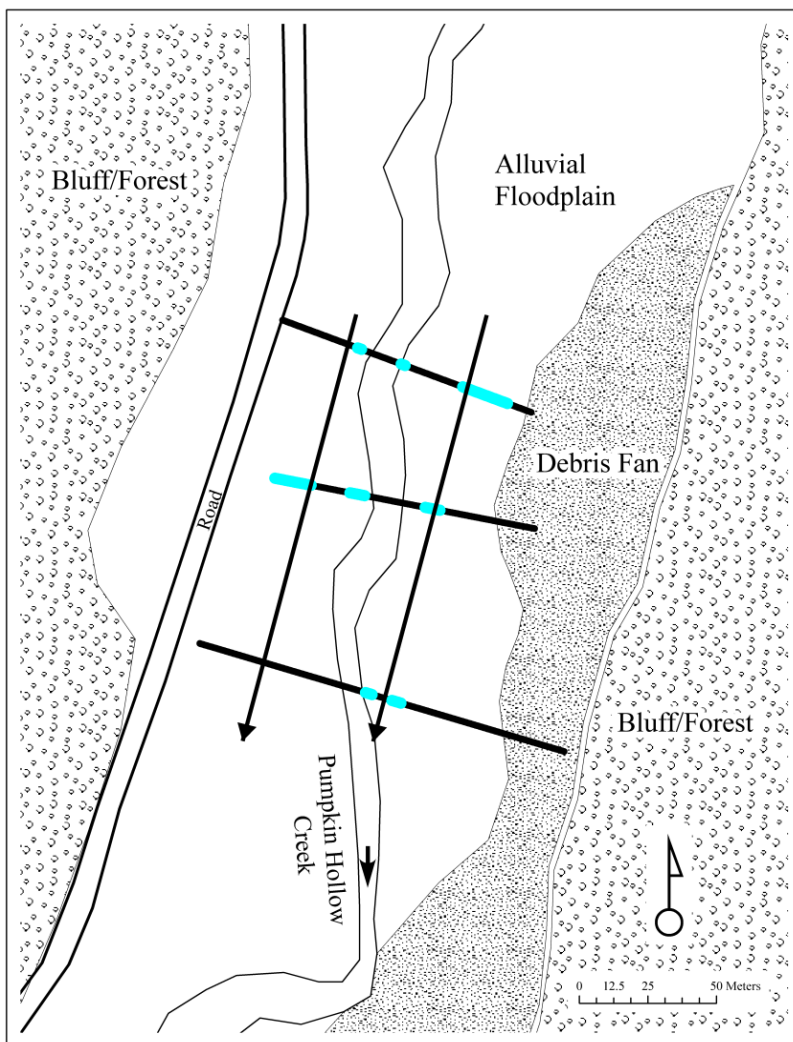


Figure 11. High resistivity feature locations on ERI lines at the Pumpkin Hollow site are shown in blue. Arrows represent potential connections between them and the direction of flow.

The Pumpkin Hollow ERI profiles also had a unique configuration consisting of a low resistivity layer between a high resistivity surface layer and high resistivity at depth (Figure 12). Observations at the site included the close proximity of large gravel debris fans originating from nearby upland areas. Jacobson and Gran (1999) noted similar pulses of gravel in Ozark streams in Missouri and Arkansas originating from 19th and early 20th century deforestation of plateau surfaces, implying that a possible interpretation of the low resistivity layer in the ERI profiles was a soil layer buried by gravel from the nearby plateau surfaces. The streambed elevation was approximately 262 m with the general floodplain surface being about 1 m above that elevation. The area of interest included the elevations above 262 m (note that the mean elevation was 262.9 m and that the maximum elevation 265 m occurred at the valley edge) and was therefore thin compared to the other study sites. The resistivity at Pumpkin Hollow ranged from 58 to 3110 Ω -m with a mean of 387 Ω -m. Like the other sites, the Pumpkin Hollow resistivity suggested a pattern of discrete areas of high resistance that indicated gravel outcrops (Figure 12). These were generally associated with topographic high areas and appeared to have the potential to direct flow down-valley parallel to the stream.

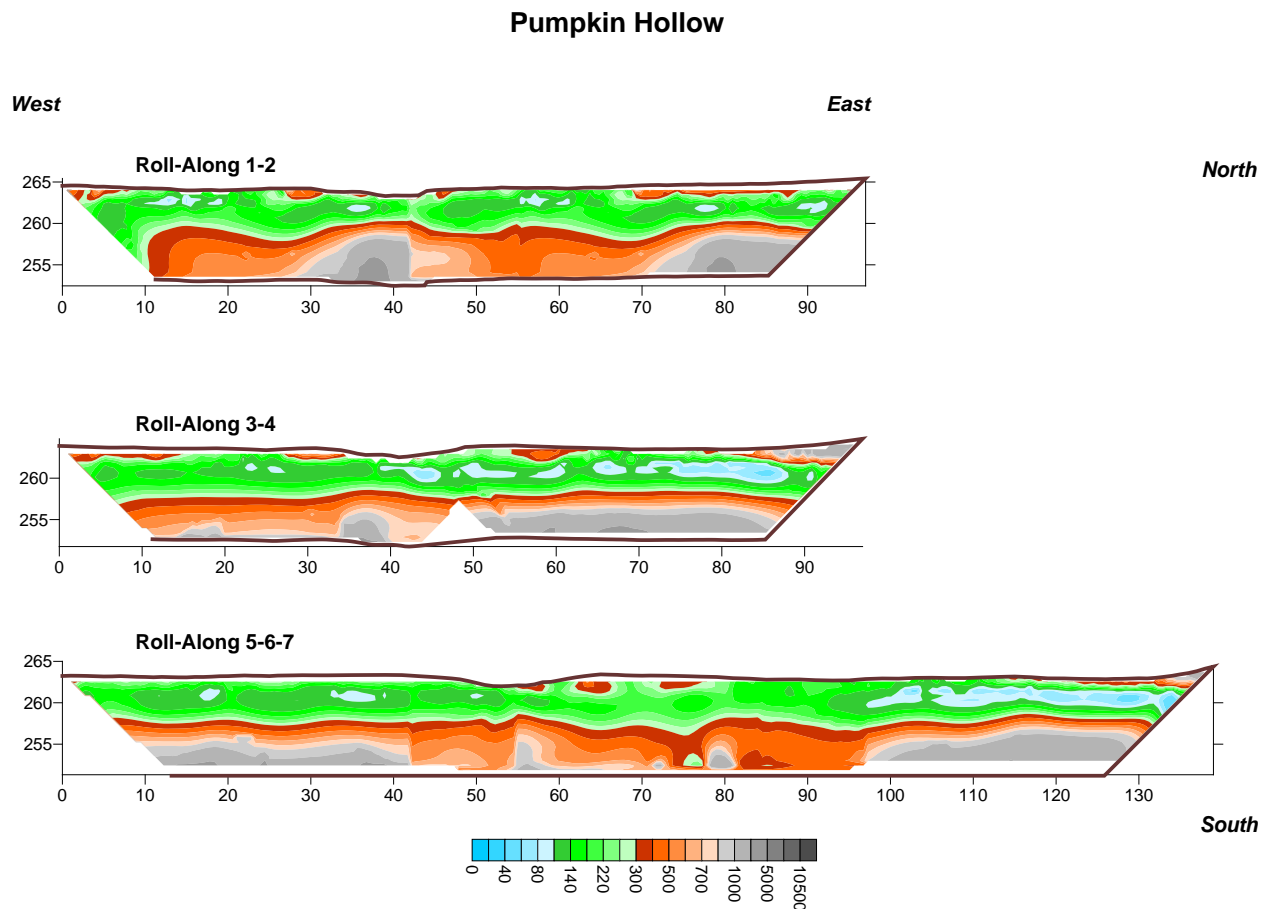


Figure 12. ERI images of three “roll-along” lines for the Pumpkin Hollow site. The *x*-axis represents the horizontal distance along the ground; the *y*-axis is elevation above mean sea level. The color bar is the electrical resistivity in Ohm-meters.

Clear Creek

Geophysical mapping was first performed between the overflow channel and Clear Creek shown in Figure 7; however, limited gravel outcrops were observed in this area and therefore the control (non-gravel outcrop) leaching experiments will be performed at this location (Figure 13a). Most of the shallow profile possessed electrical resistivities less than 450 Ω -m. On the east side of Clear Creek, layered profiles demonstrated the potential for lateral flow and transport to the stream, and this feature was clearly visible based on exposed streambanks and supported by the ERI data. Electrical resistivities at the surface were on the order of 600 to 1000 Ω -m with lower resistivity soils below this surface feature (Figure 13b).

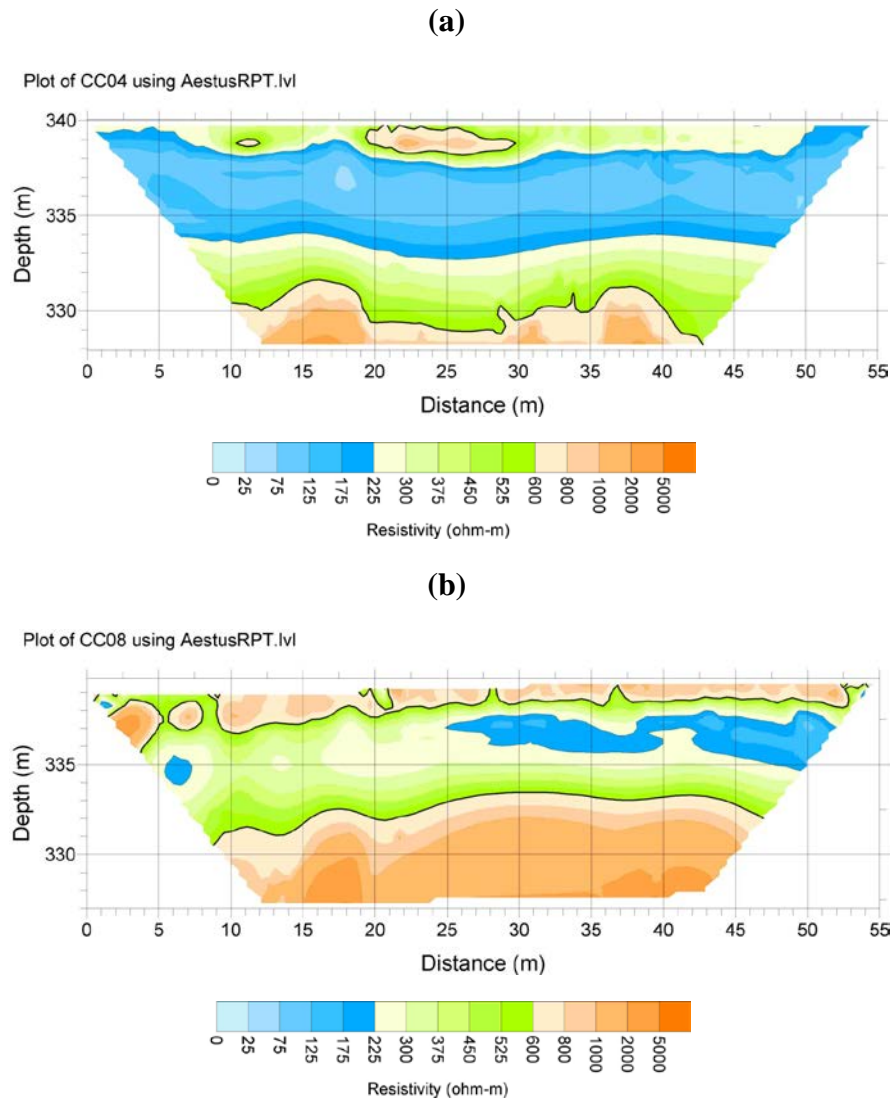


Figure 13. ERI images of two lines at the Clear Creek site where (a) is a line between the overflow channel and the creek with limited gravel outcrop area and (b) is a line on the east side of Clear Creek with gravel outcrops at the surface. The x-axis represents the horizontal distance along the ground; the y-axis is elevation above mean sea level.

Point Scale Laboratory Testing: Flow-Cell Experiments

Fine material (diameter less than 2.0 mm) from the Clear Creek site in Arkansas was used in laboratory flow-through experiments to investigate the P sorption characteristics with respect to the flow velocity (DeSutter et. al., 2006). Approximately 5.0 g of the fine materials was placed in each flow-through cell. A Whatman 42 filter was placed at the bottom of each cell to prevent the fine material from passing through the bottom. Each cell had a nozzle at the bottom with a hose running from the nozzle to a peristaltic pump (Figure 14). The pump pulled water with predetermined P and potassium chloride (KCl) concentrations through the cells and fine material at a known flow rate (mL/min).

Two different flow rates were used on the peristaltic pumps to evaluate the effect of velocity on P sorption. The flow rates were 0.20 mL/min for the low flow experiments and 0.75 mL/min for the high flow experiments. These flow rates corresponded to average flow velocities of 0.42 and 1.59 m/d, respectively. First, a 0.01M KCl solution was pulled through the soil to determine the background P that was removed from the soil. Then, a KH_2PO_4 and 0.01M KCl solution was injected into each cell at different concentrations (1.0 to 10.0 mg/L of P) and kept at a constant head using a Mariott bottle system (Figure 14). The experiments were run for approximately 8 hours. Samples were taken periodically throughout each experiment. The samples were analyzed in the laboratory for P using the Murphy-Riley (1962) method.

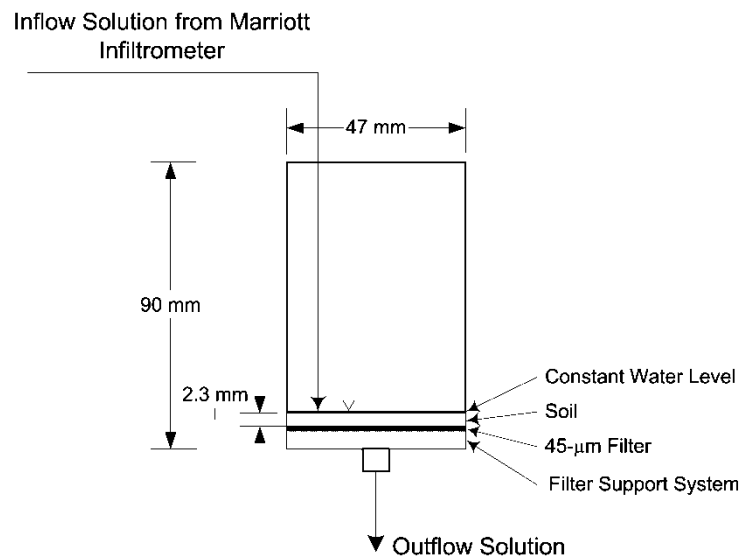


Figure 14. Laboratory flow-through experimental setup. The experimental setup follows that of DeSutter et al. (2006) and Fuchs et al. (2009).

Data were analyzed based on concentrations of P in the outflow compared to the total amount of P added to the system for both low flow and high flow scenarios. The principle of this method was that the measured P concentrations in the outflow should be approximately equal if flow

velocity does not have an effect on P sorption. The mass of P added per kilogram of soil (mg P/kg soil) was found by multiplying Q (mL/min) by the inflow P concentration (mg/L) and by the elapsed time of the experiment (min). These data were plotted against the P concentrations (mg/L) detected in the outflow solutions for both flow velocities. If equivalent sorption was occurring, the curves associated with each data set would be approximately equal. Data were also analyzed using contaminant transport theory relative to the dimensionless concentration and number of pore volumes passed through the soil.

Both the contaminant transport and load perspectives suggested that the flow velocities in the experimental range had no effect on the sorption capabilities of the system, but instead illustrated that the initial P concentrations were important (Figure 15).

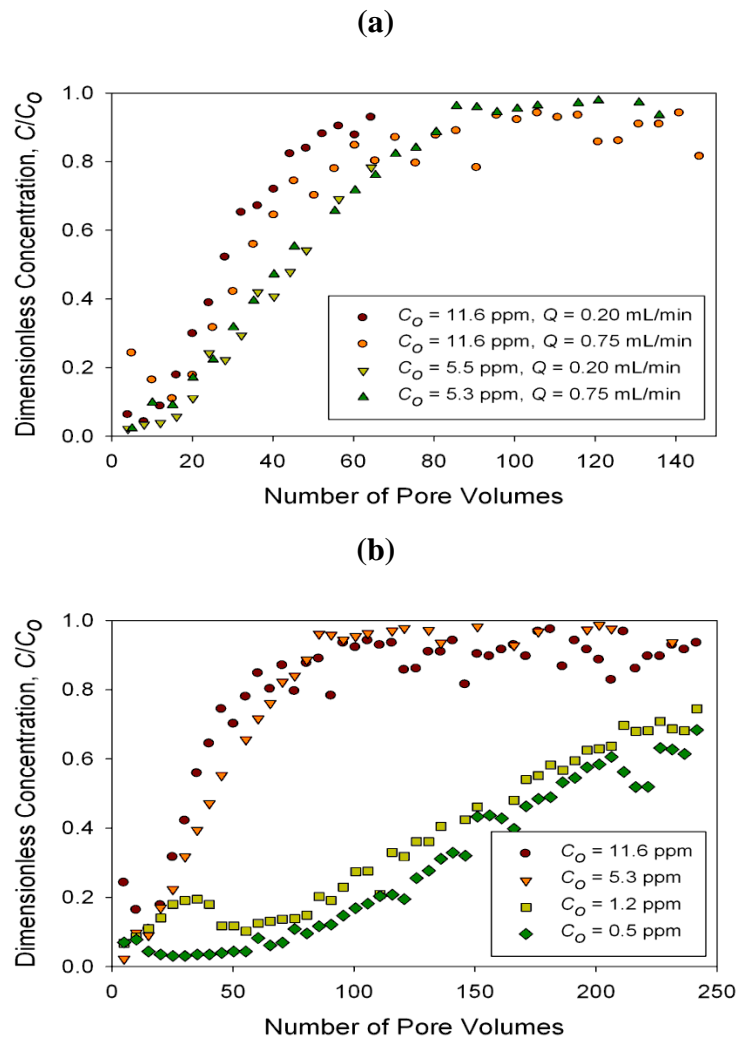


Figure 15. Phosphorus (P) breakthrough curves demonstrating (a) no influence of flow velocity on transport at the range of conditions studied and (b) influence of initial P concentration on transport.

Additional flow cell experiments have been completed to more appropriately characterize leaching potential and velocity-dependent sorption relative to all the field sites investigated in this research. Soils were sieved to 2mm and placed in a flow-through sorption cell where a synthetic P solution (1 and 10 ppm) was added at a constant rate (0.2 and 0.75 mLs min⁻¹, corresponding to a contact time of 10 and 3 min). Leachate was collected every 30 min and analyzed for P. Phosphorus sorption was normalized based on the mass of P added per mass of soil. Prior to desorption flow-through tests, soils were equilibrated with a known amount of P in a batch setting; treated soils were then subjected to flow-through cells at 0.2 and 0.75 mL min⁻¹ of DI water.

Soils (100 mg) were placed in a calorimeter titration cell, suspended in 0.75 mLs of DI water, stirred, and subjected to two different titration tests: (a) 25 titrations of a 0.1 M NaH₂PO₄⁻ solution at 0.01 mL per titration (5 minutes apart), and (b) one single titration of 0.25 mLs using the same P solution. A blank titration consisting of DI water only was subtracted from the soil titrations. The resulting thermograms were examined for the timeliness of peaks (i.e. kinetics) and integrated for total area under each peak (i.e. total heat produced or consumed during reaction).

Flow-through P sorption results clearly showed that contact time (i.e. flow rate) impacted P sorption for one of the soils; in this case, P sorption was limited by chemical kinetics. In regard to the soil in which contact time did not affect P sorption, this suggests fast chemical kinetics of P sorption, and perhaps a physical limitation in flow from the bulk flow to slow flow near the mineral surfaces. The single shot P titration thermogram also supported this observation in that the soil with fast chemical kinetics required only 3 minutes for reaction completion compared to the “slower” soil requiring 12 minutes. Area under the thermogram peaks also supported observed differences in P sorption by single point batch P additions. Thermograms from the 25 individual titrations suggest P sorption mechanisms by mostly ligand exchange onto Al and Fe hydroxides, and Ca phosphate precipitation; however, the thermogram for one soil suggested precipitation of Al and Fe phosphates as oxyhydroxides became saturated with P. Desorption of P treated soils under flow-through conditions suggested that the slower flow rate (i.e. higher contact time) could result in a greater desorption of P; however, further statistical analysis is required to determine this.

The results of this study suggest that leaching flow rates (i.e. contact time) through riparian soils will have an impact on the sorption of dissolved P onto soils as flow moves downward or laterally. Simple tests with titration calorimetry could be used estimate the potential impact of flow rate.

Plot Scale Testing: Tracer/Rhodamine WT/P Infiltration Tests

As of May 2012, all the 1 m by 1 m and 3 m by 3 m plot scale infiltration and leaching tests have been performed. Remaining field experiments include the 10 m by 10 m plots at the three field sites. Data analysis has been completed at the Barren Fork Creek site at this time, and analyses are continuing at the remaining sites.

Description of the Berm Infiltration/Leaching Technique – 1 m by 1 m and 3 m by 3 m Plots

The berm was constructed of four sections of 15 cm vinyl hose attached to four 90° elbows constructed from 15 cm steel pipe (Figure 16). Each elbow had an air vent and one elbow had a gate valve with a garden hose fitting for water. The vinyl hoses were secured to the elbows with stainless steel hose clamps and sealed with silicone sealant. The berms were then partially filled with water to add weight, but excess pressure was avoided to ensure the vinyl did not separate from the elbows.

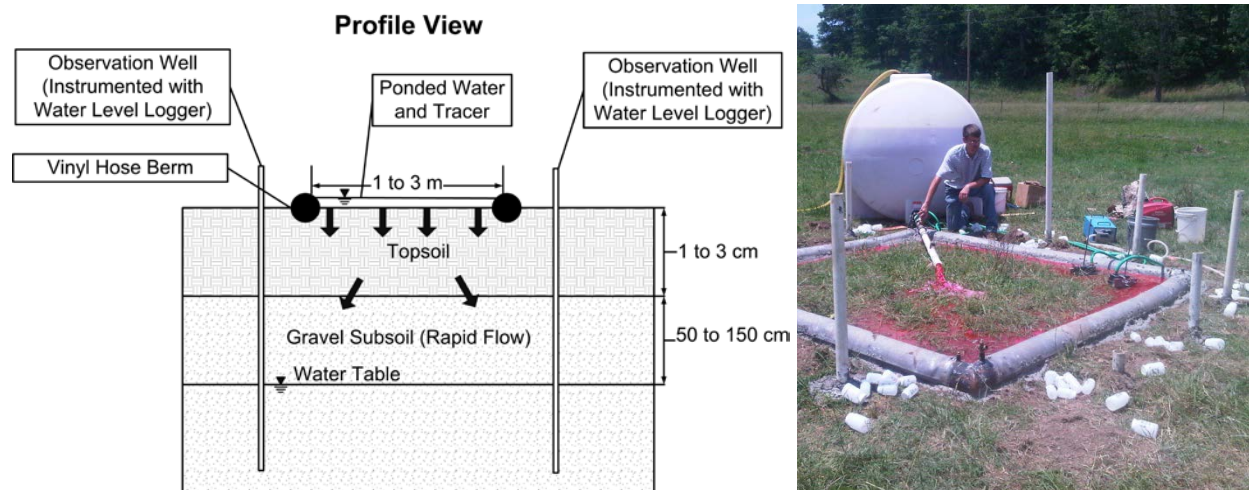


Figure 16. Berm infiltration method, including vinyl berms to contain water-tracer solution and observation wells for collecting groundwater samples: design (left) and implementation at the Pumpkin Hollow floodplain site in eastern Oklahoma (right).

Plots were located on relatively level areas in an attempt to maintain uniform water depths. Larger plots required shallower slopes to ensure that the entire plot could be inundated without overflowing the berm. The vinyl hose was placed in a shallow trench (3 to 5 cm) cut through the surface thatch layer to minimize lateral flow at the surface. A thick bead of liquid bentonite was also placed on the inside and outside of the berm to create a seal between the berm and the soil. High-density polyethylene tanks, 4.9 and 0.76 m³, were used for the 3 m by 3 m and the 1 m by 1 m plots, respectively, to mix water and a potassium chloride tracer, Rhodamine WT, and a phosphorus solution. Tanks were instrumented with automated water level data loggers with an accuracy of 0.5 cm (HoboWare U20, Onset Computer Corp., Cape Cod, MA) to monitor water depth (pressure) and temperature at one minute intervals. An additional water level data logger was used to monitor atmospheric pressure. Logger data were processed with HoboWare Pro software, which adjusted for changes in atmospheric pressure and water density. Tank water depth over time was used to calculate flow rate with a volumetric rating curve.

A combination of 5.1 cm diameter Polyvinyl chloride (PVC) pipe with a manual gate valve and vinyl garden hoses with float valves were used to deliver gravity fed water from the tanks to the plots. For low flow rates, one to two garden hoses with float valves were sufficient. When higher flow rates were required to achieve the desired constant head, flow was dominated by the larger PVC pipe and the garden hoses with float valves were relatively ineffective. For these cases a

fine-adjustment gate valve was required to manually control the flow rate to achieve a relatively constant head in the plots. When a tank was nearly empty, flow was temporarily stopped while water and tracer was added to the tank. Chloride was used as a conservative tracer and Rhodamine WT as a visual tracer with injection concentrations 20 to 30 times background levels. Phosphorus was also injected into the plot. Depth in each plot area was monitored with a water level data logger. Heads were maintained between 3 and 10 cm across the plots.

A Geoprobe Systems drilling machine (6200 TMP, Kejr, Inc., Salina, KS), which has been found to be effective in coarse gravel soils (Heeren et al., 2011; Miller et al., 2011), was used to install four to twelve observation wells around each plot. Boreholes were sealed with liquid bentonite to avoid water leaking down the hole. Observation wells were instrumented with water level data loggers. Reference water table elevations, obtained with a water level indicator and laser level data for each well, were then calculated. Water table elevation data had an accuracy of 1 cm. Low flow sampling with a peristaltic pump was used to collect water samples from the top of the water table, which ranged from 50 to 150 cm below ground surface.

Finite Element Modeling

Porous media flow from hypothetical 1 m by 1 m infiltration plots were simulated using HYDRUS-3D (Šimůnek et al., 2006) for three different soil types: sand, loam, and silt. This method was not expected to be used on soils finer than silt. HYDRUS is a finite element model for simulating two- and three-dimensional movement of water, heat, and multiple solutes in variably saturated media (Šimůnek et al., 2006; Akay et al., 2008). The HYDRUS code numerically solves the Richards equation for saturated-unsaturated water flow (Šimůnek et al., 2006).

The finite element grid consisted of triangular prism elements spaced equally every 25 cm in the horizontal, lateral, and vertical directions. The simulation domain consisted of a 1 m by 1 m constant head infiltration plot centered within a 10 m by 10 m area with a 3-m deep soil profile (Figure 17). All cells on the surface of the simulation domain outside the infiltration plot were no-flux boundaries. A constant head boundary condition was used to simulate the infiltration plot with constant heads ranging from 2.54 to 15.24 cm. The initial water table depth was varied between simulations, which included depths of 1.0, 2.0, and 2.5 m below ground surface. Below the water table, a no flux boundary condition was specified for the shell and bottom of the simulation domain to simulate the presence of a regional groundwater system. Above the water table, the shell boundary condition was a possible seepage face (Figure 17). At the water table depth, observation nodes were added to the simulation domain located at various distances (0 to 450 cm) away from the edge of the infiltration plot.

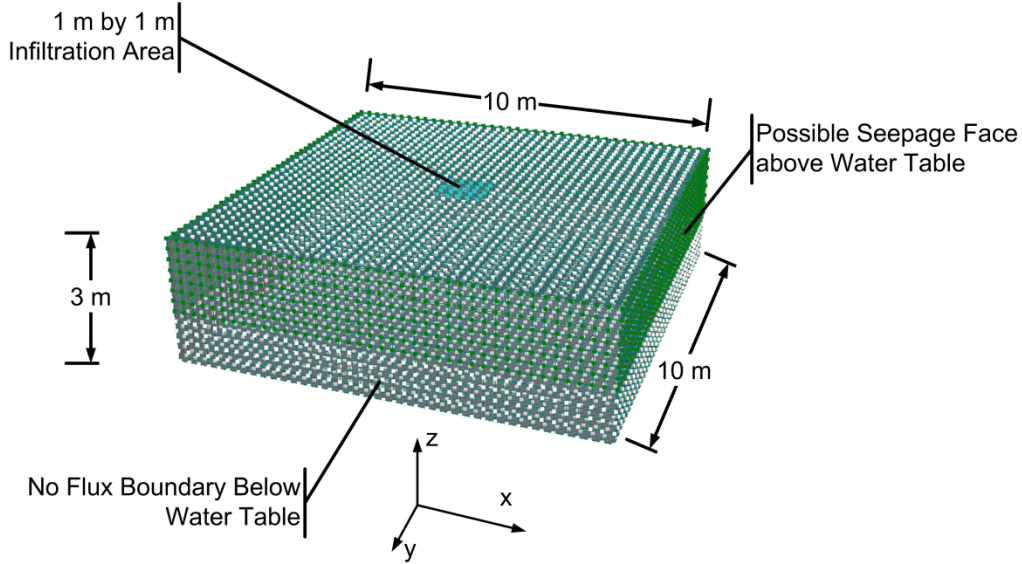


Figure 17. Simulation domain for HYDRUS-3D modeling of hypothetical infiltration experiments with a 1 m by 1 m infiltration plot.

The van Genuchten-Mualem model (van Genuchten, 1980) was used to describe the water retention, $\theta(h)$, and conductivity, $K(h)$, functions for the assumed homogeneous soil matrix:

$$\theta(h) = \begin{cases} \theta_r + \frac{\theta_s - \theta_r}{\left[1 + |\alpha h|^n\right]^m} & h < 0 \\ \theta_s & h \geq 0 \end{cases} \quad (1)$$

$$K(h) = K_s S_e^l \left[1 - (1 - S_e^{1/m})^m\right]^2 \quad m = 1 - 1/n, \quad n > 1 \quad (2)$$

where $S_e = (\theta - \theta_r)/(\theta_s - \theta_r)$ is the effective saturation; α (L^{-1}), n , and l are empirical parameters; θ_s is the saturated water content (L^3L^{-3}); θ_r is the residual water content (L^3L^{-3}); and K_s (LT^{-1}) is the saturated hydraulic conductivity. Hydraulic parameters for the sand, loam, and silt soils were acquired from the soil catalog in HYDRUS, derived from Carsel and Parrish (1988), in order to represent average values for these different textural classes (Table 1).

HYDRUS simulations were conducted to determine the time at which a detectable water table rise, defined as 1 cm, was observed in the observation nodes. This information was used to correlate the response time in observation wells installed next to the infiltration plot relative to the soil type, head in the infiltration plot, distance the observation well was installed from the infiltration plot edge, and the water table depth.

Table 1. Soil properties for the sand, loam, and silt soils simulated by HYDRUS-3D for the hypothetical 1 m by 1 m infiltration experiments. Soil properties were from the soil catalog for the textural classes in HYDRUS.

Soil Type	Residual Water Content, θ_r ($\text{cm}^3 \text{cm}^{-3}$)	Saturated Water Content, θ_s ($\text{cm}^3 \text{cm}^{-3}$)	α^* (cm^{-1})	n^*	Saturated Hydraulic Conductivity, K_s (cm min^{-1})	Pore-Connectivity Parameter, l
Sand	0.045	0.430	0.145	2.68	0.495	0.5
Loam	0.078	0.430	0.036	1.56	0.017	0.5
Silt	0.034	0.460	0.016	1.37	0.004	0.5

*Empirical constants.

As an example, infiltration rates measured at Pumpkin Hollow ranged from 5 to 70 cm/hr, indicating considerable heterogeneity in the infiltration rates of the floodplains due to the occurrence of gravel outcrops. These data were higher than the U.S. Natural Resources Conservation Service (NRCS) Adair County, Oklahoma Soil Survey (NRCS, 2012), indicating the need for larger scale field measurements of infiltration rate. The NRCS Soil Survey (NRCS, 2012) estimated permeability of the limiting layer to be in the range of 1.5 to 5 cm/hr for the Razort gravelly loam. This method was successful in quantifying high infiltration rate soils (i.e., gravels) even for large 3 m by 3 m plots, and lower infiltration rates could be easily measured. Larger plot sizes may require excessively large tanks, and thus continuous pumping and dosing to inject tracers directly into the pump hose may provide a better alternative for adequate mixing.

Figure 18 shows the relationship between flow rate and the time to empty the tank, which can be used to aid the design of infiltration experiments. For example, one of the 3 m by 3 m plots had a quasi-steady state infiltration rate of 6.3 cm/hr, which required an average flow rate of 9.5 L/min. According to Figure 18, the tank will need to be refilled every 8 hr for a 4.9 m³ tank. Actual times to empty the tank after quasi-steady state was reached were 6.5, 6.0, and 8.0 hr at Pumpkin Hollow for example, which is consistent with the fact that refills were performed before the tank was completely empty.

A constant head assumption was considered valid if the water depth in the infiltration plot was within 1.5 cm of the mean depth at least 85% of the time. All experiments met this requirement (Figure 19). Float valves were reliable and effective, allowing the system to run automatically for several hours at a time. Manual gate valves required attentive monitoring in order to be effective. Observed response times based on chloride detection in groundwater wells (located 0.5 m from the edge of the berm) ranged from 18 minutes (coarse gravel outcrop) to more than 32 hours. All plots had at least some wells where chloride was never detected above background levels (duration of experiments ranged from 3 to 32 hours), again indicating significant heterogeneity within the floodplain soils.

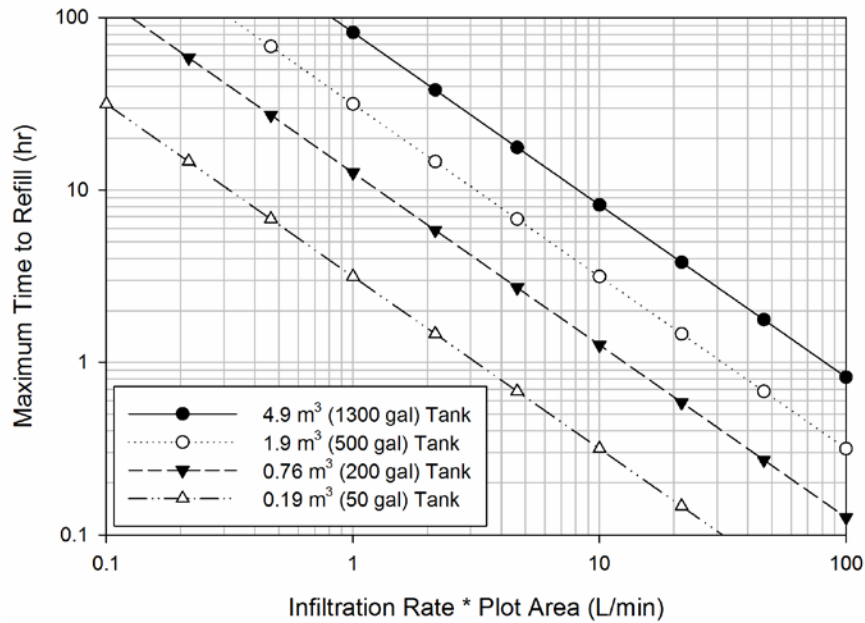


Figure 18. Relationship between expected infiltration flow rate and time to empty water tank for different size water tanks.

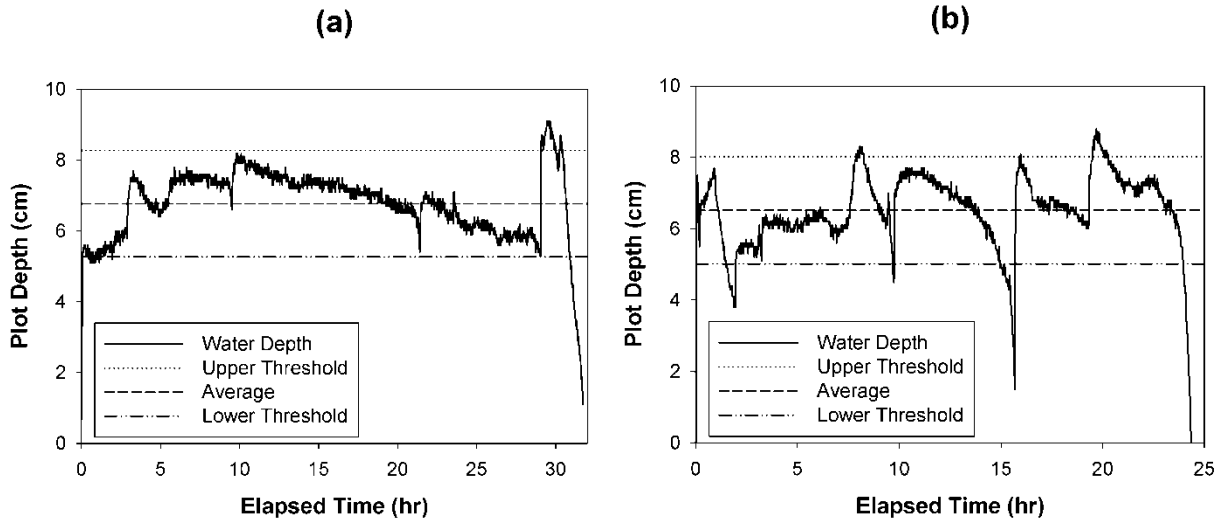


Figure 19. Measured plot water depth over time for a 1 m by 1 m plot with flow controlled primarily by an automatic float valve (a) and for a 3 m by 3 m plot with flow controlled primarily by a manual gate valve (b). Water depths were within 1.5 cm of the mean depth 92% (left) and 89% (right) of the time, meeting the prescribed requirements for constant head infiltration.

Modeled response times using HYDRUS-3D were more dependent on water table depth than distance from the plot edge. In sand and coarser soils (Figure 20), response times were predicted to be less than 200 minutes (approximately 3 hrs), even with a deep water table (250 cm) and observation wells installed as much as 4 m from the edge of the infiltration plot. For silt and finer soils, experiments would need to be conducted for multiple days when sampling from a groundwater table 200 cm below ground surface (Figure 20).

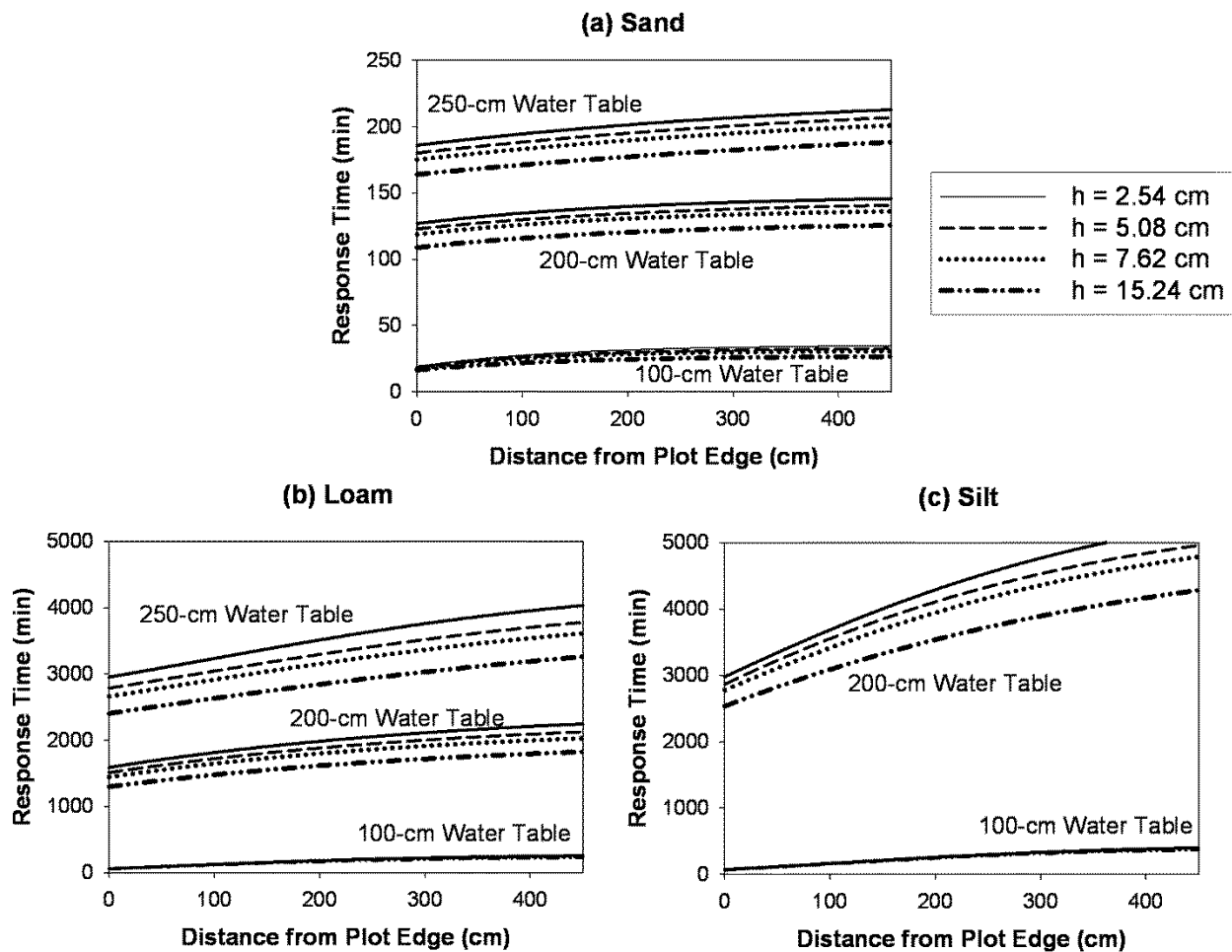


Figure 20. HYDRUS-3D predicted response times in observation wells installed next to infiltration plots as a function of soil type, head in the infiltration plot (h), distance the observation well was installed from the infiltration plot edge, and the depth to water table.

This research successfully demonstrated an innovative method for quantifying infiltration rates and leaching in highly conductive gravelly soils at the plot scale, maintaining a constant head at least 85% of the time during experiments. Guidelines have been provided for future infiltration experiments. The berm infiltration method allows investigations of various plot sizes and was demonstrated to be capable of measuring infiltration rates ranging from 5 to 70 cm/hr. Larger

plot sizes may require continuous pumping and tracer injection directly into the pump hose instead of using tanks. Numerical modeling indicated that experimental times in homogeneous soils were more dependent on water table depth than distance from the plot edge, especially for coarser soils. Experimental durations may be less than 200 minutes in sand and coarser soils to multiple days for silt and finer soils.

Data Analysis from 1 m by 1 m and 3 m by 3 m Plot Experiments at Barren Fork Creek

Locations for the 1 m by 1 m and 3 m by 3 m plots were selected based upon a relatively flat surface in order to ensure an even distribution of water within the plots. Locations were also determined from previous surveys conducted with electrical resistivity imaging that determined where gravel outcrops below the surface of the soil were located. The given sites were located approximately 10 m to 20 m from the streambank for the 1 m by 1 m and 3 m by 3 m plots, respectively.

Observation wells were installed with a Geoprobe Direct Push Drill (TMP) to a depth just below the water table to monitor the groundwater surrounding the plots, which was located approximately 3.0 to 3.5 m below the surface of the soil. Five wells (A through E) were installed around the 1 m by 1 m plot and 12 wells (I through T) were installed surrounding the 3 m by 3 m plot. The wells were located 0.5 m outside the berm (Figure 16). The wells were 5.1-cm diameter PVC pipe with approximately 3 m of screened section. Sand was packed around the screen, and bentonite was then poured and packed around the rest of well to ensure surface and lateral flow containing the injected solutes did not enter the wells before the depth of the screen. Water level loggers were installed in the wells to measure changes in the water table.

For the study, conservative and non-conservative tracers were injected into the area inside the berm (inflow water) and water samples were collected from the wells surrounding the plot. The tracers were premixed with water located in tanks (Figure 16) before distribution to the plots, with target concentrations of 100 mg/L Cl^- , 20 mg/L Rhodamine WT (RhWT, where WT means water tracing), and 10 mg/L P (in the form of PO_4^{3-}). Water added to the tanks to mix the solutions was pumped directly from the Barren Fork Creek using water pumps. The water pumped from the stream was drawn from the edge of the current, ensuring it was not drawn from stagnant pools. Water level loggers were used in both tanks to measure the head of the water in the tank, and another logger was put on the ground outside of the tanks to record the atmospheric pressure.

Both the 1 m by 1 m and 3 m by 3 m plots were started at 5:30 P.M. on June 30, 2011. An attempt was made to keep the water level in both plots at approximately 0.05 to 0.10 m to ensure a constant head on the soil. Water level loggers were placed at the lowest point in each plot to record any variability in the depth of water present in the plots.

When determining whether to collect water samples from a given well, an electrical conductivity (EC) meter, calibrated against background EC levels, was used to determine whether the Cl^- tracer had reached the well. Wells were checked approximately every 30 minutes for the first two hours of the experiment, then on the hour for the next two hours, then every four hours for the remainder of the experiment. If the EC of the water in a given well increased, a sample would be

taken at that time. Another indicator used to determine whether the tracers had reached a well was to examine the water being drawn from the well to visually determine whether it had any RhWT, a pink dye. Generally, Cl^- would increase before RhWT, which in turn would appear before the P, due to the increasing magnitude of sorption, with Cl^- being conservative or non-reactive. Samples were collected to measure RhWT, Cl^- , and P concentrations. The P samples were filtered within 24 hours using $0.45 \mu\text{m}$ filters to remove any possible particulate P. The samples were then sent to the University of Arkansas to measure the Cl^- and P concentrations. To measure the concentrations of RhWT, a Trilogy laboratory fluorometer was used with the fluorescence module to measure the relative fluorescence units (RFU). Then, the RFU was used to calculate the RhWT concentration in ppb.

Using rating curves for the tanks, the change in the volume of water in the tank was calculated for the duration of the test, with the change in volume over time being equivalent to the rate of water being distributed to the plot. Then, using the plot area and the rate of distribution, the infiltration rate of the water was calculated for the two scales (1 m^2 and 9 m^2). These infiltration rates were compared to infiltration rates from small-scale infiltration tests conducted using double ring infiltrometers.

The infiltration throughout the experiments for both plots was relatively consistent. The average infiltration rate for the 1 m by 1 m and 3 m by 3 m plots was 10.7 (Figure 21) and 12.6 cm/hr , respectively. For a two to four hour period, the 3 m by 3 m plot was not covered with water due to equipment malfunction. This may have led to variations in the concentrations for wells I through T.

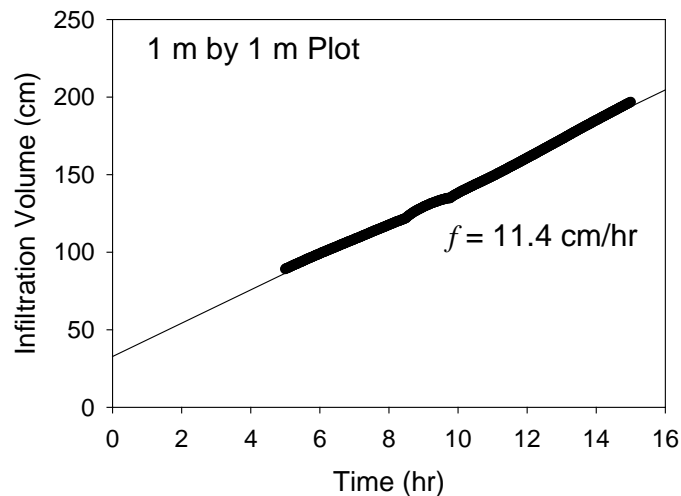


Figure 21. Infiltration of water on the 1 m by 1 m plot for a specific period in which the infiltration rate was constant. The slope of the line indicates the average infiltration rate.

Nonetheless, the average infiltration for the 3 m by 3 m was greater than the 1 m by 1 m plot, which in turn was greater than the infiltration of the soil conducted with a double ring

infiltrometer at the same site the previous year (Figure 22). This in turn is leading to future research to determine whether the size of a given plot will affect the rate of P absorption due to the velocity of water moving through the soil. The difference in the rates of infiltration appear to follow a logarithmic relationship (Figure 22); additional 10 m by 10 m plots are going to be tested in the same manner, and the infiltration rates will be compared in the future to confirm whether there is indeed a scaling factor when conducting experiments dealing with water infiltration.

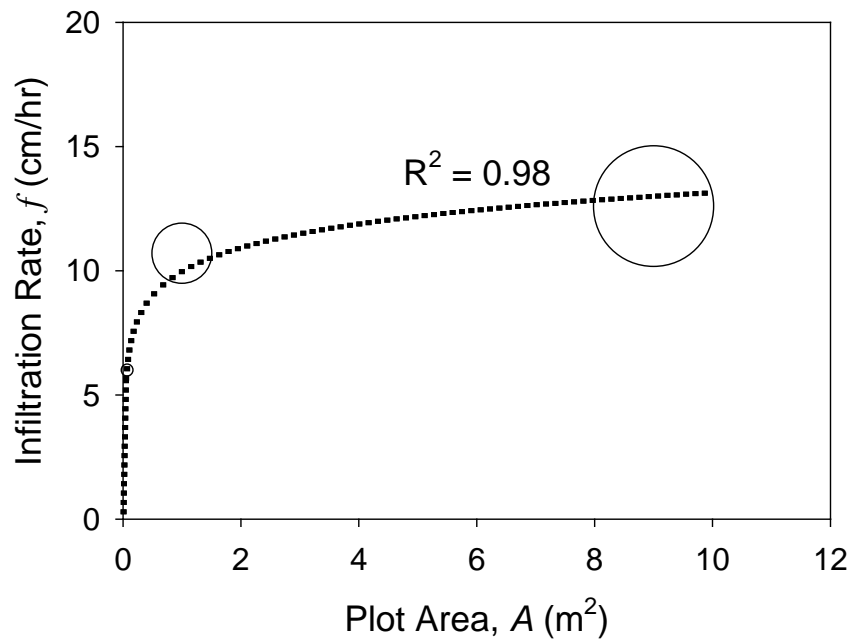


Figure 22. Infiltration rate versus the size of the plot at the Barren Fork Creek floodplain site. The smallest plot size was a 30-cm diameter double-ring infiltrometer.

For all wells, the RhWT and Cl⁻ concentrations increased by the second sample after the start of the experiment, which was approximately two hours after the start of the experiment. In fact, slight increases in concentrations of both RhWT and Cl⁻ were observed after the first sample in some wells, which was taken approximately thirty minutes to one hour after the start of the experiment. The concentration of the wells reached approximately 50% of the applied chloride within two hours of the initial introduction of the tracers. The water collected from the wells was approximately 3 m below the surface, meaning the tracers could have had an average transport rate of up to 10 cm/min. The NRCS Soil Survey (NRCS) estimated permeability of the limiting layer to be in the range of 1.5 to 5.0 cm/hr for Razort gravelly loam, the soil found at the Barren Fork Creek field site. This suggests the possibility of preferential pathways being present on the plots, meaning that water could be moving through macropores at a rate much faster than the average soil infiltration. Also, another possibility is that the soil is not homogeneous, and there is a thinner layer of soil on top of the gravel in smaller areas that allowed for an introduction of tracers to the groundwater at a faster rate than the average of the entire plot.

The concentration ratio between the concentration in the well and the concentration injected into the plot for RhWT, Cl^- , and P (i.e. dissolved P) were used to examine changes in the wells (Figure 23). The timing of when the tracers reach the well should be in the following order: Cl^- , RhWT, and P. The Cl^- should reach the wells first due to the fact that it does not bind with soil particles. RhWT only binds to organic materials, but does not bind to any other particles to a large extent. P, on the other hand, binds to both organic matter and mineral surfaces.

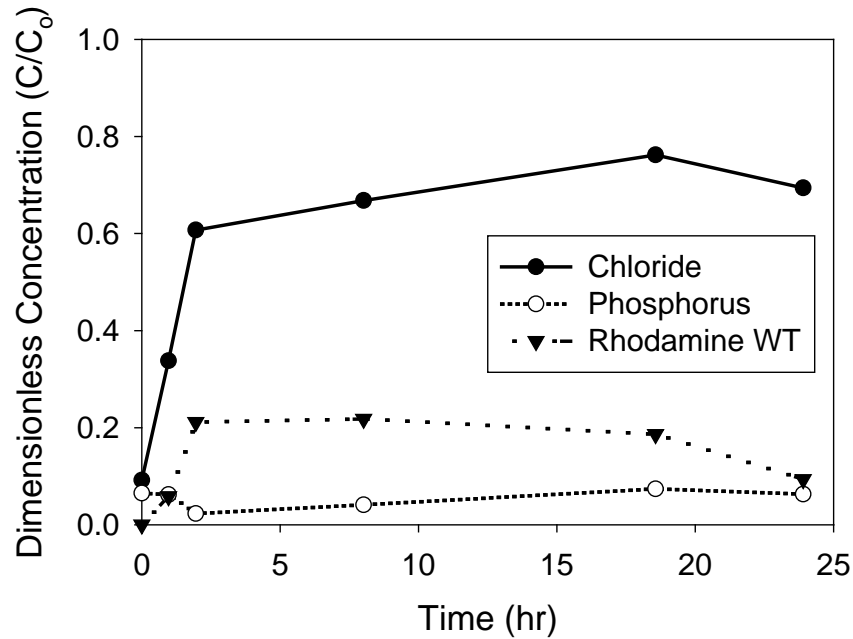


Figure 23. Dimensionless concentration calculated as the ratio of the concentration in the well (C) to the injected concentration (C_0) into the berm versus time for well B in the 1 m by 1 m plot.

Consider the example shown in Figure 23, RhWT and Cl^- concentration ratios were directly proportional for all measurements taken until the last measurement, where the concentration of the RhWT decreased while the Cl^- concentration increased. The P concentration appeared to be high at the beginning, and then after the first two readings, a low concentration of P was observed, and then the P concentration increased for the rest of the experiment.

The soils in the alluvial floodplain were extremely heterogeneous, as shown by previous studies conducted by Oklahoma State University (Heeren et al., 2011). Further, when testing on a larger scale plot (3 m by 3 m), the flow containing tracers did not follow the expected flow for soils of homogeneous composition; the wells surrounding the 3 m by 3 m plot did not show equal maximum concentrations of RhWT, Cl^- , nor P. The wells that showed a significant difference in RhWT, Cl^- , and P concentrations were all adjacent on the southern corner of the plot (wells O, P, W, R, and S, Figure 24) with some variability in the P concentrations.

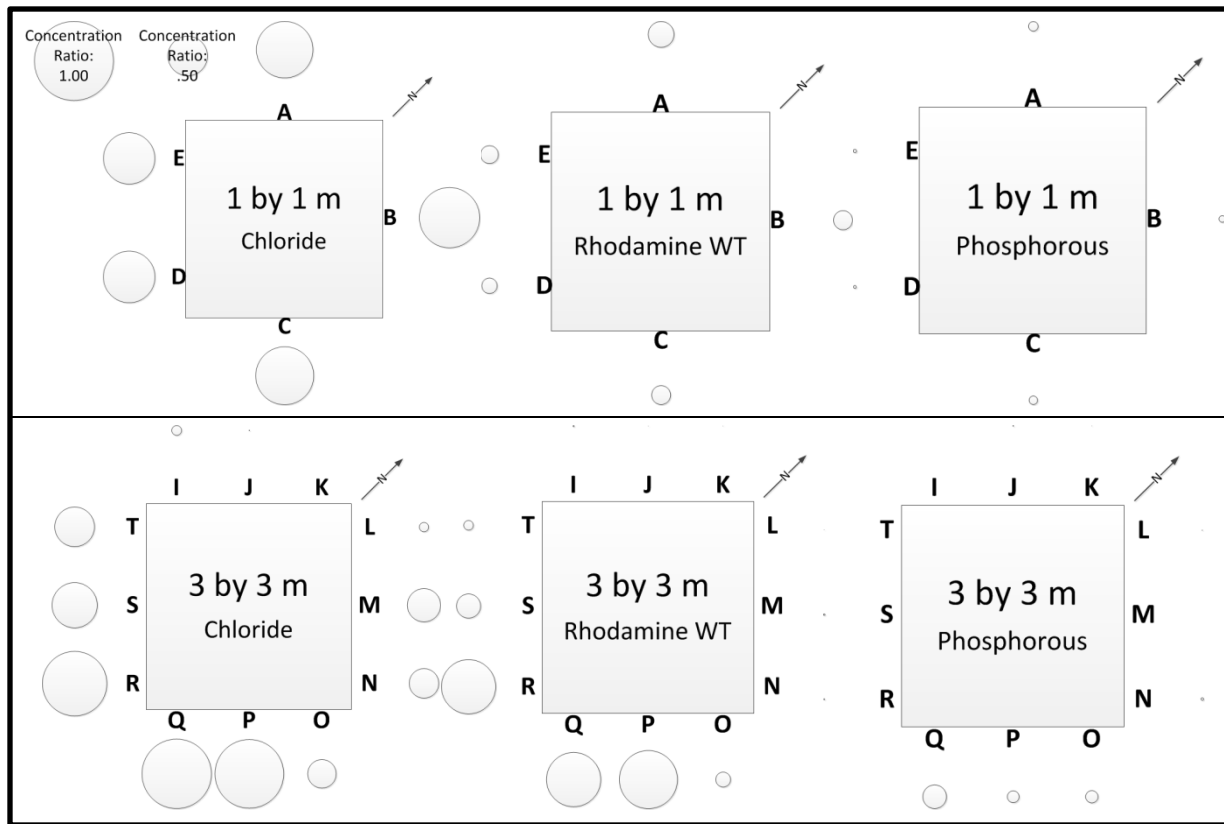


Figure 24. Maximum concentration ratios (C/C_0 , where C_0 is the inflow concentration) of samples from each well. Note that the plots are not drawn to scale. Size of the circle around each given well represents the concentration ratio.

These results show that infiltrated water may not be necessarily flowing vertically to the groundwater, but can flow laterally, potentially following preferential pathways. Conversely, the tracers may have reached the groundwater, and then moved laterally prior to reaching the wells surrounding the plot. When comparing the 3 m by 3 m to the 1 m by 1 m plot (Figure 24), it must be noted that the wells surrounding their given plots are located the same distance. For the 1 m by 1 m plot, RhWT was present in all wells at approximately the same concentration magnitude, unlike the 3 m by 3 m plot. This points to a lack of homogeneous composition of soils in this given floodplain because the tracers did not move the same distance to the wells on the 3 m by 3 m plot than they did on the 1 m by 1 m plot. The results of these experiments demonstrated a significant amount of infiltration by the Cl^- levels within this time period. While Cl^- was the only tracer to reach over 50% of the initial tracer concentration within the 26 hr timeframe of the experiment, it is possible that the RhWT and the P levels would become elevated past 50% of the initial tracer concentration given enough time. Future research should include modeling of the soil profile to predict how P leaching increases over longer time scales.

When considering the effectiveness of the plot size to realistic conditions, two factors come into play: how realistically does water move into the soil compared to natural conditions, and how can measurements and samples be taken from directly underneath the plume, where lateral flow

of tracers is not a dependent factor for accurately sampling the concentration of the tracers in the groundwater? While there are not currently any effective techniques for taking measurements from underneath a given plot in these gravelly soils, plot scale experiments realistically simulate field conditions compared to smaller infiltrometers and laboratory testing. It was shown that infiltration rate is correlated to plot size, with the data suggesting a logarithmic relationship between infiltration rate and the area of the plot. Further investigations into this relationship should be, and are being investigated; there will be a 10 m by 10 m plot experiment conducted at the Barren Fork Creek site as well as two other field sites both in Oklahoma and Arkansas.

These experiments showed a relationship between plot size and infiltration rate of water. The injected Cl⁻, RhWT, and P were observed in groundwater samples, but due to the movement patterns seen in the wells, it can be deduced that the soils in these alluvial floodplains are complex and not homogeneous.

Two-dimensional and three-dimensional HYDRUS simulation models are now being completed to simulate these infiltration and leaching experiments. The objective of this research was to use finite element modeling to develop a long-term model for this phenomenon for future predictions. HYDRUS-3D was used to simulate the infiltration plots with initial P transport parameters derived from P isotherms. For each experiment, the soil hydraulic parameters of the model were calibrated based on collected data from observation wells. The fate and transport parameters in the model were then calibrated based on electrical conductivity (chloride), Rhodamine WT and P concentrations in the groundwater. Model parameter sets for water flow and P transport were derived based on plots with and without gravel outcrops. Relationships were then derived from HYDRUS-3D for P concentrations and loads reaching the groundwater under different surface P concentrations and soil depths.

References

- Akay, O., G.A. Fox, and J. Simunek. 2008. Numerical simulation of flow dynamics during macropore/subsurface drain interaction using HYDRUS. *Vadose Zone Journal* 7(3): 909-918, DOI: 10.2136/vzj2007.0148.
- Archie, G.E. 1942. The electrical resistivity log as an aid in determining some reservoir characteristics. *Petroleum Technology* Technical Paper 1422.
- Carsel, R. F., and R. S. Parrish. 1988. Developing joint probability distributions of soil water retention characteristics. *Water Resources Research* 24: 755-769.
- DeSutter, T.M., G.M. Pierzynski, and L.R. Baker. 2006. Flow through and batch methods for determining calcium-magnesium and magnesium-calcium selectivity. *Soil Sci. Soc. Am. J.* 70:550-554.
- Fuchs, J.W., G.A. Fox, D.E. Storm, C. Penn, and G.O. Brown. 2009. Subsurface transport of phosphorus in riparian floodplains: Influence of preferential flow paths. *Journal of Environmental Quality* 38(2): 473-484.
- Halihan, T., S. Paxton, I. Graham, T. Fenstermaker, and M. Riley. 2005. Post-remediation evaluation of a LNAPL site using electrical resistivity imaging. *Journal of Environmental Modeling* 7: 283-287.

- Heeren, D.M., R.B. Miller, G.A. Fox, D.E. Storm, C.J. Penn, and T. Halihan. 2010. Preferential flow path effects on subsurface contaminant transport in alluvial floodplains. *Transactions of the ASABE* 53(1): 127-136.
- Jacobson, R.B., and K.B. Gran 1999. Gravel sediment routing from widespread, low-intensity landscape disturbance, Current River Basin, Missouri. *Earth Surface Processes and Landforms* 24: 897-917.
- Loke, M.H., and T. Dahlin. 2002. A comparison of the Gauss–Newton and quasi-Newton methods in resistivity imaging inversion. *Journal of Applied Geophysics* 49: 149–162.
- McNeill, J.D. 1980. Electrical Conductivity of Soils and Rocks. Technical Note TN-5, Geonics Limited, Ontario, Canada.
- Murphy, J., and J.R. Riley. 1962. A modified single solution method for the determination of phosphate in natural waters. *Anal. Chim. Acta* 27: 31-36.
- Najm, M.R., J.D. Jabro, W.M. Iverson, R.H. Mohtar, and R.G. Evans. 2010. New method for the characterization of three-dimensional preferential flow paths in the field. *Water Resources Research* 46, W02503, doi:10.1029/2009WR008594.
- Natural Resources Conservation Service (NRCS). 2012. Web Soil Survey (WSS). Washington, D.C.: USDA-NRCS. Available at: <http://websoilsurvey.nrcs.usda.gov/>. Accessed February, 2012.
- Šimůnek, J., M. Th. van Genuchten, and M. Šejna. 2006. The HYDRUS software package for simulating two- and three-dimensional movement of water, heat, and multiple solutes in variably-saturated media, Technical Manual, Version 1.0, PC Progress, Prague, Czech Republic, pp. 241.
- Thomas, G.W., and R.E. Phillips. 1979. Consequences of water movement in macropores. *Journal of Environmental Quality* 8(2): 149-152.
- van Genuchten, M. Th. 1980. A closed-form equation for predicting the hydraulic conductivity of unsaturated soils. *Soil Science Society of America Journal* 44: 892–898.

(2) PUBLICATIONS

Storm, P.Q. and G.A. Fox. 2013. Plot-scale leaching of phosphorus in an alluvial floodplain in the Ozark ecoregion. *Oklahoma State University Undergraduate Journal of Research* (provisionally accepted).

Heeren, D.M., G.A. Fox, and D.E. Storm. 2013. Technical Note: A berm infiltration method for conducting leaching tests at various spatial scales. *Journal of Hydrologic Engineering* (In Press, Accepted February 6, 2013), DOI: 10.1061/(ASCE)HE.1943-5584.0000802.

Heeren, D.M., G.A. Fox, and D.E. Storm. 2013. Scale analysis of infiltration measurements in heterogeneous soils. *Proceedings of the World Environmental and Water Resources Congress*, ASCE, Cincinnati, OH.

(3) INFORMATION TRANSFER PROGRAM

A project website on subsurface P transport has been created with links to relevant publications and data from the project (<http://biosystems.okstate.edu/Home/gareyf/AlluvialPTransport.htm>). Two presentations were given during the annual report period with two additional presentations and conference proceedings paper to be submitted in June 2012 for the American Society of Agricultural and Biological Engineers Annual International Meeting (AIM):

Heeren, D.M., G.A. Fox, R.B. Miller, D.E. Storm, and A.R. Mittelstet. 2011. Groundwater phosphorus preferential transport in alluvial floodplains. ASABE Annual International Meeting, Louisville, KY, 10 August 2011.

Heeren, D.M., G.A. Fox, D.E. Storm, B. Haggard. 2011. Influence of Scale on Quantifying Phosphorus Leaching in Ozark Floodplains. Arkansas Water Resources Center, Annual Watershed and Research Conference, July 6-7, 2011, Fayetteville, Arkansas.

Correll, D., D.M. Heeren, G.A. Fox, C. Penn, and T. Halihan. 2013. Transient Resistivity Imaging of a Phosphorous Tracer Test. Geological Society of America's South-Central Regional Meeting, April 4, 2013, Austin, TX.

Research results and field methods have been incorporated into an environmental contaminant transport class for graduate students during the summer of 2011 and spring 2012 semesters.

(4) STUDENT SUPPORT

Support has been provided for two graduate students (Ph.D. student in Biosystems and Agricultural Engineering at Oklahoma State and a Master of Science student in Environmental Sciences at Oklahoma State University) and four undergraduate students. Also, the research supported a 2010-2011 Oklahoma State University Wentz Research Scholars project for an additional undergraduate student.

Student Status	Number	Disciplines
Undergraduate	6	Biosystems Engineering
M.S.	1	Environmental Sciences (Geology)
Ph.D.	1	Biosystems Engineering
Post Doc	1	Biosystems Engineering
Total	9	

(5) STUDENT INTERSHIP PROGRAM

No students completed an internship during the reporting period.

(6) NOTABLE ACHIEVEMENTS AND AWARDS

None to report at this time.

Incorporating Ecological Costs and Benefits into Environmental Flow Recommendations for Oklahoma Rivers: Phase 1, Southeastern Oklahoma

Basic Information

Title:	Incorporating Ecological Costs and Benefits into Environmental Flow Recommendations for Oklahoma Rivers: Phase 1, Southeastern Oklahoma
Project Number:	2011OK207B
Start Date:	3/1/2011
End Date:	8/30/2012
Funding Source:	104B
Congressional District:	4
Research Category:	Not Applicable
Focus Category:	Ecology, Hydrology, Models
Descriptors:	None
Principal Investigators:	Caryn Vaughn, Jason P. Julian

Publications

There are no publications.

Title: Incorporating Ecological Costs and Benefits into Environmental Flow Recommendations For Oklahoma Rivers: Phase 1, Southeastern Oklahoma.

Authors' Names and Affiliations: Caryn C. Vaughn, Director and Presidential Professor, Oklahoma Biological Survey and Biology, University of Oklahoma; Jason P. Julian, Assistant Professor, Geography and Environmental Sustainability, University of Oklahoma.

Start Date: 8/1/11

End Date: 2/28/13

Congressional District: 2 and 4

Focus Category: COV, DROU, ECL, HYDROL, MOD, SW, WQN

Descriptors: stream, environmental flows, flow-ecology, hydrology, temperature, solar radiation, freshwater mussel, Unionidae

Publications: None to date.

Problem and Research Objectives:

Providing a safe and sustainable water supply to the growing Oklahoma population while also providing for economic growth and maintaining natural ecosystems is the most serious challenge facing Oklahoma policy makers in the coming decades. Accomplishing this will require consideration of both the economic and ecological costs and benefits of different water allocation and management strategies (Arthington et al. 2006, Richter 2010). Multiple approaches have been used to attempt to quantify the amount of water needed by natural water bodies in Oklahoma. In-stream flows (ISFs) quantify the amount of water that needs to be left in a stream to maintain non-consumptive uses such as fisheries or riparian areas (OWRB 2009). Currently, there are over 200 methods for determining ISFs, ranging from designation of minimum flows to those that mimic natural flow regimes (Turton et al. 2009).

Rivers in the Ouachita and Gulf Coastal Plains ecoregions of southeastern Oklahoma provide an excellent test system for examining the ecological costs and benefits of different environmental flows/in-stream flow recommendations. These rivers are known for their relatively abundant and pristine water and harbor the highest aquatic biological diversity in the state (Matthews et al. 2005). However, the water in these rivers also is in high demand to meet regional, human water needs (<http://www.owrb.ok.gov/supply/ocwp/ocwp.php>). In particular, the Kiamichi River is at the center of intense conflict over water use and governance between Oklahoma City, the State of Oklahoma, the Tarrant County Water District (Fort Worth, TX), and the Choctaw and Chickasaw nations. The source of conflict is over who gets to use water from a storage reservoir. Sardis Lake is an impoundment on a tributary to the Kiamichi. The Corps of Engineers built this reservoir in 1982 for flood control, water supply and recreation. However, Oklahoma owed money to the federal government for constructing the reservoir, and in 2011 90% of the water storage rights to Sardis Lake were sold to Oklahoma City. The Tarrant County Water District disputes this ownership. Under the 1978 Red River Compact (<http://www.oscn.net/applications/oscn/deliverdocument.asp?id=97778&hits=>), they claim to have rights to 25% of the water from Sardis Lake, and they want Oklahoma to sell it to them.

They have sued the state to get access to the water and the U.S. Supreme Court is reviewing this case this spring (US Supreme Court 2013). Finally, both the Choctaw and Chickasaw nations also claim to own the water in the Kiamichi watershed, including that in Sardis Lake. The river flows through the jurisdictional Choctaw Nation in southeastern Oklahoma, and the historical Choctaw Nation capital abuts the banks of the Kiamichi in the town of Tuskahoma. Together, Sardis and Hugo (a reservoir at the most downstream end of the Kiamichi) lakes are the water supply for people in 29 Oklahoma counties. Current and planned inter-basin water transfers will extract hundreds of thousands of acre-feet of freshwater per year out of southeastern Oklahoma, with 220,000 acre-feet/year going to Oklahoma City alone by 2050 via the Atoka Pipeline (OWRB 2008). In addition to the Supreme Court case, there are multiple, ongoing and pending lawsuits over who gets to use and sell the water from Sardis Lake.

Missing from the above dispute are the needs of the fish and wildlife that live in and around the Kiamichi River. The Kiamichi River is known for its high aquatic biodiversity (Vaughn 2000, Matthews et al. 2005). It is home to over 86 species of fish and 30 species of freshwater mussels, including 3 federally listed endangered mussel species (Vaughn et al. 1996, Pyron et al. 1998, Matthews et al. 2005, Galbraith et al. 2008). In 1998 the river was selected by The Nature Conservancy, arguably the most influential conservation organization globally, as one of the most critical rivers in the U.S. for preserving biodiversity (Master et al. 1998). The water now impounded by Sardis Lake historically provided 30% of the water flowing into the lower Kiamichi River. However, in recent drought years the organisms in the lower river have suffered because water has been held in Sardis Lake rather than being released to flow down stream. This has occurred during hot summer months and has led to drying of the lower river (Figure 1), high water temperatures (in some cases exceeding 100° F because of the extremely shallow water), massive mussel and fish mortality (Galbraith et al. 2010; W.J. Matthews personal communication), and record low lake levels downstream in Hugo Reservoir (USACE 2012). This has occurred because Sardis Lake has no designated “non-consumptive” uses and Oklahoma has no in-stream flow regulations, which means that water managers are not required to release water for mussels, fish and other river organisms during droughts. While periodic heat waves and drought are normal in this region (Stambaugh et al. 2011), the last two summers have been the hottest on record and most of this area is entering an unprecedented 3rd year of extreme to exceptional drought that is predicted to persist for the foreseeable future.

Freshwater mussels are large, long-lived bivalve mollusks. Mussels are very sensitive to changes in flow regimes and temperature (Strayer et al. 2004, Pandolfo et al. 2010, 2012, Galbraith et al. 2012). Adult mussels are highly sedentary; they move very slowly and only short distances if they move at all (Allen and Vaughn 2009). Thus, unlike fish, mussels cannot move to new habitat, such as the bottom of a pool, when flows are inappropriate, and in-stream flow models developed for fish and other mobile organisms typically do not work well for mussel populations (Layzer and Madison 1995, Gore et al. 2001). Establishing environmental flows that safeguard mussel populations will protect the three endangered mussel species and hopefully prevent future litigation related to these species. In addition, because mussels provided important habitat and other services for other river organisms such as insects and fish, protecting mussels also protects these other groups (Vaughn and Spooner 2006, Aldridge et al. 2007).

Ecosystem services describe the benefits that humans derive from natural ecosystems. These include *provisioning services* obtained directly from the ecosystem such as water, food and timber, *regulating services* such as water purification, climate control, carbon storage and

pollination, and *cultural services*, which are the benefits that people obtain through tourism, aesthetic experiences or spiritual enrichment (Daily and Matson 2008, Perrings et al. 2011, Wainger and Mazzotta 2011). Rivers and the organisms that inhabit them provide many important ecosystem services to people such as provisioning of freshwater, nutrient processing and water filtration, and recreation and ecotourism (Brauman et al. 2007). Freshwater mussels are filter feeders that move large amounts of water over their gills (Vaughn et al. 2004) resulting in multiple ecosystem services including biofiltration, nutrient cycling and storage (Vaughn and Hakenkamp 2001, Vaughn 2010). This “pre-filtration” or biofiltration by mussels means that water extracted for human uses from rivers with healthy mussel populations should require less treatment than water from rivers without mussels, saving money (Kreeger and Bushek 2008).

Like most invertebrates, mussels are ectotherms whose physiological processes are governed by external, environmental temperatures. Vaughn’s laboratory has discovered that different mussel species prefer different environmental temperatures and perform ecosystem services differently at these different temperatures (Spooner and Vaughn 2008). Because of these differences in thermal preferences and performance, the amount of water filtered by mussels and nutrient cycling rates differ with the species makeup of mussel communities, water volume, and water temperature (Vaughn et al. 2008, Vaughn 2010).

Water temperatures in rivers are influenced by numerous factors, including quantity of groundwater inputs, volume of surface water, watershed snow coverage, incoming solar radiation, air temperature, and wind speed (Allan and Castillo 2007). The direct absorption of solar radiation is the main heat input into large rivers, while convective warming by the air is more influential in small streams. Indeed, many stream studies have found strong linear relationships between air and water temperature (Wetzel 2001). Anthropogenic inputs/outputs can also affect water temperatures in rivers. Man-made reservoirs, in particular, have the potential to warm downstream waters (via greater absorption of solar radiation from increased water surface area, and longer water residence times) or cool downstream waters (via cool-water releases from the bottom of the reservoir) (Stanford et al. 1996, Allan and Castillo 2007). Because of the various unobservable pathways and interactions of water throughout a watershed, it is practically impossible to derive a numerical model that accounts for all water-heat fluxes. A much more practical strategy of predicting river water temperatures is the use of an empirical model, one that takes into account the dominant control on water temperature for that size of stream.

We need to determine the appropriate volume and timing of water diversions from the Kiamichi and other rivers to meet human needs while maintaining natural ecological function. In this project we combined information on discharge and water temperature under various stream flows with information on how mussel communities perform the ecosystem services of water filtration, nutrient cycling and nutrient storage under those conditions to determine how different stream flows influence the ecosystem services provided by mussels. We focused on the Kiamichi River because we already have rigorous data on mussel communities (Galbraith et al. 2005) and the physical characteristics of river reaches where these communities occur (Jones and Fisher 2005), and because this river is under the most pressure for regional water diversions as described above. From previous work by Vaughn’s laboratory, we already had strong data on the ecosystem services performed by various mussel species under different temperature regimes (Vaughn and Spooner 2008). We added to this dataset by obtaining additional thermal preference/performance data for a wider variety of mussel species. We also gathered data on

how water temperature in the Kiamichi River is dictated by atmospheric and flow (regulated vs. unregulated) conditions. Finally, we used these data to produce multivariate models that predict water temperature from air temperature and water depth, and in turn allow us to determine the amount of water required to be released from Sardis Reservoir to maintain target stream temperatures. We then compare these targeted stream temperatures with mussel success and ecosystem services.

Objectives:

1. Conduct laboratory experiments to measure mussel thermal preference and performance (respiration rates, filtration rate, and nitrogen and phosphorus recycling rates and storage) for species of freshwater mussels from southeastern Oklahoma. Combine these data with mussel community biomass data to estimate ecosystem services.
2. Place automatic recording level loggers in river reaches/mussel beds in the Kiamichi River to obtain daily information on flow discharge and water temperature across seasons.
3. Create a GIS-based model that quantifies (i) incoming solar radiation to the Kiamichi watershed (using Oklahoma Mesonet data); (ii) water-surface reflection and topographic and riparian shading (using methods from Julian et al. 2008b); and (iii) water budgets (using flow and hydrographic data). This GIS-based model will be combined with empirical data from Objective 2 to develop predictive relationships of water temperature based on variable flow and atmospheric conditions.
4. Compare model results with various in-stream flow scenarios to make environmental flow recommendations that protect mussel populations and system-wide ecological function.

METHODS

Objective 1: *Conduct laboratory experiments to measure mussel thermal preference and performance (respiration rates, filtration rate, and nitrogen and phosphorus recycling rates and storage) for species of freshwater mussels from southeastern Oklahoma. Combine these data with mussel community biomass data to estimate ecosystem services.*

Spooner and Vaughn (2008) measured respiration rates, algal clearance rates, and nitrogen and phosphorus recycling rates for eight species of mussels from southeastern Oklahoma at 15, 25, and 35 °C. We added to this dataset by measuring the above rates for six additional species of mussels across the three temperatures. Mussels were acclimated to experimental temperatures for two weeks in 500-L Frigid Unit Living Streams®. Mussels were fed cultured algae during acclimation, and then starved for 24 hours before conducting the experiments (Vaughn et al. 2004). Measurements on individual mussels were conducted in continuously stirred, covered glass beakers (500 ml or 1500 ml, depending on mussel size) housed in 1.8 m³ temperature-controlled chambers. Following Spooner and Vaughn (2008) we added an aliquot of cultured algae to each beaker, allowed mussels to filter for 1.5 hours, and measure filtration rate as the mass-specific change in chlorophyll concentration. Each mussel was then placed in a second beaker with pre-filtered water for an additional 1.5 hours where we measured respiration rate as the change in oxygen concentration and collect water samples to determine excretion (NH₃, PO₄) rates. At the end of the experiment, mussels were measured for shell dimensions and weighed. All rate were expressed on a gram dry weight basis.

On July 31, 2011 and June 10, 2012, we quantitatively sampled mussels at the Paine's site on the Kiamichi River. This is a long-term mussel-monitoring site established in 1991 (Site 7 from Vaughn and Pyron 1995; Site KM11 Hobo logger). We divided the site into three sections; the upstream pool, the downstream riffle that had water (hereafter "riffle"), and the most downstream riffle that was completely dry (hereafter "dry riffle")(Figure 1). In the pool and riffle sections, we excavated 15, 0.25 m² quadrats following Vaughn et al. (1997). Mussels were identified, measured for length, and returned to the stream. In the riffle there were many freshly dead mussels (tissue still attached), so we separately tallied densities and sizes for live and dead mussels. In the dry riffle we established eight transects across the riverbed spaced 10 meters apart. Then, at each one meter interval across each transect we counted freshly dead mussel individuals that could be observed from the surface for one meter to either side of the transect line.

We used length-dry weight regressions to estimate mean mussel biomass for each species. We combined this information with our measured densities to estimate the total biomass of each species in the pool and riffle. We multiplied the dry-weight corrected nitrogen and phosphorus excretion rates and algal clearance rates from our laboratory experiment by mussel biomass from our field survey to get areal rates (rates per g dry weight per square meter of riverbed), and summed across species to get community wide ecosystem service rates (N recycling, P recycling and biofiltration) based on the species actually present in the pool and riffle. We did not use the dry riffle in our ecosystem services estimates because we did not have mussel length data for that area and thus could not estimate biomass. We used mussel biomass and stoichiometric data to estimate the amount of nitrogen, phosphorus and carbon stored in mussel soft tissue and shell (Christian et al. 2008, Atkinson et al. 2010).

Objective 2: Place automatic recording level loggers in ten river reaches/mussel beds in the Kiamichi River to obtain daily information on flow discharge and water temperature across seasons.

We installed 8 Onset[®] HOBO[®] data loggers (model U20-001-01) that measured water depth and water temperature across the Kiamichi River watershed (Figure 2; Table 1). These sites were strategically selected to capture influences from Sardis Reservoir and tributaries. We also installed 3 Onset[®] HOBO[®] data loggers (model U20-001-01) that measured atmospheric pressure and air temperature across the watershed. These data were used to calibrate and compare the water temperature and depth data. Daily solar radiation data was collected from OK Mesonet stations distributed across the Kiamichi watershed. The Mesonet is a network of 120 environmental monitoring stations distributed across Oklahoma (<http://www.mesonet.org/index.php/site/about>). All of these stations collect air temperature (°C) and solar radiation (400-1100 nm; W/m²) in 5-minute intervals.

Objective 3: Create a GIS-based model that quantifies (i) incoming solar radiation to the Kiamichi watershed (using Oklahoma Mesonet data); (ii) water-surface reflection and topographic and riparian shading (using methods from Julian et al. 2008b); and (iii) water budgets (using flow and hydrographic data). This GIS-based model will be combined with empirical data from Objective 2 to develop predictive relationships of water temperature based on variable flow and atmospheric conditions.

With the intention of developing a GIS-based model that estimates water temperatures using solar radiation budgets (BLAM; Julian et al. 2008a), we collected 22 hemispherical canopy photographs throughout the watershed (Figure 2). We analyzed these canopy photos with Gap Light Analyzer (GLA) software and derived canopy shading and the percentage of incoming solar radiation that reached the stream surface on an average summer day. We then used these values to calibrate a canopy-shading map for the entire watershed based on an Enhanced Vegetation Index (EVI) derived from Landsat imagery taken close to the same period as the canopy photos. This canopy-shading map can be used to calculate daily solar radiation budgets at the ground/stream surface, which can then be used to develop empirical mechanistic models for river water temperature.

Objective 4: *Compare model results with various in-stream flow scenarios to make environmental flow recommendations that protect mussel populations and system-wide ecological function.*

Using data from Objective 2, we developed multivariate regression models for each monitoring station (Figure 2, Table 1) that uses air temperature and water depth to predict water temperature. These models were then used to (1) develop an historical timeline of water temperatures in the Kiamichi River; and (2) determine what flows need to be released from Sardis Dam to maintain healthy mussel communities downstream and/or maximize the ecosystem services they provide.

PRINCIPAL FINDINGS AND SIGNIFICANCE

Objective 1: *Mussel thermal preference and performance and estimated ecosystem services.*

We measured respiration (Figure 3), nitrogen excretion (Figure 4) and phosphorus excretion rates (Figure 5) and clearance (filtration) rates (Figure 6) for five unionid mussel species (*Lampsilis teres*, *Plectomerus dombeyanus*, *Potamilus purpuratus*, *Pyganodon grandis* and *Quadrula verrucosa*) and the invasive clam *Corbicula fluminea*.

Mussel densities at the Paine's site mussel bed (Vaughn site 7) were strongly associated with water depth and temperature. In late July 2011-12, the upper pool portion of this mussel bed was covered by water depths of 30-to-100 cm, with midday water temperatures < 30°C. In contrast the portion of the riffle that still had water covering it was extremely shallow with hot water temperatures. On July 31, 2011 the average depth in the riffle was 10 cm and the midday temperature was 40°C, well above the thermal tolerances for both juvenile and adult mussels (Pandolfo et al. 2010, Galbraith et al. 2012). In past surveys mussel densities in the pool and riffle/run portion of this site have been approximately equal (Vaughn and Pyron 1995), however in 2011-12 mussel densities in the pool were approximately 12 times higher than in the shallower riffle (Figure 7A). In the riffle freshly dead mussels (tissue still attached) were twice as abundant in quadrats as live mussels (Figure 7B). In the completely dry lower riffle we found 19 species of freshly dead mussels.

We estimated ecosystem services for the Paine's site mussel bed based on the actual community composition, densities and rates for species we found in quadrats at the site in 2011-12: *Actinonaias ligamentina*, *Amblema plicata*, *Ellipsaria lineolata*, *Fusconaia flava*, *Lampsilis cardium*, *Obliquaria reflexa*, *Potamilus purpuratus*, *Quadrula pustulosa*, *Quadrula verrucosa* and *Truncilla truncata*. Rates for *P. purpuratus* and *Q. verrucosa* were estimated from data

collected in this study. Rates for the other species are from Spooner and Vaughn (2008). We estimated ecosystem services separately for the pool, live mussels in the riffle, and lost services due to mussel death (the freshly dead mussels in the riffle). Community nitrogen and phosphorus recycling rates were highest in the pool and lowest in the riffle and increased with temperature (Figure 8). This is because mussel metabolic rates rise with temperature and they excrete at higher rates because they are stressed (Spooner and Vaughn 2008). What is interesting is that the N and P recycling capability lost through mussel death in the riffle was much higher than that provided by surviving, live mussels in the riffle (Figure 9). The same pattern can be seen for biofiltration (Figure 9) and nutrient storage (Figure 10).

Objective 2: Discharge and water temperature time-series.

Because of the extremely low flows to no flows in the watershed during the summers of 2011 and 2012, we were not able to construct stage-discharge rating curves for each monitoring station. Instead, we relied on water discharge data from four federal monitoring stations located within our study area (Table 2). We obtained daily precipitation, air temperature (for verification of HOBO data), and solar radiation data from three Oklahoma Mesonet stations located around the watershed (Table 3). All of these data were used to create time-series for each station that displayed mean water temperatures (Appendix 1) and maximum water temperatures (Appendix 2). During our study period (June 8, 2011 – September 30, 2012), there were 4 days at the Kiamichi River station @ Clayton in which water temperatures exceeded 35 C – the temperature at which adult mussels begin to die. Kiamichi River @ Antlers had 21 days where water temperature exceeded 35 C. During these days, there were no releases from Sardis Dam or in the case of Antlers, releases did not convey all the way to Antlers due to the lower Kiamichi River being a losing stream during extended droughts in the post-Sardis Dam hydrologic regime. The effect of lack of releases from Sardis Dam on downstream reaches during droughts is illustrated in Figure 11. Sardis Dam captures approximately 25% of the Kiamichi River watershed above the Antlers gage. When none of this runoff is released during extended droughts, the lower reaches behave like the upper reaches in terms of hydrologic drought. Before Sardis Dam (1982) downstream reaches such as Antlers were not as susceptible to hydrologic drought as the upper reaches on account of a larger contributing watershed.

In addition to numerous days of lethal water temperatures, there were also long periods of no flow days at many of the stations (Table 4) that also led to mass mortality of mussels (USFWS, unpublished data; C.L. Atkinson, unpublished data).

Objective 3: Predictive relationships of water temperature based on variable flow and atmospheric conditions.

We analyzed the canopy photos with Gap Light Analyzer (GLA) software and derived canopy shading and the percentage of incoming solar radiation that reached the stream surface on an average summer day (Table 5). We then used these values to calibrate a canopy-shading map for the entire watershed based on an Enhanced Vegetation Index (EVI) derived from Landsat imagery taken close to the same period as the canopy photos (Figure 12).

Solar radiation at the stream surface was not a good predictor of water temperatures (Figure 13), which we attribute to the extremely low flow volumes of the Kiamichi streams during the drought of 2011-12. Under these flow conditions, water temperature is more influenced by heat

diffusion at the air-water interface than by solar radiation heating. That is, the air temperature is the dominant control on water temperature for low flow conditions. Thus, we changed our strategy to model water temperatures using a multivariate regression model that incorporates air temperature and flow depth. These multivariate regression models predicted mean daily water temperatures (Appendix 3) and maximum daily water temperatures (Appendix 4) accurately. The coefficient of determination (r^2) for mean daily water temperature ranged from 0.77 to 0.85 for all the stations except Antlers (K9), which had an $r^2 = 0.64$ (Appendix 3). We attribute the lower predictability for K9 to the extreme variability in groundwater-surface water exchanges over our study period. Similarly, r^2 for maximum daily water temperature ranged from 0.62 to 0.83 (Appendix 4). For all models, water temperature increased predictably with increasing air temperature, and decreased predictably with increasing water depth. These models were used to determine how different water releases from Sardis Dam affect downstream water temperatures (Figure 14; Objective 4).

Objective 4: Compare model results with various in-stream flow scenarios to make environmental flow recommendations that protect mussel populations and system-wide ecological function.

The managed daily water releases of 0.59 cms (21 cfs) from Sardis Dam beginning on August 2, 2011 did not increase discharge at the Antlers site until August 27, 2011 (25 days later). The likely reason for this lack of conveyance is that the water table was considerably lower than the stream bed at the end of July 2011, and thus all water released by Sardis Dam was quickly lost to the subsurface until the local water table rose high enough to intersect the channel bed, which occurred on August 27, 2011. Note that there were three small rainfall events (> 1 cm) during this period that also helped to raise the water table. What all of these data mean is that the Kiamichi River is a losing stream (i.e. discharge is lost to the subsurface due to the water table being lower than the stream bed) during extended periods of drought, particularly when 25% of its watershed runoff is held behind Sardis Dam without daily releases.

Figures 15 and 16 show the discharge-temperature rating curves that can be used to determine the required discharge for the Kiamichi River near Clayton (USGS 07335790) in order to reduce maximum water temperature to the target water temperatures that ensure mussel survival and allow them to provide ecosystem services. At the bare minimum, we recommend that maximum water temperatures be kept below 35°C, which is the temperature at which almost all juvenile mussels and many adult mussels start to die (Pandolfo et al 2010, 2012; Galbraith et al. 2010, 2012). For example, on a day with a mean daily air temperature of 40°C, enough water needs to be released from Sardis Dam to ensure 1.8 cms at the Clayton gage and prevent mussel mortality (Table 6). Note that these recommendations are based on empirical data and do not directly take into account the water temperature of Sardis Reservoir. Even more important than regulating water temperature, we recommend that during droughts, enough water should be released from Sardis Dam to maintain flow at both the Clayton and Antlers gages (> 0.01 cms) as the reach between these two gages is critical mussel habitat with 3 federally listed endangered species.

Adult freshwater mussels are sedentary and dispersal is via their larvae (glochidia) that are obligate parasites on fish (Strayer et al. 2004). While no flow days have occurred in the river in the past, in pre-reservoir construction droughts the river would have been recolonized by fish hosts moving up from the Red River (Vaughn 2012). The presence of Hugo Dam downstream prevents recolonization from the Red River and its tributaries and creates an isolated mussel

community above Hugo Lake. Vaughn has been monitoring mussels in the Kiamichi River since 1990 and has found that mussel populations have declined following the drought in the early 2000s (Galbraith et al. 2010) and the 2011-12 drought. As an example, at Paine's site mussel abundance has decreased 50 % since 1991 (Figure 17). The occurrence of the endangered mussel species have also decreased throughout the river (Galbraith et al. 2008), including the abundance of *Arkansia wheeleri*. The Kiamichi River contains the only viable population in the world of *A. wheeleri* (Vaughn and Pyron 1995). Thus, it is imperative that we manage releases from Sardis Dam to maintain flows in the river between Sardis Lake and Hugo Lake.

Freshwater mussels provide important ecosystem services to humans, including pre-filtration of water and nutrient recycling and storage. Different mussel species perform these services differently at various temperatures, but when the contributions of whole mussel communities are considered biofiltration and nutrient recycling generally increase with temperature up to a point because mussel metabolic rates increase with temperature. However, when water temperatures become so warm that mussels can no longer filter or excrete nutrients in a normal manner or actually die, these ecosystem services are lost. For the Kiamichi River, the maximum temperature that mussel communities can continue to perform normally is 35°C, although some species begin to decrease their performance at temperatures above 25 or 30°C (for example, *Actinonaias ligamentina*, see Vaughn et al. 2008). In addition, once mussels die it may take decades for populations to recover and provide lost ecosystem services, assuming flows are maintained in the river. Mussels have very long life spans (30 to 50 years), don't reach reproductive maturity until around age 6, and often don't reproduce every year. In mussel beds hard hit by the 2011-12 drought, such as the riffle at Paine's site, it will likely take approximately 30 years to achieve enough mussel biomass to restore ecosystem services.

REFERENCES:

- Aldridge, D. C., T. M. Fayle, and N. Jackson. 2007. Freshwater mussel abundance predicts biodiversity in UK lowland rivers. *Aquatic Conservation-Marine and Freshwater Ecosystems* **17**:554-564.
- Allan, D. J. and M. M. Castillo. 2007. *Stream ecology: Structure and Function of Running Waters*. Springer, Dordrecht.
- Allen, D. C. and C. C. Vaughn. 2009. Burrowing behavior of freshwater mussels in experimentally manipulated communities. *Journal of the North American Benthological Society* **28**:93-100.
- Arthington, A. H., S. E. Bunn, N. L. Poff, and R. J. Naiman. 2006. The challenge of providing environmental flow rules to sustain river ecosystems. *Ecological Applications* **16**:1311-1318.
- Atkinson, C. L., S. P. Opsahl, A. P. Covich, S. W. Golladay, and L. M. Conner. 2010. Stable isotopic signatures, tissue stoichiometry, and nutrient cycling (C and N) of native and invasive freshwater bivalves. *Journal of the North American Benthological Society* **29**:496-505.
- Berg, D. J., W. R. Haag, S. I. Guttman, and J. B. Sickel. 1995. Mantle biopsy: a technique for nondestructive tissue-sampling of freshwater mussels. *Journal of the North American Benthological Society* **14**:577-581.
- Bogan, A. E. and K. Roe. 2008. Freshwater bivalve (Unioniformes) diversity, systematics, and evolution: status and future directions. *Journal of the North American Benthological Society* **27**:349-369.
- Bovee, K. D. 1994. Data collection procedures for the Physical Habitat Simulation system. U.S. Geological Survey, Biological Resources Division, Fort Collins, CO.
- Brauman, K. A., G. C. Daily, T. K. Duarte, and H. A. Mooney. 2007. The nature and value of ecosystem services: An overview highlighting hydrologic services. Pages 67-98 *Annual Review of Environment and Resources*.
- Christian, A. D., B. G. Crump, and D. J. Berg. 2008. Nutrient release and ecological stoichiometry of freshwater mussels (Mollusca : Unionidae) in 2 small, regionally distinct streams. *Journal of the North American Benthological Society* **27**:440-450.
- Daily, G. C. and P. A. Matson. 2008. Ecosystem services: From theory to implementation. *Proceedings of the National Academy of Sciences of the United States of America* **105**:9455-9456.
- Durham, B. W. and G. R. Wilde. 2006. Influence of stream discharge on reproductive success of a prairie stream fish assemblage. *Transactions of the American Fisheries Society* **135**:1644-1653.
- Frazer, G. W., C. D. Canham, and K. P. Lertzman. 1999. Gap Light Analyzer (GLA), version 2.0: Imaging software to extract canopy structure and gap light transmission indices from true-colour fisheye photographs. Users Manual and Program Documentation. Simon Fraser University and Institute of Ecosystem Studies, Burnaby, B.C. and Millbrook, NY.
- Galbraith, H. S., D. E. Spooner, and C. C. Vaughn. 2005. *Arkansia wheeleri* monitoring in the Kiamichi River. Final report to Oklahoma Department of Wildlife Conservation.
- Galbraith, H. S., D. E. Spooner, and C. C. Vaughn. 2008. Status of rare and endangered freshwater mussels in southeastern Oklahoma rivers. *Southwestern Naturalist* **53**:45-50.

- Galbraith, H. S., D. E. Spooner, and C. C. Vaughn. 2010. Synergistic effects of regional climate patterns and local water management on freshwater mussel communities. *Biological Conservation* **143**:1175-1183. .
- Galbraith, H. S., C. J. Blakeslee, and W. A. Lellis. 2012. Recent thermal history influences thermal tolerance in freshwater mussel species (Bivalvia: Unionoida). *Freshwater Science* **31**:83-92
- Gore, J. A., J. B. Layzer, and J. Mead. 2001. Macroinvertebrate instream flow studies after 20 years: a role in stream management and restoration. *Regulated Rivers: Research & Management* **17**:527-542.
- Graf, D. L. and K. S. Cummings. 2007. Review of the systematics and global diversity of freshwater mussel species (Bivalvia : Unionoida). *Journal of Molluscan Studies* **73**:291-314.
- Jones, C. and W. L. Fisher. 2005. Final report for project T-8-P. Instream flow modeling for mussels and fishes in southeastern Oklahoma. Oklahoma Department of Wildlife Conservation.
- Julian, J., M. W. Doyle, and E. H. Stanley. 2008a. Empirical modeling of light availability in rivers. *Journal of Geophysical Research*. DOI: 10.1029,2007JG000601. 16 pp.
- Julian, J., E. H. Stanley, and M. W. Doyle. 2008b. Basin-scale consequences of agricultural land use on benthic light availability and primary production along a sixth-order temperate river. *Ecosystems* **11**:1091-1105.
- Kehmeier, J. W., R. A. Valdez, C. N. Medley, and O. B. Myers. 2007. Relationship of fish mesohabitat to flow in a sand-bed southwestern river. *North American Journal of Fisheries Management* **27**:750-764.
- Kreeger, D. and D. Bushek. 2008. From the headwaters to the coast: A watershed-based perspective on bivalve shellfish restoration. *Journal of Shellfish Research* **27**:1022-1022.
- Labbe, T. R. and K. D. Fausch. 2000. Dynamics of intermittent stream habitat regulate persistence of a threatened fish at multiple scales. *Ecological Applications* **10**:1774-1791.
- Layzer, J. B. and L. M. Madison. 1995. Microhabitat use by freshwater mussels and recommendations for determining their instream flow needs. *Regulated Rivers: Research & Management* **10**:329-345.
- Master, L. M., S. R. Flack, and B. A. Stein. 1998. Rivers of life: critical watersheds for protecting freshwater diversity. The Nature Conservancy, Arlington, VA.
- Matthews, W. J., C. C. Vaughn, K. B. Gido, and E. Marsh-Matthews. 2005. Southern plains rivers. In, A. Benke and C. E. Cushing, editors. *Rivers of North America*. Academic Press.
- Naimo, T. J., E. D. Damschen, R. G. Rada, and E. M. Monroe. 1998. Nonlethal evaluation of the physiological health of unionid mussels: methods for biopsy and glycogen analysis. *Journal of the North American Benthological Society* **17**:121-128.
- OWRB (Oklahoma Water Resources Board). 2009. Oklahoma Comprehensive Water Plan 2011 Update: Technical Memorandum, Instream Flows in Oklahoma and the West.
- Pandolfo, T. J., W. G. Cope, C. Arellano, R. B. Bringolf, M. C. Barnhart, and E. Hammer. 2010. Upper thermal tolerances of early life stages of freshwater mussels. *Journal of the North American Benthological Society* **29**:959-969.
- Pandolfo, T. J., T. J. Kwak, and W. G. Cope. 2012. Thermal tolerances of freshwater mussels and their host fish: species interactions in a changing climate. *Walkerana* **15**:69-82.
- Perrings, C., S. Naeem, F. S. Ahrestani, D. E. Bunker, P. Burkill, G. Canziani, T. Elmqvist, J. A. Fuhrman, F. M. Jaksic, Z. Kawabata, A. Kinzig, G. M. Mace, H. Mooney, A. H. Prieur-

- Richard, J. Tschirhart, and W. Weisser. 2011. Ecosystem services, targets, and indicators for the conservation and sustainable use of biodiversity. *Frontiers in Ecology and the Environment* **9**:512-520.
- Poff, N. L., B. D. Richter, A. H. Arthington, S. E. Bunn, R. J. Naiman, E. Kendy, M. Acreman, C. Apse, B. P. Bledsoe, M. C. Freeman, J. Henriksen, R. B. Jacobson, J. G. Kennen, D. M. Merritt, J. H. O'Keeffe, J. D. Olden, K. Rogers, R. E. Tharme, and A. Warner. 2010. The ecological limits of hydrologic alteration (ELOHA): a new framework for developing regional environmental flow standards. *Freshwater Biology* **55**:147-170.
- Richter, B. D. 2010. Re-thinking environmental flows: from allocations and reserves to sustainability boundaries. *River Research and Applications* **26**:1052-1063.
- Spooner, D. E. and C. C. Vaughn. 2008. A trait-based approach to species' roles in stream ecosystems: climate change, community structure, and material cycling. *Oecologia* **158**:307-317.
- Stanford, J. A., J. V. Ward, W. J. Liss, C. A. Frissell, R. N. Williams, J. A. Lichatowich, and C. C. Coutant. 1996. A general protocol for restoration of regulated rivers. *Regulated Rivers-Research & Management* **12**:391-413.
- Strayer, D. L., J. A. Downing, W. R. Haag, T. L. King, J. B. Layzer, T. J. Newton, and S. Nichols. 2004. Changing perspectives on pearly mussels, North America's most imperiled animals. *BioScience* **54**:429-439.
- Turton, D., W. L. Fisher, T. Seilheimer, and R. Esralew. 2009. An assessment of environmental flows for Oklahoma. Oklahoma Water Resources Board.
- United States Supreme Court. 2013.
<http://www.supremecourt.gov/Search.aspx?FileName=/docketfiles/11-889.htm>
- Vaughn, C. C. 2000. Changes in the mussel fauna of the Red River drainage: 1910 - present. Pages 225-232 in R. A. Tankersley, D. I. Warmolts, G. T. Watters, B. J. Armitage, P. D. Johnson, and R. S. Butler, editors. *Proceedings of the First Freshwater Mussel Symposium*. Ohio Biological Survey, Columbus, Ohio.
- Vaughn, C. C. 2010. Biodiversity losses and ecosystem function in freshwaters: emerging conclusions and research directions. *BioScience* **60**:25-35.
- Vaughn, C. C. 2012. Life history traits and abundance can predict local colonisation and extinction rates of freshwater mussels. *Freshwater Biology* **57**:982-992.
- Vaughn, C. C., C. M. Mather, M. Pyron, P. Mehlhop, and E. K. Miller. 1996. The current and historical mussel fauna of the Kiamichi River, Oklahoma. *Southwestern Naturalist* **41**:325-328.
- Vaughn, C. C., C. M. Taylor, and K. J. Eberhard. 1997. A comparison of the effectiveness of timed searches vs. quadrat sampling in mussel surveys. Pages 157-162 in K. S. Cummings, A. C. Buchanan, and L. M. Koch, editors. *Conservation and Management of Freshwater Mussels II: Initiatives for the Future*.
- Vaughn, C. C. and C. C. Hakenkamp. 2001. The functional role of burrowing bivalves in freshwater ecosystems. *Freshwater Biology* **46**:1431-1446.
- Vaughn, C. C. and M. Pyron. 1995. Population ecology of the endangered Ouachita Rock Pocketbook mussel, *Arkansia wheeleri* (Bivalvia: Unionidae), in the Kiamichi River, Oklahoma. *American Malacological Bulletin* **11**:145-151.
- Vaughn, C. C. and D. E. Spooner. 2006. Unionid mussels influence macroinvertebrate assemblage structure in streams. *Journal of the North American Benthological Society* **25**:691-700.

- Vaughn, C. C. and C. M. Taylor. 1999. Impoundments and the decline of freshwater mussels: a case study of an extinction gradient. *Conservation Biology* **13**:912-920.
- Vaughn, C. C., K. B. Gido, and D. E. Spooner. 2004. Ecosystem processes performed by unionid mussels in stream mesocosms: species roles and effects of abundance. *Hydrobiologia* **527**:35-47.
- Vaughn, C. C., S. J. Nichols, and D. E. Spooner. 2008. Community and foodweb ecology of freshwater mussels. *Journal of the North American Benthological Society* **27**:41-55.
- Wainger, L. and M. Mazzotta. 2011. Realizing the Potential of Ecosystem Services: A Framework for Relating Ecological Changes to Economic Benefits. *Environmental Management* **48**:710-733.
- Wetzel, R. G. 2001. *Limnology: Lake and River Ecosystems*. Academic Press.

Table 1. Locations of HOBO data loggers that measure water depth and water temperature. Period of data collection may not be continuous due to logger displacements (flood or anthropogenic) and to days with no flow.

ID	Description	Location (WGS 84)	Elevation (m)	Period of Data (MM/DD/YYYY)
K1	Atmosphere, Upper watershed	N34 38.359 W94 36.733	280	06/08/2011 – 09/30/2012
K2	Kiamichi River @ Big Cedar	N34 38.351 W94 36.724	279	06/08/2011 – 09/30/2012
K3	Buffalo Creek	N34 43.711 W95 14.141	203	06/08/2011 – 09/30/2012
K4	Jackfork Creek above Sardis Reservoir	N34 36.063 W95 33.956	193	06/08/2011 – 07/19/2011
K5	Atmosphere, Middle watershed	N34 34.428 W95 21.435	164	06/08/2011 – 09/30/2012
K6	Kiamichi River @ Tuskahoma	N34 36.715 W95 16.640	155	06/08/2011 – 09/30/2012
K7	Jackfork Creek below Sardis Dam	N34 36.377 W95 20.091	160	06/08/2011 – 09/30/2012
K8	Kiamichi River @ Clayton	N34 34.531 W95 20.406	154	06/08/2011 – 09/30/2012
K9	Kiamichi River @ Antlers	N34 14.933 W95 36.317	126	06/08/2011 – 09/30/2012
K10	Atmosphere, Lower watershed	N34 14.846 W95 36.451	141	06/08/2011 – 09/30/2012
K11	Kiamichi River @ Paine's	N34.42720 W95.58134	139	8/01/2011 – 09/24/2011

Table 2. Water discharge gages in the watershed. The Sardis Lake gage is maintained by USACE (USACE station ID: CYD02).

ID	Name	Location (NAD27)	Elevation (m)	Watershed area (km²)	Period of Data (MM/YYYY)
USGS 07335700	Kiamichi River near Big Cedar, OK	N34 38.300 W94 36.750	270	102.6	10/1965 – current ¹
USGS 07335790	Kiamichi River near Clayton, OK	N34 34.483 W95 20.433	158	1810	11/1980 – current
USGS 07336200	Kiamichi River near Antlers, OK	N34 14.917 W95 36.300	128	2924	10/1972 – current
USGS 07335775	Sardis Lake near Clayton, OK	N34 37.750 W95 21.050	161	712	11/1994 – current

¹USGS began recording water temperature at this site 2/2012.

Table 3. Oklahoma mesonet stations in the watershed used to characterize and verify air temperature and precipitation.

ID (number)	Name	Location (NAD27)	Elevation (m)	Period of Data (MM/YYYY)
TALI (93)	Talihina	N34.71070 W95.01152	204	03/1997 – present
CLAY (29)	Clayton	N34.65657 W95.32596	186	03/1997 – present
ANTL (4)	Antlers	N34.22438 W95.70059	179	03/1997 – present

Table 4. No flow days at each of the four discharge monitoring stations for Summer 2011 (June 8 – September 30) and Summer 2012 (June 1 – September 30). Except during large floods, discharge on Jackfork Creek below Sardis Dam is set by controlled releases from the dam.

ID	Name	Watershed area (km²)	No Flow Days	
			Summer 2011	Summer 2012
USGS 07335700	Kiamichi River near Big Cedar, OK	102.6	95	112
USGS 07335790	Kiamichi River near Clayton, OK	1810	13	32
USGS 07336200	Kiamichi River near Antlers, OK	2924	52	31
USGS 07335775	Jackfork Creek below Sardis Dam	712	55	67

Table 5. Locations and data from canopy photographs that measure stream shading.

ID	Date (MM/DD/YYYY)	Location (WGS 84)	Elevation (m)	Width (m)	Canopy shading (%)	Stream surface solar radiation (%)
CP1	06/7/2011	N34 38.244 W94 39.153	264	8.8	64.0	54.4
CP2	06/7/2011	N34 38.396 W94 36.669	267	14.6	59.2	60.1
CP3	06/7/2011	N34 38.411 W94 36.620	280	4.5	88.4	18.2
CP4	06/7/2011	N34 38.448 W94 37.304	285	5.9	86.5	26.9
CP5	06/7/2011	N34 40.942 W94 53.174	210	30.1	51.2	72.0
CP6	06/7/2011	N34 39.463 W95 02.522	187	30	46.4	84.5
CP7	06/7/2011	N34 43.717 W95 14.151	201	14	68.8	66.6
CP8	06/7/2011	N34 36.068 W95 33.953	197	15	65.0	63.2
CP9	06/8/2011	N34 36.715 W95 16.640	155	36	45.8	86.8
CP10	06/8/2011	N34 36.850 W95 17.969	154	14.7	47.5	82.9
CP11	06/8/2011	N34 36.826 W95 17.850	171	10	84.8	28.3
CP12	06/8/2011	N34 36.375 W95 20.096	171	11.3	66.9	55.9
CP13	07/14/2011	N34 40.863 W94 55.682	183	25	61.6	65.7
CP14	07/14/2011	N34 40.790 W94 56.538	192	28	49.0	64.3
CP15	07/14/2011	N34 40.812 W94 56.543	188	37.5	40.9	89.0
CP16	07/14/2011	N34 40.375 W94 56.275	198	4.5	86.7	21.6
CP17	07/14/2011	N34 40.385 W94 56.285	200	3.9	82.6	26.1
CP18	07/14/2011	N34 40.361 W94 56.269	198	4.9	79.8	33.7
CP19	07/14/2011	N34 40.018 W94 57.585	200	10	80.5	38.4
CP20	07/14/2011	N34 34.500 W95 21.263	182	40	44.4	87.2
CP21	07/14/2011	N34 34.389 W95 21.425	157	37.5	46.8	84.3
CP22	07/14/2011	N34 14.953 W95 36.428	130	42	41.1	89.7

Table 6. Required discharge (in mean daily cubic meters per second) for Kiamichi River near Clayton (USGS 07335790) to prevent maximum water temperatures from exceeding 35°C, and thus preventing mussel mortality. Releases from Sardis Dam can be used to supplement discharge at the Clayton gage.

Mean daily air temperature (C)	Required discharge at Clayton gage (cms)
36	0.1
37	0.2
38	0.2
39	0.3
40	1.8
41	4.4
42	8.3
43	13.4
44	19.7
45	27.2
46	35.9
47	45.8

Figure 1. Google image of Paine's site showing the areas sampled for mussels (pool, riffle and dry lower riffle).



Figure 2. Study area and environmental variables monitoring network.

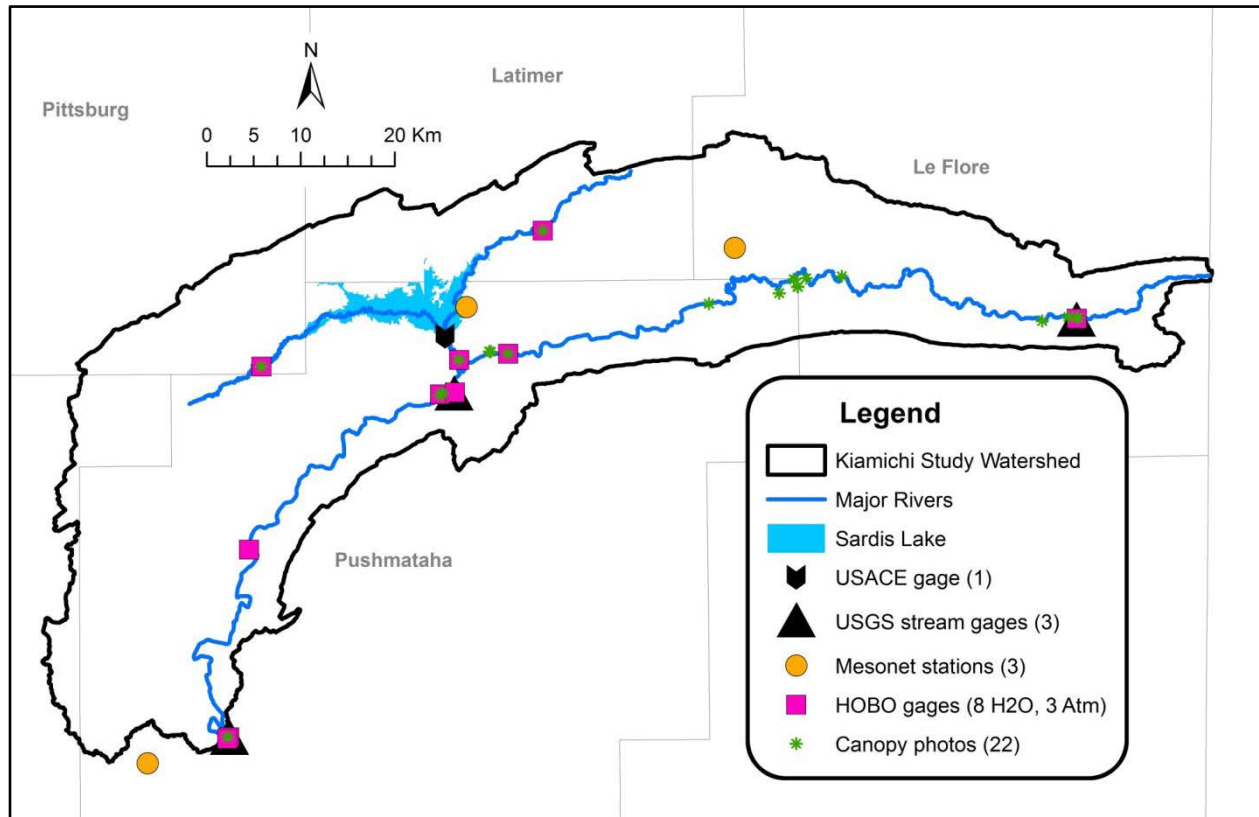


Figure 3. Mussel respiration rates.

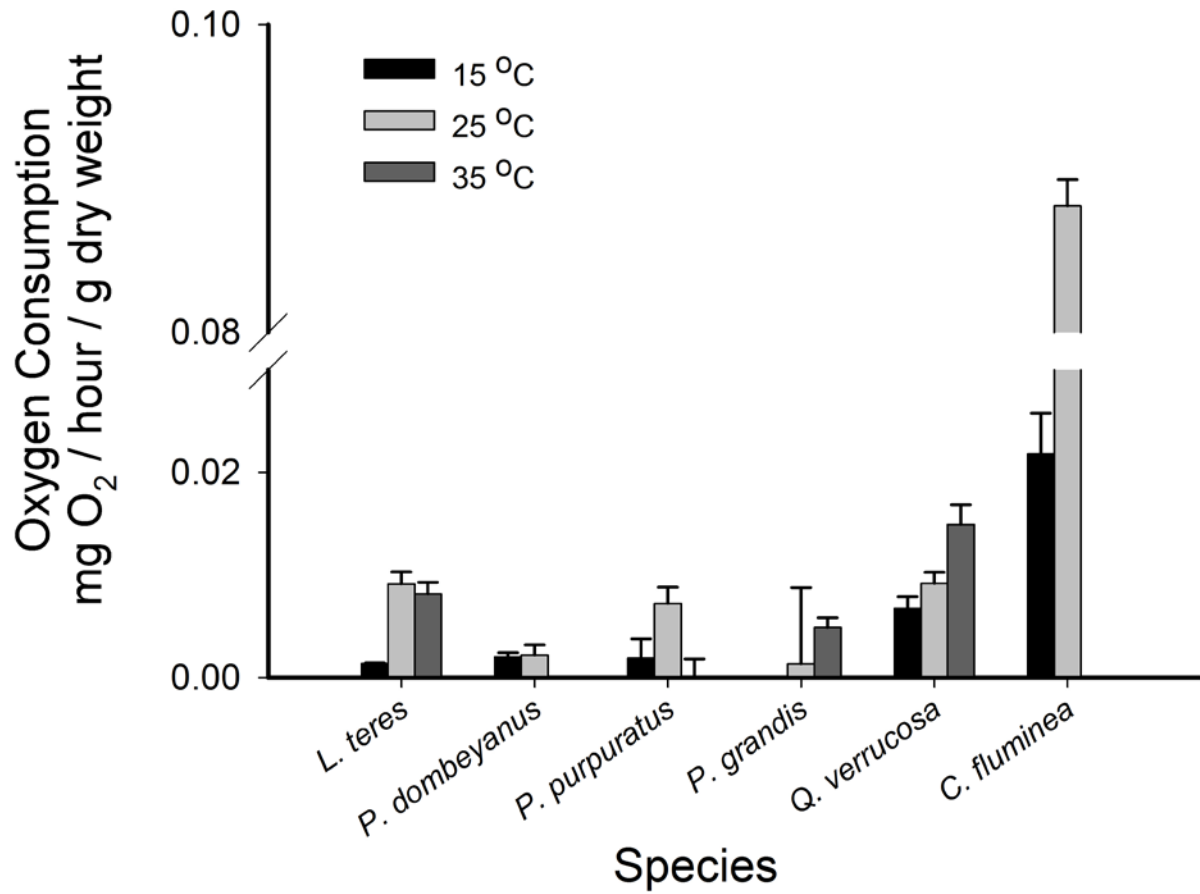


Figure 4. Mussel nitrogen excretion rates.

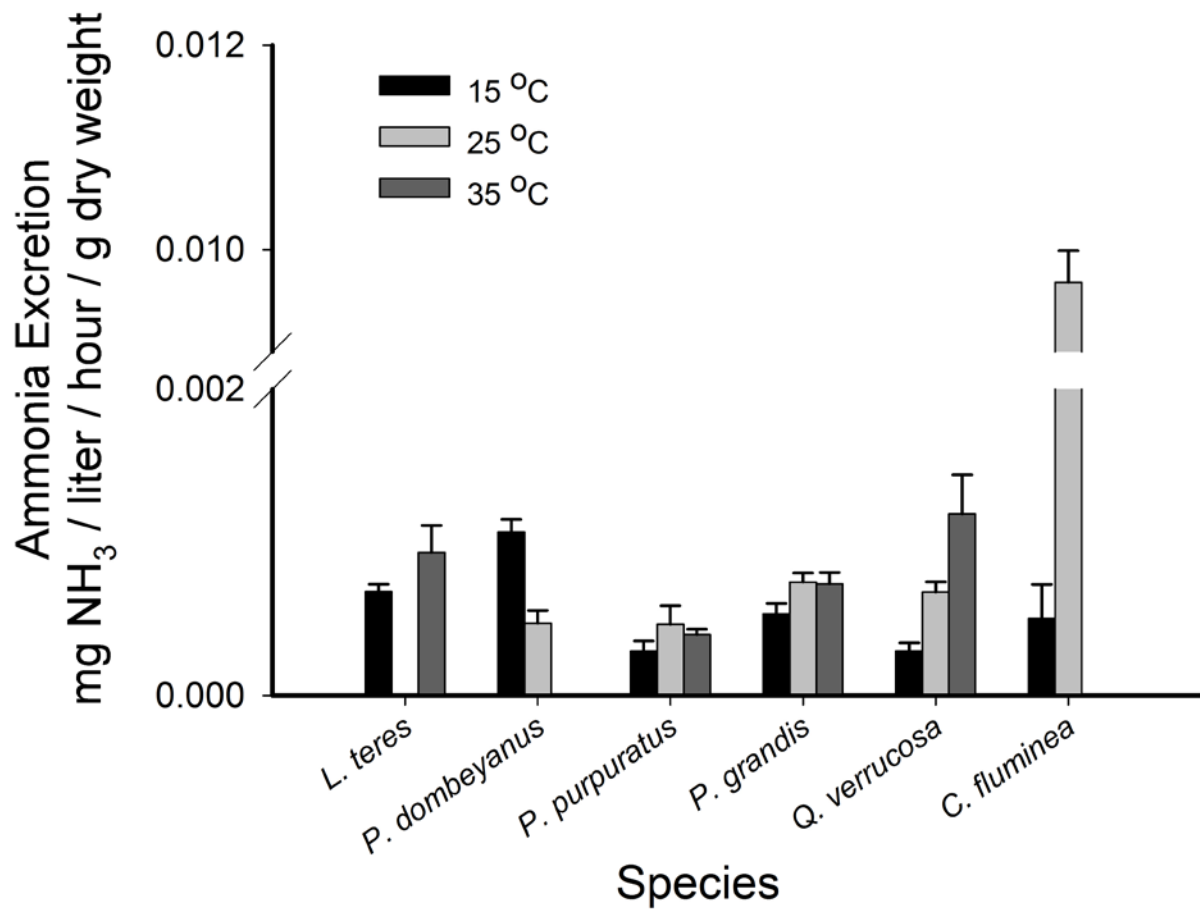


Figure 5. Mussel phosphorus excretion rates.

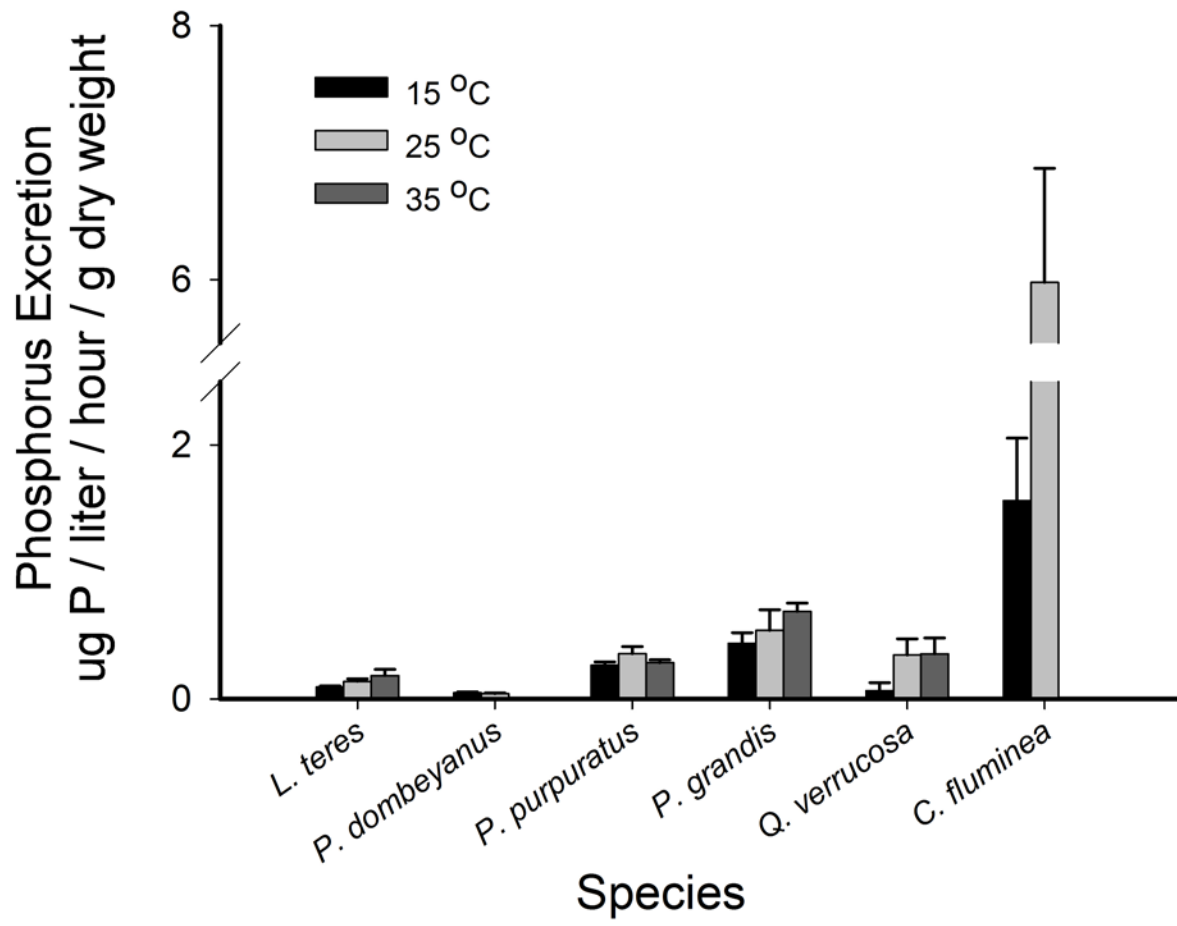


Figure 6. Mussel filtration rates.

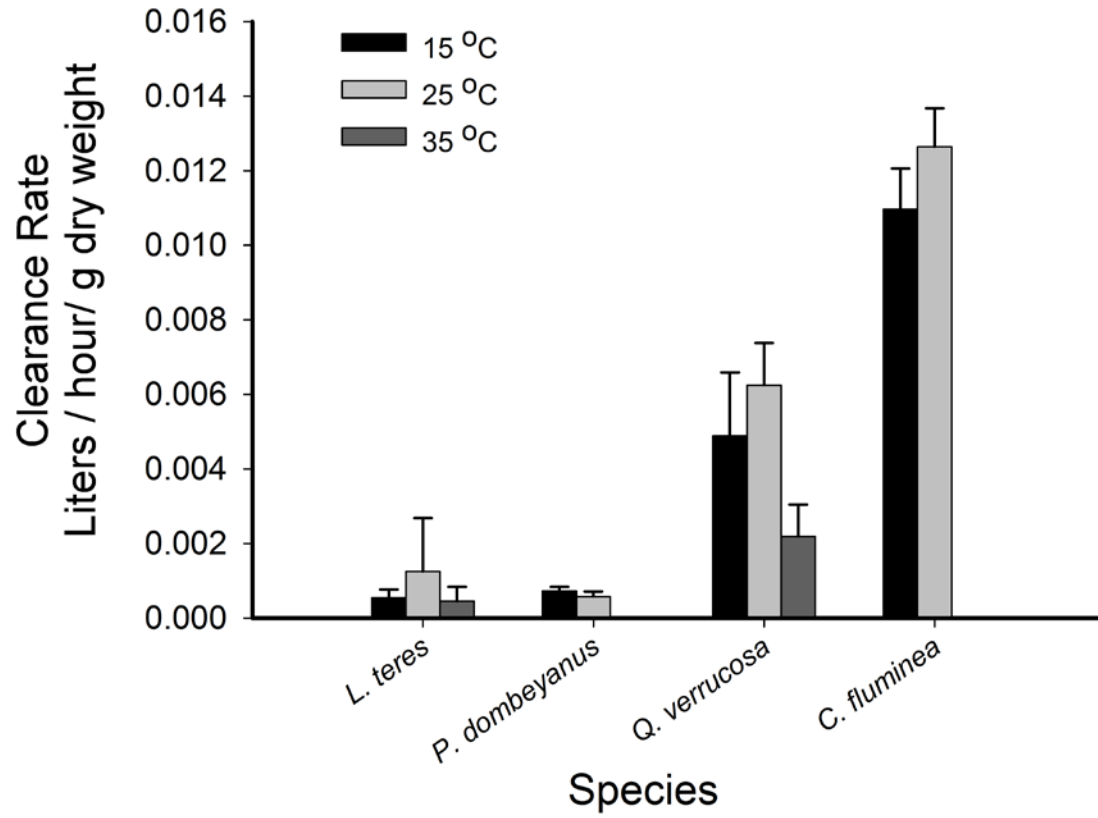


Figure 7. Mussel densities (± 1 S.E.) at Paine's site (Vaughn site 7 from Vaughn and Pyron (1995). A: Comparison of pool and riffle densities. B: Comparison of live and dead mussels in the riffle.

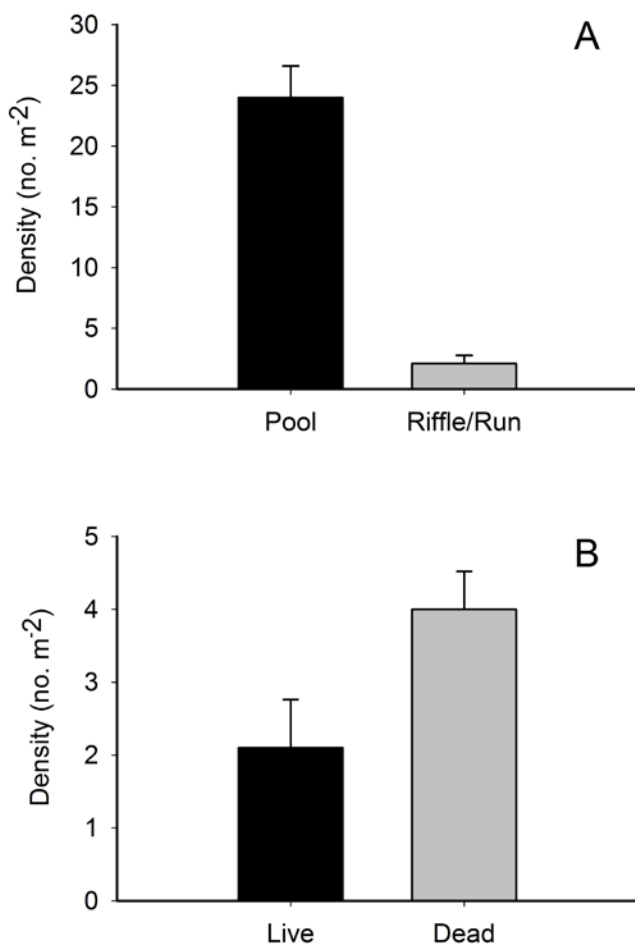


Figure 8. Mussel nitrogen and phosphorus recycling at Paine's site.

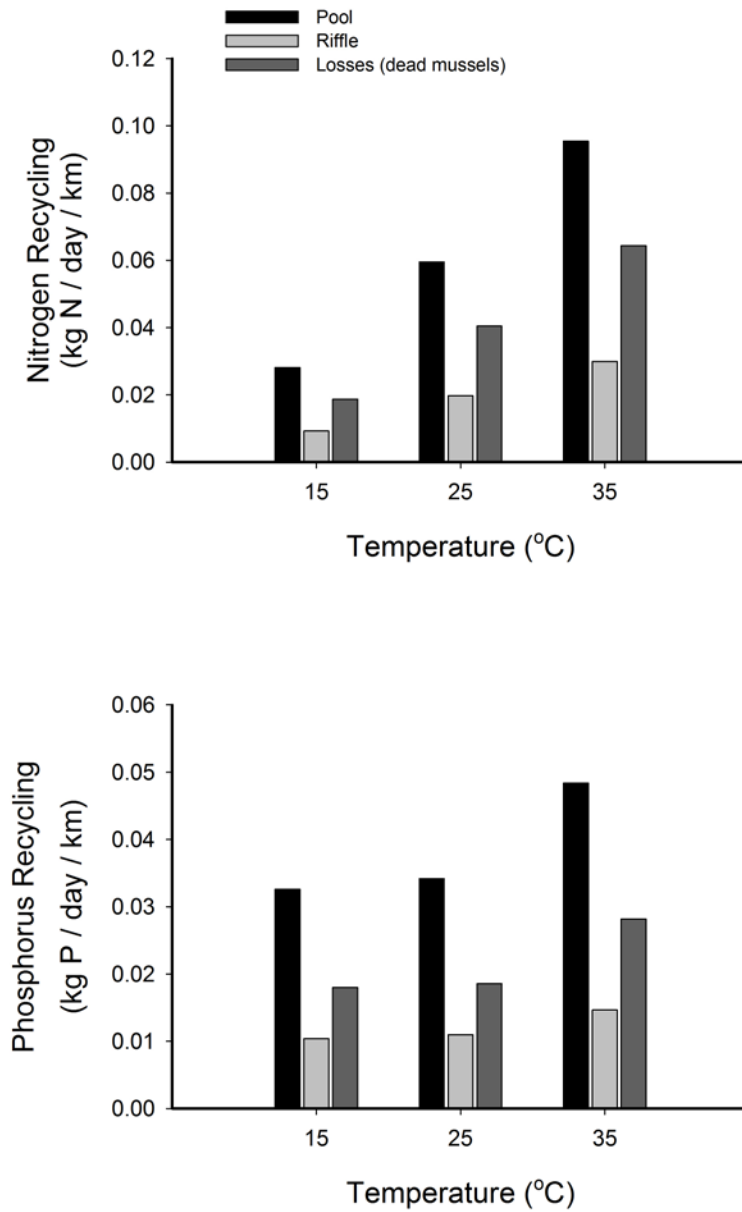


Figure 9. Mussel biofiltration at Paine's site.

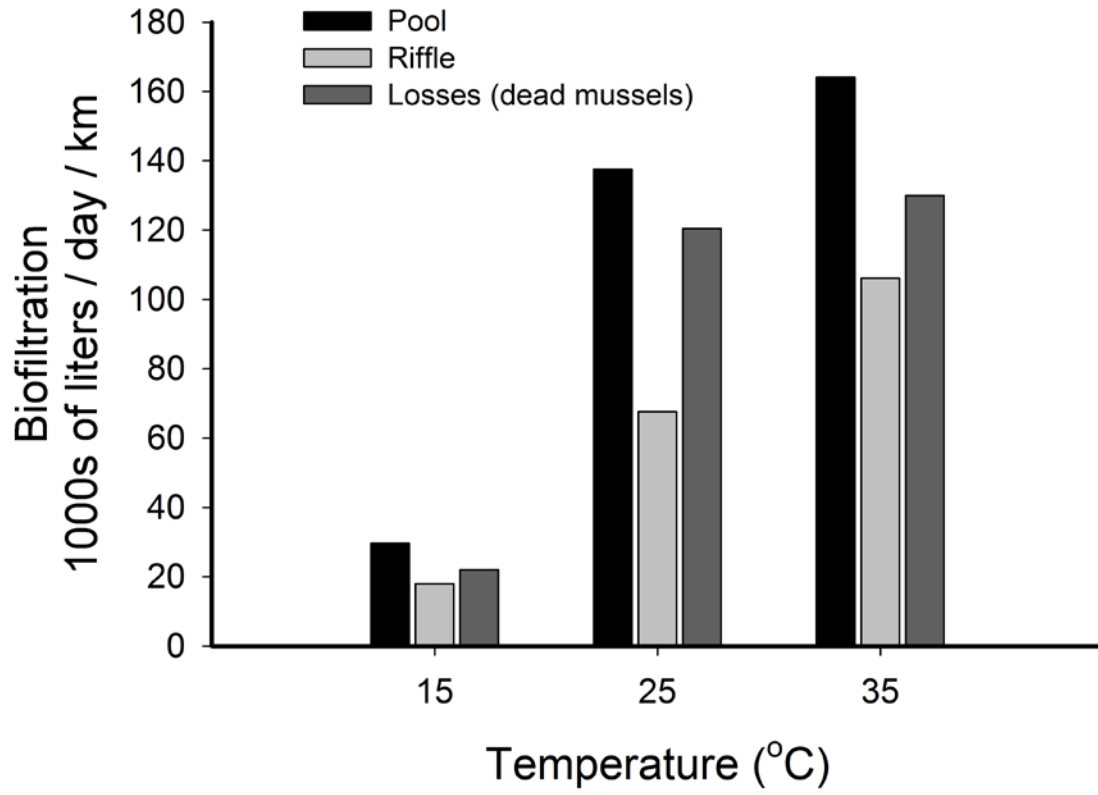


Figure 10. Mussel nutrient storage at Paine's site.

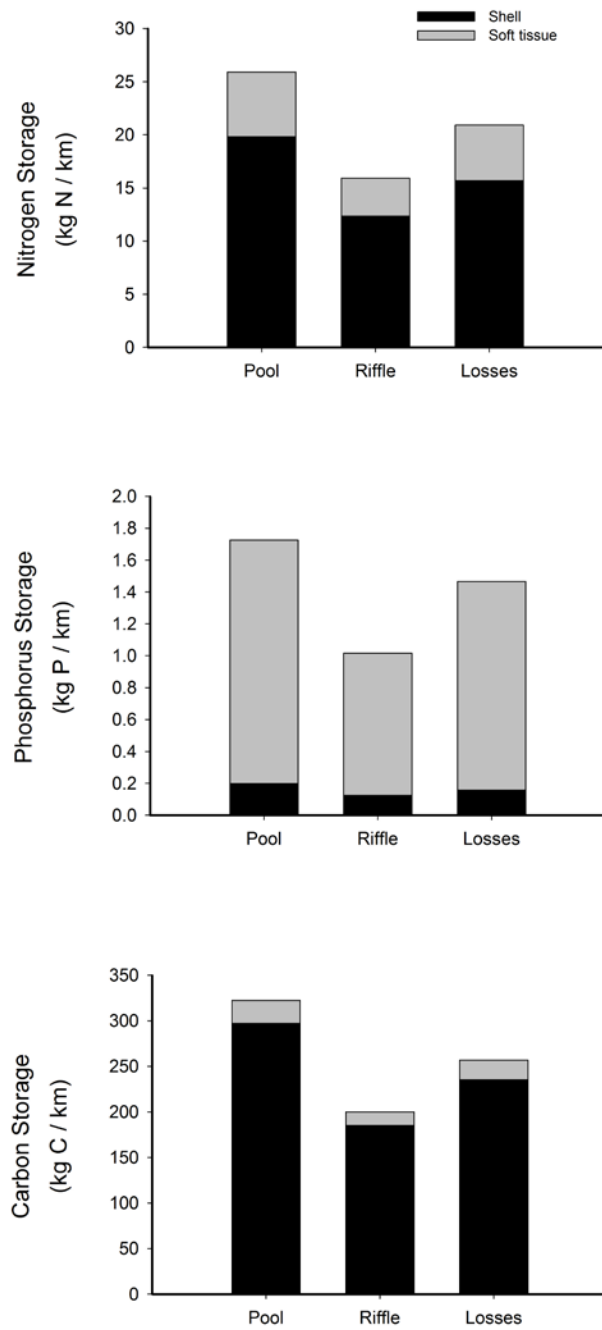


Figure 11. Severe hydrologic drought frequency for Kiamichi River at Big Cedar (upper watershed) and at Antlers (downstream extent of study area). Discharge data were obtained from the USGS gages listed in Table 2. The Kiamichi River at Antlers should be less susceptible to drought given it has a much larger watershed, which the displayed trends show from 1973 to 2004. Beginning in 2005, the two locations along the river exhibit the same drought behavior, which we attribute to the lack of releases from Sardis Dam (which captures approximately 25% of the total watershed's runoff). That is, the lack of releases from Sardis Dam during drought periods increases the magnitude and frequency of hydrologic drought in downstream reaches.

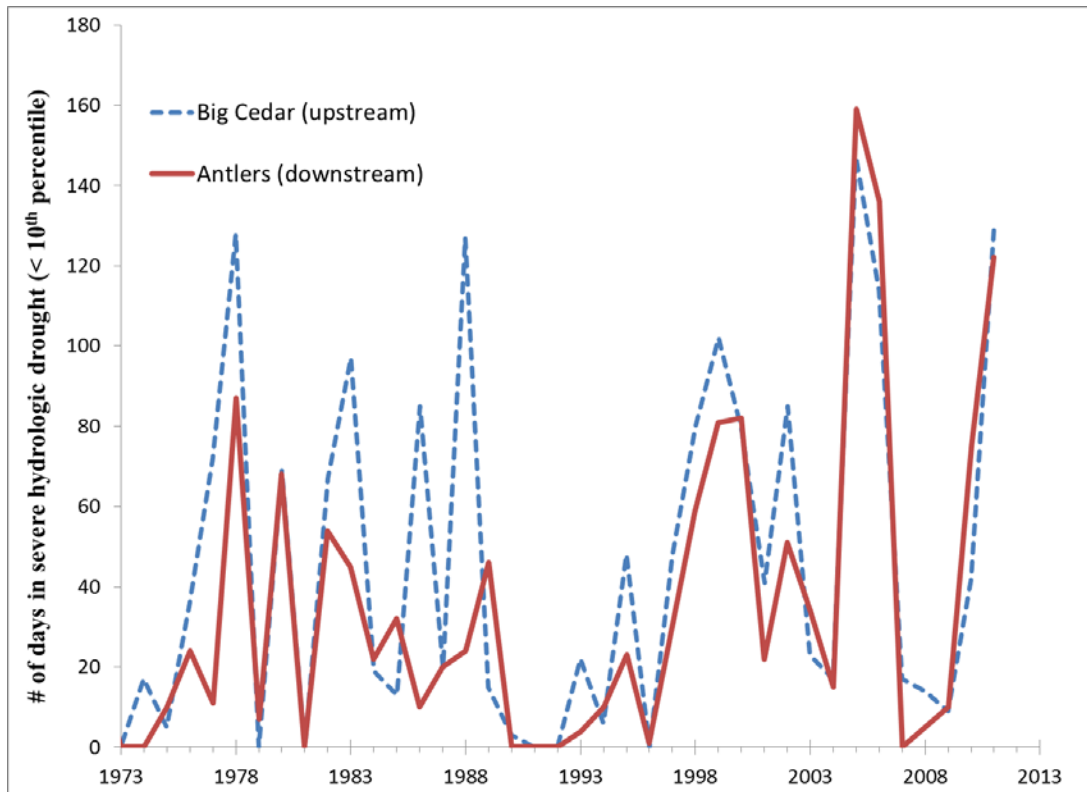


Figure 12. Map of canopy shading across the Kiamichi River watershed, derived using canopy photograph analyses in combination with subpixel mapping of Landsat imagery.

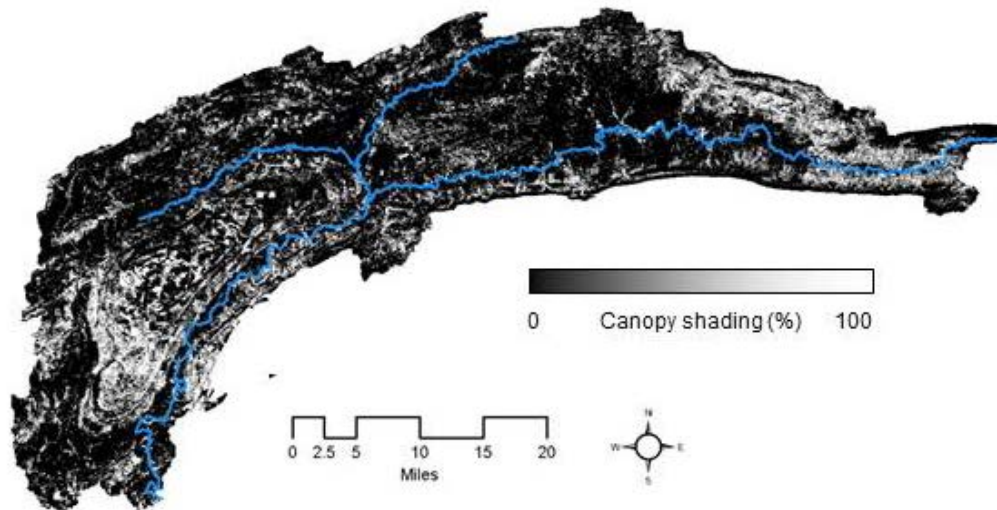


Figure 13. Relationship between mean daily water temperature of Kiamichi River @ Clayton and total daily solar radiation reaching watershed stream surface for the summer of 2011 (6/8/2011 – 9/30/2011). There was not a strong relationship between these two variables ($r^2 = 0.23$), and thus the GIS model based on solar radiation budgets was not pursued. Note that prior to Sardis Dam releases on August 2, 2011, water temperature remained above 29 C.

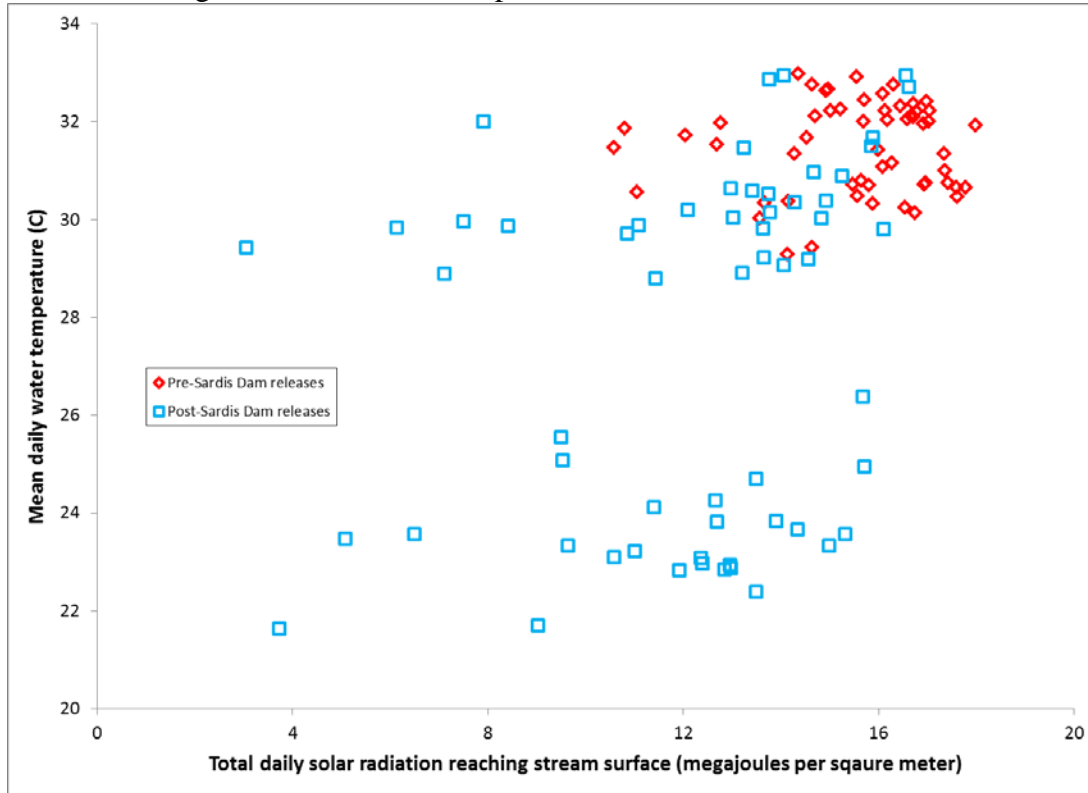


Figure 14. The effect of different water releases from Sardis Dam on downstream water temperatures in the Kiamichi River, at Clayton in this case during Summer 2011. Water temperatures were calculated using actual air temperatures with modeled water depths (Appendix 5E). Refer to Appendix 3F for the multivariate regression model used.

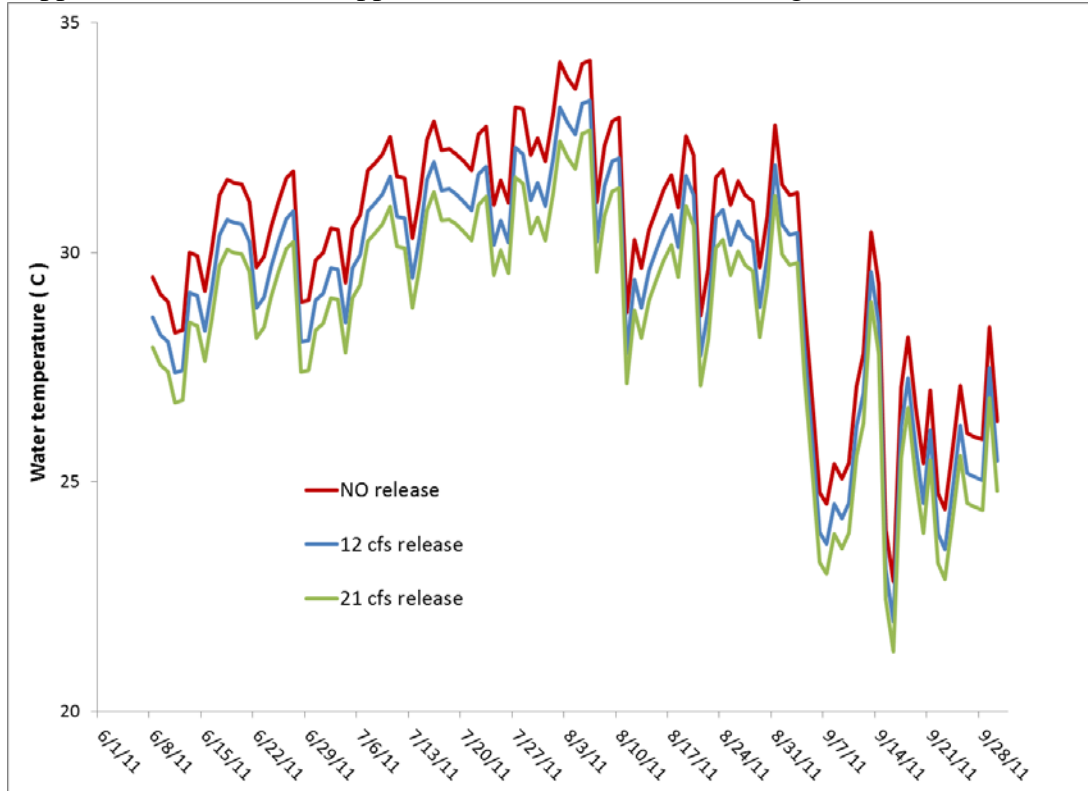


Figure 15. Discharges required for Kiamichi River near Clayton (USGS 07335790) to reduce maximum water temperature below target water temperatures assessed in Objective 1. Empirical rating curves were developed using Appendix 4F in combination with Appendix 5C.

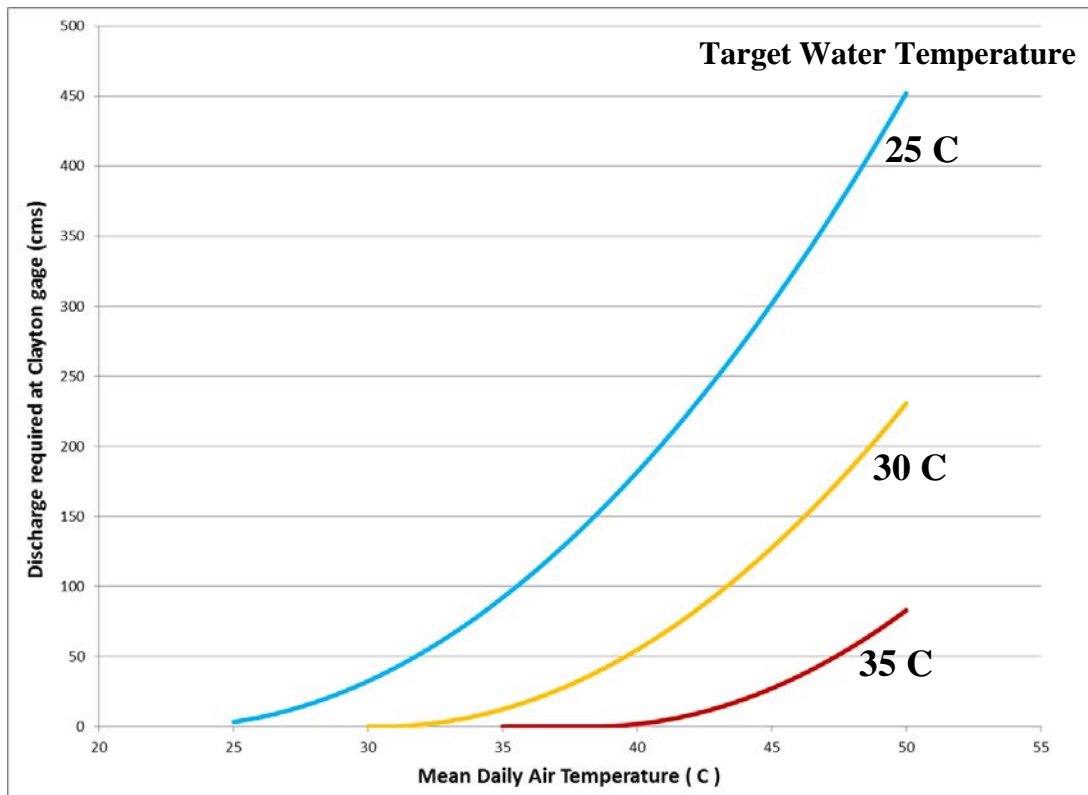


Figure 16. Discharges (under 100 cms) required for Kiamichi River near Clayton (USGS 07335790) to reduce maximum water temperature below target water temperatures assessed in Objective 1. Empirical rating curves were developed using Appendix 4F in combination with Appendix 5C. This is the same figure as Figure 15, just with shorter ranges for visual simplicity.

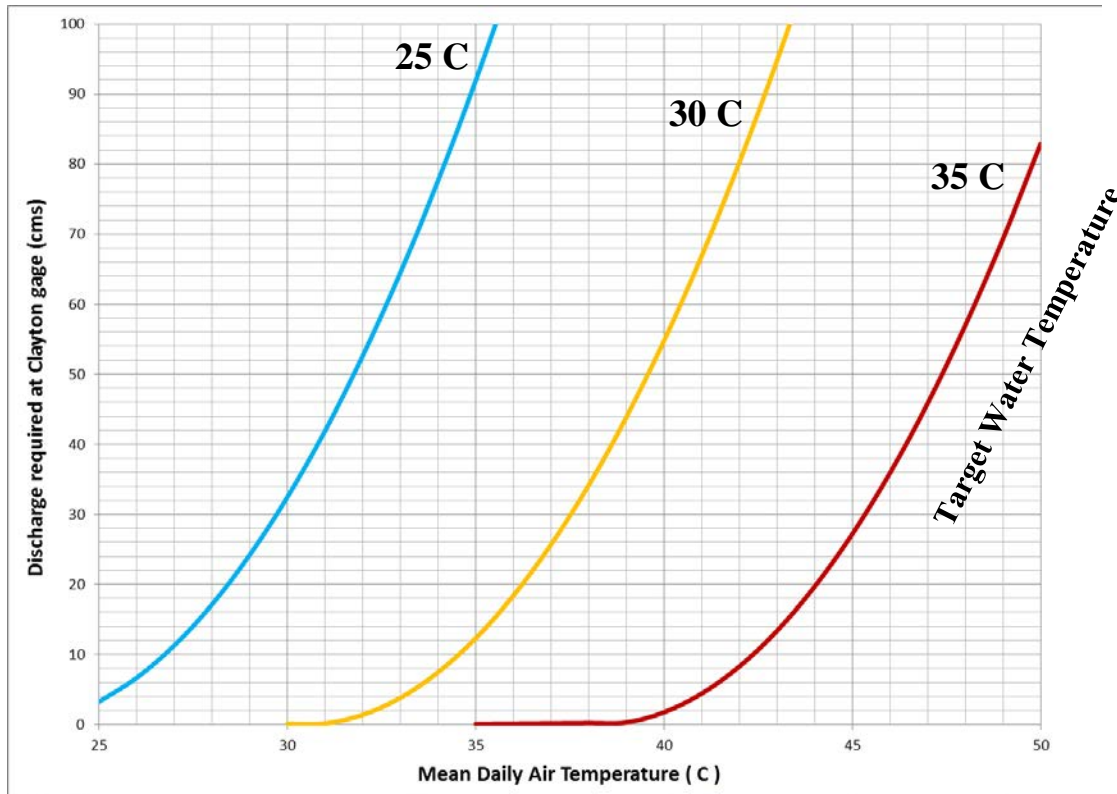
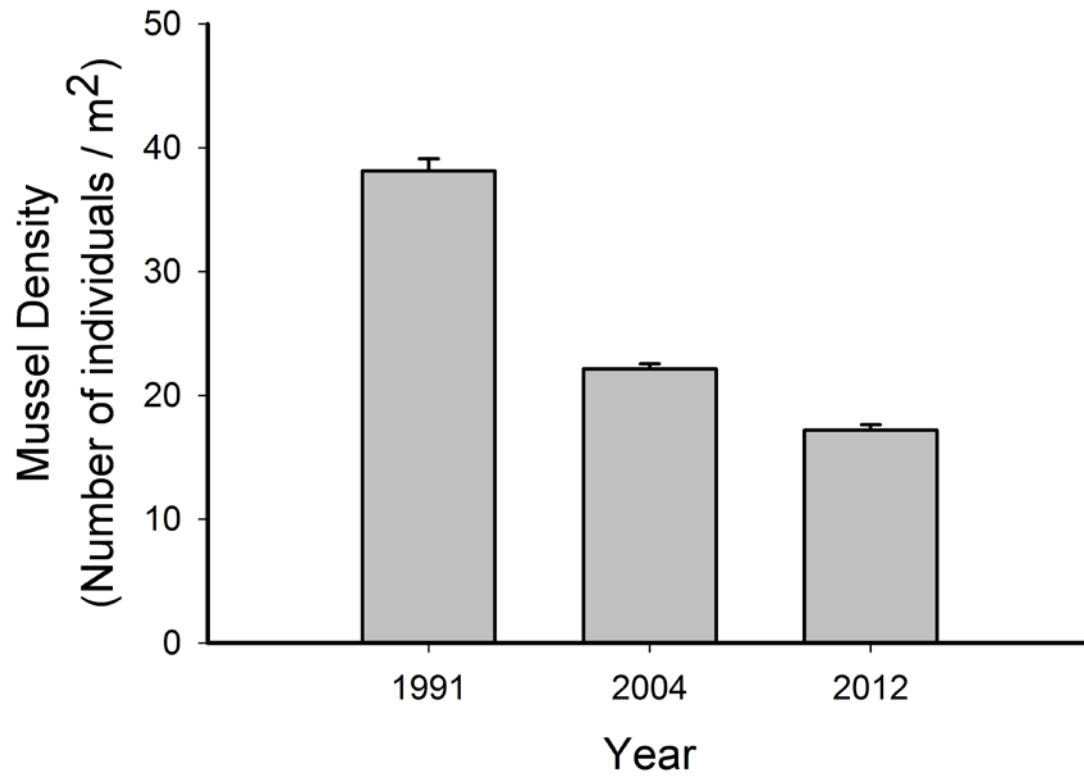
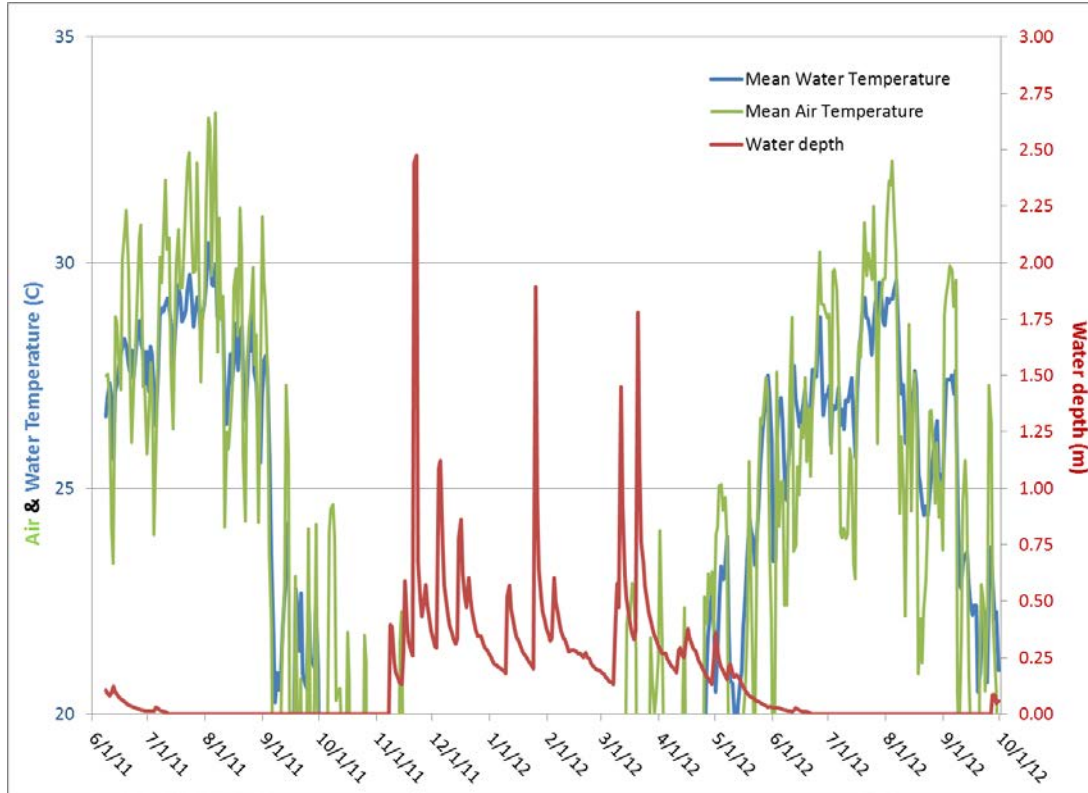


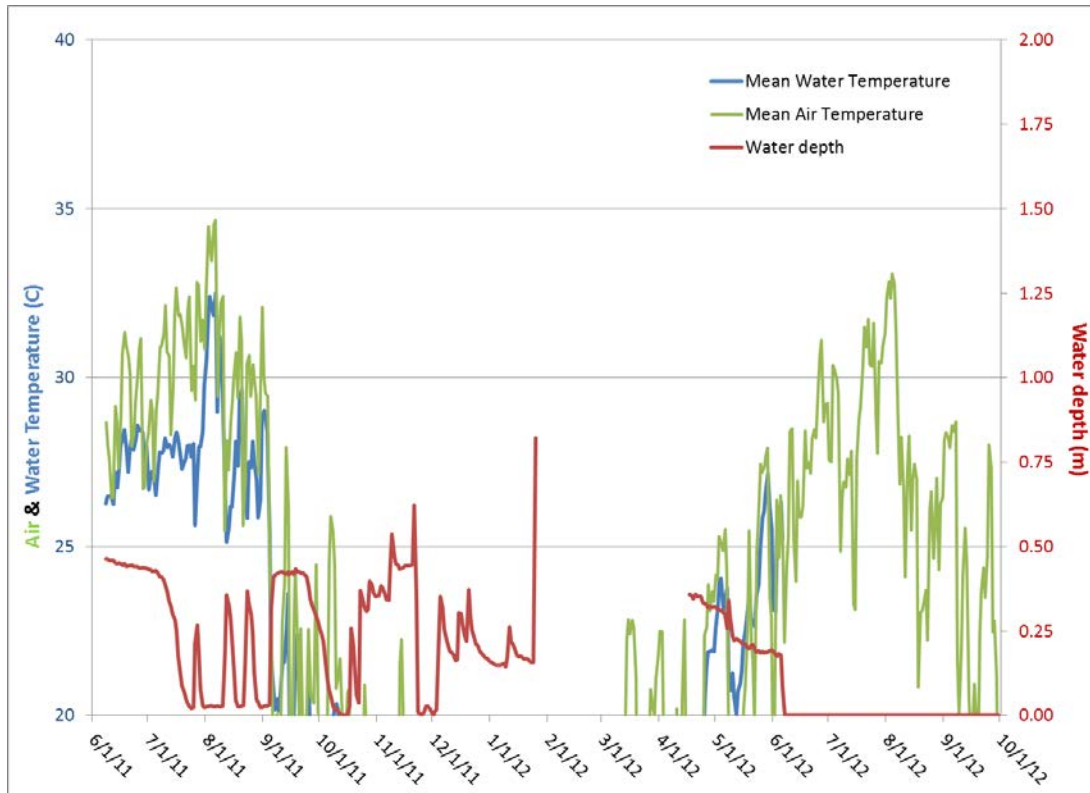
Figure 17. Average mussel densities at Paine's site (Vaughn site 7, Hobo logger site K11 across three decades – 1991, 2004 and 2012. From Vaughn and Pyron (1995), Galbraith et al. (2010) and Vaughn unpublished.



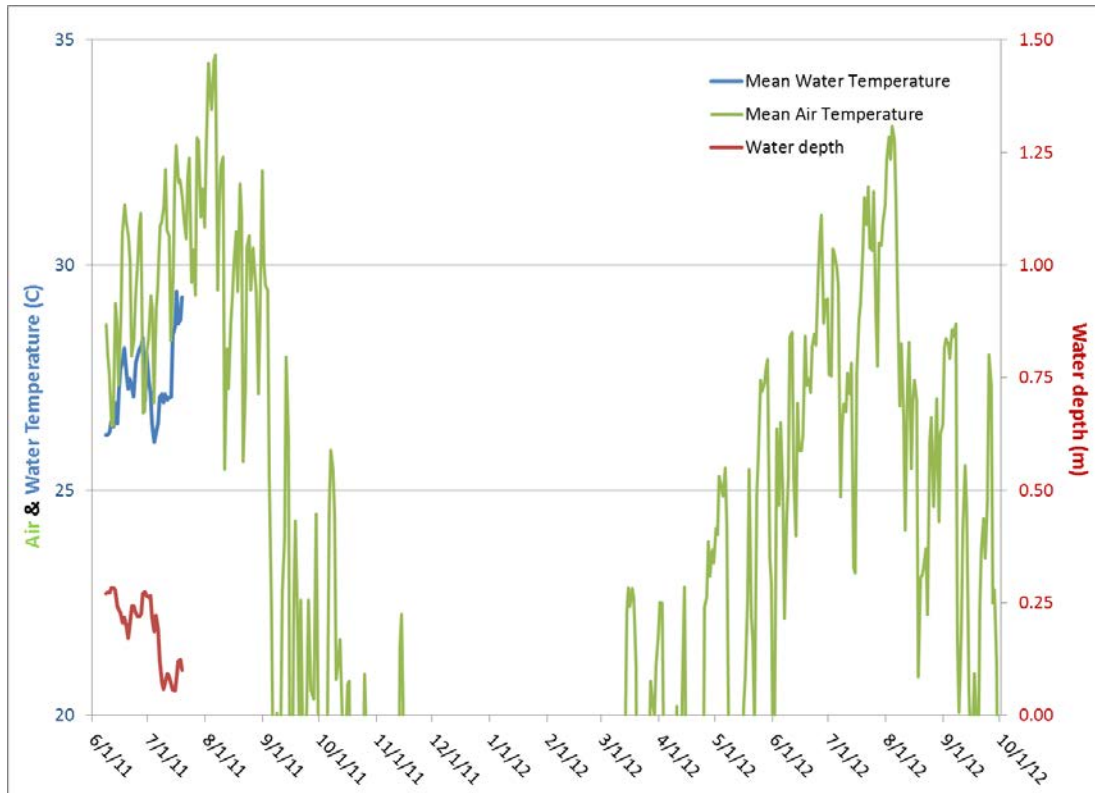
Appendix 1 – Mean water temperature time-series



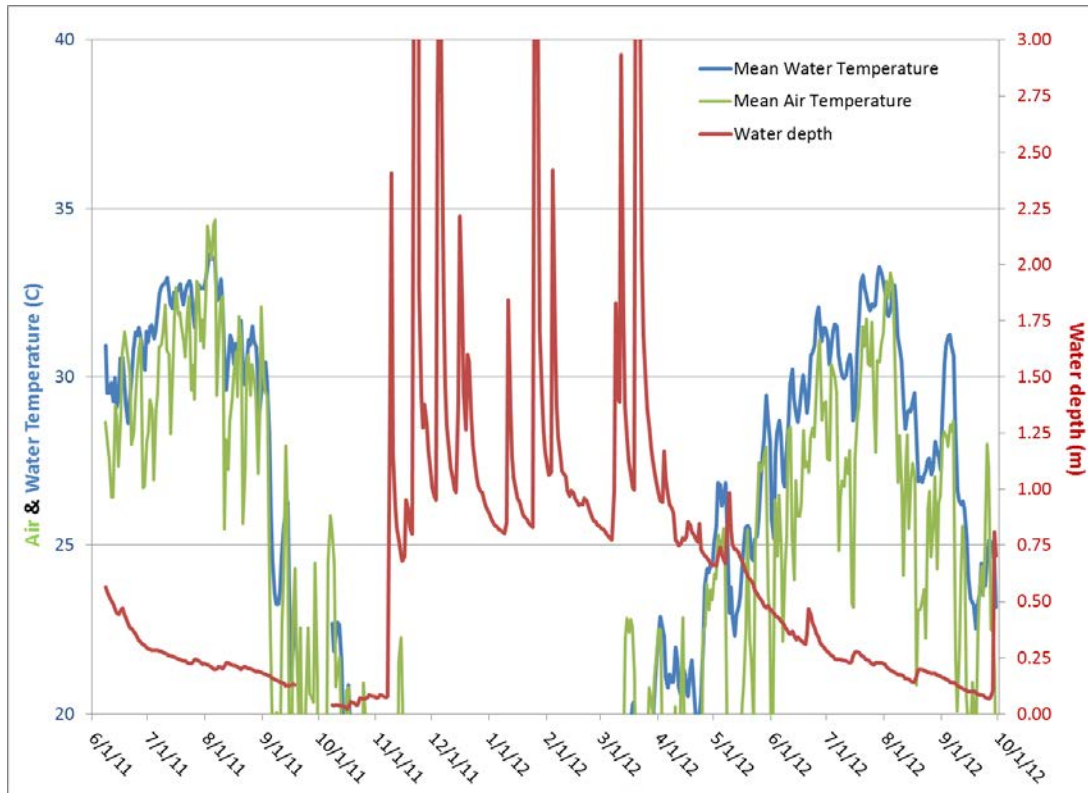
Appendix 1A. Water depth and mean daily air & water temperature for Kiamichi River station at Big Cedar (K2), the most upstream station of the study area. Because our HOBO gage was displaced on several occasions, water depth was obtained from the USGS gage at the same site. Water temperature for 2012 was also obtained from the USGS gage due to our HOBO gage being out of water during most of this period.



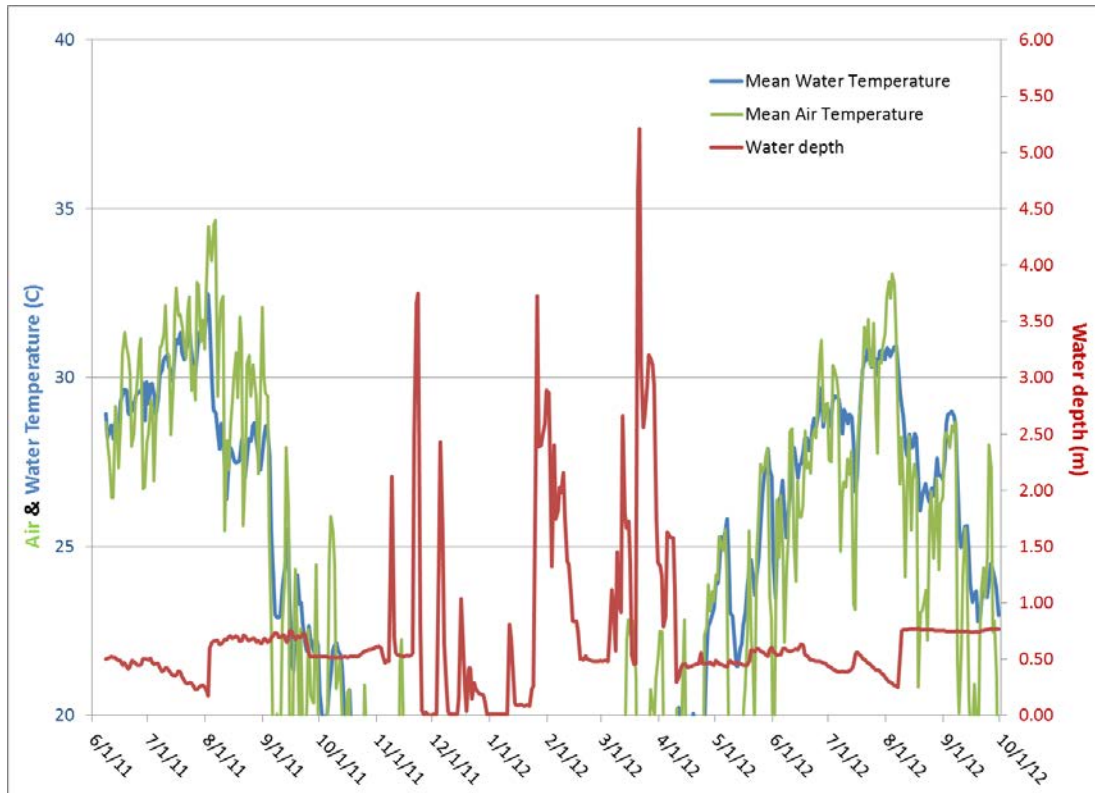
Appendix 1B. Water depth and mean daily air & water temperature for Buffalo Creek station (K3), one of the two main inputs to Sardis Lake. The HOBO gage was displaced by a flood on January 25, 2012 and was not replaced until April 17, 2012. The creek was dry from June 7 to September 30, 2012 and thus no water temperature data for this period.



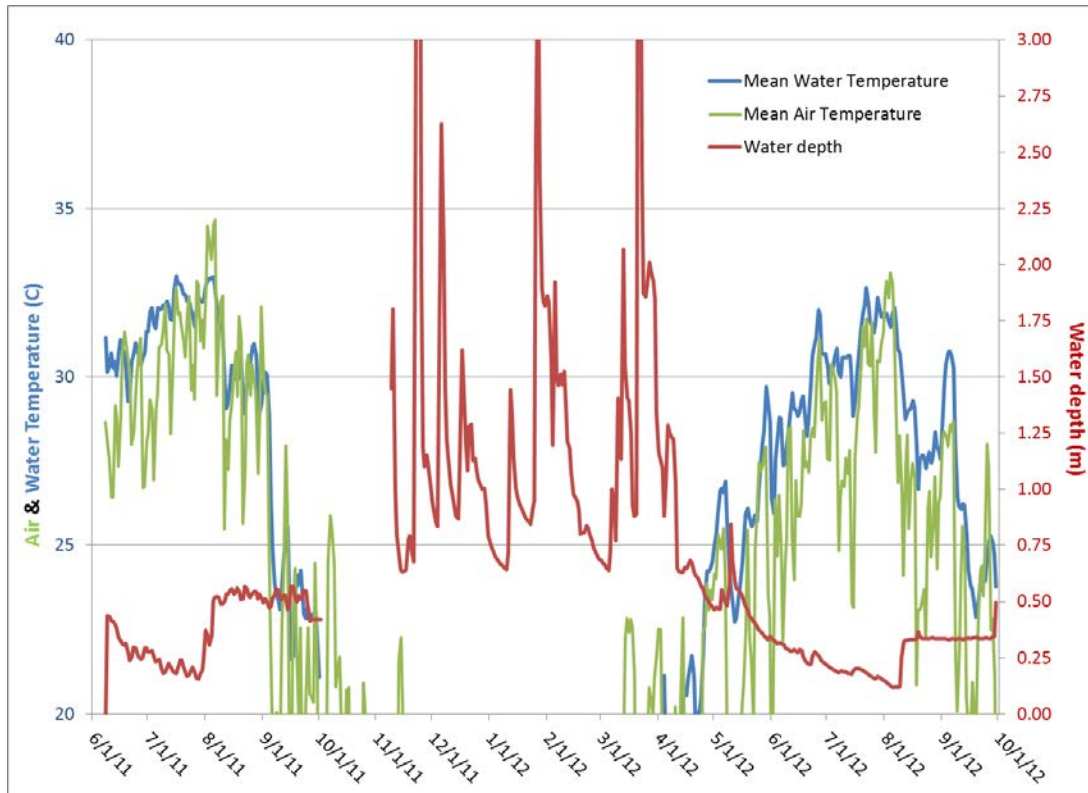
Appendix 1C. Water depth and mean daily air & water temperature for Jackfork Creek station above Sardis Reservoir (K4), one of the two main inputs to Sardis Lake. The logger malfunctioned on July 19, 2011, with no usable data after this date.



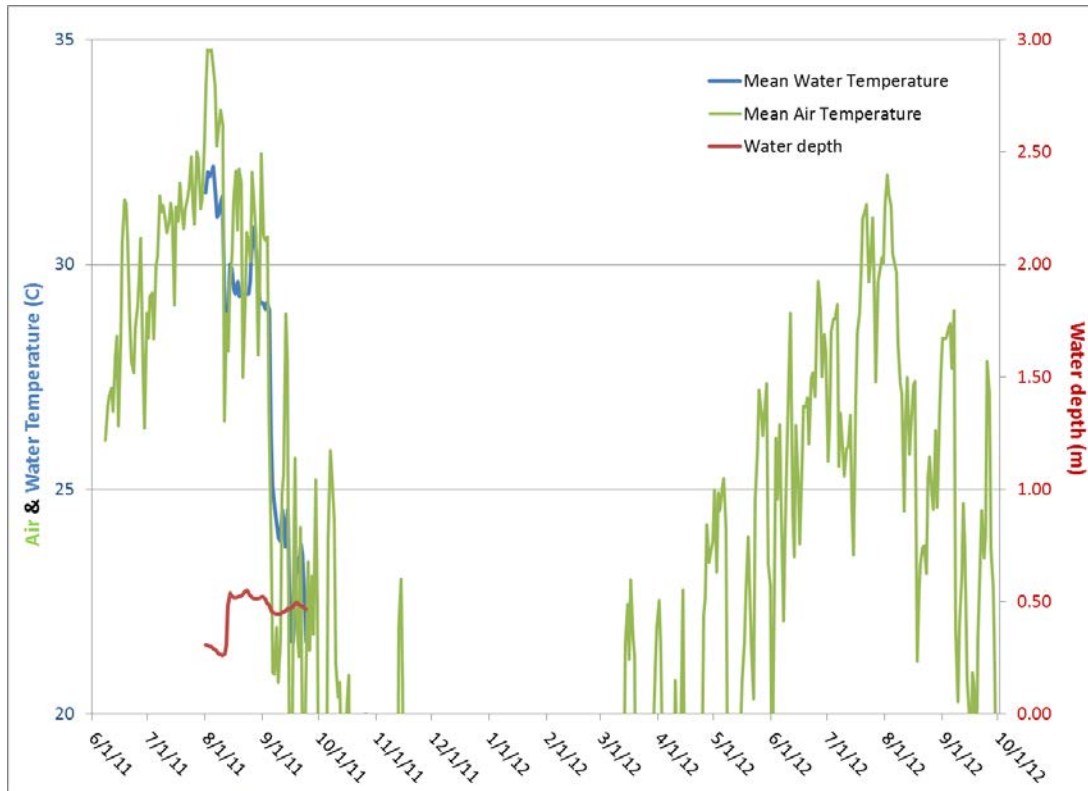
Appendix 1D. Water depth and mean daily air & water temperature for Kiamichi River station at Tuskahoma (K6), upstream of the Jackfork Creek confluence.



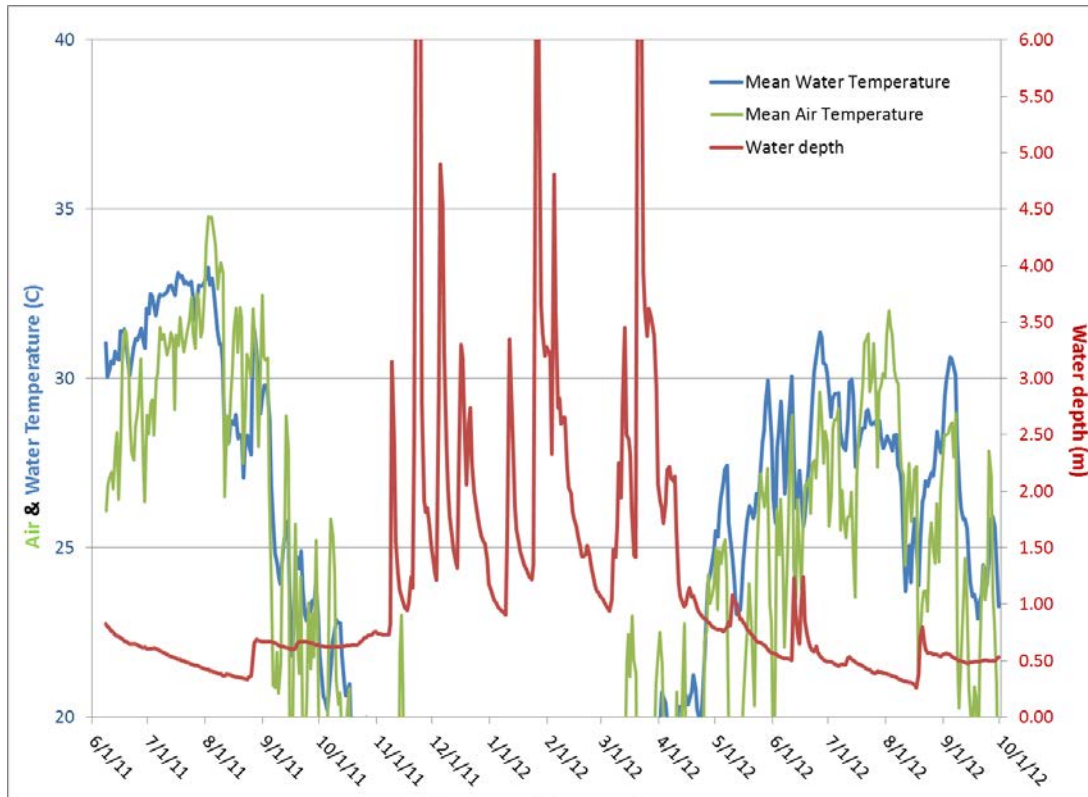
Appendix 1E. Water depth and mean daily air & water temperature for Jackfork Creek station below Sardis Dam (K7). This station measures releases from Sardis Dam. Note the spikes in water depth on August 3, 2011 and August 8, 2012 from managed Sardis Dam releases of 21 cfs and 12 cfs, respectively.



Appendix 1F. Water depth and mean daily air & water temperature for Kiamichi River station at Clayton (K8), downstream of the Jackfork Creek confluence. Note the spikes in water depth on August 3, 2011 and August 8, 2012 from managed Sardis Dam releases of 21 cfs and 12 cfs, respectively.

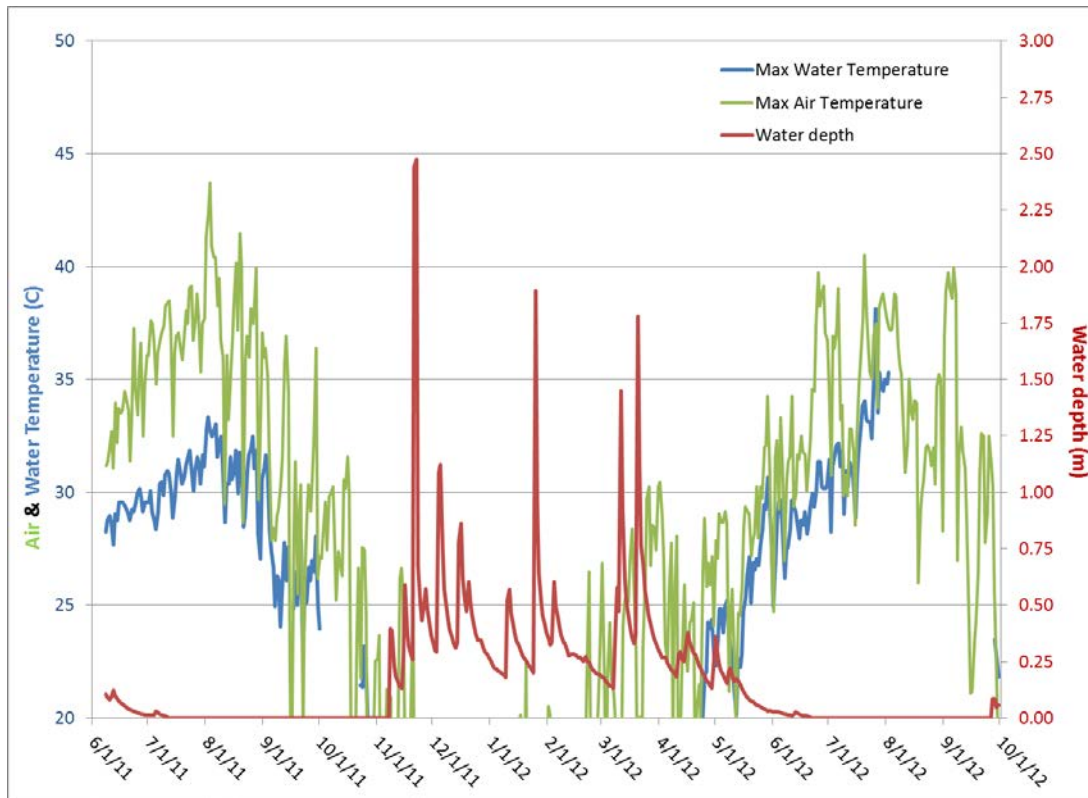


Appendix 1G. Water depth and mean daily air & water temperature for Kiamichi River station at Paine's (K11). Note the spike in water depth on August 13, 2011 from managed Sardis Dam releases of 21 cfs. Due to access issues, logger was not installed until July 31, 2011. After September 24, 2011, logger was buried under large debris jam and was not accessible. With such little data from this site, it was not modeled for water temperature changes. These data are useful, however, to show the flow timing and magnitude effects from Sardis Dam releases on downstream reaches.

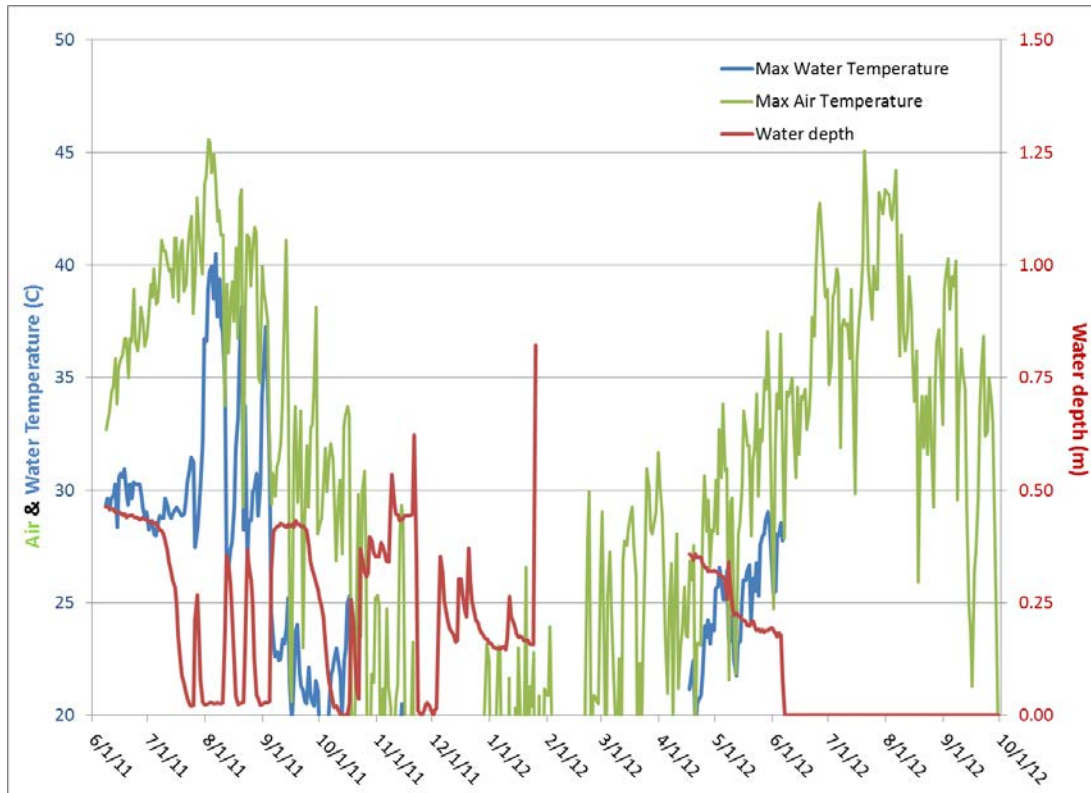


Appendix 1H. Water depth and mean daily air & water temperature for Kiamichi River station at Antlers (K9), downstream extent of study area. Note the spikes in water depth on August 27, 2011 and August 19, 2012 from managed Sardis Dam releases of 21 cfs and 12 cfs, respectively.

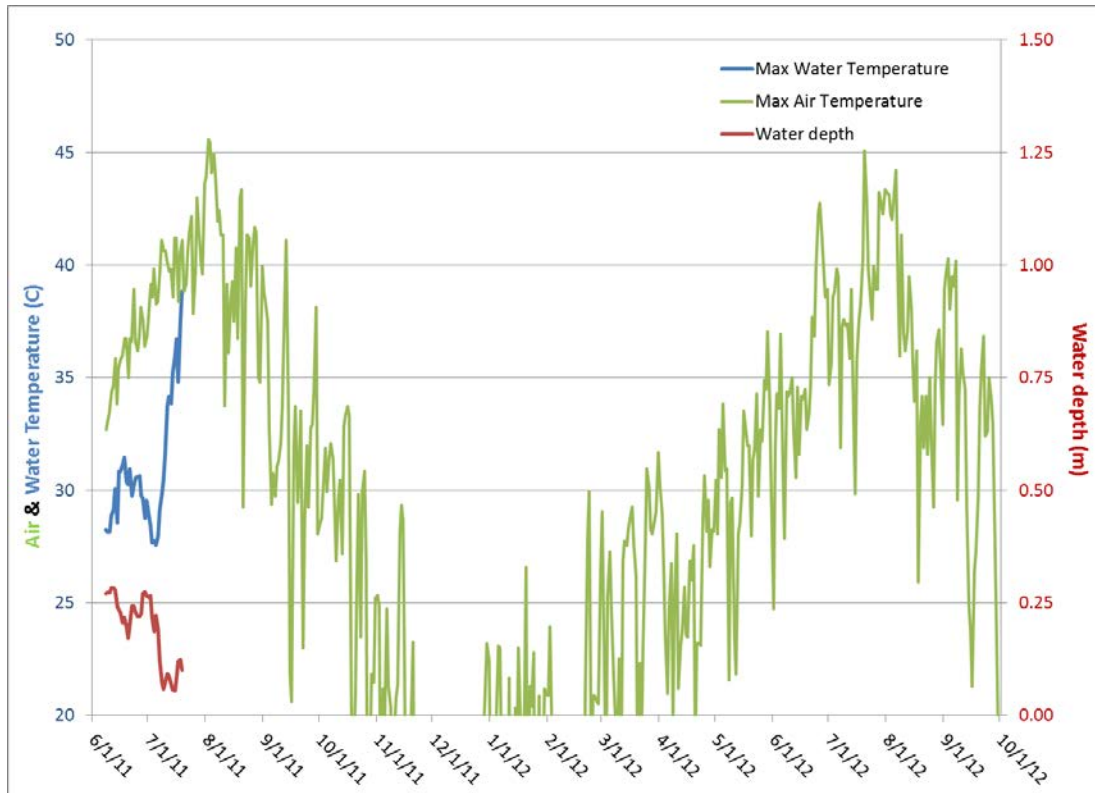
Appendix 2 – Maximum water temperature time-series



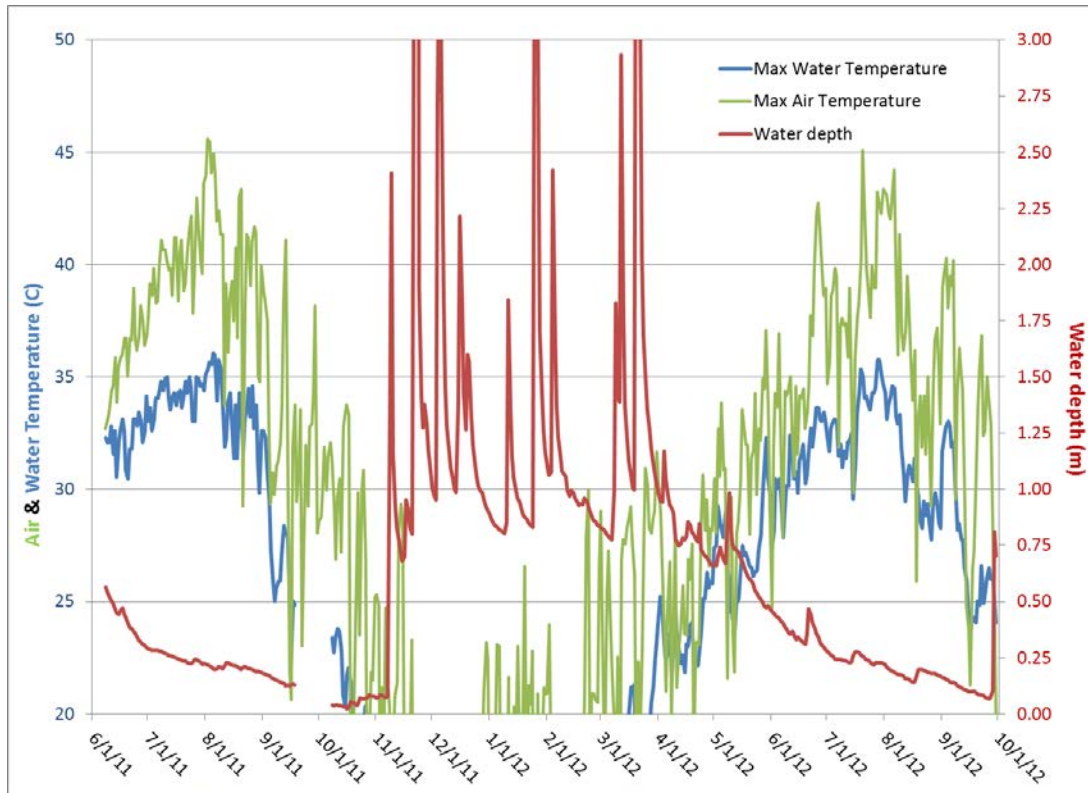
Appendix 2A. Water depth and maximum daily air & water temperature for Kiamichi River station at Big Cedar (K2), the most upstream station of the study area. Because our HOBO gage was displaced on several occasions, water depth was obtained from the USGS gage at the same site. Maximum water temperature is not reported for most of 2012 because our HOBO gage was out of water during most of this period.



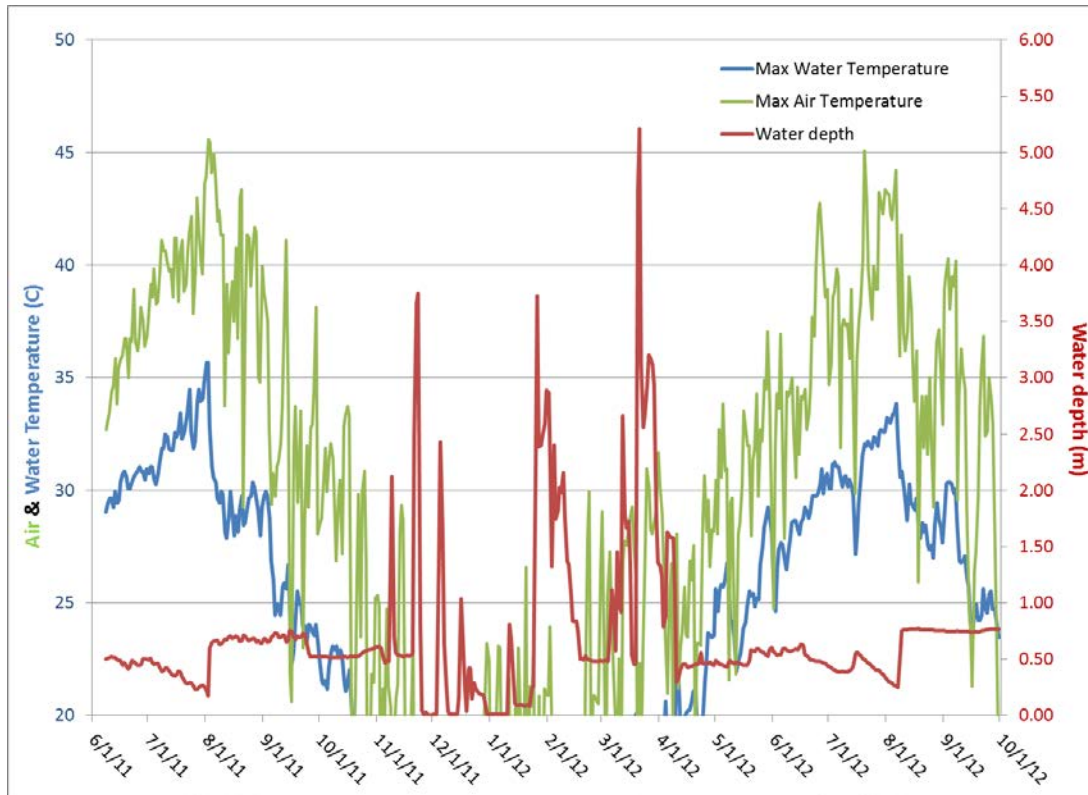
Appendix 2B. Water depth and maximum daily air & water temperature for Buffalo Creek station (K3), one of the two main inputs to Sardis Lake. The HOBO gage was displaced by a flood on January 25, 2012 and was not replaced until April 17, 2012. The creek was dry from June 7 to September 30, 2012 and thus no water temperature data for this period.



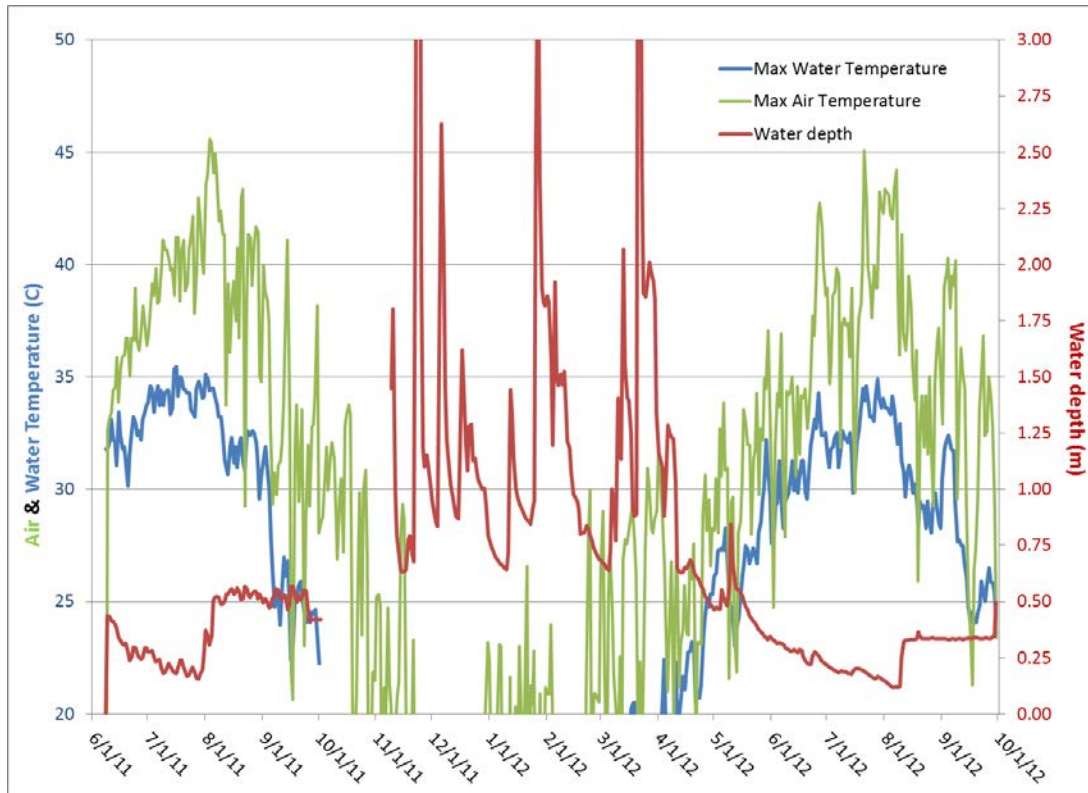
Appendix 2C. Water depth and maximum daily air & water temperature for Jackfork Creek station above Sardis Reservoir (K4), one of the two main inputs to Sardis Lake. The logger malfunctioned on July 19, 2011, with no usable data after this date.



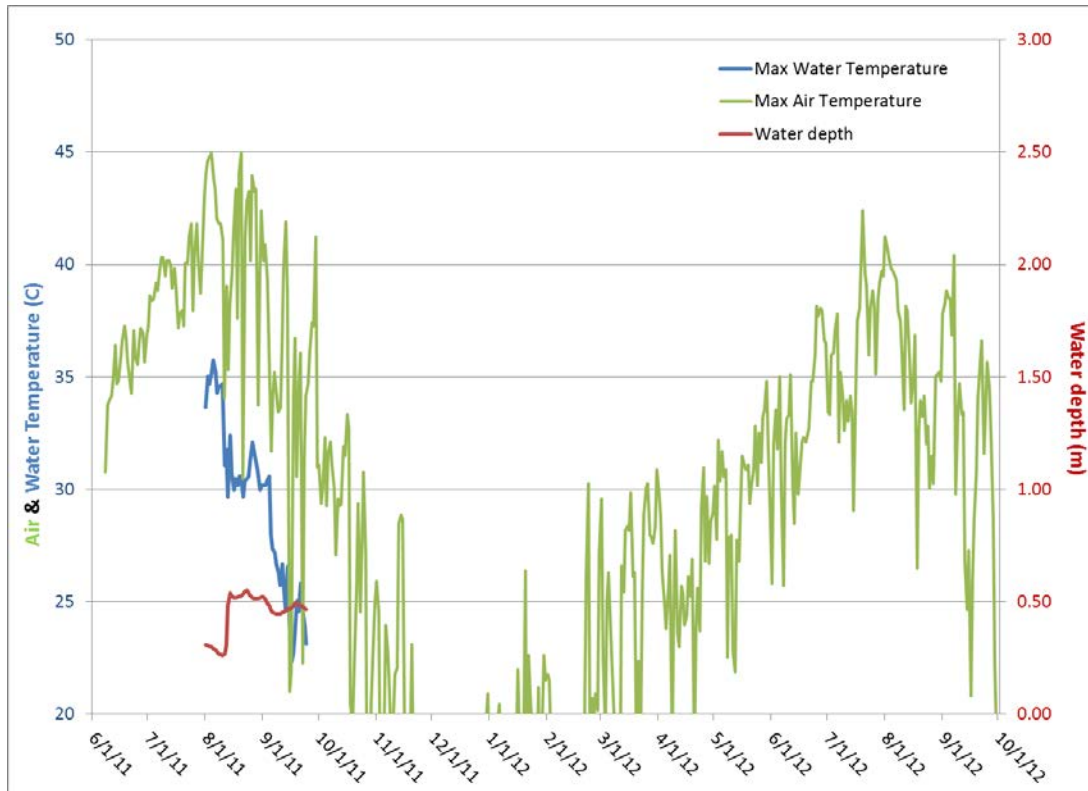
Appendix 2D. Water depth and maximum daily air & water temperature for Kiamichi River station at Tuskahoma (K6), upstream of the Jackfork Creek confluence.



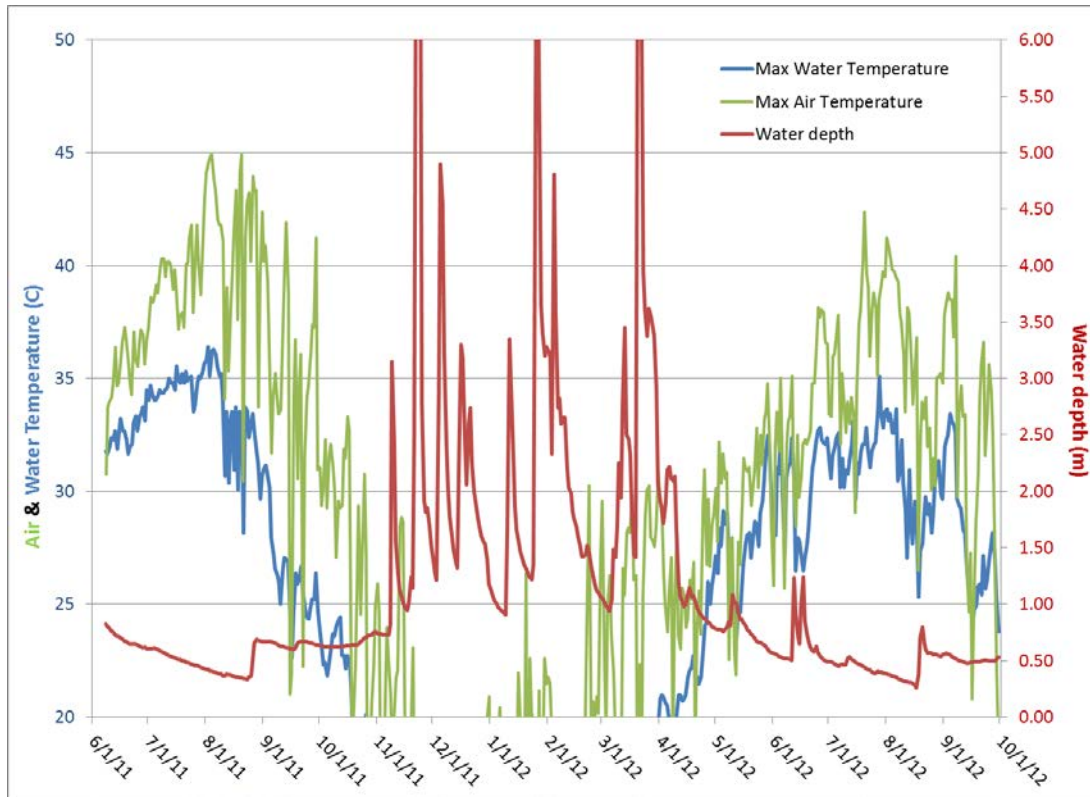
Appendix 2E. Water depth and maximum daily air & water temperature for Jackfork Creek station below Sardis Dam (K7). This station measures releases from Sardis Dam. Because Sardis Reservoir is such a large body of water, its water temperatures will be considerably lower than air temperatures during the summer. Note the spikes in water depth on August 3, 2011 and August 8, 2012 from managed Sardis Dam releases of 21 cfs and 12 cfs, respectively.



Appendix 2F. Water depth and maximum daily air & water temperature for Kiamichi River station at Clayton (K8), downstream of the Jackfork Creek confluence. Note the spikes in water depth on August 2, 2011 and August 8, 2012 from managed Sardis Dam releases of 21 cfs and 12 cfs, respectively.

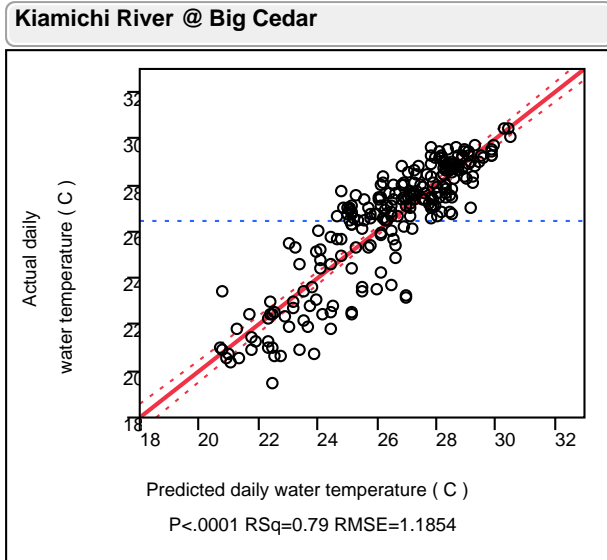


Appendix 2G. Water depth and maximum daily air & water temperature for Kiamichi River station at Paine's (K11). Note the spike in water depth on August 13, 2011 from managed Sardis Dam releases of 21 cfs. Due to access issues, logger was not installed until July 31, 2011. After September 24, 2011, logger was buried under large debris jam and was not accessible. With such little data from this site, it was not modeled for water temperature changes. These data are useful, however, to show the flow timing and magnitude effects from Sardis Dam releases on downstream reaches.

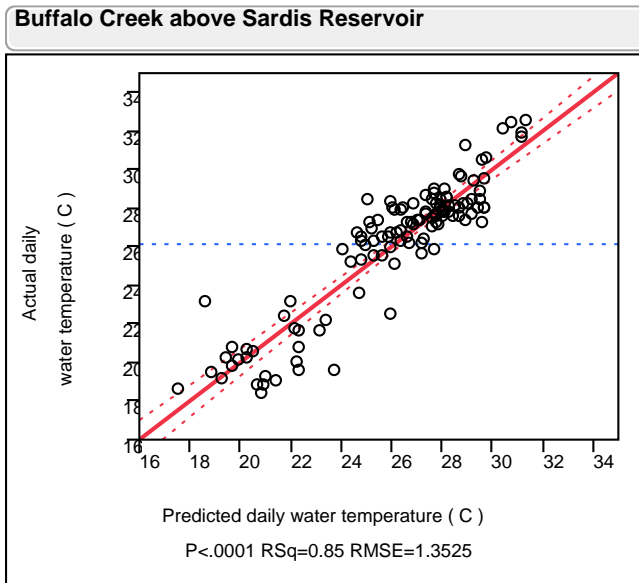


Appendix 2H. Water depth and maximum daily air & water temperature for Kiamichi River station at Antlers (K9), downstream extent of study area. Note the spikes in water depth on August 27, 2011 and August 19, 2012 from managed Sardis Dam releases of 21 cfs and 12 cfs, respectively.

Appendix 3 – Mean daily water temperature regression models



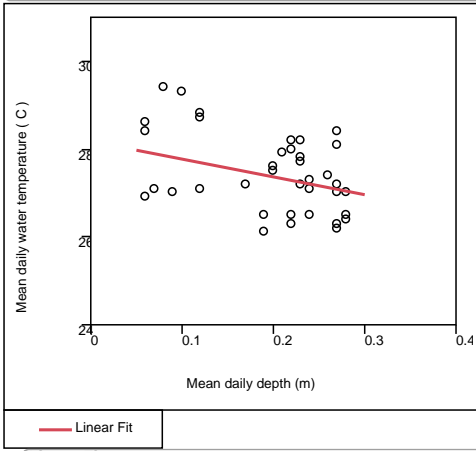
Appendix 3A. Actual vs. predicted mean daily water temperature (T_w) for Kiamichi River at Big Cedar (K2) using a bivariate model with mean daily air temperature (T_{air}). Water depth (D) was not used for this station because of its narrow range (0 – 0.12 cm). Horizontal blue dotted line represents the mean value. Diagonal solid red line represents $y=x$, and diagonal red dashed lines are 95% confidence intervals. Model equation: $T_w = 0.58T_{air} + 11.09$.



Appendix 3B. Actual vs. predicted mean daily water temperature (T_w) for Buffalo Creek above Sardis Reservoir (K3) using a multivariate model that includes mean daily air temperature (T_{air}) and mean daily water depth (D) at the station. Horizontal blue dotted line represents the mean value. Diagonal solid red line represents $y=x$, and diagonal red dashed lines are 95% confidence intervals. Model equation: $T_w = 0.69T_{air} - 1.69D + 7.26$.

Jackfork Creek above Sardis Reservoir

Bivariate Fit of Tw and D



Linear Fit

Linear Fit

$$T_w = 28.176366 - 4.0509241 \cdot D$$

Summary of Fit

RSquare	0.129377
RSquare Adj	0.107612
Root Mean Square Error	0.81769
Mean of Response	27.40476
Observations (or Sum Wgts)	42

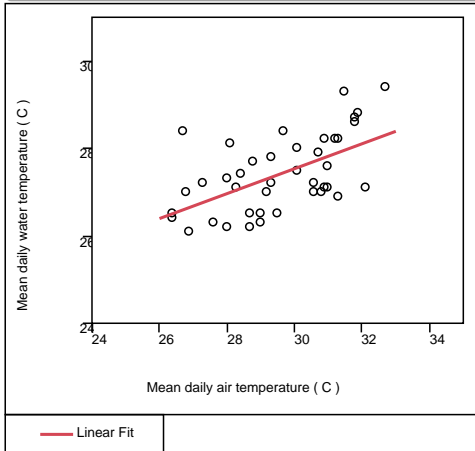
Analysis of Variance

Source	DF	Sum of Squares	Mean Square	F Ratio
Model	1	3.974342	3.97434	5.9441
Error	40	26.744705	0.66862	Prob > F
C. Total	41	30.719048		0.0193

Parameter Estimates

Term	Estimate	Std Error	t Ratio	Prob> t
Intercept	28.176366	0.340707	82.70	<.0001
Average of Depth_m	-4.050924	1.661538	-2.44	0.0193

Bivariate Fit of Tw and Tair



Linear Fit

Linear Fit

$$T_w = 18.982302 + 0.2851159 \cdot T_{air}$$

Summary of Fit

RSquare	0.32793
RSquare Adj	0.311128
Root Mean Square Error	0.718425
Mean of Response	27.40476
Observations (or Sum Wgts)	42

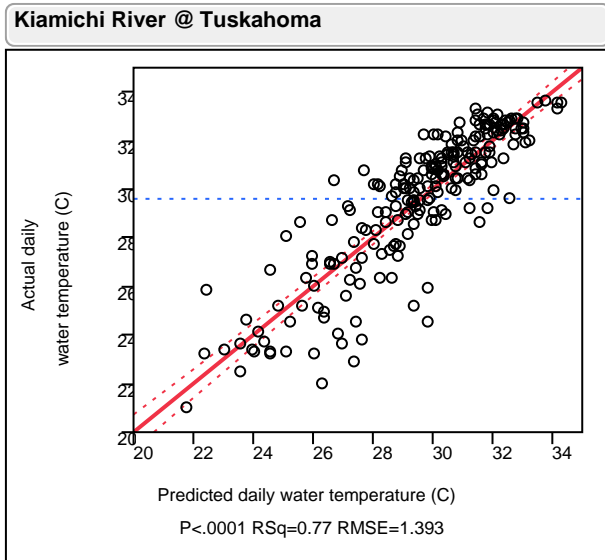
Analysis of Variance

Source	DF	Sum of Squares	Mean Square	F Ratio
Model	1	10.073689	10.0737	19.5176
Error	40	20.645359	0.5161	Prob > F
C. Total	41	30.719048		<.0001

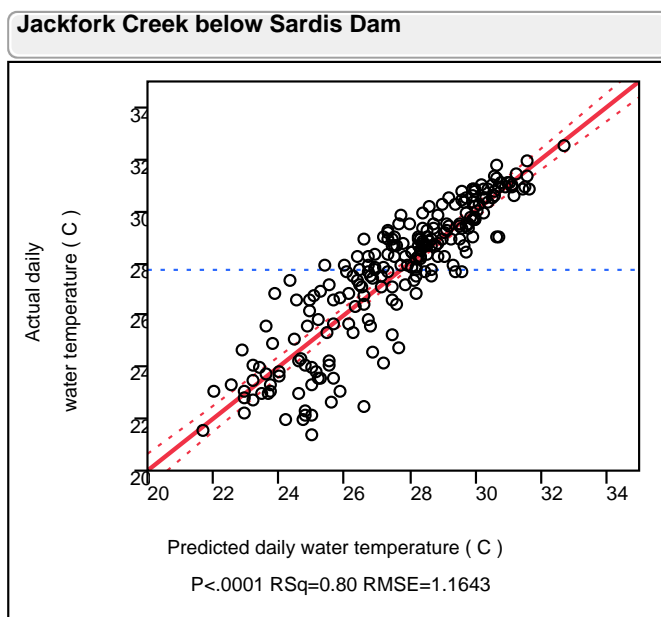
Parameter Estimates

Term	Estimate	Std Error	t Ratio	Prob
Intercept	18.982302	1.909672	9.94	<.000
Mean_Air_Temp_C	0.2851159	0.064537	4.42	<.000

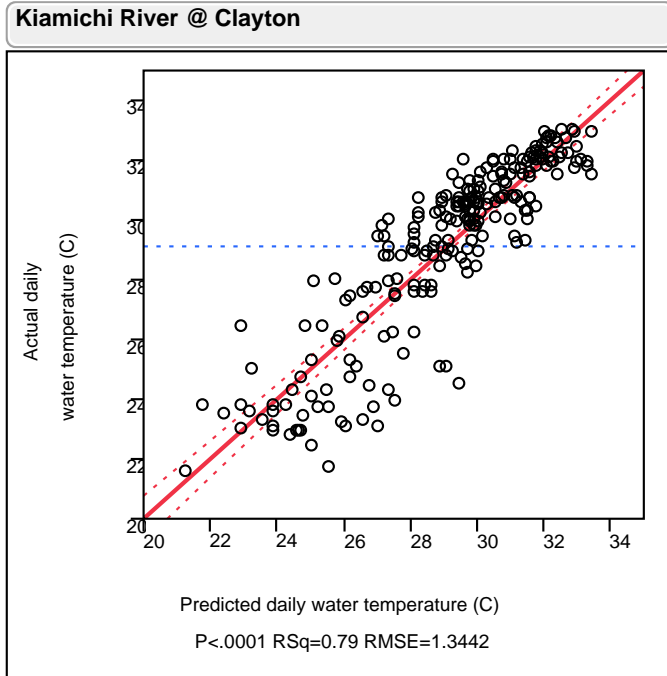
Appendix 3C. Bivariate plots of mean daily water temperature (T_w) vs. water depth (D) and mean daily air temperature (T_{air}) for Jackfork Creek station above Sardis Reservoir (K4). The plots show that T_w has a significant negative correlation with D and a significant positive correlation with T_{air} . There were not enough measurements to derive a robust model for T_w .



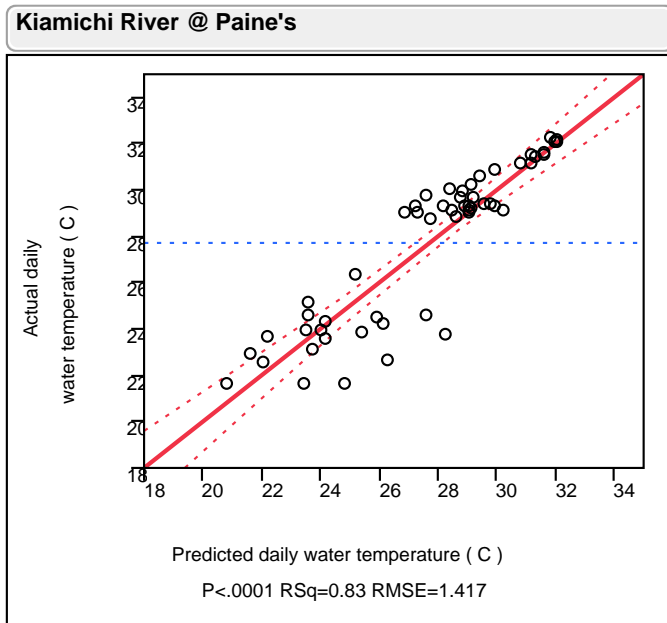
Appendix 3D. Actual vs. predicted mean daily water temperature (T_w) for Kiamichi River at Tuskahoma (K6) using a bivariate model with mean daily air temperature (T_{air}). Mean daily water depth (D) could not be included in the multivariate model for this station because it had a nonlinear relationship with water temperature. Horizontal blue dotted line represents the mean value. Diagonal solid red line represents $y=x$, and diagonal red dashed lines are 95% confidence intervals. Model equation: $T_w = 0.66T_{air} + 11.26$.



Appendix 3E. Actual vs. predicted mean daily water temperature (T_w) for Jackfork Creek below Sardis Dam (K7) using a multivariate model that includes mean daily air temperature (T_{air}) and mean daily water depth (D) at the station. Horizontal blue dotted line represents the mean value. Diagonal solid red line represents $y=x$, and diagonal red dashed lines are 95% confidence intervals. Model equation: $T_w = 0.46T_{air} - 4.23D + 17.54$.

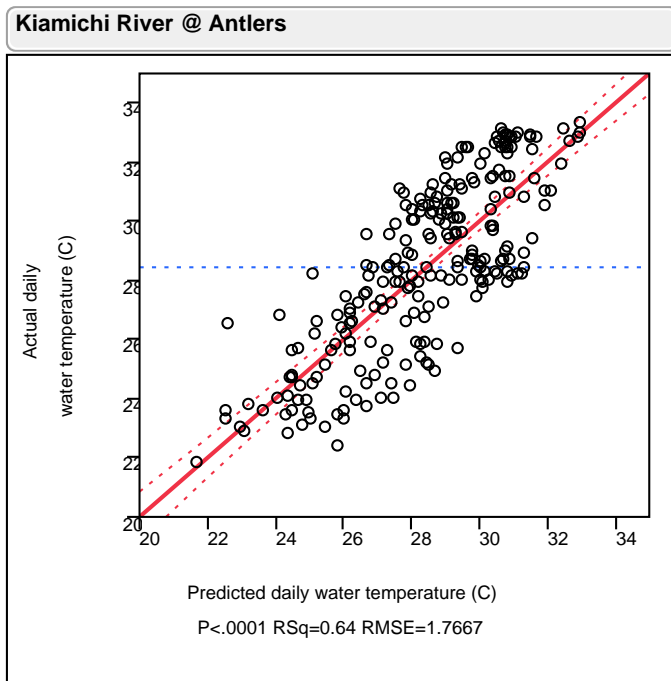


Appendix 3F. Actual vs. predicted mean daily water temperature (T_w) for Kiamichi River at Clayton (K8) using a multivariate model that includes mean daily air temperature (T_{air}) and mean daily water depth (D) at the station. Horizontal blue dotted line represents the mean value. Diagonal solid red line represents $y=x$, and diagonal red dashed lines are 95% confidence intervals. Model equation: $T_w = 0.59T_{air} - 4.37D + 14.36$.



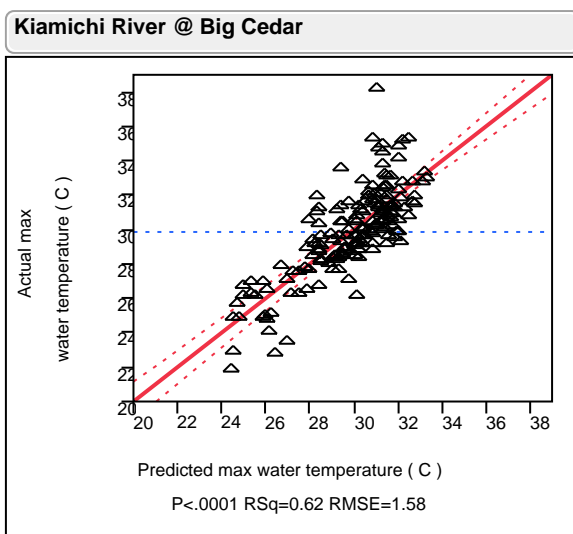
Appendix 3G. Actual vs. predicted mean daily water temperature (T_w) for Kiamichi River at Paine's (K11) using a multivariate model that includes mean daily air temperature (T_{air}) and mean daily water depth (D) at the station. Horizontal blue dotted line represents the mean value.

Diagonal solid red line represents $y=x$, and diagonal red dashed lines are 95% confidence intervals. Model equation: $T_w = 0.58T_{air} - 2.47D + 12.52$.

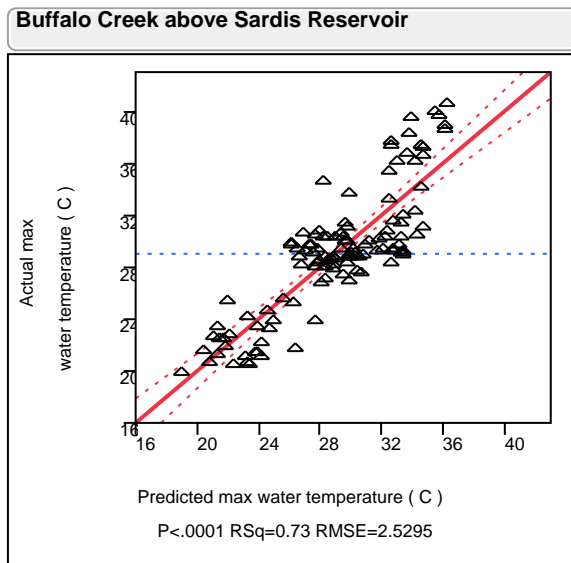


Appendix 3H. Actual vs. predicted mean daily water temperature (T_w) for Kiamichi River at Antlers (K9) using a bivariate model with mean daily air temperature (T_{air}). Water depth (D) was not used for this station because of collinearity with air temperature (i.e. lower flow occurred on warmer days). Model equation: $T_w = 0.61T_{air} + 11.83$.

Appendix 4 – Maximum daily water temperature regression models



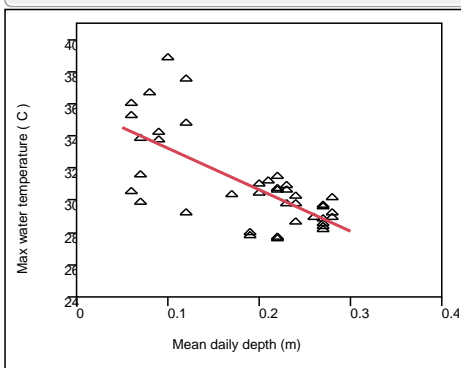
Appendix 4A. Actual vs. predicted maximum daily water temperature (T_w) for Kiamichi River at Big Cedar (K2) using a bivariate model with mean daily air temperature (T_{air}). Water depth (D) was not used for this station because of its narrow range (0 – 0.12 cm). Horizontal blue dotted line represents the mean value. Diagonal solid red line represents $y=x$, and diagonal red dashed lines are 95% confidence intervals. Model equation: $T_w(\text{max}) = 0.53T_{air} + 15.75$.



Appendix 4B. Actual vs. predicted maximum daily water temperature (T_w) for Buffalo Creek above Sardis Reservoir (K3) using a multivariate model that includes mean daily air temperature (T_{air}) and mean daily water depth (D) at the station. Horizontal blue dotted line represents the mean value. Diagonal solid red line represents $y=x$, and diagonal red dashed lines are 95% confidence intervals. Model equation: $T_w(\text{max}) = 0.71T_{air} - 9.82D + 11.85$.

Jackfork Creek above Sardis Reservoir

Bivariate Fit of Max Tw and D



— Linear Fit

Linear Fit

$$T_w(\max) = 35.810794 - 25.76917 \cdot D$$

Summary of Fit

RSquare	0.493621
RSquare Adj	0.480962
Root Mean Square Error	2.030906
Mean of Response	30.90238
Observations (or Sum Wgts)	42

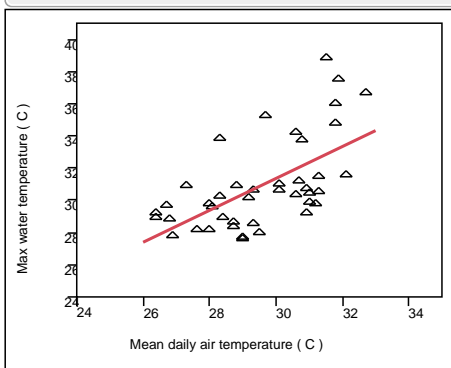
Analysis of Variance

Source	DF	Sum of Squares	Mean Square	F Ratio
Model	1	160.82662	160.827	38.9923
Error	40	164.98314	4.125	Prob > F
C. Total	41	325.80976		≈.0001

Parameter Estimates

Term	Estimate	Std Error	t Ratio	Prob> t
Intercept	35.810794	0.846217	42.32	≈.0001
Average of Depth_m	-25.76917	4.126779	-6.24	≈.0001

Bivariate Fit of Max Tw and Tair



— Linear Fit

Linear Fit

$$T_w(\max) = 1.646827 + 0.9903549 \cdot T_{air}$$

Summary of Fit

RSquare	0.373047
RSquare Adj	0.357373
Root Mean Square Error	2.259798
Mean of Response	30.90238
Observations (or Sum Wgts)	42

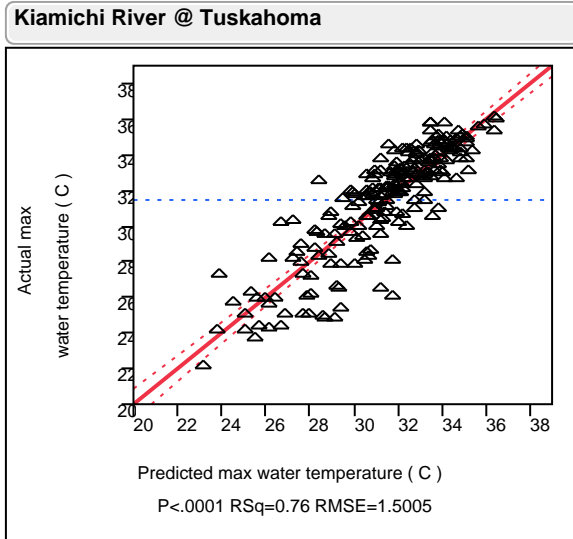
Analysis of Variance

Source	DF	Sum of Squares	Mean Square	F Ratio
Model	1	121.54224	121.542	23.8006
Error	40	204.26752	5.107	Prob > F
C. Total	41	325.80976		≈.0001

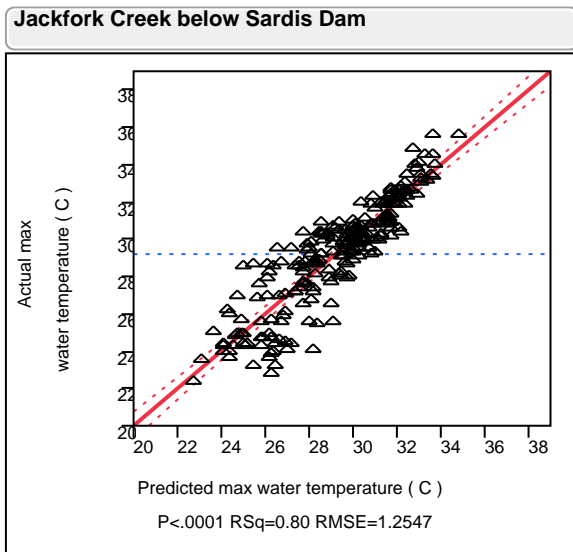
Parameter Estimates

Term	Estimate	Std Error	t Ratio	Prob
Intercept	1.646827	6.006857	0.27	0.785
Mean_Air_Temp_C	0.9903549	0.203	4.88	≈.000

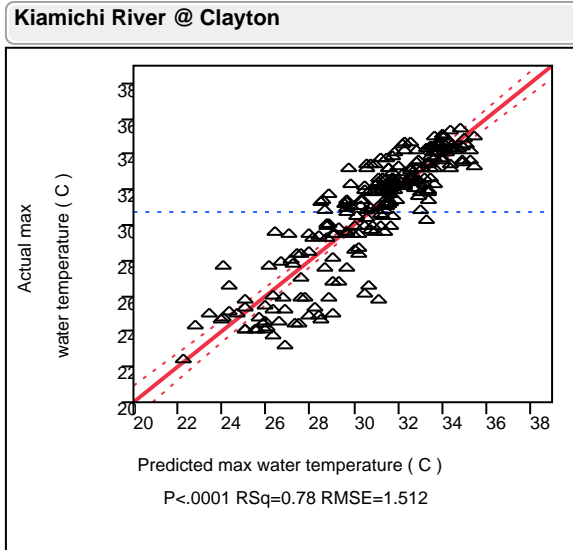
Appendix 4C. Bivariate plots of maximum daily water temperature (T_w) vs. water depth (D) and mean daily air temperature (T_{air}) for Jackfork Creek station above Sardis Reservoir (K4). The plots show that $T_w(\max)$ has a significant negative correlation with D and a significant positive correlation with T_{air} . There were not enough measurements to derive a robust model for $T_w(\max)$.



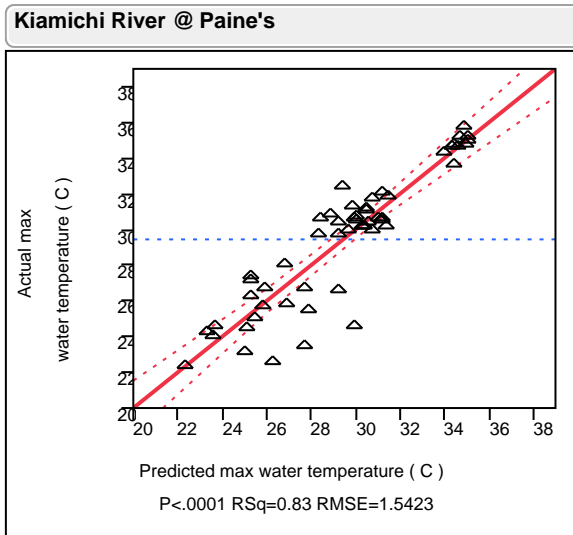
Appendix 4D. Actual vs. predicted maximum daily water temperature (T_w) for Kiamichi River at Tuskahoma (K6) using a bivariate model with mean daily air temperature (T_{air}). Mean daily water depth (D) could not be included in the multivariate model for this station because it had a nonlinear relationship with water temperature. Horizontal blue dotted line represents the mean value. Diagonal solid red line represents $y=x$, and diagonal red dashed lines are 95% confidence intervals. Model equation: $T_w(\max) = 0.71T_{air} + 11.89$.



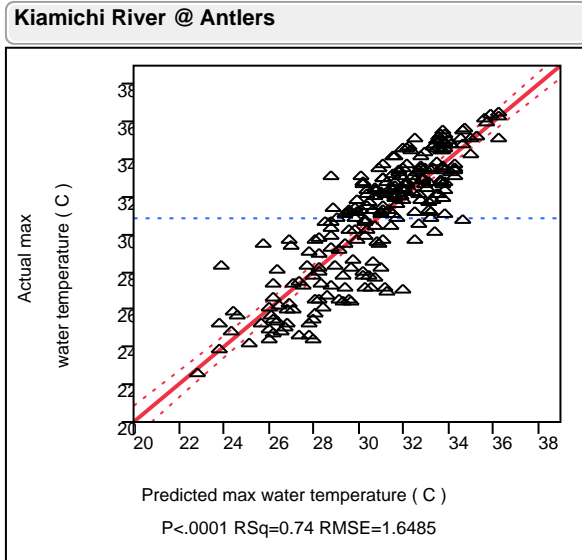
Appendix 4E. Actual vs. predicted maximum daily water temperature (T_w) for Jackfork Creek below Sardis Dam (K7) using a multivariate model that includes mean daily air temperature (T_{air}) and mean daily water depth (D) at the station. Horizontal blue dotted line represents the mean value. Diagonal solid red line represents $y=x$, and diagonal red dashed lines are 95% confidence intervals. Model equation: $T_w(\max) = 0.47T_{air} - 5.78D + 19.58$.



Appendix 4F. Actual vs. predicted maximum daily water temperature (T_w) for Kiamichi River at Clayton (K8) using a multivariate model that includes mean daily air temperature (T_{air}) and mean daily water depth (D) at the station. Horizontal blue dotted line represents the mean value. Diagonal solid red line represents $y=x$, and diagonal red dashed lines are 95% confidence intervals. Model equation: $T_w(\max) = 0.64T_{air} - 4.84D + 14.75$.

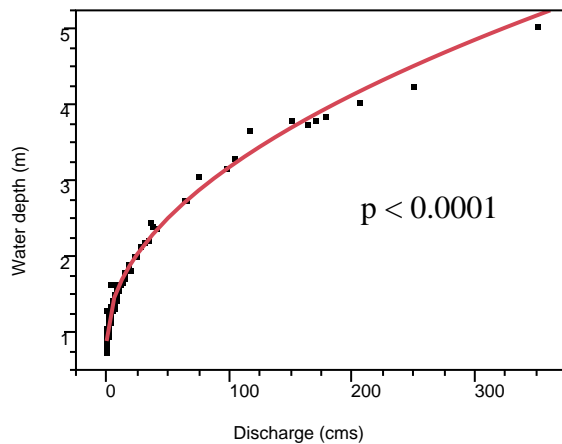


Appendix 4G. Actual vs. predicted maximum daily water temperature (T_w) for Kiamichi River at Paine's (K11) using a multivariate model that includes mean daily air temperature (T_{air}) and mean daily water depth (D) at the station. Horizontal blue dotted line represents the mean value. Diagonal solid red line represents $y=x$, and diagonal red dashed lines are 95% confidence intervals. Model equation: $T_w(\max) = 0.59T_{air} - 10.41D + 17.73$.

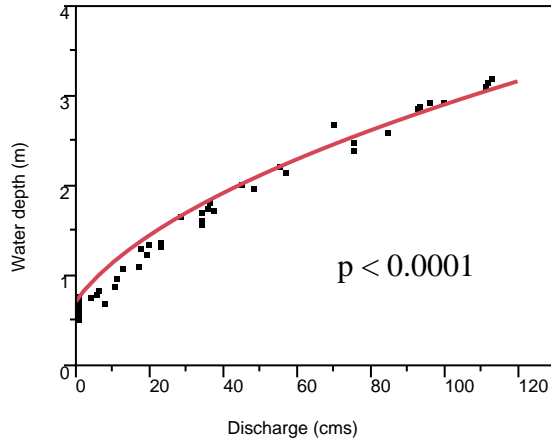


Appendix 4H. Actual vs. predicted maximum daily water temperature (T_w) for Kiamichi River at Antlers (K9) using a bivariate model with mean daily air temperature (T_{air}). Water depth (D) was not used for this station because of collinearity with air temperature (i.e. lower flow occurred on warmer days). Model equation: $T_w(\max) = 0.72T_{air} + 11.08$.

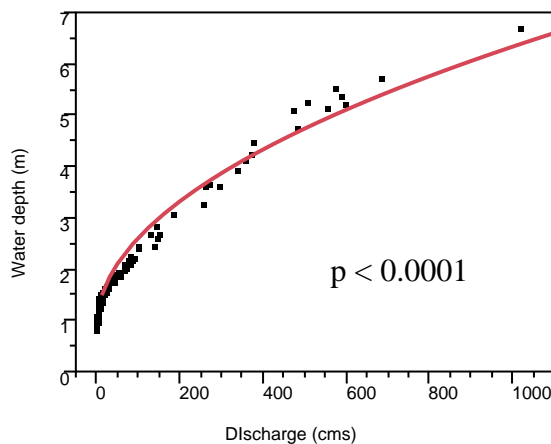
Appendix 5 – Hydrology data



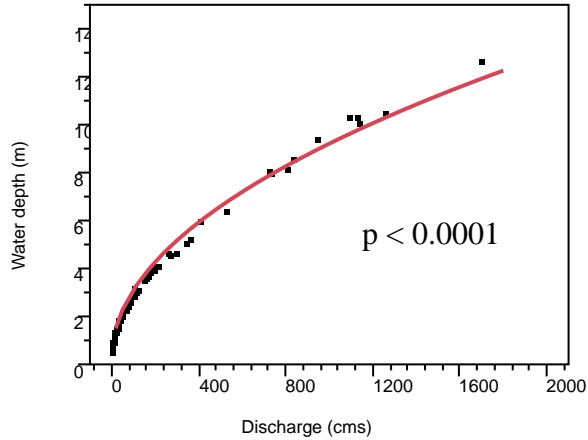
Appendix 5A. Depth-Discharge rating curve for Kiamichi River near Big Cedar (USGS 07335700). Use the following equation to calculate water depth at Big Cedar gage (D_{BIGC}) using the discharge reported on the USGS waterdata site (Q_{BIGC}): $D_{BIGC} = 0.88 + 0.23(Q_{BIGC})^{0.5}$



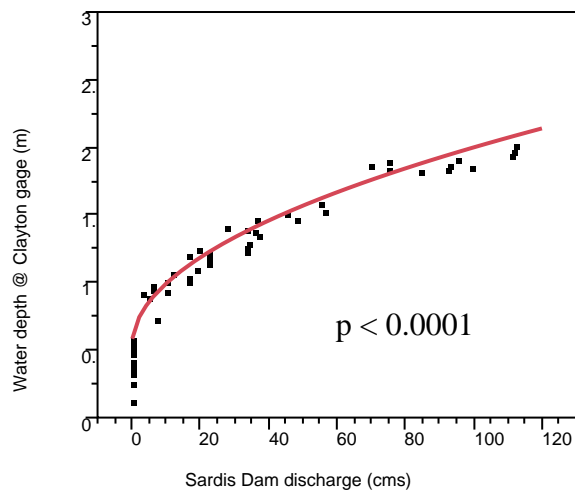
Appendix 5B. Depth-Discharge rating curve for Jackfork Creek below Sardis Dam using releases from Sardis Lake near Clayton (USGS 07335775) for discharge. Use the following equation to calculate water depth below Sardis Dam (D_{SARD}) using the discharge reported on the USGS waterdata site (Q_{SARD}): $D_{SARD} = (0.52 + 0.08 * Q_{SARD})^{0.5}$



Appendix 5C. Depth-Discharge rating curve for Kiamichi River near Clayton (USGS 07335790). Use the following equation to calculate water depth at Clayton gage (D_{CLAY}) using the discharge reported on the USGS waterdata site (Q_{CLAY}): $D_{CLAY} = 0.88 + 0.17(Q_{CLAY})^{0.5}$



Appendix 5D. Depth-Discharge rating curve for Kiamichi River near Antlers (USGS 07336200). Use the following equation to calculate water depth at Clayton gage (D_{ANTL}) using the discharge reported on the USGS waterdata site (Q_{ANTL}): $D_{ANTL} = 0.28 + 0.28(Q_{ANTL})^{0.5}$



Appendix 5E. Relationship between Sardis Dam releases (Q_{SARD}) and water depth of Kiamichi River @ Clayton (D_{CLAY}): $D_{CLAY} = 0.525 + 0.147(Q_{SARD})^{0.5}$. This equation was used to determine the necessary releases from Sardis Dam to prevent maximum water temperatures (via Appendix 4F) from exceeding target temperatures identified in Objective 1.

Investigation of the Viability of Rainfall Harvesting for Long-term Urban Irrigation: Bioaccumulating Organic Compounds and the First Flush in Rooftop Runoff

Basic Information

Title:	Investigation of the Viability of Rainfall Harvesting for Long-term Urban Irrigation: Bioaccumulating Organic Compounds and the First Flush in Rooftop Runoff
Project Number:	2011OK213B
Start Date:	3/1/2011
End Date:	12/31/2012
Funding Source:	104B
Congressional District:	3
Research Category:	Engineering
Focus Category:	Water Use, Non Point Pollution, Conservation
Descriptors:	None
Principal Investigators:	Jason Vogel, Jason B Belden, Glenn Brown

Publications

1. Vogel, J.R., J.J. Lay, J.B. Belden, and G.O. Brown, 2012 Investigation of the Viability of Rainfall Harvesting for Long-term Urban Irrigation: Bioaccumulating Organic Compounds and the First Flush in Rooftop Runoff. 2012 ASCE EWRI World Environmental and Water Resources Congress. Albuquerque, NM, May 21-24, 2012.
2. Lay, J.J., J.R. Vogel, J.B. Belden, and G.O. Brown, 2011. Quantifying the First Flush in Rooftop Rainwater Harvesting through Continuous Monitoring and Analysis of Stormwater Runoff, National Low Impact Development Symposium. Philadelphia, PA, Sep. 25-28, 2011.
3. Lay, J.J., J.R. Vogel, J.B. Belden, and G.O. Brown, 2011. Quantifying the First Flush in Rooftop Rainwater Harvesting through Continuous Monitoring and Analysis of Stormwater Runoff. 2011 International Conference of the ASABE. Louisville, KY, Aug. 7-10, 2011.

Project Update: Investigation of the Viability of Rainfall Harvesting for Long-term Urban Irrigation: Bioaccumulating Organic Compounds and the First Flush in Rooftop Runoff

May 13, 2013

Jason R. Vogel, Jason B. Belden, Glenn O. Brown, and Jessica J. Lay

Introduction

Rooftop stormwater runoff has been shown to be a major source and pathway of heavy metals and bacterial load into local surface waters (Lye, 2009; Van Metre and Mahler, 2003). Polycyclic aromatic hydrocarbons (PAHs), contaminants of emerging concern known to cause carcinogenic and mutagenic effects in humans and biota, have been found in stormwater runoff due to atmospheric deposition on rooftops, especially in urban areas (Forster, 1999; Van Metre and Mahler, 2003). Polybrominated diphenyl ethers (PBDEs), which are used as flame retardants, are also being found in water, surface sediments, and marine biota (Oros et al., 2005). PBDEs are of concern as research has shown that they bioaccumulate and have potential endocrine disrupting properties (Rahman et al., 2001).

Rainwater harvesting (RWH) is a low impact development (LID) stormwater best management practice (BMP) that involves the capture, diversion and storage of rainwater for later non-potable and sometimes potable use while also helping reduce stormwater runoff volume. The majority of a rooftop's dust and debris is thought to be washed away during the initial periods of a rainfall event, a phenomenon known as the "first flush" (Martinson and Thomas, 2005). If it occurs in the classical sense, the removal of the first flush in RWH can dramatically increase the collected water's quality (Lye, 2009). Research has shown varied conclusions in how much runoff should be diverted in the first flush in order to have satisfactory water quality in the RWH system. Yaziz et al. (1989) suggested diverting five liters for galvanized-iron and concrete tile roofs with catchment areas of 18 m² from the RWH system. Martinson and Thomas (2005) proposed that contamination will be halved for each mm of rainwater that is diverted from the RWH system. The *Texas Manual on Rainwater Harvesting* recommends diverting one to two gallons of the first flush for every 9.29 m² of catchment area (TWDB, 2005). While research has shown that diverting the first flush does play a significant role in harvested rainwater quality, there has yet to be a universal consensus on what exactly constitutes a first flush (Lye, 2009; Martinson and Thomas, 2005).

There are many variables that play a role in the water quality of roof runoff. For example, the roofing material, catchment parameters, precipitation events, local weather, chemical properties of the pollutants, and geographical location of the RWH system all need to be taken into consideration when designing a first flush device (Forster, 1996; Forster, 1999). This paper focuses on the research materials and methodology utilized in testing the hypothesis that a more site-specific first flush can be quantified based on the roofing material, roof orientation, and geographical location by continuous monitoring and analysis of contaminants, including PAHs and PBDEs, found in the rooftop runoff throughout a storm event in the state of Oklahoma.

Materials and Methods

This study was conducted at two different locations in Oklahoma: the Oklahoma State University Oklahoma City campus (OSU-OKC) and the OSU Agronomy Farm, located in Stillwater. The OSU-OKC campus is located west of Interstate 44 (I – 44) and the OSU Agronomy Farm is

located north of Highway 51. The sites' close proximity to the two highways allows for a more accurate representation of the environmental occurrence of PAHS and other contaminants from anthropogenic sources (i.e. motor vehicles) as dust from the highway is expected to become atmospherically deposited onto the buildings and roof structures.

OSU – OKC

Three different roof types were analyzed for contaminants in the rooftop runoff at the OSU – OKC site. Runoff samples were collected from two commercial buildings, the Horticulture Pavilion and the Maintenance Shop, representing metal and built-up (tar and gravel) roof types, respectively, as well as from a constructed asphalt-shingle roof structure located next to the Maintenance Shop. A single downspout on both the Horticulture Pavilion and the Maintenance Shop have been replaced and modified with a PVC pipe configuration in order to allow for continuous water quality readings and auto sampling with a Hach® Hydrolab MS5 Water Quality Multiprobe and Teledyne Isco 6712 portable sampler. The same PVC downspout configuration was also placed on the constructed asphalt shingle structure. In addition, a 90° V-notch weir box was placed at the outlet of each downspout configuration in order to measure stormwater runoff flow in conjunction with a Teledyne Isco 720 Submerged Probe Flow Module.

In order to help quantify the first flush occurrence, the OSU – OKC site had continuous monitoring of specific conductance and turbidity as well as auto sampling for total suspended solids (TSS), PAHs, PBDEs, bacteria, metals and nitrate throughout the duration of the storm event. Each roof had 24 1000 mL water samples collected by the sampler during each sampled storm event. The sampler will be set to take samples at irregular time intervals, with the majority of the samples programmed to be collected during the rising limb of the storm. Six grab samples were collected from the 24 1000 mL water samples based on the storm hydrograph. Samples were collected from 10 storms between the months of March and June 2012.

OSU Agronomy Farm

Eighteen simulated roof structures were constructed and placed at the Agronomy Farm in Stillwater, OK, for evaluation of first flush occurrence from simulated rainfall events for new TAMKO® Elite Glass-Seal® three tab asphalt shingles, new MasterRib® acrylic coated Galvalume® sheeting, and 60 year-old clay tile roofing materials. Each roofing material is replicated six times. Nine roofs, consisting of three replicates of each roofing material, are oriented north-south while the remaining nine roofs are oriented east-west in order to determine if roof orientation in relation to the sun and prevailing wind direction have a significant impact on rooftop runoff water quality.

A rainfall simulator will be used to simulate a high, medium and low intensity storm on the roofs, resulting in a total of three experimental runs on each roof throughout the duration of the study. Water used in the simulations will pass through a reverse osmosis (RO) filter before passing through the simulator nozzle in order to mimic rainwater quality. Six samples, five individual and one composite, will be manually collected from each roof during the three simulated rainfall events. Collected samples will then be analyzed for specific conductance, turbidity, TSS, PAHs, PBDEs, metals and nitrate. In addition to the water samples, the surface temperature will be recorded on each of the simulated structures at each rainfall simulation. Weathering of the roofing materials will also be evaluated throughout the duration of the study.

Analytical Methods

Water samples from both sites were analyzed for PAHs and PBDEs using solid-phase extraction of whole water samples and then frozen until analysis can be completed. Of the six

water samples collected from each roof, the first sample and the composite sample were initially analyzed for PAHs and PBDEs; if there is no detection in these samples, the remaining four samples were not analyzed. Analysis of extracts was conducted using gas chromatography coupled with mass spectrometry detection. Electron ionization was used for detection of the PAHs while negative chemical ionization will be used for PBDE detection. Detection was performed using select ion-monitoring using three-ions per analyte.

Samples were analyzed for the following PAHs listed in Table 1, of which 16 are designated by the Environmental Protection Agency (EPA) as Priority Pollutants. PBDEs selected for detection analysis are listed in Table 2.

Table 1. PAHs highlighted in research study.

Polycyclic Aromatic Hydrocarbons (PAHs)	Acenaphthene	
	Acenaphthylene	
	Anthracene	
	Benzo(a)anthracene	Probable Human Carcinogen
	Benzo(a)pyrene	Probable Human Carcinogen
	Benzo(b)fluoranthene	Possible Human Carcinogen
	Benzo(ghi)perylene	
	Benzo(k) fluoranthene	Probable Human Carcinogen
	Chrysene	Probable Human Carcinogen
	Dibenzo(a,h)anthracene	Probable Human Carcinogen
	Fluoranthene	
	Fluorine	
	Ideno(1,2,3-cd)pyrene	Possible Human Carcinogen
	1-methylnaphthalene	
	2-methylnaphthalene	
	Naphthalene	
	Phenanthrene	
	Pyrene	

Table 2. Select congeners of PBDEs highlighted in research study.

Polybrominated Diphenyl Ethers (PBDEs) – Select Congeners	28
	47
	99
	100
	153
	154
	183
	209

QA/QC

Replicate and field blank samples were collected at a rate of 10% of the environmental sample count for quality assurance/quality control of the results. Prior to analyzing samples for PAHs and PBDEs, accuracy and precision studies, as well as method detection limit studies, were performed. Laboratory blanks and spikes were run at a frequency of 10% the number of samples.

Objectives and Hypotheses

The objective of this research are to investigate two questions that remain regarding the widespread implementation of rainwater harvesting as a solution for decreasing demand on water systems from water used for urban irrigation. These two questions are:

1. Does the runoff from the beginning part of a storm, also referred to as the “first flush” contribute a substantial portion of contaminants in rooftop runoff, and, if it does, can design of the rainfall harvesting system decrease the concentration and bioaccumulation potential of contaminants in harvested rainfall?
2. Do PAHs, PBDEs, and pyrethroid insecticides occur in rooftop runoff, and what is the bioaccumulation potential of these compounds in lawns if the water is used for urban irrigation?

This objective is being investigated by testing two hypotheses: (1) a site specific first flush can be quantified based on the roofing material, roof orientation, and geographical location by continuous monitoring and analysis of contaminants found in the rooftop runoff throughout a storm event, and (2) PAHs, PBDEs, and selected pyrethroid insecticides have the potential for long-term accumulation in soils from harvested rainfall used as urban irrigation.

The hypotheses to be tested are being investigated discrete monitoring of simulated rainfall from 18 smaller structures to be constructed near Stillwater, Oklahoma; by a combination of continuous and discrete monitoring of harvested rainfall from three buildings with different roof types in central Oklahoma; a field survey of accumulation concentrations of PAHs, PBDEs, and selected pyrethroid insecticides in soils below downspouts from 30 buildings (representing 3 roof types) in central Oklahoma; and, a leaching test on the parent roofing material to determine leaching potential.

Results

Full results from all four tasks are not currently interpreted and/or completed because my graduate student is currently completing a Fulbright project in Sierra Leone that was not anticipated at the time this grant was received. A full project report will be completed by December 31, 2013.

Simulated Harvested Rainfall from Different Roofs and Intensities. Between July 2011 and January 2012 three separate rainfall simulations were performed on 18 roofs. In general, the results indicate that the poorest water quality comes from asphalt roofs compared to clay tile and metal roofs. The first flush was prevalent and dependent on rainfall intensity and roof type. It appears that PAH's are being transported in from roof as shown by a decrease in concentration during the storm. Example results for turbidity, specific conductance, and benzo(a)pyrene are shown in Figures 1, 2, and 3. Full results will be presented in the final project report.

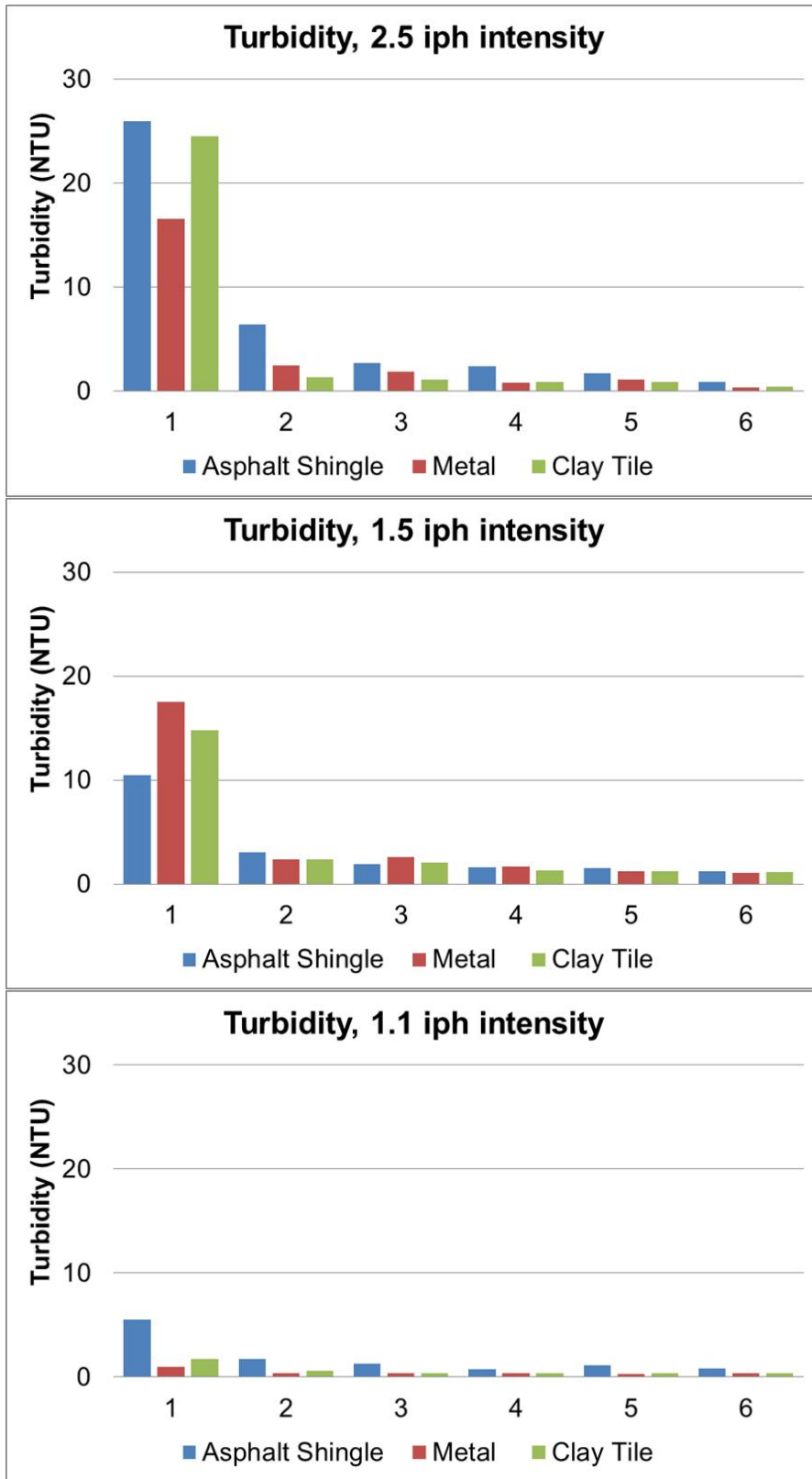


Figure 1. Average turbidity measurements for rooftop runoff at different intensities and roof types.

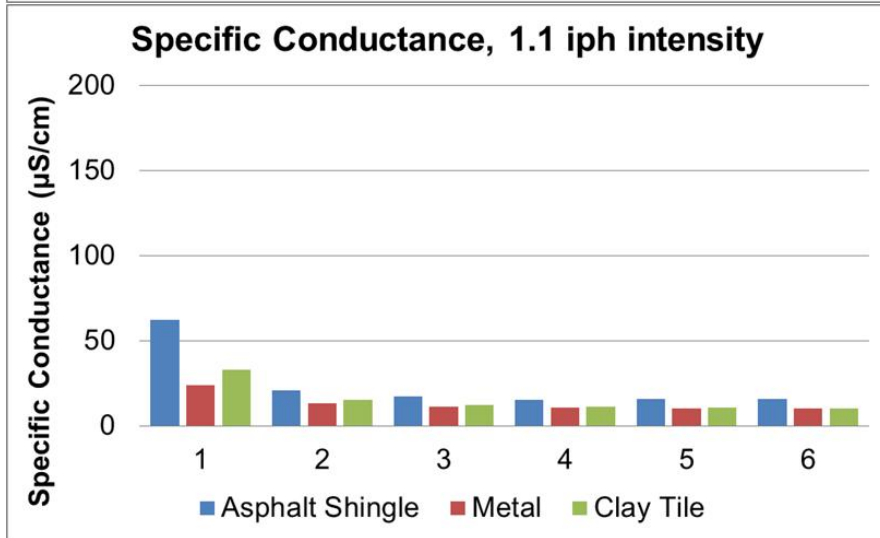
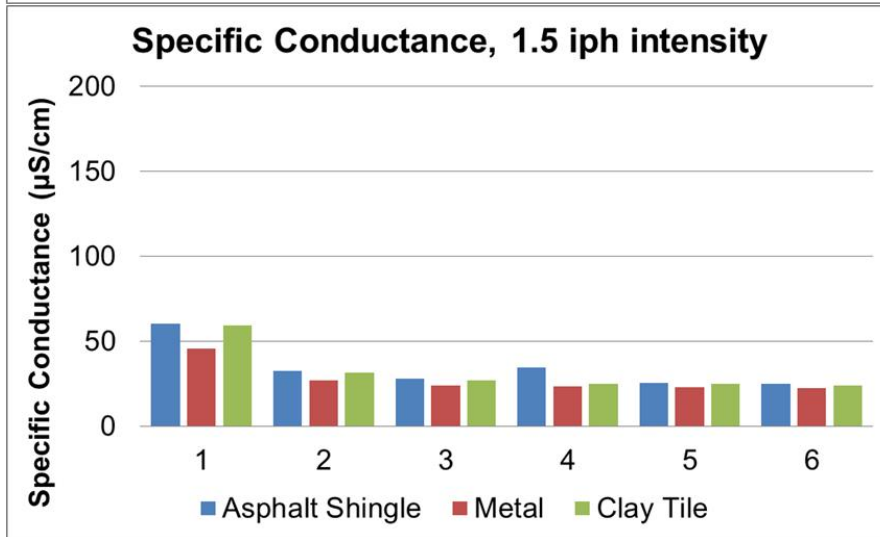
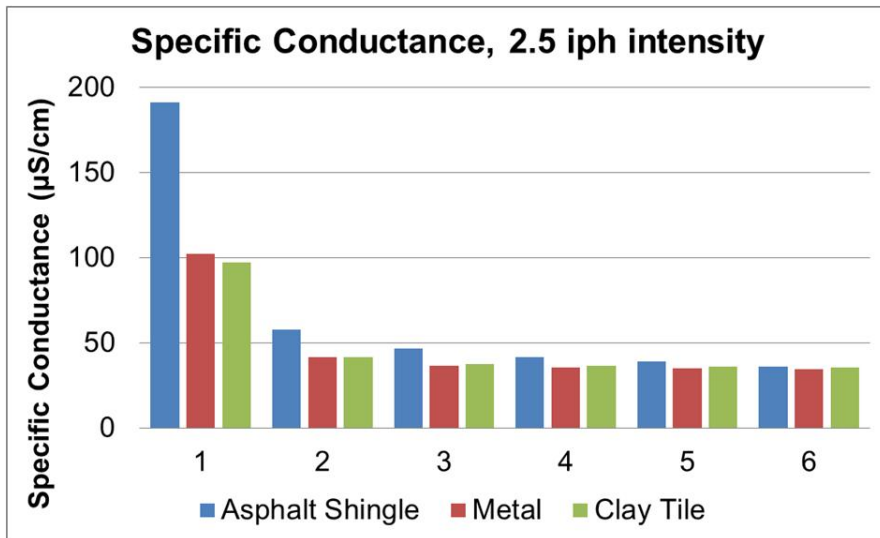


Figure 2. Average specific conductance measurements for rooftop runoff at different intensities and roof types.

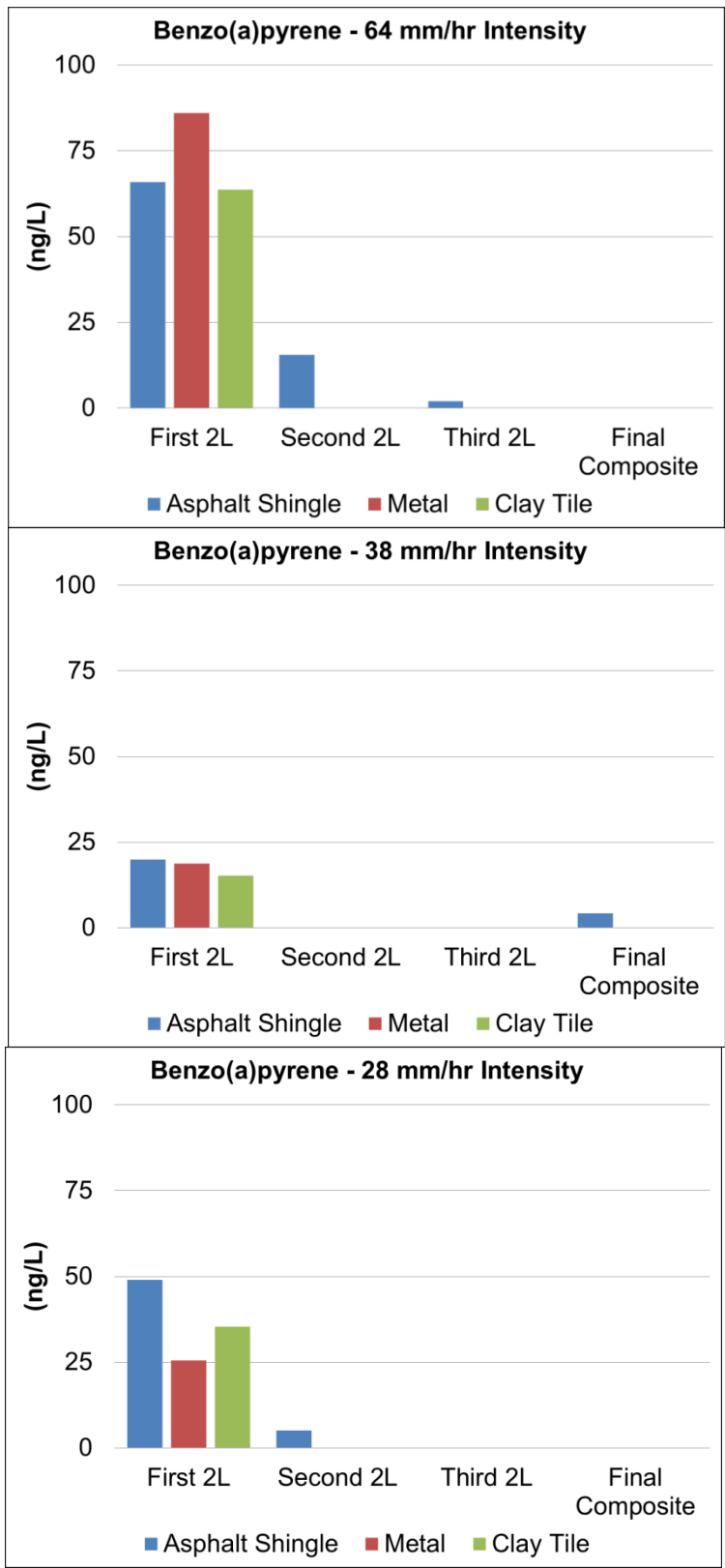


Figure 3. Average benzo(a)pyrene concentration for rooftop runoff at different intensities and roof types.

Oklahoma City Harvested Rainfall. Between April and July 2012, water samples were collected from the rooftop runoff during 10 storms. These samples have been analyzed in the laboratory, but interpretation of the results has not yet been completed. Full analysis is completed in the final report that will be submitted in December 2013.

Soil sampling below downspouts. Between April and July 2012, soil samples were collected from below downspouts and in nearby areas not affected by rooftop runoff from 30 different buildings—10 buildings with three different types of roofing materials. These samples have been analyzed in the laboratory, but interpretation of the results has not yet been completed. Full analysis is completed in the final report that will be submitted in December 2013.

Leaching studies. These studies are currently in progress, with final results expected in fall 2013. The results of these studies will be included in the final report.

Impact of Wastewater Treatment Plant Effluent on Nitrogen Cycling by Stream Bacteria

Basic Information

Title:	Impact of Wastewater Treatment Plant Effluent on Nitrogen Cycling by Stream Bacteria
Project Number:	2012OK241B
Start Date:	3/1/2012
End Date:	2/28/2013
Funding Source:	104B
Congressional District:	2
Research Category:	Water Quality
Focus Category:	Nutrients, Wastewater, Hydrogeochemistry
Descriptors:	None
Principal Investigators:	Cindy R Cisar, Jonathan Fisher, Joy Van Nostrand

Publications

There are no publications.

Student Status	Number	Disciplines
Undergraduate	4	Biology
M.S.	2	Biology
Ph.D.	0	
Post Doc	0	
Total	6	

Technical Report

Title: Impact of Wastewater Treatment Plant Effluent on Nitrogen Cycling by Stream Bacteria

Authors' Names and Affiliations

Cindy R. Cisar
Associate Professor
Department of Natural Sciences
Northeastern State University
cisar@nsuok.edu
918-444-3841

Jonathan Fisher
Assistant Professor
Department of Natural Sciences
Northeastern State University
fisher10@nsuok.edu
918-444-3831

Joy Van Nostrand
Research Scientist
Institute for Environmental Genomics, University of Oklahoma
joy.vannostrand@ou.edu
405-325-4403

Start Date: 03/01/12

End Date: 02/28/13

Congressional District: 2

Focus Category: NU, SED, SW, WW

Descriptors: nitrogen cycle, bacteria, wastewater treatment plant effluent, antibiotics

Principal Investigators:

Cindy R. Cisar
Associate Professor
Department of Natural Sciences
Northeastern State University
cisar@nsuok.edu
918-444-3841

Jonathan Fisher
Assistant Professor
Department of Natural Sciences
Northeastern State University
fisher10@nsuok.edu
918-444-3831

Joy Van Nostrand
Research Scientist
Institute for Environmental Genomics, University of Oklahoma
joy.vannostrand@ou.edu
405-325-4403

Publications: None at the time this report was prepared. We anticipate that at least two manuscripts will be prepared for submission. The OWRRI will be notified of any future publications that result from this work.

Problem and Research Objectives:

Treated wastewater contains nutrients, such as ammonium (NH_4^+), and organic compounds, such as antibiotics. Nitrogen is both an essential nutrient and a potential pollutant that can lead to degradation of water quality when levels in the environment are high. Antibiotics at high concentrations can kill or inhibit the growth of bacteria. However, it has also been suggested that low concentrations of antibiotics play a role in bacterial communication in natural ecosystems and can cause changes in bacterial gene expression. The effects of contaminants, including nitrogen and antibiotics, in wastewater treatment plant effluent on nitrogen cycling in downstream bacterial populations are not well understood.

This study had four objectives.

1. To characterize bacterial diversity in a stream that receives wastewater treatment plant effluent, and compare upstream and downstream populations
2. To determine the abundance of bacterial genes encoding enzymes involved in nitrogen cycling in bacterial populations upstream and downstream of a wastewater treatment plant
3. To examine the expression of genes involved in nitrogen cycling in bacteria downstream of a wastewater treatment plant and compare to the upstream population
 - a. In addition, in-stream uptake of ammonium (NH_4^+) upstream and downstream of the Tahlequah WWTP will be measured and compared.
4. To examine ammonium (NH_4^+) uptake by sediment bacteria and the effect(s) of antibiotics on bacterial nitrogen metabolism

Methodology:

Extraction of nucleic acids from stream sediments

Tahlequah Creek sediments, 200m upstream and 100m downstream of the Tahlequah wastewater treatment plant, (WWTP) were sampled twelve times over the course of this study. Sediment samples were stored on ice until processed. All samples were processed within 6 hrs of sampling. A MoBio Power Max® Soil DNA isolation kit was used to purify high quality DNA from 5g of sediment. DNA samples were concentrated by ethanol precipitation and stored at -80°C in 10mM Tris pH 7.4 buffer. A MoBio PowerSoil® Total RNA Isolation kit was used to purify RNA from 2g of sediment. Although yields were high using the MoBio kit the RNA was contaminated with RNases, which resulted in degradation of the RNA when we attempted to purify mRNA from total RNA. mRNA is preferred over total RNA in gene expression studies as signal intensities are increased. Several attempts were made to obtain RNase-free total RNA including additional phenol extraction of the RNA samples, use of two RNA Capture columns during purification with the MoBio kit, and use of an RNA-binding column (MEGAclean™ Kit, Invitrogen) for removal of contaminants from RNA. However, none of the treatments was successful. Therefore, we decided to use total RNA rather than mRNA for preparation of fluorescently labeled cDNA. The RNA pellets obtained from the MoBio PowerSoil® Total RNA Isolation kit were resuspended in RNA Storage Solution (Ambion®) and stored at -80°C. Nucleic acids were quantitated using a Qubit® 2.0 fluorometer and dsDNA Broad Range Assay or RNA Assay kits (Invitrogen). Nucleic acids were purified from triplicate biological replicates (sediment samples) taken at the upstream and downstream locations.

GeoChip hybridization and scanning

Fluorescently labeled genomic DNA (gDNA) was prepared and hybridized to GeoChip 4.0 (NimbleGen) arrays as described previously (Wu et al. 2006; Lu et al. 2011). In brief, 1 µg of gDNA was labeled with Cy-3 by random priming. Labeled gDNA was suspended in hybridization buffer containing a universal standard DNA labeled with the fluorescent dye Cy-5 (Liang et al. 2010). Fluorescently labeled cDNA was prepared from total RNA as described by He et al. (He et al. 2005). In brief, 500ng of total RNA was amplified using a MessageAmp™ II-Bacteria Kit (Invitrogen). Ten micrograms of amplified RNA (aRNA) was then used to prepare Cy-5 labeled cDNA using random primers and reverse transcriptase. Labeled cDNA was suspended in hybridization buffer containing a universal standard DNA labeled with the fluorescent dye Cy-3. Fluorescently labeled nucleic acids were denatured and loaded onto GeoChip 4.0 microarrays. Twelve arrays were used in these experiments: 3 arrays were hybridized with Cy-5 labeled gDNA from replicate upstream sediment samples, 3 arrays were hybridized with Cy-5 labeled gDNA from replicate downstream sediment samples, 3 arrays were hybridized with Cy-3 labeled cDNA derived from replicate upstream sediment RNA samples, and 3 arrays were hybridized with Cy-3 labeled cDNA derived from replicate downstream sediment RNA samples. Hybridization was performed overnight using a Hybridization Station (Maui; Roche). Arrays were washed and scanned using an MS 200 Microarray Scanner (NimbleGen).

GeoChip 4.0 data analyses

Raw data were analyzed using the Institute for Environmental Genomics data analysis pipeline (ieg.ou.edu) as described previously (He et al. 2010). Signal intensities of GeoChip hybridization spots were normalized across samples using the universal standards included in the hybridization

buffers. Positive spots were selected based on signal-to-noise ratios [(signal intensity-background intensity)/background standard deviation]. Cy-5 labeled gDNA positive spots had signal-to-noise ratios (SNRs) ≥ 2.0 . Cy-3 labeled cDNA (from RNA) positive spots had SNRs ≥ 2.0 and SNRs ≥ 1.0 for the corresponding gDNA probes. All signal intensities were log-normal transformed. A minimum of two valid values was required for each gene included in the analyses.

Statistical analyses included calculation of diversity indices (Shannon and Simpson), cluster analysis, dissimilarity analysis, and analysis of gene categories and genes using a T-test.

Bacterial diversity based on pyrosequencing of 16S rRNA genes

Artificial substrates (Fluval Biomax bio rings, Hagen) were buried in Tahlequah Creek sediments upstream and downstream of the Tahlequah WWTP (200 m and 100 m, respectively) 30d prior to sampling to allow for colonization by resident bacteria. The bio rings are porous ceramic media designed for biological filtration in aquarium systems. A MoBio Power Max® Soil DNA isolation kit was used to purify high quality DNA from 10-12 g of bio rings and from 5g of sediment. Artificial substrate and sediment samples were harvested simultaneously from the locations described above. All samples were placed on ice and processed within 6 hours of sampling or stored at -20°C until processed. DNA samples were concentrated by ethanol precipitation and stored at -80°C in 10mM Tris pH 7.4 buffer.

Bacterial FLX-Titanium amplicon pyrosequencing (TEFAP) and data processing were performed at the Research and Testing Laboratory (Lubbock, TX) as described previously (Handl et al. 2011). In brief, small subunit rRNA gene primers, forward28F (GAGTTTGATCNTGGCTCAG) and reverse519R (GTNTTACNGCGGCKGCTG), were used to generate sequence data that included the V1–V3 hypervariable regions. Analysis of sequence data was performed in two stages. Stage I, sequence reads were checked for quality and denoised. Chimeras and poor quality sequences were removed. Stage II, sequencing data was used to examine bacterial diversity in the samples. Sequences were queried against a database of high quality sequences derived from NCBI (KrakenBLAST www.krakenblast.com) and classified at the appropriate taxonomic levels using the following criteria. Sequences with $> 97\%$ identity were resolved at the species level, between 95% and 97% at the genus level, between 90% and 95% at the family level, between 85% and 90% at the order level, between 80 and 85% at the class level, and between 77% to 80% at the phyla level. Files containing taxonomic information for each read and the number and percentage of each taxonomic group within each sample were generated.

Artificial substrate and stream sediment communities were compared to determine if the bacterial populations were similar or different using principal components analysis (CANOCO for Windows 4.53).

In-stream nitrogen uptake

Ammonium chloride was introduced to the stream at a constant rate 100m upstream from each sample site (upstream and downstream of the Tahlequah WWTP). Specific conductivity was used as a conservative tracer in-stream and to correct for dilution in samples analyzed in the laboratory. Once in-stream conductivity reached a stable maximum water samples were taken every 10m downstream of the injection point for 100m. These samples were placed on ice and transported back to the laboratory for analysis of total ammonia, nitrite, nitrate, total nitrogen,

and conductivity. These experiments were replicated three times at each site during the summer and fall of 2012.

Summary statistics, linear regressions, and graphical representations of data were accomplished in MS Excel.

Nitrogen cycling by bacteria on colonized artificial substrates with and without antibiotics

Artificial substrates (Fluval Biomax bio rings, Hagen) buried in Tahlequah Creek sediments for 60d were harvested and taken to the laboratory in sterile containers. Individual rings were placed in sterilized 300ml BOD bottles containing Tahlequah Creek water from the relevant study site (upstream or downstream of the Tahlequah WWTP). Ammonium chloride was added to achieve a concentration of 1mg/liter total ammonia as nitrogen, with and without an antibiotic. Dissolved oxygen was measured in each bottle. Bottles were then incubated at 20°C in the dark for 5d after which dissolved oxygen, total ammonia, nitrite, nitrate, and total nitrogen were measured in each replicate. Antibiotic concentrations were chosen to represent 0x, 1x, and 10x concentrations where x represents a previously measured environmental concentration for that antibiotic. The antibiotics used were azithromycin, ciprofloxacin, erythromycin, sulfamethoxazole, triclosan, trimethoprim, and tylosin (Table 1). Four replicates of each antibiotic concentration were analyzed for each site.

Table 1. Nominal concentrations and literature source for each of the antibiotics used in the experiments described above. Concentrations represent the 1x or environmental concentrations.

Antibiotic	Nominal Concentration	Units	Source
Triclosan	0.250	ug/L	(Haggard et al. 2006)
Erythromycin	0.175	ug/L	(Haggard et al. 2006)
Trimethoprim	0.190	ug/L	(Haggard et al. 2006)
Tylosin	0.012	ug/L	(Haggard et al. 2006)
Ciprofloxacin	0.039	ug/L	(Haggard et al. 2006)
Sulfamethoxazole	0.500	ug/L	(Haggard et al. 2006)
Azithromycin	0.042	ug/L	(Cisar <i>et al.</i> , manuscript submitted)

One-way ANOVA's with Fisher's LSD post-hoc comparisons to test a-priori comparisons of antibiotic screening experiments were done using IBM SPSS Statistics 19.

Principal Findings and Significance:

Bacterial diversity in sediments upstream and downstream of the Tahlequah wastewater treatment plant based on 16S rRNA gene pyrosequencing (Objective 1)

Bacterial operational taxonomic units (OTUs) identified in sediment samples from upstream and downstream of the Tahlequah wastewater treatment plant (WWTP) were not the same. At the phylum level, bacteria from 22 phyla were present in Tahlequah Creek sediments (Table 2). However, only 20 of the 22 phyla were present at each location. Chrysiogenetes and Aquificae were present only in sediments downstream of the WWTP while Deferribacteres and Fusobacteria were present only in sediments upstream of the WWTP. The abundance of some phyla could be quite different between upstream and downstream sediments. For example, the percentage of Acidobacteria downstream of the WWTP was almost two times the percentage upstream of the WWTP. Upstream of the WWTP eight phyla were abundant (present at levels > 1%) making up > 96% of bacteria identified. Downstream of the WWTP nine phyla were abundant (present at levels > 1%) making up > 97% of bacteria identified. Most of these phyla were abundant (defined as 1% or greater of the total bacteria) in both upstream and downstream sediments. However, Cyanobacteria and Actinobacteria were present at < 1% in upstream sediment and Firmicutes were present at < 1% in downstream sediment. Two of the phyla, Nitrospirae and Cyanobacteria, were more abundant in downstream sediment than in upstream sediment and are particularly interesting as they play important roles in cycling of nitrogen in streams. Species of Nitrospirae convert nitrite (NO₂⁻) to nitrate (NO₃⁻). Cyanobacteria are more abundant in streams polluted with nitrogen and high numbers of cyanobacteria can be indicative of poor water quality.

Table 2. Bacteria Present in Tahlequah Creek Sediments by Phylum

Phylum	Upstream of WWTP (%)	Downstream of WWTP (%)
Proteobacteria	39.311	37.765
Bacteroidetes	20.368	12.804
Nitrospirae	17.963	24.333
Acidobacteria	6.888	13.569
Verrucomicrobia	5.879	1.902
Chloroflexi	3.593	2.745
Firmicutes	1.455	0.725
Planctomycetes	1.099	1.647
Cyanobacteria	0.831	1.784
Actinobacteria	0.445	1.000
Fibrobacteres	0.445	0.431
Lentisphaerae	0.386	0.510
Chlorobi	0.386	0.176
Gemmatimonadetes	0.297	0.078
Deinococcus-Thermus	0.267	0.157
Dictyoglomi	0.148	0.196
Spirochaetes	0.119	0.020
TM7	0.059	0.118
Deferribacteres	0.030	0
Fusobacteria	0.030	0
Chrysiogenetes	0	0.020
Aquificae	0	0.020

16S rRNA gene sequences obtained by pyrosequencing were used to compare bacterial diversity in sediments upstream and downstream of the Tahlequah WWTP at the phylum, genus, and species levels (Table 3). The data indicates that the bacterial populations at the two locations (sediments upstream and downstream of the WWTP) were similar, but not identical, at the phylum level. However, the populations appeared more different at the genus and species levels.

Table 3. Shannon diversity index and number of OTU's observed at the phylum level (20% sequence dissimilarity), genus level (5% sequence dissimilarity), and species level (3% sequence dissimilarity).

	Upstream sediment	Downstream sediment
Phylum level (20% dissimilarity)		
Shannon diversity index (H)	1.74	1.77
OTUs	20	20
Genus level (5% dissimilarity)		
Shannon diversity index (H)	4.12	5.17
OTUs	261	281
Species level (3% dissimilarity)		
Shannon diversity index (H)	4.25	3.92
OTUs	322	339

Pyrosequencing of 16S rRNA genes from bacteria in sediment samples taken upstream and downstream of a wastewater treatment plant showed that bacterial diversity was high at both sites (Table 3). Although the bacterial populations share similarities they also differ at all three levels with regard to their specific makeup. For example, Cyanobacteria is a highly diverse phylum. Current estimates of described species of Cyanobacteria range from 3,234 to 2,664 different species (<http://www.environment.gov.au/biodiversity/abrs/publications/other/species-numbers/2009/pubs/08-nlsaw-others.pdf>). Seventeen cyanobacterial species were identified in upstream sediment and sixteen cyanobacterial species were identified in downstream sediment (Table 4). Only nine of these species were present at both locations although the sites are only 300m apart. Preliminary analysis of data indicates that the wastewater treatment plant effluent, which is essentially the only environmental factor that is different between the two locations, does have an impact on downstream bacterial populations.

Table 4. Cyanobacterial species present in sediments

Species	Upstream sediment (%)	Downstream sediment (%)
Cyanothece sp ¹	0.089073634	0.294117647
Gloeocapsa sp	0.059382423	0.019607843
Gloeotheca sp	0	0.039215686
Microcystis aeruginosa	0.059382423	0
Synechococcus sp	0	0.156862745
Chamaesiphon subglobosus	0	0.019607843
Tolypothrix sp	0.089073634	0
Anabaena sp	0.089073634	0.098039216
Cylindrospermum sp	0.029691211	0
Dolichospermum lemmermanii	0.029691211	0
Nodularia spumigena	0	0.019607843
Nostoc sp	0.029691211	0
Scytonema sp	0.029691211	0
Geitlerinema sp	0.029691211	0.078431373
Leptolyngbya frigida	0	0.019607843
Leptolyngbya sp	0.059382423	0.058823529
Lyngbya sp	0	0.019607843
Pleurocapsa sp	0.089073634	0.450980392
Dermocarpella sp	0.029691211	0.098039216
Myxosarcina sp	0.029691211	0.039215686
Solentia sp	0.029691211	0
Xenococcus sp	0	0.019607843
Gloeobacter violaceus	0.029691211	0
Chroococciopsis sp	0.029691211	0.352941176

¹Due to incomplete taxonomic data for some organisms some entries have no specific species name. These are abbreviated <Genus> sp.

Analysis of microbial communities from sediments upstream and downstream of a WWTP using a functional gene array probed with genomic DNA (Objective 2)

The GeoChip 4.0 array contains 83,992 50-mer oligonucleotide probes targeting 152,414 genes in 410 gene categories for different microbial functional and biogeochemical processes. Functional gene categories include antibiotic resistance, bacteriophage, bioleaching, carbon cycling, energy processes, fungal genes, metal resistance, nitrogen cycling, organic remediation, phosphorous cycling, stress proteins, sulphur cycling, beneficial in soil, soil borne pathogens, and virulence. Arrays were hybridized with fluorescently labeled genomic DNA (gDNA) extracted from sediments upstream and downstream of the Tahlequah WWTP. Similar numbers of genes were detected on each array (Table 5). In addition, the gene overlap between arrays was high: 73-92% overlap among upstream samples, 85-89% overlap among downstream samples, 70-80% overlap between upstream and downstream samples.

Table 5. Total number of genes detected per GeoChip array and gene overlap between arrays¹

	U/S I	U/S J	U/S K	D/S I	D/S J	D/S K
U/S I		24333(74.10%)	30049(91.50%)	26282(77.75%)	25414(75.47%)	25558(75.93%)
U/S J			24007(73.11%)	22589(71.81%)	22603(74.24%)	22211(71.73%)
U/S K				26612(80.28%)	25830(78.43%)	26011(79.11%)
D/S I					26213(88.11%)	26339(88.53%)
D/S J						25342(85.18%)
D/S K						
Total	31607	25565	31281	28480	27483	27609

¹Triplicate biological replicates (I, J, K) were used in these experiments. U/S = upstream sediment, D/S = downstream sediment.

Microbial diversity and species evenness in upstream and downstream sediments was also measured using GeoChip array data (Table 6). Results indicate high levels of microbial diversity in both locations, upstream and downstream of the WWTP, and very high levels of species evenness.

Table 6. Diversity indices and species evenness for microorganisms in sediments upstream and downstream of the Tahlequah WWTP

	Shannon Index (H)	Simpson Index (D)	Pielou evenness (J)	Simpson evenness (Si)
Upstream	10.28 +0.12	29235.7 +3313.7	0.9996 +0.00	0.9917 +0.00
Downstream	10.23 +0.02	27649.6 +534.8	0.9996 +0.00	0.9925 +0.00

Cluster analysis of the GeoChip array data revealed that the microbial populations in upstream and downstream sediments are different (Figure 1). However, one of the upstream sediment samples (T1S J) is more similar to the downstream sediment samples than the other two upstream samples (T1S I and K).

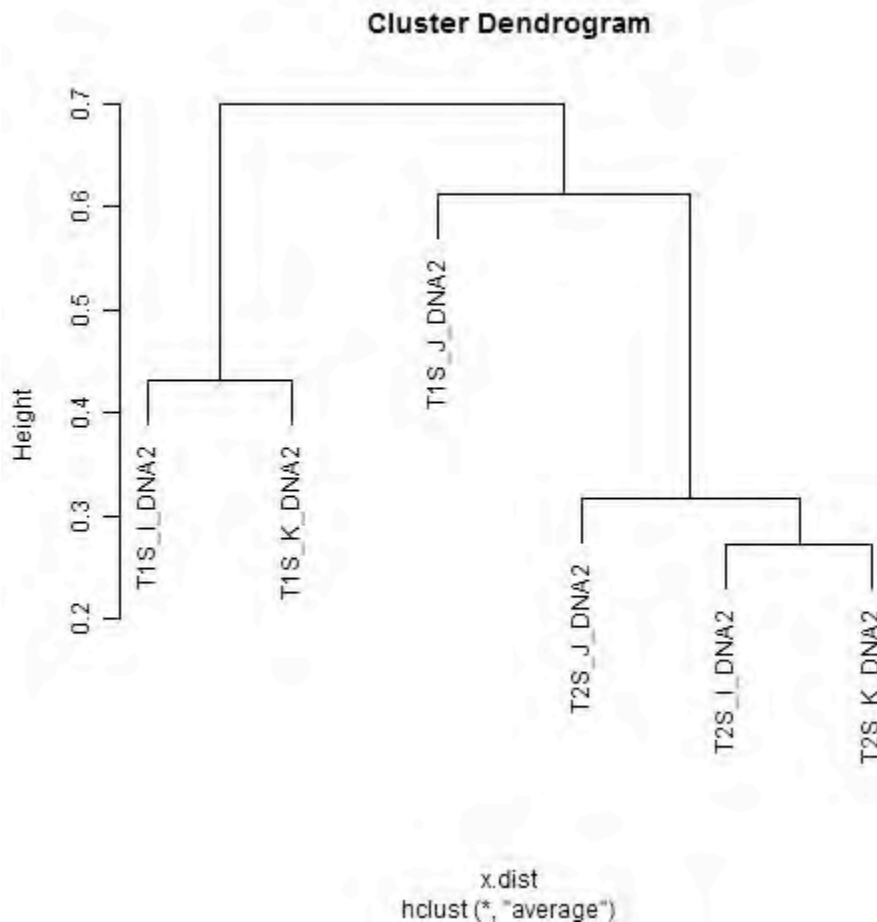


Figure 1. Hierarchical cluster analysis of GeoChip array data. T1S = upstream sediment (I, J and K are biological replicates). T2S = downstream sediment (I, J and K are biological replicates).

Figure 2 shows the relative abundance of the different categories of functional genes in sediments upstream and downstream of the Tahlequah WWTP. Very similar percentages of gene groups in upstream and downstream samples were observed. However, statistically significant differences were observed for ‘other category’ genes (T-test; $p=0.03$), which includes *gyrB* and genes for chlorophyllide reductase. Further examination of these results is planned.

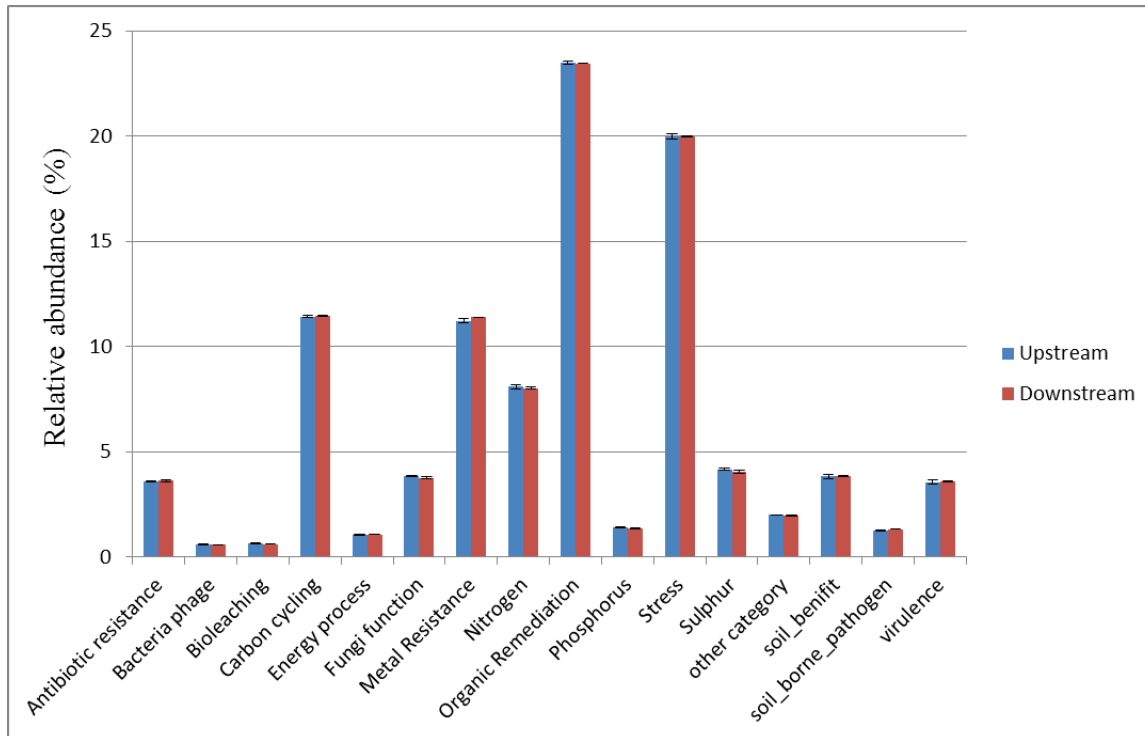


Figure 2. Relative abundances of functional genes by category on GeoChip 4.0 arrays hybridized with genomic DNA from sediment samples from upstream and downstream of a WWTP. Error bars are SD.

The analyses of the GeoChip 4.0 array data described above suggest that the microbial communities upstream and downstream of the WWTP are similar, *i.e.* in terms of diversity (Table 6), functional ability (Figure 2) and even community members (Table 5). However, when examining the structure of the communities (presence/absence and abundance of individual sequences) via clustering and dissimilarity analysis, differences between the upstream and downstream communities are apparent (Table 7).

Table 7. Dissimilarity analysis of upstream and downstream microbial communities at the level of gene category

adonis	euclidean		manhattan		bray curtis		binomial	
	Delta	p-value	Delta	p-value	Delta	p-value	Delta	p-value
Organic Remediation	0.36	0.038	0.393	0.001	0.398	0.042	0.434	0.001
Soil_benefit	0.372	0.046	0.429	0.033	0.433	0.056	0.483	0.07
Antibiotic resistance	0.366	0.001	0.405	0.063	0.406	0.011	0.449	0.068
Carbon cycling	0.376	0.001	0.428	0.049	0.432	0.059	0.475	0.056
Stress	0.363	0.001	0.405	0.001	0.407	0.065	0.445	0.04
Sulfur cycling	0.388	0.001	0.442	0.001	0.45	0.053	0.486	0.001
Virulence	0.388	0.001	0.442	0.001	0.445	0.001	0.499	0.001
Phosphorus cycling	0.367	0.001	0.428	0.016	0.433	0.055	0.464	0.057
Fungi function	0.378	0.001	0.446	0.035	0.45	0.033	0.497	0.001
Nitrogen cycling	0.389	0.001	0.445	0.001	0.448	0.061	0.49	0.075
Metal Resistance	0.369	0.001	0.419	0.043	0.421	0.001	0.467	0.036
Other category	0.384	0.017	0.445	0.001	0.452	0.059	0.491	0.001
Soil_borne_pathogen	0.382	0.001	0.456	0.072	0.454	0.054	0.509	0.001
Bioleaching	0.338	0.049	0.346	0.127	0.347	0.162	0.377	0.137
Energy process	0.289	0.001	0.299	0.183	0.308	0.088	0.326	0.049
Bacteriophage	0.366	0.001	0.407	0.05	0.416	0.001	0.44	0.046

Examination of expression of nitrogen cycling genes in sediments upstream and downstream of the Tahlequah WWTP using a functional gene array, GeoChip 4.0 (Objective 3)

The experimental results above describe microbial community functional structure, or more specifically, the similarities and differences between the upstream and downstream sediment communities based on the abundance of certain genes. The presence/abundance of genes in a habitat indicates the *potential* for that population to perform a particular function. However, knowledge of the *amount of messenger RNA* (a measure of gene expression) produced by these bacteria is a *better indicator of their actual capacity* for nitrogen cycling. Therefore, GeoChip arrays were hybridized with fluorescently-labeled cDNA prepared from RNA extracted from the sediments described above. As expected, far fewer genes were expressed than were present in these communities (compare Tables 5 and 8).

Table 8. Total number of genes expressed per GeoChip array and gene overlap between arrays¹

	U/S I	U/S J	U/S K	D/S I	D/S J	D/S K
U/S I		6588(97.72%)	6596(97.81%)	6631(98.22%)	6131(90.87%)	6522(96.55%)
U/S J			6613(98.22%)	6634(98.22%)	6146(91.21%)	6529(96.67%)
U/S K				6649(98.52%)	6150(91.19%)	6540(96.85%)
D/S I					6185(91.62%)	6576(97.29%)
D/S J						6130(91.48%)
D/S K						
Total	6662	6668	6678	6720	6216	6615

¹Triplicate biological replicates (I, J, K) were used in these experiments. U/S = upstream sediment, D/S = downstream sediment.

In-stream Nitrogen Uptake Experiments (Objective 3a)

Though stream discharge was always similar between sites on the same day, there was variability in discharge between sampling days. Results from the nitrogen uptake experiments were converted to percent of ambient concentrations for each experiment to help correct for this variability. A significant relationship ($P < 0.05$) for total ammonia and none of the other measured nutrients uptake was developed (Figure 4). This relationship was similar for both sites (Upstream = -0.0105 and Downstream = -0.0112) with the slope of the simple linear regression approximating the rate of nitrogen uptake or conversion by resident nutrient cycling communities. These uptake regressions also explained the majority of variability (Upstream = 59.39% and Downstream = 83.69%) in measured total ammonia concentrations.

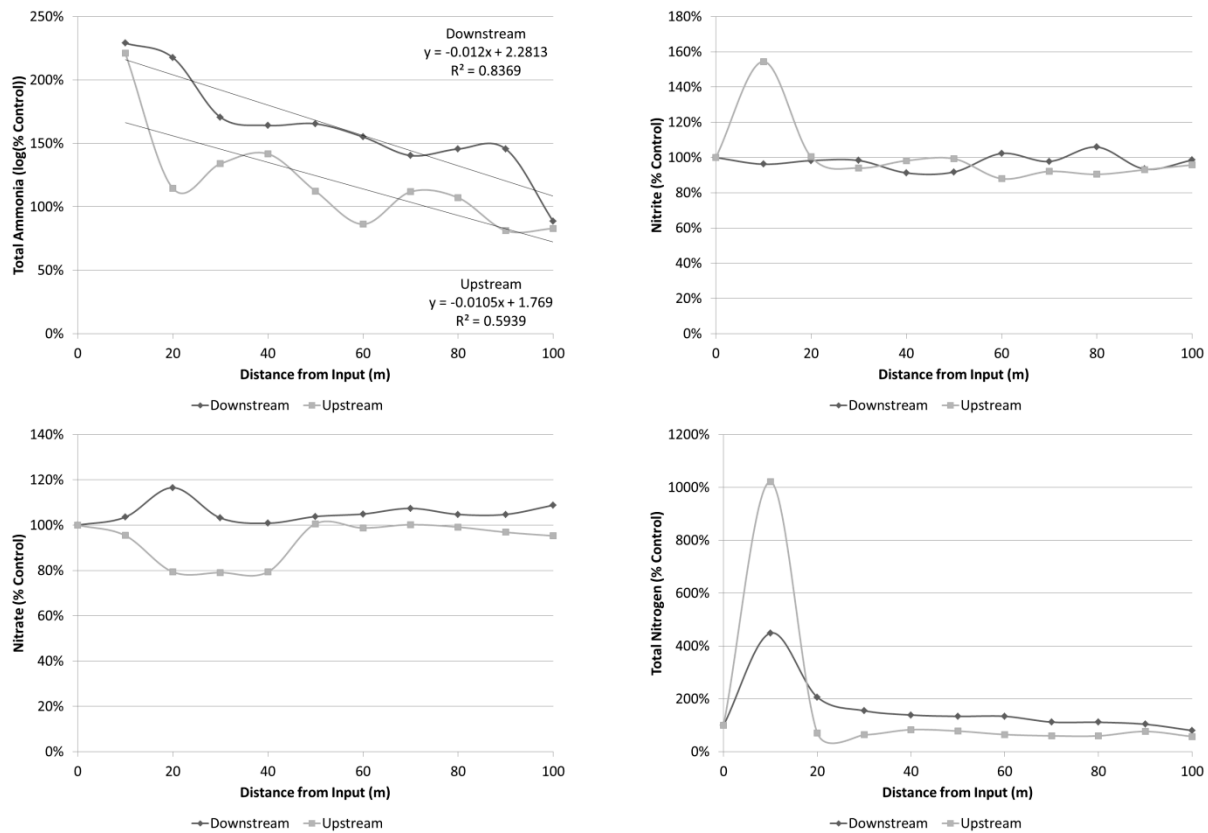


Figure 4. Results for both sites when Ammonium chloride was added to the stream. Uptake rates (linear slopes) could only be derived for ammonia concentrations (top left). Uptake rates for nitrite (top right), nitrate (bottom left) and total nitrogen (bottom right) did not differ from zero.

Comparison of bacterial communities in stream sediments and colonized artificial substrates (Objective 4)

16S rRNA gene sequences were used to identify bacteria present in stream sediments and on artificial substrates buried in stream sediments upstream and downstream of the WWTP for 30d. Bacterial phyla data were analyzed for correlations using a principal components analysis (PCA) (Figure 5). The first two axes of the PCA accounted for 73.71% of the variability in the observed data. The first axis represented the differences between the sediment samples and artificial substrates. The artificial substrates were positively correlated with Planctomycetes, whereas the sediment samples were positively correlated with all other phyla, especially Chloroflexi, Cyanobacteria, Verrucomicrobia, and Actinobacteria. The second axis plots the differences between the phyla present at the two different sample sites, but only for the sediment samples. Firmicutes and Verrucomicrobia were positively correlated with the upstream site, while Actinobacteria, Acidobacteria, Planctomycetes, Proteobacteria, and Nitrospirae were all strongly correlated with the downstream sediment. Preliminary analysis of the data indicates that based on bacterial phyla the artificial substrates were more similar to each other than to stream sediments. However, this analysis is ongoing.

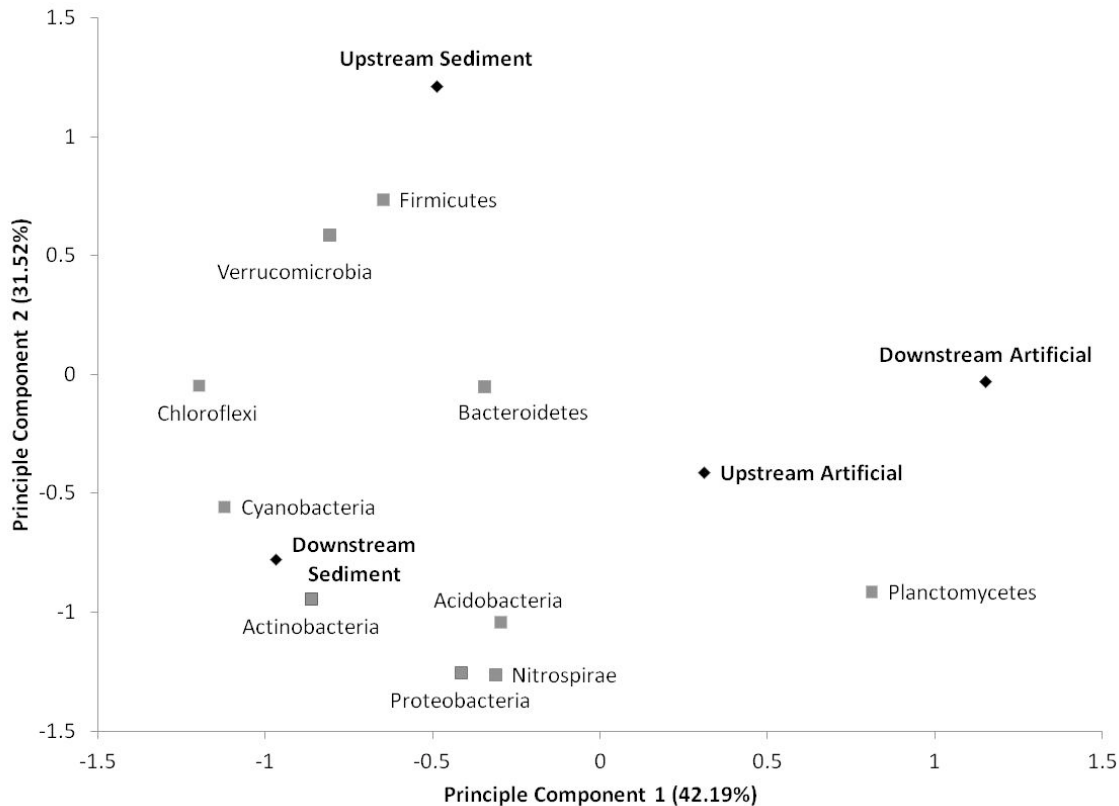


Figure 5. Symmetric biplot of a principal components analysis of bacterial phyla counts from sediment and artificial substrate samples from both study locations (upstream and downstream of the WWTP). Percentages on each axis label represent the percent of variability in the observed data explained by that axis. Sample types and locations are plotted as black diamonds. Bacterial phyla representing at least 1% of the sequences in one sample are plotted as gray squares.

Nitrogen cycling by bacteria on colonized artificial substrates with and without antibiotics (Objective 4)

Although preliminary analysis of the data on bacterial taxa present on artificial substrates colonized by stream bacteria and bacterial taxa present in stream sediments indicated that these populations may be different, experiments examining the effects of antibiotics on bacterial processes using colonized artificial substrates were still deemed valuable and were performed.

Experiments were performed to measure the effect of antibiotics on biochemical oxygen demand (BOD) using colonized artificial substrates from upstream and downstream of the WWTP. Five out of the seven antibiotics applied to laboratory microcosms containing stream water and artificial substrates significantly altered BOD (Figure 6). Sulfamethoxazole, triclosan, and tylosin at environmental (1x) concentrations significantly increased BOD in experiments with upstream colonized artificial substrates. Environmental concentrations (1x) of tylosin also affected BOD in experiments with artificial substrates harvested from the downstream site, but the effect was to reduce BOD. Erythromycin, sulfamethoxazole, triclosan, and trimethoprim increased BOD significantly at ten times (10x) environmental concentrations in experiments with artificial substrates harvested from both sites.

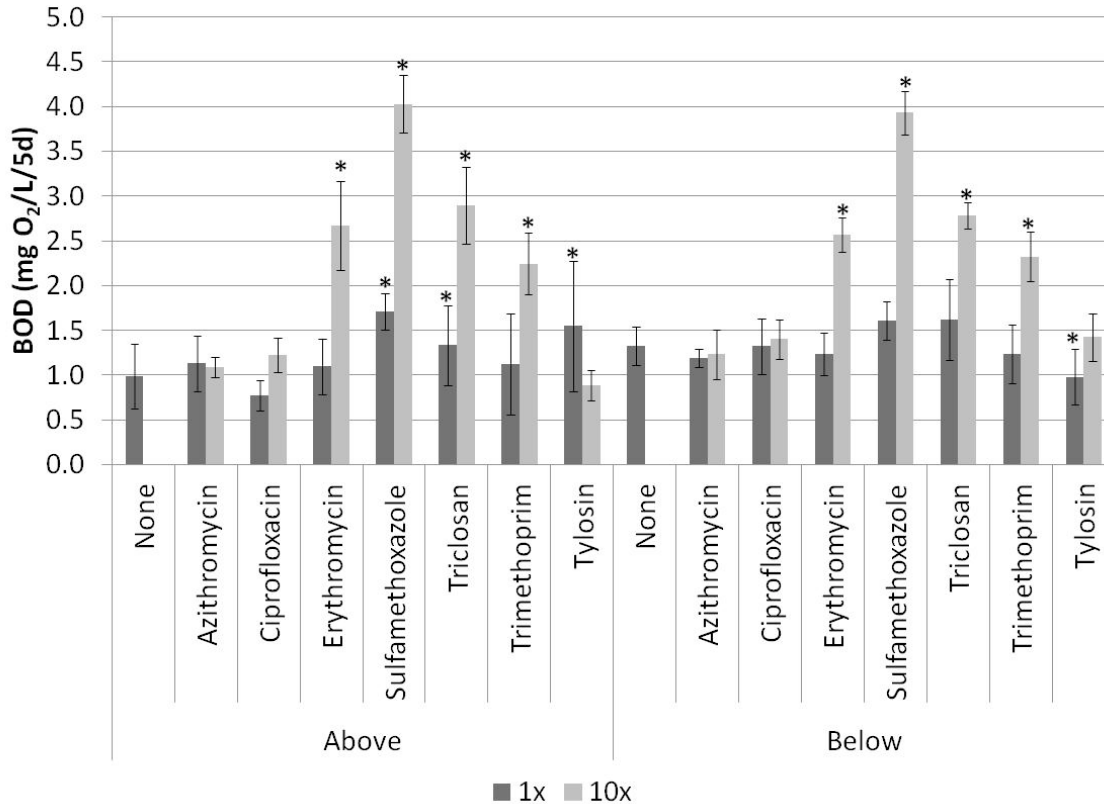


Figure 6. Bar chart representing the mean BOD (Biochemical Oxygen Demand) with colonized artificial substrates in the presence of ammonium chloride and the indicated antibiotics. Each grouping of bars indicates one antibiotic treatment within a site treatment (Above = upstream of WWTP and Below = downstream of WWTP). Dark gray bars represent 1x previously reported environmental antibiotic concentrations and light gray bars represent 10 times those reported concentrations. Asterisks indicate means that significantly differ from the treatment containing no antibiotics within each sampling location. Error bars are standard deviation for each treatment.

Four out of the seven antibiotics significantly affected nitrite production in the laboratory microcosms (Figure 7). At environmental concentrations, only experiments including the antibiotic tylosin showed a significant change in nitrite concentrations. In experiments with colonized artificial substrates from upstream of the WWTP nitrite levels were significantly higher in the presence of 1x tylosin. In experiments with colonized artificial substrates from downstream of the WWTP nitrite levels were significantly lower in the presence of 1x tylosin. Azithromycin, sulfamethoxazole, and triclosan, all at 10x environmental concentrations, significantly decreased nitrite concentrations in downstream treatments.

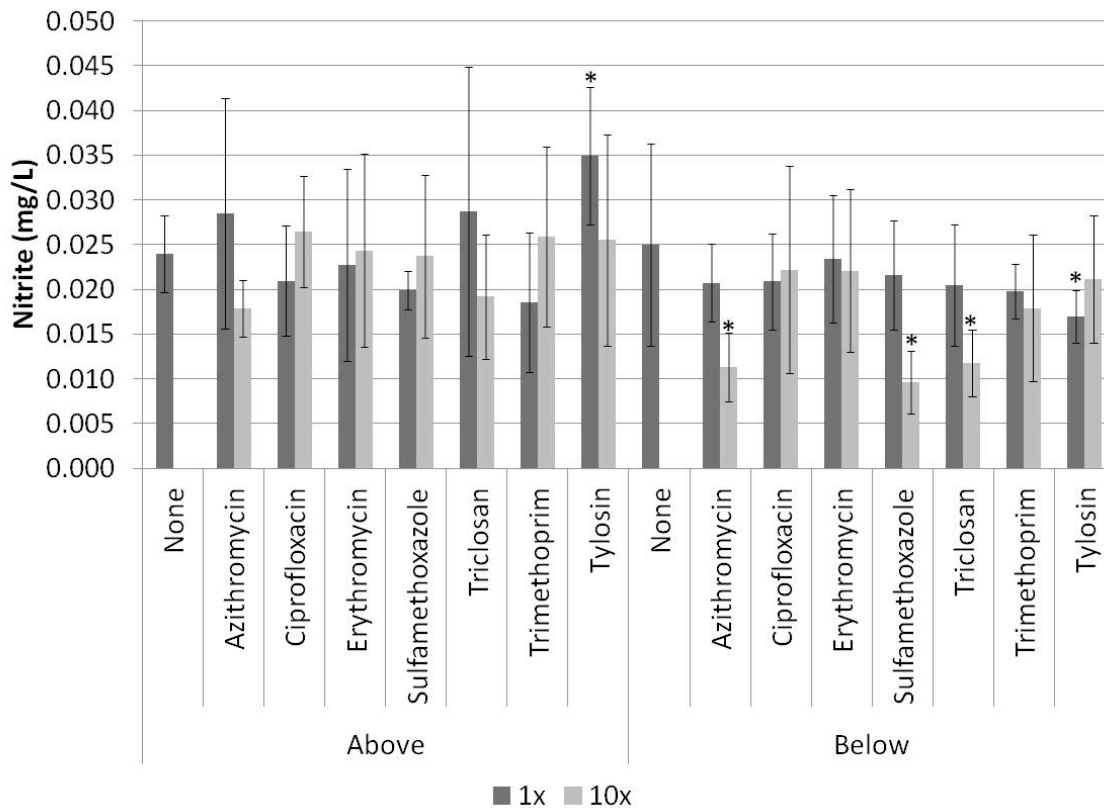


Figure 7. Bar chart representing the mean nitrite concentrations generated with colonized artificial substrates in the presence of ammonium chloride and the indicated antibiotics. Each grouping of bars indicates one antibiotic treatment within a site treatment (Above = upstream of WWTP and Below = downstream of WWTP). Dark gray bars represent 1x previously reported environmental antibiotic concentrations and light gray bars represent 10 times those reported concentrations. Asterisks indicate means that significantly differ from the treatment containing no antibiotics within each sampling location. Error bars are standard deviation for each treatment.

All seven antibiotics affected nitrate concentrations in our experiments, though most of the effects were limited to the downstream treatments (Figure 8). Sulfamethoxazole (10x concentration, upstream treatment) and azithromycin (10x concentration, downstream treatment) significantly reduced nitrate concentrations. In the downstream experimental units environmental concentrations of azithromycin, ciprofloxacin, triclosan, and trimethoprim significantly increased nitrate concentrations. Also in the downstream microcosms 10x concentrations of erythromycin, sulfamethoxazole, trimethoprim, and tylosin resulted in increased nitrate concentrations.

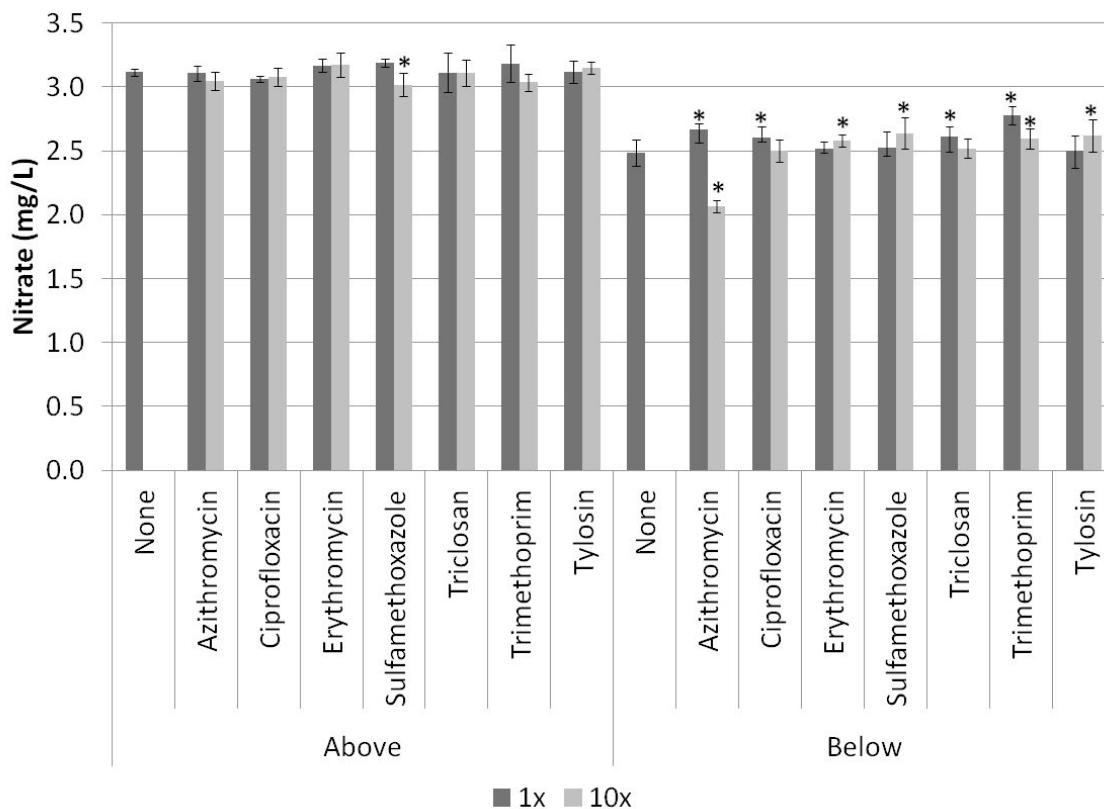


Figure 8. Bar chart representing the mean nitrate concentrations generated with colonized artificial substrates in the presence of ammonium chloride and the indicated antibiotics. Each grouping of bars indicates one antibiotic treatment within a site treatment (Above = upstream of WWTP and Below = downstream of WWTP). Dark gray bars represent 1x previously reported environmental antibiotic concentrations and light gray bars represent 10 times those reported concentrations. Asterisks indicate means that significantly differ from the treatment containing no antibiotics within each sampling location. Error bars are standard deviation for each treatment.

Summary

No differences were observed in ammonium uptake rates at the upstream and downstream study sites, indicating that the wastewater treatment plant has no effect on the ecological function of stream communities responsible for nitrogen processing. However, other data indicate that some aspects of nitrogen processing may be affected in downstream sediments, though more research

is needed, and that wastewater treatment plant effluent does have an impact on downstream microorganisms. For example, the upstream and downstream bacterial communities are different based on 16S rRNA gene pyrosequencing data. Dissimilarity analysis of the data from GeoChip 4.0 arrays probed with genomic DNA from sediment also indicates differences between the upstream and downstream sediment microbiota. Furthermore, several genes encoding enzymes involved in nitrogen cycling have been found to be expressed at lower levels in microbial communities downstream of the wastewater treatment plant. Analysis of abundance and expression of nutrient cycling genes in these populations is ongoing.

The data presented here indicate that environmentally relevant concentrations of antibiotics can significantly affect nutrient cycling in microbial stream communities. Several antibiotics increased the oxygen demand of these communities. The current data set does not indicate whether the increase in oxygen use is from stressing or stimulating the communities. Decreased nitrite concentrations in the presence of antibiotics could indicate that less nitrite was being produced or that the conversion of nitrite to other products was stimulated. Similarly, increased nitrate concentrations in the presence of antibiotics could indicate the stimulation of cellular processes that stimulate nitrate production, or that nitrate uptake/processing was inhibited. The experiments presented here are preliminary studies on the effects of environmentally relevant antibiotics on nutrient cycling. Additional experiments will be required to more precisely describe the impact of antibiotics on nitrogen cycling by microbial communities and to correlate laboratory results with ecological data.

References

- Haggard, B. E.; Galloway, J. M.; Green, W. R.; Meyer, M. T. (2006) Pharmaceuticals and Other Organic Chemicals in Selected North-Central and Northwestern Arkansas Streams. *J Environ Qual*, 35, 1078-1087.
- Handl, S.; Dowd, S. E.; Garcia-Mazcorro, J. F.; Steiner, J. M.; Suchodolski, J. S. (2011) Massive Parallel 16s Rrna Gene Pyrosequencing Reveals Highly Diverse Fecal Bacterial and Fungal Communities in Healthy Dogs and Cats. *FEMS Microbiol Ecol*, 76, 301-310.
- He, Z.; Deng, Y.; Van Nostrand, J. D.; Tu, Q.; Xu, M.; Hemme, C. L.; Li, X.; Wu, L.; Gentry, T. J.; Yin, Y.; Liebich, J.; Hazen, T. C.; Zhou, J. (2010) Geochip 3.0 as a High-Throughput Tool for Analyzing Microbial Community Composition, Structure and Functional Activity. *ISME J*, 4, 1167-1179.
- He, Z.; Wu, L.; Fields, M. W.; Zhou, J. (2005) Use of Microarrays with Different Probe Sizes for Monitoring Gene Expression. *Appl Environ Microbiol*, 71, 5154-5162.
- Liang, Y.; He, Z.; Wu, L.; Deng, Y.; Li, G.; Zhou, J. (2010) Development of a Common Oligonucleotide Reference Standard for Microarray Data Normalization and Comparison across Different Microbial Communities. *Appl Environ Microbiol*, 76, 1088-1094.
- Lu, Z.; Deng, Y.; Van Nostrand, J. D.; He, Z.; Voordeckers, J.; Zhou, A.; Lee, Y.-J.; Mason, O. U.; Dubinsky, E. A.; Chavarria, K. L.; Tom, L. M.; Fortney, J. L.; Lamendella, R.; Jansson, J. K.; D'haeseleer, P.; Hazen, T. C.; Zhou, J. (2011) Microbial Gene Functions Enriched in the Deepwater Horizon Deep-Sea Oil Plume. *ISME J*, 6, 1751-1762.
- Wu, L.; Liu, X.; Schadt, C. W.; Zhou, J. (2006) Microarray-Based Analysis of Subnanogram Quantities of Microbial Community Dnas by Using Whole-Community Genome Amplification. *Appl Environ Microbiol*, 72, 4931-4941.

Quantitative assessment of climate variability and land surface change on streamflow decrease in the Upper Cimarron River

Basic Information

Title:	Quantitative assessment of climate variability and land surface change on streamflow decrease in the Upper Cimarron River
Project Number:	2012OK244B
Start Date:	3/1/2012
End Date:	2/28/2013
Funding Source:	104B
Congressional District:	3
Research Category:	Climate and Hydrologic Processes
Focus Category:	Hydrology, Surface Water, Water Quantity
Descriptors:	None
Principal Investigators:	Chris Zou, William J Andrews, Juanjun Ge

Publications

1. Ge J and Zou C. 2013. Impacts of woody plant encroachment on regional climate in the Southern Great Plains of the USA. *Journal of Geophysical Research - Atmospheres* (In revision)
2. Zou C, Andrews W, Ge J, Smith J, Dale J. 2013. Climate variability and land surface change on streamflow decrease in the Upper Cimarron River. (In preparation for submission to) *Journal of the American Water Resources Association*

Quantitative assessment of climate variability and land surface change on streamflow decrease in the Upper Cimarron River

Chris Zou

Assistant Professor
Oklahoma State University
562 Agricultural Hall, Stillwater, OK 74078-6013
Tel.: 405-744-9637; Fax: (405) 744-3530
E-mail: chris.zou@okstate.edu

William J. Andrews

Report Specialist, Water-Use Specialist, Hydrologist
USGS, Oklahoma Water Science Center
202 NW 66th Street, Bldg. 7, Oklahoma City, OK 73116
Tel.: 405-810-4416
E-mail: wandrews@usgs.gov

Jianjun Ge

Assistant Professor
GIS Certificate Coordinator
Oklahoma State University
Tel.: 405-744-2864
E-mail: jianjun.ge@okstate.edu

S. Jerrod Smith

Hydrologist
USGS, Oklahoma Water Science Center

Joseph Dale

Graduate Research Assistant
Oklahoma State University
007C Agricultural Hall, Stillwater, OK 74078-6013
E-mail: dalejj@okstate.edu

Start Date: 03/01/2012

End Date: 02/28/2013

Congressional District: 3rd, Ok

Focus Category: AG, CP, GW, HYDTOL, INV, IRRIGATION, MODELS, SURFACE WATER, WATER QUANTITY

Descriptors: Climate variability, Cimarron River, Groundwater withdrawal, Streamflow trend, Woody plant expansion,

Principal Investigators: Chris Zou, Assistant Professor, Oklahoma State University

Publications:

Ge J and Zou C. 2013. Impacts of woody plant encroachment on regional climate in the Southern Great Plains of the USA. *Journal of Geophysical Research – Atmospheres* (In revision)

Zou C, Andrews W, Ge J, Smith J, Dale J. 2013. Climate variability and land surface change on streamflow decrease in the Upper Cimarron River. Preparation for submission to *Journal of the American Water Resources Association*

Number of students supported by the project

Student Status	Number	Disciplines
Undergraduate	1	Engineering
M.S.	1	NREM
Ph.D.	0	
Post Doc	0	
Total	2	

Contents

Problem and Research Objectives	4
Problem statement	4
Scope and objectives	5
Methods and Procedures	6
Climate variability and hydrological cycle trends	6
Precipitation and temperature	6
Water consumption	7
Streamflow.....	7
Groundwater.....	8
Land use and land cover change.....	9
Mapping land use and cover change	9
Nonparametric Estimator of Climate Elasticity and Land Surface Elasticity of Streamflow.....	10
Stepwise Regression	11
Principal Findings and Significance	11
Precipitation and air temperature	11
Consumptive water use	13
Streamflow.....	14
Groundwater storage	15
Hydrologic cycle estimates	17
Land-surface change.....	17
Climatic elasticity and vegetation impact.....	19
Conclusion and Future Research	20
References	21

Problem and Research Objectives

Problem statement

A recent report by Oklahoma Water Resource Board and USGS highlighted the apparent downward trend in long-term streamflow of rivers in northwest and north-central Oklahoma such as the North Canadian River and the Cimarron River (Esralew and Lewis 2008). For example, the 10-year average discharge rate for the Cimarron River since the 1970s is nearly half of that measured in the 1940s and 1950s (**Fig. 1**). Similar downward trends exist for several other rivers in this region.

Continued reduction in river flows could impose profound social, economic and ecological impacts in the northwest and central Oklahoma region. Namely, the North Canadian River provides more than half of the water supply to the City of Oklahoma. The Cimarron River is an important habitat for many fish species including the federally threatened Arkansas River shiner *Notropis girardi* (a priority species identified in the Oklahoma Comprehensive Wildlife Conservation Strategy and the Great Plains Landscape Conservation Cooperative Action Plan).

Despite its importance, streamflow accounts for only a small component of the water budget for semiarid regions (Wilcox 2002), usually less than 10% of precipitation. An increase in precipitation is positively related to total streamflow, in general, but this relation is not linear and depends on climate condition and land surface characteristics (Yang and Yang 2011). This relation varies with time even for the same river basin due to land cover change and human activities (Zheng et al. 2009). Therefore quantifying weighted precipitation (Esralew and Lewis 2008, Wine and Zou 2011) may not completely reveal interactions and feedbacks among climate, land use/land cover changes, and human activities.

Climate variability, including changes in precipitation regime, temperature, vapor pressure, and wind speed, can cause changes in streamflow directly or indirectly (Dam 1999). Land use and land cover change, on the other hand, are believed to affect infiltration and evapotranspiration, which consequently causes changes in groundwater levels and streamflow (Zhang et al. 2001).

Climate elasticity of streamflow proposed by Schaake (Schaake 1990) is an effective indicator identifying the sensitivity of streamflow to climate change (Dooge 1992, Dooge et al. 1999, Sankarasubramanian et al. 2001). After climate elasticity is defined, theoretically, the land surface change elasticity of streamflow can be estimated. Then one can compare the land surface elasticity index to change of land uses, woody cover change (data extracted from the historic aerial images), and groundwater withdrawal data to evaluate the relative effects components other than climate on streamflow.

Scope and objectives

This is a one year, collaborative research project involving faculty and students from Oklahoma State University and a USGS Oklahoma Water Science Center scientist. Originally, we proposed to focus on the upper Cimarron River from the Waynoka USGS Station (36°31'02", Longitude 98°52'45") to the Dover station (Latitude 35°57'06", Longitude 97°54'51"). We later decided to expand the contribution area to Guthrie to utilize the longer streamflow records. The contribution area includes the entire Lower Cimarron-Skeleton Watershed (HUC11050002) which has a contribution area of 8,375.26 square kilometers or 3233.68 square miles (U.S. Environmental Protection Agency, 2012).

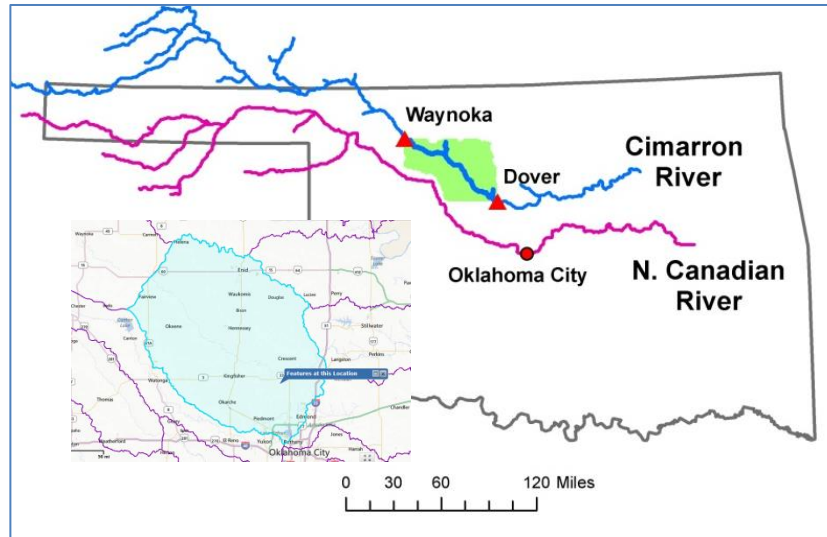


Fig. 1: Map showing location of the proposed study area between Waynoka and Dover in north-central Oklahoma and revised area from Waynoka to Guthrie (inset).

The overarching goal of this project is to quantitatively assess the effects of climate change, land surface change, and human activities on long-term streamflow characteristics of the upper Cimarron River. The area along the upper Cimarron River has a diverse land use history and pattern and is experiencing a rapid increase in woody vegetation cover (both riparian and upland) and increases in groundwater withdrawals from alluvial aquifers. Specific project objectives include:

Objective 1: Archive and digitize multi-temporal aerial photos from the 1930s to the 2010s and produce a time series of land use and land cover change history for the studied area; quantify and archive the long-term trends of climate variability, groundwater levels, and water withdrawals during the study period.

Objective 2: Quantify the effects of climate related change on streamflow and groundwater trends and understand the contribution of non-climatic factors including land use, woody plant encroachment, and groundwater withdrawal on streamflow and groundwater levels.

Objective 3: Apply stepwise regression to determine which variables (land use change, encroachment of woody plants (primarily eastern redcedar) and change in surface storage such as reservoir construction are significant predictors of land surface change elasticity index, therefore streamflow trends.

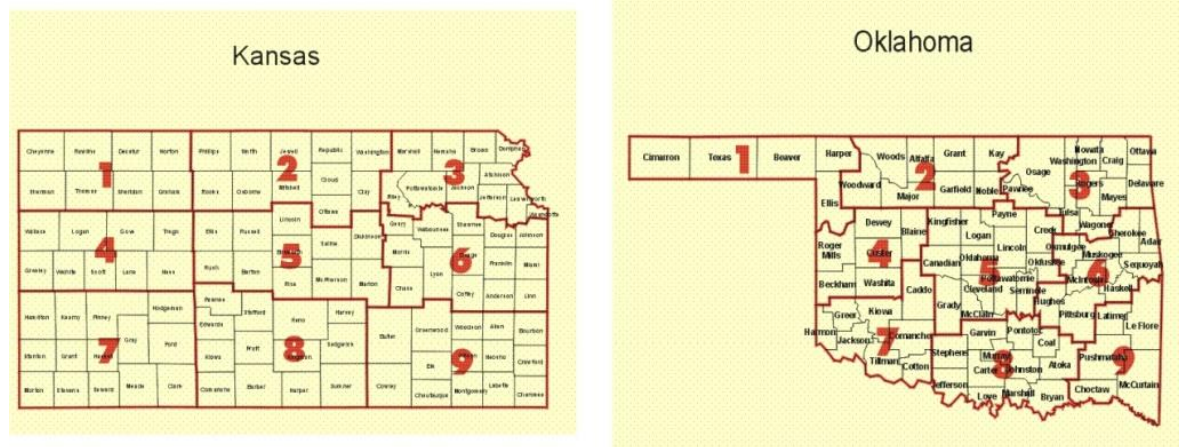
Methods and Procedures

Climate variability and hydrological cycle trends

Two streamflow-gaging stations (Cimarron River near Waynoka, Oklahoma, #070185000; and Cimarron River near Guthrie, Oklahoma, #071860000) and contributing areas upstream of those stations comprise the study area of this paper. Types of data collected to determine climate variability and trends in hydrologic cycle components in the watersheds in this study area included annual precipitation and mean annual air temperature, estimated consumptive water use, streamflow and contributing areas (areas from which runoff is likely to flow to streams), and groundwater levels.

Precipitation and temperature

Because the contributing areas to the streamflow-gaging stations on the Cimarron River near Waynoka and near Guthrie, Oklahoma span approximately equal areas in several climate divisions in parts of Oklahoma, Kansas, and Colorado (**Fig. 1**), the averages of mean annual precipitation and mean annual air temperature data collected by the National Weather Service in five-year increments from 1950 through 2005 in those climate divisions (National Oceanic and Atmospheric Administration, 2012a) were used to represent mean annual precipitation and temperature in those contributing areas. Mean annual precipitation and air temperature data from Oklahoma Climate Division 2, and Kansas Climate Divisions 7 and 8 (**Fig. 2A**) were used to represent annual precipitation and air temperature for the contributing area of the streamflow-gaging station near Waynoka, Oklahoma. For the contributing area to the streamflow-gaging station near Guthrie, Oklahoma, averages of climate data from those climate divisions plus climate data from Oklahoma Climate Division 5 (**Fig. 2B**) were used to represent mean annual precipitation and mean annual air temperature.



Images from National Weather Service (2012)

Fig. 2: Climate Division maps for Kansas and Oklahoma showing contribution area for Waynoka and Guthrie gauge stations.

Water consumption

Water-use data compiled at 5-year increments from 1950-2005 for parts of 8-digit hydrologic unit code watersheds in contributing areas of these streamflow-gaging stations (**Fig. 2**) were estimated from data obtained from the Aggregate Water Use Data System (AWUDS) of the USGS (U.S. Geological Survey 2012a), water-use data supplied by the USGS Kansas Water Science Center (written commun. Joan Kenny, U.S. Geological Survey, 2012), and data used to compile Tortorelli (2009). Major water-use categories included in this compilation included: domestic use from public water supplies, domestic self-supplied, self-supplied irrigation from groundwater, self-supplied irrigation from surface water, self-supplied groundwater for livestock, self-supplied surface water for livestock, industrial self-supplied groundwater, industrial self-supplied surface water, industrial from public water supplies, commercial from public water supplies, and self-supplied withdrawals of freshwater for mining. The AWUDS system contains water-use data compiled every five years from watersheds from 1985, 1990, and 1995. For 2000 and 2005, commercial and domestic water obtained from public-water supply systems in Kansas were not available, so data from 1995 were substituted for those missing data. For 2005, water-use data were not compiled by watershed in Kansas, so the remaining water-use categories were carried over from 2000 data. Water-use data for four watersheds (hydrologic unit codes 11040006, 11040007, 11040008, 11050001, and 11050002) were scaled to the approximate proportions of contributing areas in those watersheds to total land area (33, 50, 90, 100, and 95 percent, respectively). Water-use data from prior to 1985 were estimated by developing coefficients for major water-use categories in Tortorelli (2009) relative to 1985 water-use data available in the AWUDS system. Consumptive water use is an estimate of the portion of water withdrawn from aquifers and streams that is evaporated to the atmosphere or removed from the areas of withdrawal in commercial and industrial products. Estimates of consumptive water use were made by multiplying industrial and commercial water withdrawals by 7 percent, domestic water withdrawals by 30 percent, and irrigation and livestock water withdrawals by 100 percent. Water-use data from 1950-2005 were obtained from data used to compile Tortorelli (2009). For the 2010 USGS National water-use compilation, water use in Oklahoma and Kansas was not computed by HUC watersheds, only by counties, so could not be compared to previously compiled water-use data without substantial recomputation..

Streamflow

To investigate long-term trends in streamflow in this area, mean annual streamflow data collected at two streamflow-gaging stations operated by the USGS from 1950-2005 (Cimarron River near Waynoka, Oklahoma; and Cimarron River near Guthrie, Oklahoma) were compiled from U.S. Geological Survey (2012b). Those streamflow-gaging stations have the longest periods of data collection (record) and are on the primary river draining the study area. Contributing drainage areas for the streamflow-gaging stations near Waynoka and near Guthrie were determined to occur in parts of four 8-digit hydrologic unit code watersheds (11040006, 11040007, 11040008, 11050001, and 11050002) having contributing drainage areas of 4,594 and 8,154 square miles, respectively, based on geographic information system coverages developed for the Oklahoma Streamstats

Program (U.S. Geological Survey, 2012c). To investigate trends in the portions of streamflow represented by baseflow (primarily groundwater seepage) and runoff (primarily overland flow from precipitation) the BFI (Baseflow Index) program (Wahl and Wahl, 2012) was used to estimate components of daily streamflow, which were summarized to mean annual baseflow and runoff at those stations.

Groundwater

Groundwater levels, annually measured in selected wells by staff of the USGS or the Oklahoma Water Resources Board during the late winter (time of minimum irrigation pumpage) were obtained from U.S. Geological Survey (2012b). Water levels in some wells were sampled more than once per year, but to avoid overweighting data from such wells, the earliest water-level measurement made in each well completed in a known aquifer in these watersheds was compiled for each year. More than 90 percent of the wells in this area with available water-level measurements were completed in the Cimarron Terrace or alluvial aquifers, rather than in underlying bedrock aquifers of Permian age. Only water levels from wells completed in the younger unconsolidated aquifers were summarized for this paper as those wells generally were shallow, unconfined, likely to respond quickly to precipitation, and likely to be in hydraulic connection with the Cimarron River or tributaries of that river.

As one of the primary purposes of this paper is to investigate relations between land-surface changes and water resources, a simple model was developed to estimate hydrologic cycle components, including those likely to be affected by land-surface changes, for the study area in 5-year increments from 1950-2005. The conceptual hydrologic cycle model (Fig. 3) incorporates existing meteorologic and hydrologic data to estimate an annual residual term for every fifth year that is likely to be associated with evapotranspiration of natural plants and non-irrigated crops, which can be substantially affected by land-surface changes.

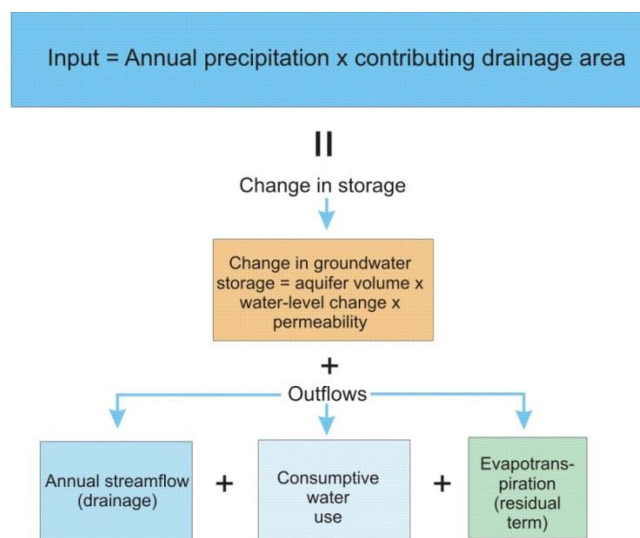


Fig. 3. Conceptual model used to summarize trends in available hydrologic data and evapotranspiration for the study watersheds

To construct the conceptual model of the hydrologic cycle, change in groundwater storage every five years was estimated from the change in the median depth to groundwater measured five years previously, multiplied by porosity of the alluvial and terrace aquifers, which was estimated to be 35 percent (Freeze and Cherry, 1979), multiplied by the surface areas of the alluvial and terrace aquifers upstream of each streamflow-gaging station (130 square miles for the contributing area upstream of the station near Waynoka, and 1,329 square miles for the contributing area upstream of the station near Guthrie, based on GIS coverages derived from Bingham and Moore (1975) and Morton (1980). Annual streamflows for each fifth year were based on the sums of mean annual baseflow and runoff at the streamflow-gaging stations on the Cimarron River near Waynoka and near Guthrie, Oklahoma. The residual amount, shown in the green box in **Fig. 3**, was assumed to represent evapotranspiration from non-irrigated crops, other plants, soils, and open-water surfaces for the contributing areas of each of those streamflow-gaging stations.

The Seasonal Kendall test (Kendall, 1938), with one test per year, was used to quantify trends of the hydrologic parameters for each fifth year from 1950-2005. Seasonal Kendall tests with p-values less than or equal to 0.05 were considered to indicate significant trends of meteorologic and hydrologic parameters with time.

Graphs and statistical computations were made using the statistical computer program TIBCO Spotfire S+ 8.1 for Windows (TIBCO Software, Inc., 2012). For some graphs, Loess trend lines were used to aid in visual analysis of trends. LOESS, or Locally Estimated Scatterplot Smoothing (also referred to as LOWESS or Locally WEighted Scatterplot Smoothing in other publications), is a nonparametric regression procedure that reduces the influence of outliers and displays a smooth or trend line for a range of data (Cleveland and Devlin, 1988; Helsel and Hirsch, 2002). Graphs were modified further using CorelDRAW X3 Graphing Suite software and Adobe Illustrator CS5 Version 15.0.2 software.

Land use and land cover change

Mapping land use and cover change

We archived and digitized the historical aerial photos and images taken around 1940s and 1960s for the study area and surrounding area. The majority of these historical aerial photos were provided by Oklahoma State University library, and the rest were provided by the Archives Division of the Oklahoma Department of Libraries, and the Oklahoma Corporation Commission. The scale of these photos ranges from 1:7,000 to 1:30,000, which is sufficient for observing individual tree canopies. These aerial photos were scanned at 800 dpi and geo-referenced for use in this project. Geo-referenced photos will be mosaiced and balanced by dodging, as described in Wine and Zou (2011).

A complete database of woody expansion and dynamics from 1975 to 2010 were developed from Landsat images. We will use most recent NAIP images as ground-truth data for defining Region-of-Interest (ROI) to support aerial photos and Landsat image classification and analysis. We propose to carry out the Classification And Regression Tree

(CART) method to process Landsat images to identify and document changes in spatial distribution of woody plants in the study area.

Nonparametric Estimator of Climate Elasticity and Land Surface Elasticity of Streamflow

The Cimarron River is one of a few Oklahoma rivers in which streamflow has not been largely regulated by hydro-power and other large diversion structures. For the drainage area of this study, there is some surface water withdrawal primarily for livestock and aquaculture (Tortorelli 2009), therefore the streamflow contributed from this drainage area (Q) can be computed based on streamflows measured at the two gaging stations and surface water withdrawals in this area. Assuming the streamflow and groundwater is completely linked and there is no observed change in groundwater level, the groundwater withdrawal was added to the streamflow to calculate the change. [Note – due to relatively stable ground water withdrawal since ..., the absolute amount of groundwater withdrawal is not critical for analysis of climate and land surface elasticity). Then Q can be modeled as a function of climatic variables and catchment land surface characteristics of the drainage area:

$$Q = f(P, E_0, V), \quad (1)$$

where Q is streamflow contributed from this drainage area; P and E_0 are precipitation and potential evapotranspiration, respectively, representing dominant climate factors on the hydrological cycle; and V is a factor that represents the integrated effects of catchment land surface characteristics such as land use, cover change and human activities on streamflow. Using the following equation (1), changes in streamflow due to changing climate and catchment surface characteristics can be approximated as (Zheng et al. 2009):

$$\Delta Q = f'_P \Delta P + f'_{E_0} \Delta E_0 + f'_V \Delta V \quad (2)$$

where ΔQ , ΔP , ΔE_0 , and ΔV are changes in streamflow, precipitation, potential evapotranspiration, and catchment surface characteristics, respectively, with $f'_P = \frac{\partial Q}{\partial P}$, $f'_{E_0} = \frac{\partial Q}{\partial E_0}$, and $f'_V = \frac{\partial Q}{\partial V}$. In terms of climate change, potential evapotranspiration instead of temperature is considered herein because potential evapotranspiration better represents the effects of climate change on water balance and because it integrates the effects of temperature, wind speed, solar radiation, sunshine duration and vapor pressure deficit.

Assuming that the land surface factors are independent of the climate factors, equation (2) can be rearranged as:

$$\Delta Q = \Delta Q_c + \Delta Q_v \quad (3a)$$

$$\Delta Q_c = f'_P \Delta P + f'_{E_0} \Delta E_0 \quad (3b)$$

$$\Delta Q_v = f'_V \Delta V \quad (3c)$$

Where ΔQ_c and ΔQ_v are changes in streamflow caused by climate change and land use and land cover change, respectively. In equation (3a), ΔQ can be estimated from observed streamflow records. If ΔQ_c is known, ΔQ_v can be calculated.

Climate elasticity of streamflow (ϵ), by definition, is the proportional change in streamflow (Q) divided by the proportional change in a climatic variable. The elasticity of streamflow to precipitation and potential evapotranspiration can be calculated as:

$$\epsilon_P = \frac{\partial Q/Q}{\partial P/P} \quad (4)$$

$$\epsilon_{E0} = \frac{\partial Q/Q}{\partial E0/E0} \quad (5)$$

Stepwise Regression

Stepwise regression was used to determine which variables were significant predictors of land surface change elasticity indices. Linear interpolation was used to fill tree cover values and land use and reservoir storage for years in which aerial photography had not been classified so that this variable could be used as a predictor in statistical analyses.

Principal Findings and Significance

Precipitation and air temperature

Mean annual precipitation in the contributing area to the streamflow-gaging stations near Waynoka and near Guthrie, Oklahoma, tended to increase from 1950 to 1960, decreased to 1975, increased to 2000, and decreased to 2005 (Fig. 4). Because much of the contributing area to the streamflow-gaging station near Guthrie, Oklahoma included the contributing area to the streamflow-gaging station near Waynoka, Oklahoma, mean annual precipitation trends for those areas were similar, though decreases in precipitation in Oklahoma Climate Division 5 in the 2000s tended to narrow the differences between precipitation in those two areas. Though indicating slight increases of mean annual precipitation with time in these contributing areas, the Seasonal Kendall test did not indicate significant upward trends in mean annual precipitation with time (Table 1).

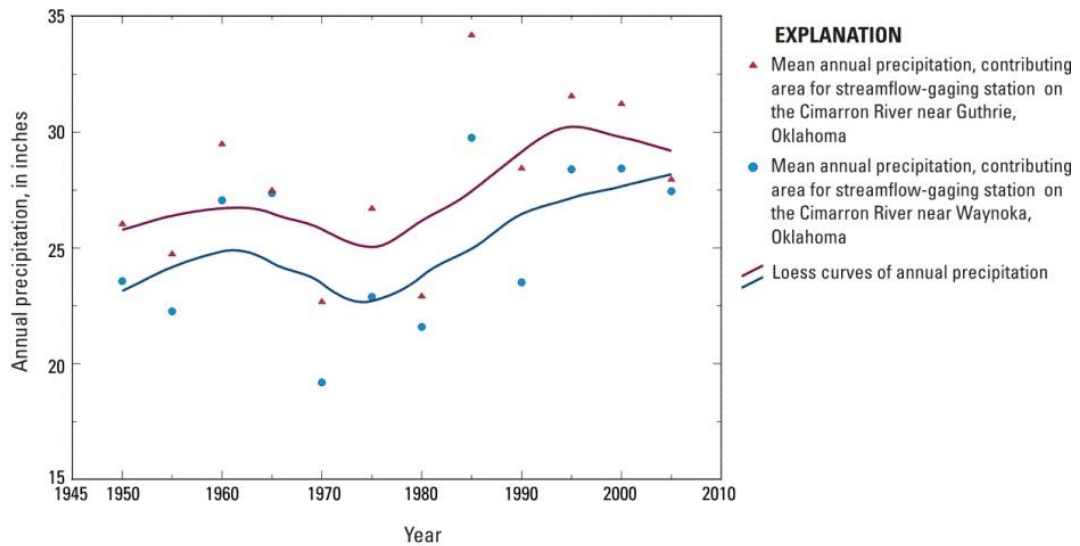


Fig. 4. Mean annual precipitation, in five-year increments for contributing areas for streamflow –gaging stations on the Cimarron River near Waynoka and near Guthrie, Oklahoma

Mean annual air temperature in the contributing area of the streamflow-gaging station near Waynoka generally was about 0.5 °C cooler than in the contributing area for the station near Guthrie (**Fig. 5**). In both areas, mean annual air temperatures increased by about 1.5 °C from 1950 to 2005, with the rate of warming increasing starting in 1990 (**Fig. 5**). Although there were general upward trends in mean annual air temperature during this period, the Seasonal Kendall test did not indicate significant increases in mean annual air temperature for these two areas during this period due to temperature increasing and decreasing notably between subsequent periods. Empirical relations between water evaporation, humidity, and air temperatures typical for this area indicate that an increase of air temperature of 1.5 °C would increase evaporation from a water surface by about 11 percent (The Engineering Toolbox, 2012), though relatively small parts of these contributing areas have free water surfaces subject to direct evaporation to the atmosphere.

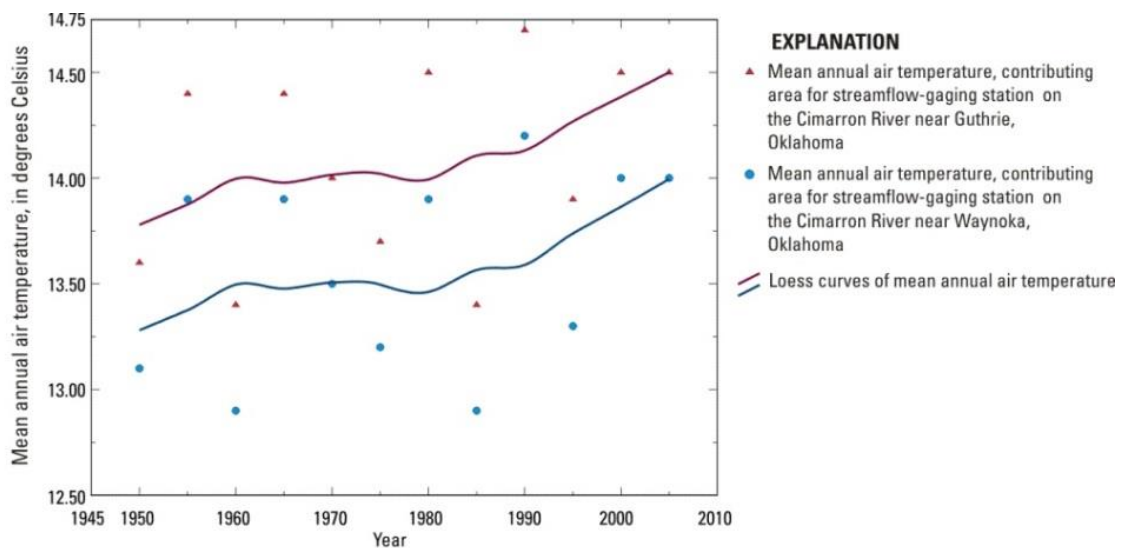


Fig. 5. Mean annual air temperature, in five-year increments for contributing areas for streamflow–gaging stations on the Cimarron River near Waynoka and near Guthrie, Oklahoma

Table 1. Seasonal Kendall tests for trend for meteorologic and hydrologic parameters for contributing areas of streamflow-gaging stations on the Cimarron River near Waynoka and near Guthrie, Oklahoma, 1950-2005.

[mgd, million gallons per day; *, not computed for 1980 because of lack of streamflow data; Waynoka, streamflow-gaging station Cimarron River near Waynoka, Oklahoma (07158000); Guthrie, streamflow-gaging station Cimarron River near Guthrie, Oklahoma (07160000), annual constituents analyzed at 5-year intervals]

Component	Contributing Area	Period	S-score	Z-score	P-value	Estimated trend equation ²
Precipitation, in inches per year	Waynoka	1950-2005	22	1.44	0.150	Precipitation =23.3 + 0.0663*year
	Guthrie		20	1.30	0.193	Precipitation =25.31 + 0.0804*year
Mean annual air temperature, in degrees Celsius	Waynoka	1950-2005	21	1.39	0.164	Temperature=13.55+0.005*year
	Guthrie		21	1.39	0.164	Temperature=14.0+0.008*year
Consumptive water use, in mgd	Waynoka	1950-2005	17	1.10	0.271	Consumptive water use=238+3.03*year
	Guthrie		18	1.17	0.244	Consumptive water use=258+3.27*year
Mean annual streamflow, in mgd	Waynoka	1950-2010	-18	-1.17	0.244	Streamflow=286-3.30*year
	Guthrie ¹		15	1.090	0.276	Streamflow=604+8.04*year
Change in groundwater storage, in mgd	Waynoka	1950-2010	11	0.737	0.461	Groundwater storage=0+0*year
	Guthrie		6	0.343	0.732	Groundwater storage=-718.3+18.0*year
Evapotranspiration, in mgd ³	Waynoka	1950-2005	16	1.03	0.304	Evapotranspiration=4488+19.1*year
	Guthrie		22	1.44	0.150	Evapotranspiration=7596+55.2*year

¹No streamflow data for 1980 due to break in operation of this streamflow-gaging station.

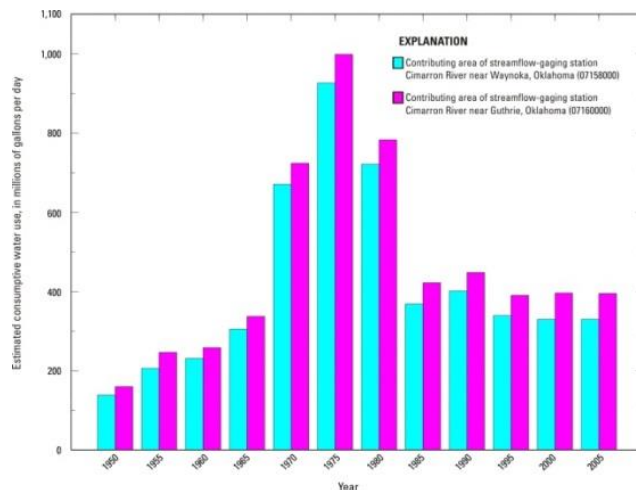
²Years computed as sequential integers, with multiplier for year being divided by 5 to account for 5-year periods.

³Residual term that does not include evapotranspiration from irrigated cropland

Consumptive water use

Estimated consumptive water use in the two watersheds in the study area peaked in 1975, due to a peak in estimated crop irrigation. A peak in crop irrigation in the study area in 1975 was validated by increases in irrigated acreage numbers in the counties in those areas from U.S. Department of Agriculture census of agriculture from 1949 through 1978 with subsequent leveling off of irrigated acreages from 1982-2007, combined with relative lack of precipitation in between 1970 - 1975 (**Fig. 4**). Declines in consumptive water use from 1975-2005 may be related to wetter conditions leading to less water applied per irrigated acre and more efficient water use in households and commercial and industrial facilities.

Fig. 6. Estimated consumptive water use in contribution areas upstream of streamflow-gaging stations on the Cimarron River near Waynoka and near Guthrie, Oklahoma.



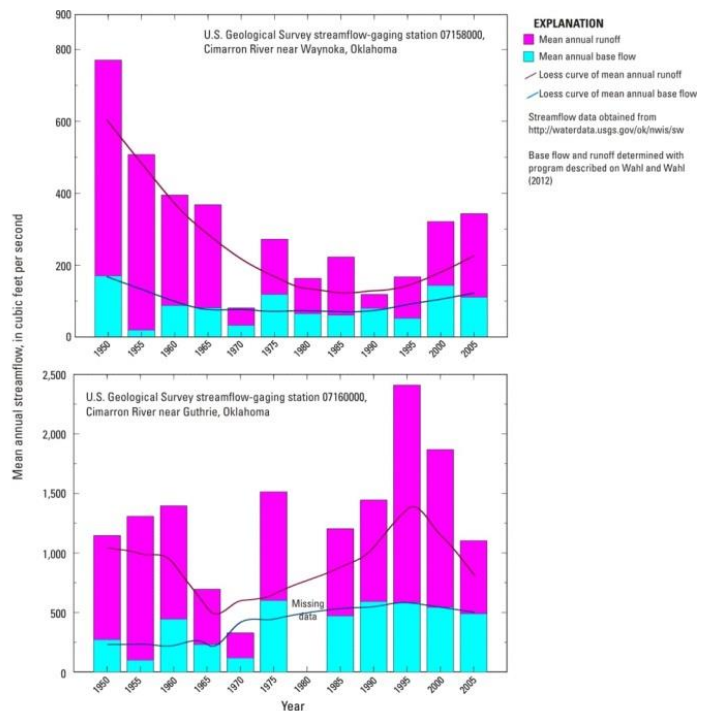
Estimated consumptive water use generally was about 20 percent greater in the contributing area of the streamflow-gaging station near Guthrie than the contributing area to the station near Waynoka because of water use by additional people, livestock, irrigated agriculture, and commercial and industrial facilities in the area between those two stations. Estimated consumptive water use in both areas was dominated by irrigated agriculture in Kansas, which far exceeded additional water use by as many as 200,000 additional people in the area between the Waynoka and Guthrie gages, which is on the fringes of the Oklahoma City metropolitan area (written commun., R.L. Tortorelli, U.S. Geological Survey, 2005). The Seasonal Kendall test did not indicate significant increases in estimated consumptive water use in these areas over this period (**Table 1**).

Streamflow

From 1950 through 2005 at the streamflow-gaging station near Waynoka, Oklahoma, mean annual baseflow (comprised mostly of groundwater seepage) in the Cimarron River decreased from 170 cubic feet per second (cfs) to about 80 cfs through 1990 (**Fig. 7**). From 1990 through 2005 baseflow at that station increased to more than 100 cfs (**Fig. 7**), probably due to a combination of trends in precipitation and estimated consumptive water use over those periods (**Fig. 6**, and **Fig. 8**). Mean annual runoff (consisting primarily of overland flow after precipitation events) at that station had a similar pattern with time, though more accentuated, decreasing from 600 cfs in 1950 to about 150 cfs in the 1980s through the 1990s, and increasing to more than 200 cfs in 2005. The Seasonal Kendall test did not indicate significant upward or downward trends in mean annual streamflow at this station during this period (**Table 1**).

Downstream at the Cimarron River streamflow-gaging station near Guthrie, Oklahoma, baseflow generally increased from about 250 cfs in 1950 to about 500 cfs in 2005 (**Fig. 7**). Reasons for increasing baseflow at that station over that period may include increasing annual precipitation, particularly during the 1980s through early 1990s (**Fig. 4**), and decreases in consumptive water use since 1980 (**Fig. 6**).

Fig.7. Mean annual base flow and runoff at two streamflowing-gaging stations on the Cimarron River, northwest Oklahoma (1950 -2005)



Groundwater storage

Changes in groundwater storage in aquifers can be estimated through periodic measurement of groundwater levels (depth to groundwater below land surface). In HUC watershed 11050001, in which the streamflow-gaging station near Waynoka, Oklahoma is located, water levels were measured at least annually in 4 to 14 wells completed in alluvial and terrace aquifers along the Cimarron River (**Fig. 8**). In HUC watershed 11050002, in which the streamflow-gaging station near Guthrie, Oklahoma is located, between 8 and 29 wells were measured at least annual for water levels from 1950 through 2005 (**Fig. 8**). As previously described for computation of hydrologic-cycle parameters, data collected at 5-year intervals were selected for analysis (**Fig. 7**). Because of lack of groundwater-level prior to 1975 for the HUC 1105002 watershed, groundwater levels in that watershed from 1950-70 were assumed to have remained constant at 1975 levels, based on relatively little change in annual precipitation for that period (**Fig. 6**).

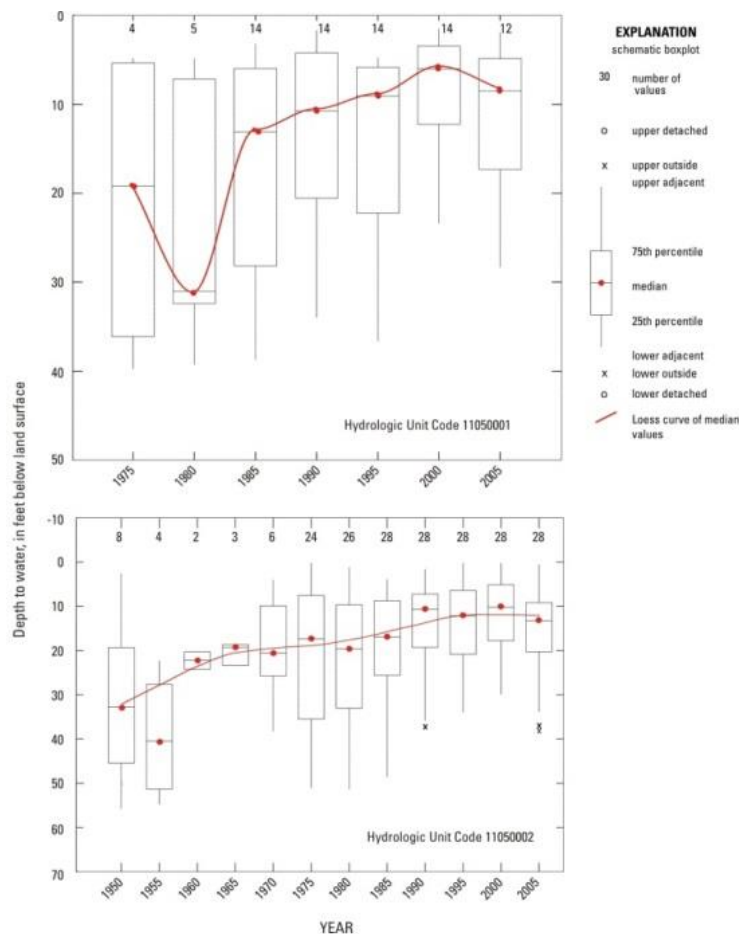


Fig. 8. Distribution of depths to groundwater in selected wells completed in alluvial and terrace aquifers of the Cimarron River in Hydrologic Unit Code watersheds 11050001 and 11050002, 1950 – 2005

For wells measured in the HUC 11050001 watershed, groundwater levels generally increased from 5 to more than 10 feet from 1975-2005, similar to the trend of increasing precipitation in that area for much of that period (**Fig. 6** and **Fig. 8**). Similarly, groundwater levels measured in the HUC 11050002 watershed increased by a median value of about 10 feet from 1975-2005, with a preceding increase of about 10 feet for the period 1950-75 (**Fig. 8**). Because the boxplots shown on **Fig. 8** represent varying numbers of different wells for successive measurement years, they may misrepresent or exaggerate water-level trends. Long-term water level measurements from selected individual wells (**Fig. 9**) also indicated that groundwater levels in alluvial and terrace aquifers of the Cimarron River in these watersheds tended to increase by at least a few feet from the mid- to late-20th century to 2005, indicating increases in groundwater stored in those aquifers during that period.

As with other hydrologic parameters, the Seasonal Kendall test did not indicate significant upward or downward trends in change in groundwater in storage in alluvial aquifers in either of these areas for this period (**Table 1**).

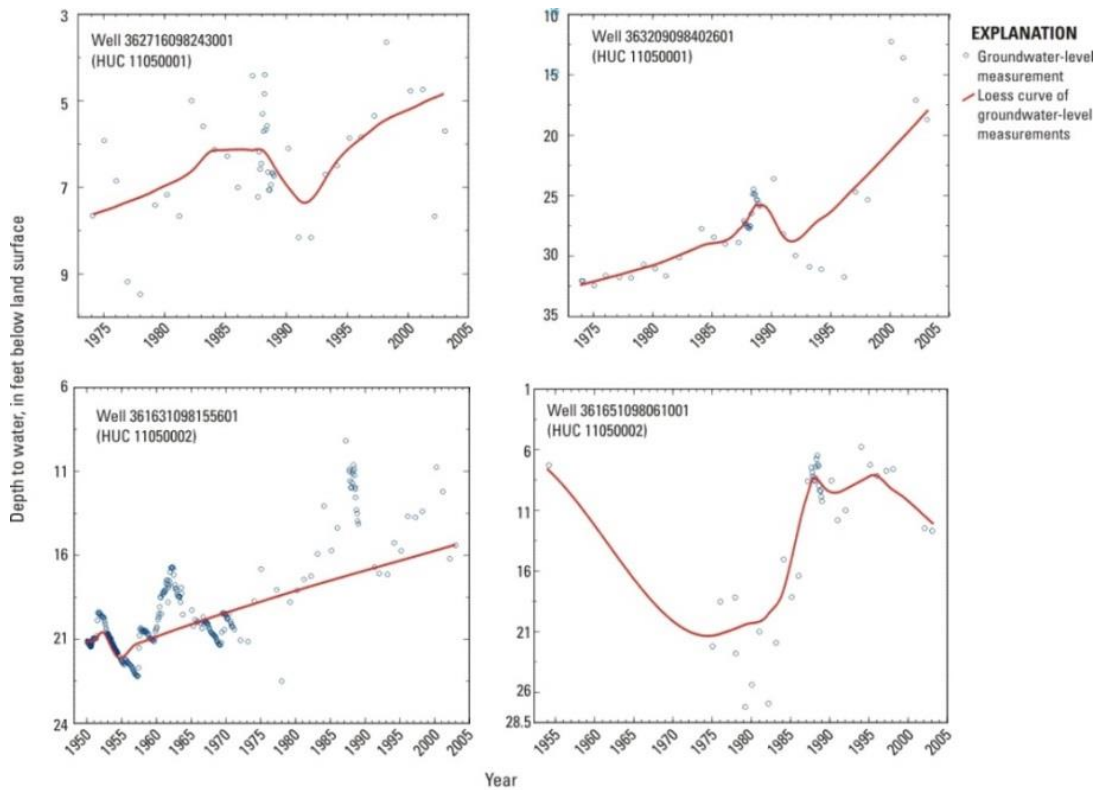


Fig.9. Depths to water in selected wells completed in alluvial and terrace aquifers of the Cimarron River in Hydrologic Unit Code watersheds 11050001 and 11050002, 1950 – 2005

Hydrologic cycle estimates

Estimated evapotranspiration, the residual of inputs, plus or minus change in storage, minus measured outputs of water from the contributing areas upstream of these streamflow-gaging stations, gradually increased for the contributing area upstream of the station near Waynoka, Oklahoma from 1950 to 2005 (**Fig. 10**). Estimated evapotranspiration increased from 1950 to 1990 in the contributing area upstream of the station near Guthrie, Oklahoma, but decreased from 1990-2010 in that area (**Fig. 10**). Decreases in estimated evapotranspiration since 1990 in the contributing area upstream of the station near Guthrie largely are attributable to decreases in annual precipitation in Climate Division 5 since 1990 (**Fig. 4**). The Seasonal Kendall test did not indicate significant upward or downward trends in estimated evapotranspiration in either of these contributing areas during this period (**Table 1**).

Fig. 10. Change in precipitation input, streamflows in Guthrie and Waynoka, Consumptive water use and estimated ET for the contribution area.

Land-surface change

Between 1975 and 2010 woody cover more than doubled in the contribution area to Cimarron River from Waynoka to Guthrie, from covering 2.7% of the total land area in 1975 to 5.7% in 2010 (approximately 477 sq kilometers or 118,000 acres). Of the total woody cover, approximately 88% consisted of evergreens.

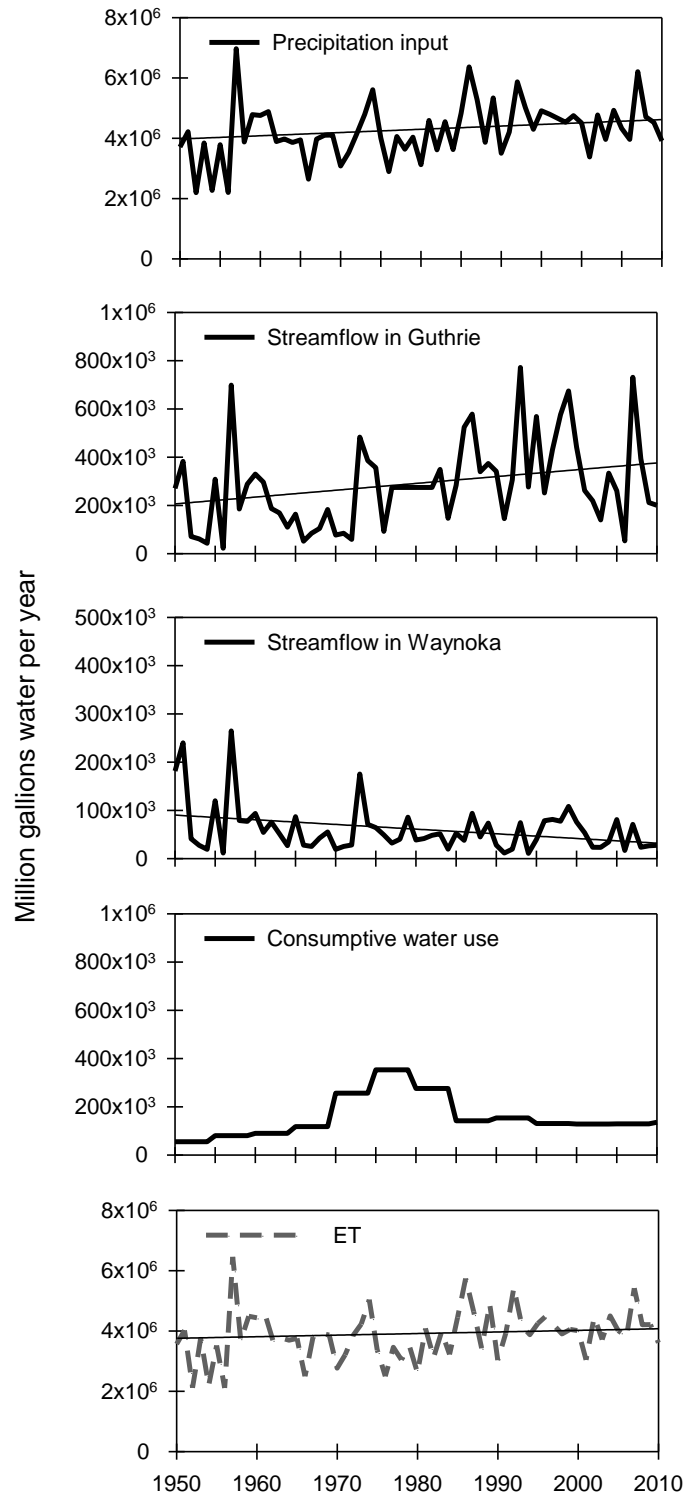


Table 2. Change of woody and herbaceous land cover between 1975 and 2010

Year	Season	Trees % total land	Herb % total land	Total vegetation cover
1975	winter	3.63	72.58	76.20
1985	winter	3.49	69.12	72.61
1995	winter	3.29	62.56	65.86
2005	winter	4.05	69.63	73.68
2010	winter	5.42	72.61	78.03
<hr/>				
1975	summer	2.71	78.10	80.81
1985	summer	3.84	74.38	78.21
1995	summer	4.22	67.32	71.54
2005	summer	4.58	73.20	77.77
2010	summer	5.66	69.93	75.59

Given the wide proliferation of the species in the state, the majority of these are likely to be eastern redcedar (*Juniperus virginiana*) and salt cedar (*Tamarix ra mosissima*). During the 35 years from 1975 to 2010, stands of these trees appear to have increased in density in the upper portion of the watershed while decreasing in the lower portion near Guthrie and Oklahoma City, OK. A substantial increase in woody cover along the river channel and riparian zone, particularly in the upper part of the river, was observed in 1995 vegetation distribution map. Expansion in the upland portion of the watershed became apparent in 2005 and 2010 vegetation distribution maps. Coincident with the increase in woody cover has been a 7% decrease in total herbaceous cover. A large portion of this reduction has been from retirement or abandonment of irrigated acreage, which has decreased by 9.2% since 1985 (**Fig. 11**).

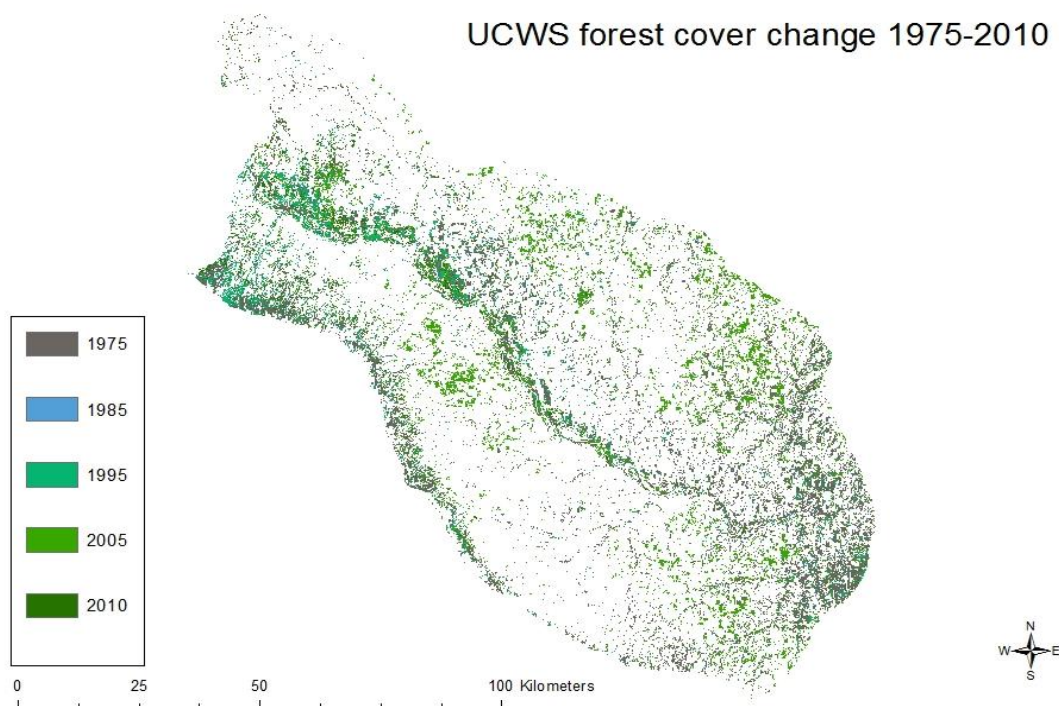


Fig. 11 Change in woody cover from 1975 to 2010 in the contribution area to Cimarron River between Waynoka and Guthrie

Climatic elasticity and vegetation impact

The calculation of climate elasticity and land surface elasticity of streamflow produced unsatisfactory results (not reported here). The main challenge in calculating climate elasticity was to precisely quantify change in streamflow ($\partial Q/Q$). In contrast to our original thoughts, we found that a substantial change (both increase and decrease) in groundwater storage during this period (**Fig. 8** and **Fig. 9**); this change has been estimated to be substantial in magnitude and its effect on streamflow is not well understood. In addition, consumptive water use might partially come from groundwater storage. A subtle error in streamflow change will affect $\partial Q/Q$ substantially, resulting unsatisfactory climate elasticity results.

Instead, we used linear and non-linear regression analysis. Regression analysis showed that precipitation in the contribution area strongly affected streamflow recorded in Guthrie gauge station. The streamflow decreased nearly linearly with increase in potential ET calculated based on mean monthly temperature and mean monthly precipitation using Thornthwaite monthly water balance model (http://wwwbrr.cr.usgs.gov/projects/SW_MoWS/Thornthwaite.html) for the contribution area (**Fig. 12**).

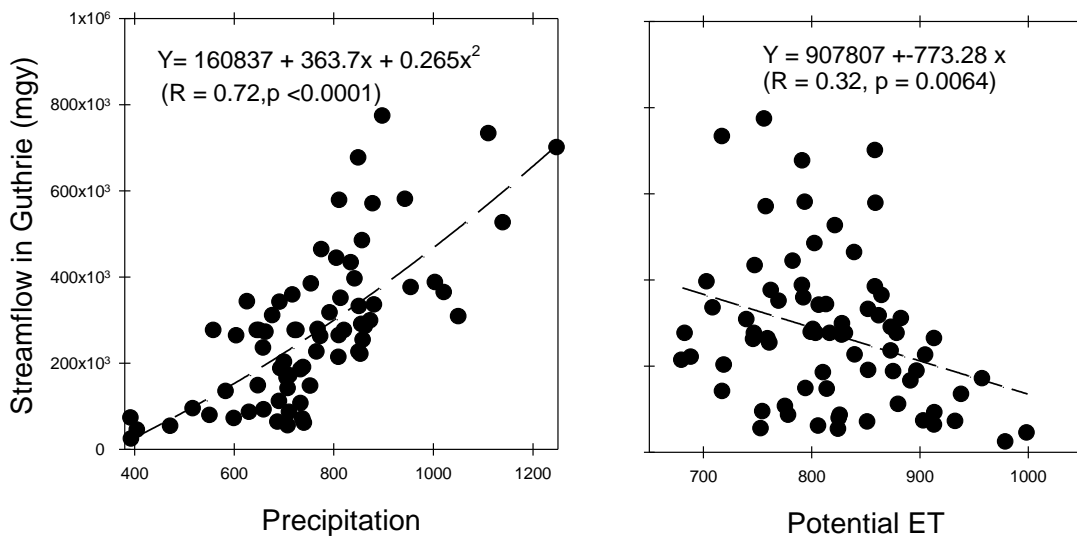


Fig. 12. Responses of streamflow in Guthrie Station to precipitation and potential ET of the contribution area.

There is an upward trend in ET/P with increase in tree cover in summer (**Fig. 13**) although the positive correlation is not statistically significant ($p = 0.2067$).

The increase in tree cover is relatively small compared with the contribution area percentage wise. However, the increased tree cover has mainly concentrated around the riparian zone and river channel. We found some positive relationship between ET/P and tree cover (in summer) although this relationship is not statistically significant.

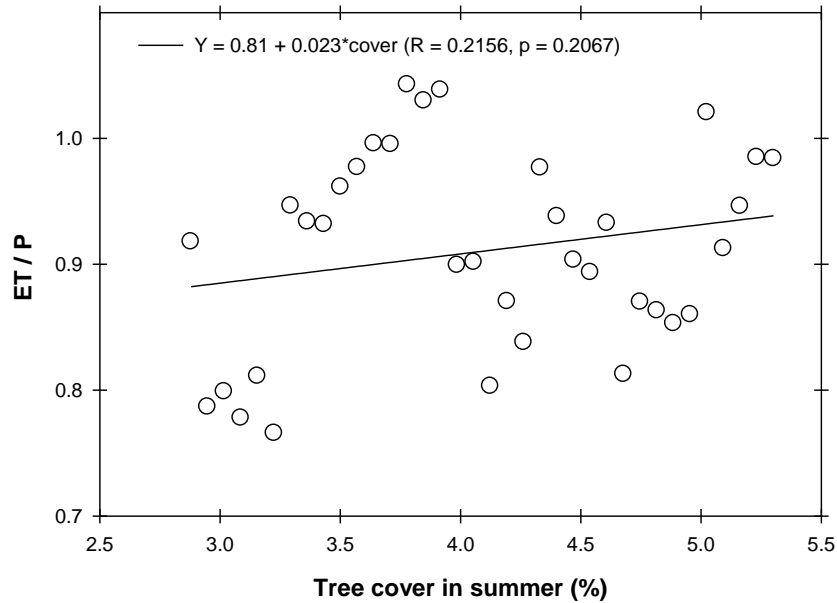


Fig. 13. Response of ET/P to increase in tree cover

Conclusion and Future Research

1. There were general upward trends in mean annual air temperature and mean annual precipitation during 1950 - 2005, but the Seasonal Kendall test did not indicate significant increases in either mean annual air temperature or mean annual precipitation during this period;
2. Consumptive water use in the contribution area peaked in 1975 and subsequently leveled off from 1982-2005;
3. Groundwater levels in alluvial and terrace aquifers in the contribution area tended to increase from the 1960s to 2005, indicating increases in groundwater stored in those aquifers during that period.
4. There was a general upward trend in streamflow for Guthrie gage station since 1970 to 2005. In contrast, there was a downward trend in streamflow for Waynoka station since 1950 although seasonal Kendall test did not indicate significant increases or decrease.
5. The magnitude of streamflow for Guthrie gage station was strongly, positively correlated with annual precipitation in the contribution area, but negatively correlated with potential ET.

6. Increase in tree cover has primarily concentrated in riparian zone and river channels. During 1975 to 2010, the tree cover has doubled from 2.7% to 5.7% (approximately 477 sq kilometers) primarily from increase in evergreen trees such as eastern redcedars.
7. There is an upward trend in ET/P with the increase in tree cover, suggesting increase of tree cover may have augmented the ET component and reduced streamflow or recharge component in the water budget.
8. Future research should focus on: 1. Quantify vegetation and land use change in riparian zone and alluvial area to investigate vegetation impact on water use and groundwater recharge; 2. Quantify change in impoundment in the contribution area, its history, its relative magnitude, and its potential impact on water budget calculation. 3. Improve potential ET estimation using Penman-monteith or other approaches with a daily step and re-evaluate the elasticity of streamflow to potential ET.

References

- Bingham, R.H., and Moore, R.L., 1975, Reconnaissance of the water resources of the Oklahoma City Quadrangle, central Oklahoma: Oklahoma Geological Survey, Hydrologic Atlas 4, 4 sheets.
- Cleveland, W.S., and Devlin, S.J., 1988, Locally-weighted regression: An approach to regression analysis by local fitting: *Journal of the American Statistical Association*, v. 83, p. 596-610.
- Christenson, S.C., Morton, R.B., and Mesander, B.A., 1992, Hydrogeologic maps of the Central Oklahoma Aquifer, Oklahoma: U.S. Geological Survey Hydrologic Investigations Atlas Map HA-724.
- U.S. Environmental Protection Agency, 2012. Watershed Assessment, Tracking & Environmental Results.
(http://iaspub.epa.gov/tmdl_waters10/attains_watershed.control?p_huc=11050002&p_cycle=&p_report_type=T)
- Esralew, R.A., and Lewis, J.M., 2010, Trends in base flow, total flow, and base-flow index of selected streams in and near Oklahoma through 2008: U.S. Geological Survey Scientific Investigations Report 2010-5104, 143 p.
- Helsel, D.R., and Hirsch, R.M., 2002, *Statistical methods in water resources*: New York, Elsevier, 522 p.
- Kendall, M.G., 1938, A new measure of rank correlation: *Biometrika*, v. 30, p. 81-93.
- Mashburn, S.L., and Magers, J., 2011, Potentiometric surface in the Central Oklahoma (Garber-Wellington) Aquifer, Oklahoma, 2009: U.S. Geological Survey Scientific Investigations Map 3147, 1 sheet.
- Morton, R.B., 1980, Reconnaissance of the water resources of the Woodward Quadrangle northwestern Oklahoma: Oklahoma Geological Survey, Hydrologic Atlas 8, 4 sheets.
- National Oceanic and Atmospheric Administration, 2012, New Access to climate data online: National Oceanic and Atmospheric Administration, National Environmental

- Satellite, Data, and Information Service, accessed on June 1, 2012 at URL:
<http://www.ncdc.noaa.gov/oa/ncdc.html>
- National Weather Service, 2012, Climate Divisions with counties: National Weather Service, Climate Prediction Center, accessed on June 20, 2012 at URL:
http://www.cpc.ncep.noaa.gov/products/analysis_monitoring/regional_monitoring/CLIM_DIVS/states_counties_climate-divisions.shtml
- The Engineering Toolbox, 2012, Evaporation from water surfaces: The Engineering Toolbox, accessed on June 22, 2012 at URL:
http://www.engineeringtoolbox.com/evaporation-water-surface-d_690.html
- TIBCO Software, Inc., 2012, TIBCO Spotfire: TIBCO Software, Inc., accessed on June 15, 2012 at URL: <http://spotfire.tibco.com/products/overview/analytics-products.aspx>
- Tortorelli, R.L., 2009, Water use in Oklahoma 1950-2005: U.S. Geological Survey Scientific Investigations Report 2009-5212, 49 p.
- U.S. Geological Survey, 2012a, The Aggregate Water Use Data System (AWUDS) of the USGS: U.S. Geological Survey, accessed on June 15, 2012 at URL:
<http://water.usgs.gov/watuse/wuawuds.html>
- U.S. Geological Survey, 2012b, USGS surface-water data for Oklahoma: U.S. Geological Survey, accessed on May 15, 2012 at URL: <http://waterdata.usgs.gov/ok/nwis/sw/>
- U.S. Geological Survey 2012c, Welcome to StreamStats, Oklahoma: U.S. Geological Survey, accessed on June 6, 2012 at URL:
<http://water.usgs.gov/osw/streamstats/oklahoma.html>
- Wahl, T.L., and Wahl, K.L., 2012, A computer program for determining an index to base flow: U.S. Bureau of Reclamation, accessed on June 6, 2012 at URL:
http://www.usbr.gov/pmts/hydraulics_lab/twahl/bfi/

Identifying Nutrient Pathways to Streams: Sediment and Phosphorus Loads from Streambank Erosion and Failure in the Illinois River Watershed

Basic Information

Title:	Identifying Nutrient Pathways to Streams: Sediment and Phosphorus Loads from Streambank Erosion and Failure in the Illinois River Watershed
Project Number:	2012OK248B
Start Date:	3/1/2012
End Date:	2/28/2013
Funding Source:	104B
Congressional District:	3
Research Category:	Water Quality
Focus Category:	Geomorphological Processes, Nutrients, Sediments
Descriptors:	None
Principal Investigators:	Garey Fox, Chad Penn, Daniel E. Storm

Publication

1. Fox, G.A., R.B. Miller, E. Daly, D.E. Storm, and C. Penn. 2013. Streambank and phosphorus loading from protected and unprotected streambanks in eastern Oklahoma. ASABE Annual International Meeting, Conference Proceedings Paper, Kansas City, MO, July 21-24, 2013.

**FY 2012 Oklahoma Water Resources Research Institute Grant
Interim Technical Report**

Title:

Identifying Nutrient Pathways to Streams: Sediment and Phosphorus Loads from Streambank Erosion and Failure in the Illinois River Watershed

Start Date:

March 1, 2012

End Date:

August 31, 2013

Congressional Districts:

03 – Stillwater, Oklahoma State University and Project Sites

Focus Category:

GEOMORPHOLOGICAL PROCESSES, HYDROLOGY, NONPOINT POLLUTION, NUTRIENTS, SEDIMENTS

Descriptors:

Streambank Erosion, Sediment, Phosphorus, Riparian Protection

Principal Investigators:

Garey A. Fox, Ph.D., P.E., Associate Professor and Buchanan Chair, Department of Biosystems and Agricultural Engineering, Oklahoma State University; Chad Penn, Associate Professor, Plant and Soil Sciences, Oklahoma State University; Dan Storm, Professor, Biosystems and Agricultural Engineering, Oklahoma State University

Publications:

Fox, G.A., R.B. Miller, E. Daly, D.E. Storm, and C. Penn. 2013. Streambank and phosphorus loading from protected and unprotected streambanks in eastern Oklahoma. ASABE Annual International Meeting, Conference Proceedings Paper, Kansas City, MO, July 21-24, 2013.

TABLE OF CONTENTS

List of Figures	iii
List of Tables.....	iv
Summary Table of Student Support.....	v
Abstract	vi
I. Problem and Research Objectives	1
II. Methodology	3
III. Principle Findings and Significance.....	6
IV. Conclusions and Future Work	11
V. Acknowledgements	11
VI. References.....	11

LIST OF FIGURES

Figure 1. Map of Barren Fork Creek watershed in eastern Oklahoma. A, B, C, and D are four sites where data/samples were collected from six streambanks.....	2
Figure 2. Typical streambank profile of Ozark Ecoregion streams in Eastern Oklahoma. BH is the bank height; FL is the bank face length; D is the depth of the water at the thalweg; and α is the bank angle.....	2
Figure 3. Eroded streambank on Barren Fork Creek after a rainfall event. Picture from Midgley et al. (2012).....	3
Figure 4. NAIP aerial images from 2003 (bottom) and 2008 (top) of a stream and the polygon (in red) showing the bank erosion during that time period.....	5
Figure 5. Water-soluble phosphorous (WSP) contour plots and NAIP aerial photographs for unprotected sites. Note that different scales were used in the contour plots to highlight P distributions.	8
Figure 6. Water-soluble phosphorous (WSP) and NAIP aerial photographs for protected sites. Note that different scales were used in the contour plots to highlight P distributions..	9
Figure 7. Percent reach failing of left and right streambanks along the Barren Fork Creek watershed (bottom line) and several other streams in eastern Oklahoma.....	10

LIST OF TABLES

Table 1. Total water-soluble phosphorous (WSP), streambank retreat, and quantified erosion for each site.	7
Table 2. Length-averaged water-soluble phosphorus (WSP) per year per length of streambank.	10

SUMMARY TABLE OF STUDENT SUPPORT

Student Status	Number	Disciplines
Undergraduate	2	Biosystems and Agricultural Engineering
M.S.		
Ph.D.	1	Biosystems and Agricultural Engineering
Post Doc	1	Biosystems and Agricultural Engineering
Total	4	Biosystems and Agricultural Engineering

ABSTRACT

Nutrients and excessive sediment are two main nonpoint source pollutants in the United States. In some watersheds, the majority of the total sediment load to streams and rivers is from streambank erosion. The presence of riparian vegetation can significantly decrease streambank erosion in some locations. Streambank erosion and failure may be one pathway for phosphorus (P) loading to streams, but insufficient data exists on actual loading from this source and the potential protective effect of riparian vegetation in most watersheds. The objective of this research was to characterize the distribution of soil phosphorus concentrations in streambanks both with and without implemented riparian protection in the Barren Fork Creek watershed in eastern Oklahoma and to estimate P loading due to bank erosion. Barren Fork Creek is a state-designated Scenic River in Oklahoma where soil phosphorus (P) levels are potentially high due to historic poultry litter application. Streambank soil samples were collected at three transects and at four vertical locations at six different reaches. Streambank core samples were collected up to 50 cm into the bank at each location. Also, lateral bank erosion over a seven year period (2003-2010) was estimated using aerial photography. Soil samples were analyzed for water-soluble phosphorus, pH, and electrical conductivity (EC). A video reconnaissance of the Barren Fork Creek throughout the entire watershed in Oklahoma was performed to estimate the average percent reach failing. Contour plots of streambank phosphorus concentrations illustrated considerable differences among reaches relative to adjacent land use. Average streambank migration rates were approximately 8 m for the three sites with riparian protection compared to 45 m for the three sites without riparian protection over the seven year period. When considering the combination of phosphorus concentrations and the extent of erosion as documented by the video reconnaissance (approximately 37.5% failing and unprotected banks), streambanks represent a considerable source of phosphorus entering Barren Fork Creek and eventually impacting water supply reservoirs. Total water soluble phosphorus from streambanks on the Barren Fork Creek from unprotected and failing banks is approximately 1540 kg per year, which represents approximately 10% of the total dissolved phosphorus load.

IDENTIFYING NUTRIENT PATHWAYS TO STREAMS: SEDIMENT AND PHOSPHORUS LOADS FROM STREAMBANK EROSION AND FAILURE IN THE ILLINOIS RIVER WATERSHED

I. PROBLEM AND RESEARCH OBJECTIVES

Nutrients and excess sediment are two of the primary pollutants of surface waters in the United States. Main sources of nutrients include fertilizer, legacy P from discharges in the upper portion of the watershed, and wastewater treatment plant discharge. However, there is currently insufficient data about many of the watersheds to determine the loading of sediment and nutrients from streambanks. Billions of dollars have been spent on streambank stabilization to help slow bank retreat and reduce sediment loading (Lavendel, 2002; Bernhardt et al., 2005). Riparian protection can drastically reduce streambank erosion in locations, but estimates of actual decreases in sediment-bound P are limited. Understanding the effects of riparian protection on sediment and phosphorous loading to streams due to streambank erosion can justify the use and demonstrate the effectiveness of such management practices.

Barren Fork Creek is a fourth order stream, originating in northwestern Arkansas which flows west through the Boston Mountains and Ozark Highlands ecoregions, and reaches its confluence with the Illinois River at Lake Tenkiller near Tahlequah, OK (Figure 1). The Barren Fork Creek watershed is within the Illinois River watershed, which has many areas listed on the 303(d) list for nutrient related impairments. Streambanks consist of cohesive topsoil underlain by noncohesive gravel (Midgley et al., 2012). Silt loam and loam topsoils (Figure 2) have high potential for P sorption (Fuchs et al., 2009; Heeren et al., 2011; Miller et al., 2011; Mittelstet et al., 2011); however, these soils can become very unstable when undercutting by fluvial erosion occurs (Figure 3). This instability, which can lead to mass failure of the bank, may be a major pathway for P loading into streams. Multiple state and federal agencies, including the Oklahoma Conservation commission (OCC), have invested heavily in riparian protection along the Barren Fork Creek watershed, and data on the behavior of the protected and unprotected streambanks is vital to determine if these management practices should be implemented throughout the watershed and in other impaired regions.

Streambank erosion is most likely to occur when the soil's resistance to fluvial erosion is low and when soil strength is low causing a geotechnically unstable bank. Fluvial erosion can lead to streambank undercutting when fluvial forces remove sediment at the toe or bottom of the bank, leading to geotechnical failure of the overlying material (Midgley et al., 2012). The growth and establishment of tree roots adds more strength to the soil structure and reduces the occurrence of streambank erosion. Therefore, adding trees to the system through the implementation of a riparian corridor or vegetative filter strip can help to stabilize the banks. The important question is how much stabilization it provides, especially in geomorphically active or rapidly eroding streams such as Barren Fork Creek (Midgley et al., 2012).

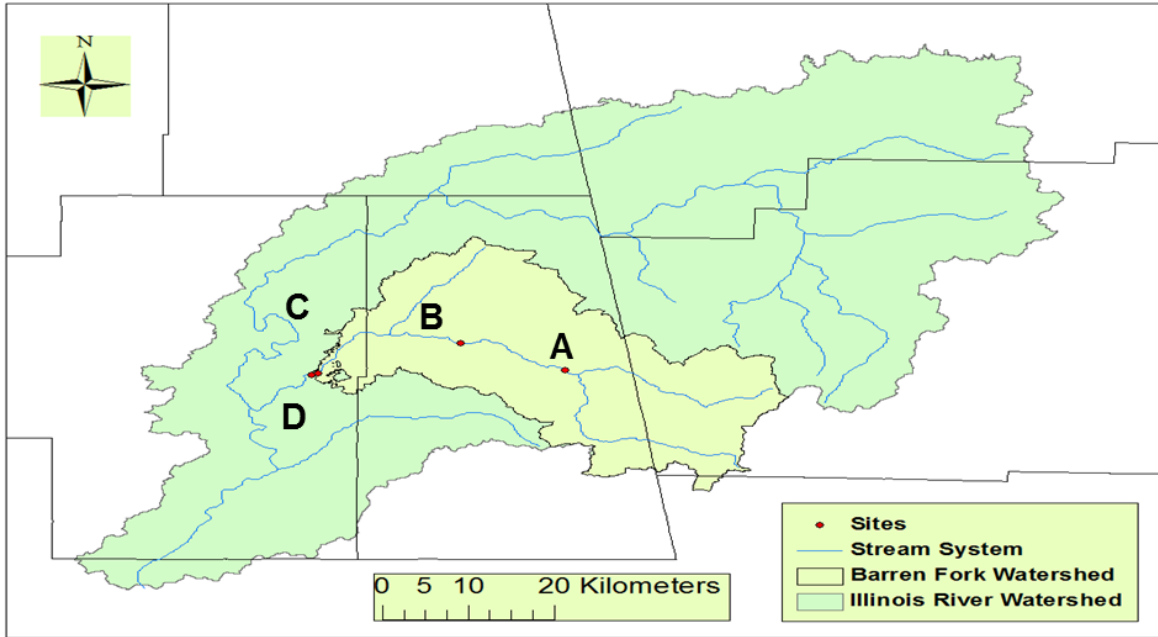


Figure 1. Map of Barren Fork Creek watershed in eastern Oklahoma. A, B, C, and D are four sites where data/samples were collected from six streambanks.

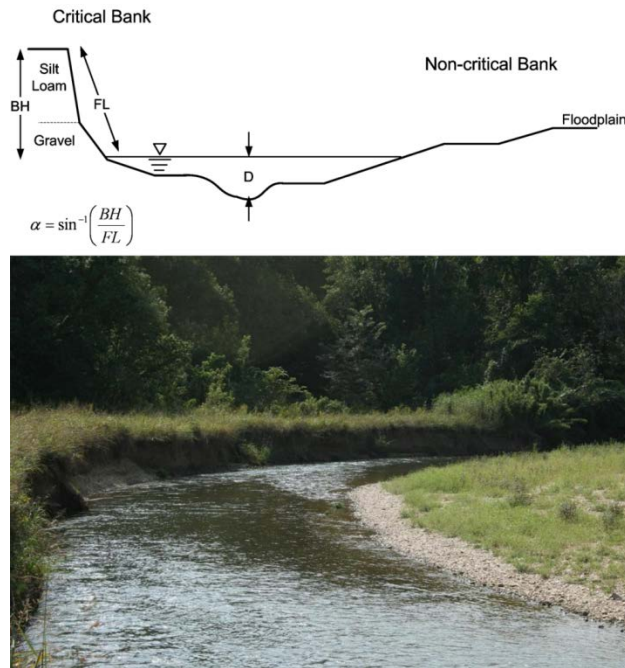


Figure 2. Typical streambank profile of Ozark Ecoregion streams in Eastern Oklahoma. BH is the bank height; FL is the bank face length; D is the depth of the water at the thalweg; and α is the bank angle.



Figure 3. Eroded streambank on Barren Fork Creek after a rainfall event. Picture from Midgley et al. (2012).

Poultry litter, a by-product of egg and poultry production, has historically been applied as fertilizer within the Barren Fork Creek watershed. These fertilizers are high in P and excess P concentrations may build up on the soil surface. Runoff of precipitation over the surface immediately after application can lead to the transport of P into the stream. Phosphorous can also be sorbed onto the soil, so erosion of the soil surface can lead to an increase in sediment and sediment-bound P in the streams (Mittelstet et al., 2011). These processes result in an excess of nutrients within the water and can lead to eutrophication which, in turn, decrease the quality and productivity of the receiving lake and/or water supply reservoir. Streams and water bodies in the eastern Oklahoma Ozarks are very sensitive to nutrient pollution, so determining loading into the waterways is important, but in this effort bank erosion as a P-load source has often been ignored.

The objective of this research was to assess the importance of bank erosion as a source of P loading to the Barren Fork Creek based on six selected streambanks distributed throughout the Barren Fork Creek watershed. To accomplish this, the study had three major goals: (1) quantify the amount of streambank erosion and failure, (2) quantify the amount of water-soluble phosphorous in streambanks, and (3) estimate the benefit of riparian management practices in the Barren Fork Creek watershed.

II. METHODOLOGY

Six streambank sites within the Barren Fork Creek watershed were selected for the study (Figure 1), and labeled from upstream to downstream as site A through D. One or two stream reaches were selected at each site that had consistent streambank characteristics (layering, height, and vegetation protection). Reach lengths ranged from 138 to 233 m. The streambanks consisted of approximately 0.9 to 2.5 m of silt loam topsoil underlain by non-cohesive and easily eroded gravel. Total bank heights varied among the sites, but typically

ranged between 2.0 and 4.0 m. Riparian tree species on protected banks included Bur Oak, Blackgum, River Birch, and Mockernut Hickory (Brabander et al., 1985).

At each study site, soil samples were collected at three transects and at four vertical locations: two near the bank surface (15 cm), one in the middle of the silt loam topsoil depth (60 cm), and one just above the interface between the topsoil and gravel layers (90 or 120 cm). Soil cores were taken 50 cm into the streambank face or until resistance occurred. Each core was then divided into three lateral sections: (1) 0 to 5 cm, (2) 5 to 20 cm, and (3) 20 to 50 cm. When possible, additional samples were acquired up to 100 cm and divided into five sections including 50 to 75 cm or 50 cm to 100 cm. Samples were acquired in June 2012 after litter application had occurred in the watershed.

Images from the National Agricultural Imagery Program (NAIP) from 2003-2010 were obtained for analysis. Based on those images, three sites had historical riparian protection and three sites did not possess riparian protection. Figure 4 shows NAIP images from one of the locations. ArcMap 10 (ESRI, Redlands, CA) was used for determining bank erosion over time (Figure 4). From the NAIP image, the total lateral retreat was measured. Total sediment loading (SL , kg or kg/yr) into the stream from each site was then determined using the estimated reach length (RL , m), the average lateral streambank retreat (SR , m), soil bulk density (ρ_b , 1500 kg/m³), and depth of the topsoil from cross-section surveys (D_{ts} , m):

$$SL = RL \times SR \times D_{ts} \times \rho_b \quad (1)$$

Subsamples from the cores were characterized for P saturation and soil properties that impact P saturation. Soil pH was measured by weighing out 5 g of sample and adding 15 mL of distilled water (DI water) to a vial to obtain a 1:3 (soil:water) ratio required for the tests. Vials were shaken for 30 seconds, ensuring that all soil was wet. Samples were then equilibrated for 20 minutes and were shaken again. After sitting for another 20 minutes the calibrated pH probe was placed into the sample mixture. Once the probe had stabilized, the reading was taken to the nearest 0.01. The probe was rinsed with DI water between each sample. The same sample preparation procedure was used for EC, but using a calibrated EC meter.

Mehlich III soil test phosphorous (STP) was also measured in the laboratory. These measurements estimate plant availability of many nutrients on soil acids. This method has been positively correlated to crop residue and fertilizer phosphorous (Zhang et al., 2009). Laboratory procedures for these tests involve weighing out 2 g of dried soil sample into a centrifuge tube, adding 20 mL of Mehlich 3 solution (having a 1:10 soil to solution ratio), putting the tubes on a shaker for 5 minutes on the high setting, and then filtering the mixture with Whatman #42 paper.

Standard ammonium oxalate tests were run to determine the extractable aluminum, iron, and phosphorous within the samples. The proper methods for these tests involved weighing out 1 g of sample and putting it in a centrifuge tube with 40 mL of the ammonium oxalate extracting solution. Each tube was wrapped in aluminum foil to keep the mixture in darkness throughout the extraction. Tubes were placed on a shaker at low speed for two hours. Next, tubes were centrifuged at 2000 rpm for 13 minutes. Whatman #42 filter paper was then used to filter the solution into a 60 mL sample bottle. These bottles were then sent to the Plant Disease and Insect Diagnostic Laboratory for ICP analysis of iron, aluminum, and phosphorous.

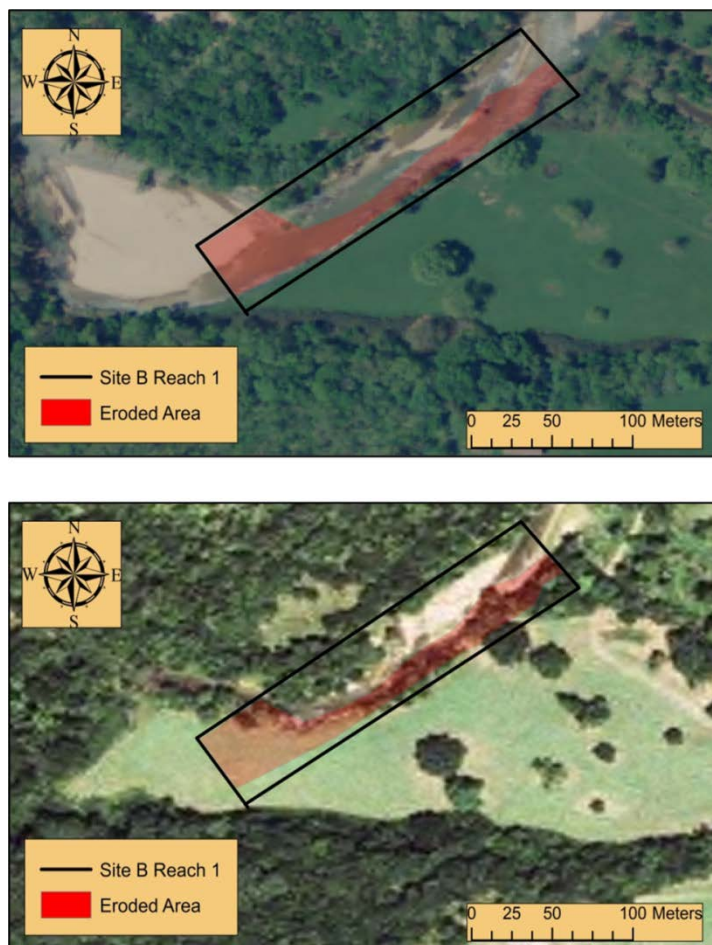


Figure 4. NAIP aerial images from 2003 (bottom) and 2008 (top) of a stream and the polygon (in red) showing the bank erosion during that time period.

Water-soluble phosphorous (WSP) was measured to determine the amount of P that is readily available for plant uptake. A 2 g subsample of soil was weighed and placed with 20 mL of DI water into a centrifuge tube, and all tubes were placed on a shaker platform at the low setting for an hour. After shaking, samples were centrifuged at 2000 rpm for 13 minutes. Each solution was then individually vacuum filtered using 0.45- μ m filters. The P concentrations in the filtered solutions were determined using the Murphy Riley colorimetric method (Murphy and Riley, 1962). The procedure called for 5 mL of the Murphy Riley reagent in each sample. Test tubes were left to equilibrate for 30 minutes and then analyzed, against standards, using a spectrophotometer. This test is the most appropriate environmental estimator of P concentrations in runoff as compared to other soil test methods (Fuhrman et al., 2005). Dissolved reactive P concentrations in runoff are correlated to a soil's WSP (Pote et al., 1996).

Transect streambank pH, EC, and P data from each site were composited. The spatial distribution of WSP at each site was plotted in a contour plot using SigmaPlot to visualize the three-dimensional P distribution in the banks. Total WSP (kg WSP) contributed at each stream site was calculated as total mass of eroded topsoil (SL, kg or

kg/yr) multiplied by the average WSP for all measurements in the streambank (WSP_{avg} , mg WSP/kg soil). The length-averaged WSP-load for each site was calculated as WSP_{avg} divided by reach length (WSP_{avg}/m). Average contributions for both unprotected and riparian protected sites were then compared to estimate the benefit of riparian vegetation in preventing WSP loading to the creek.

A video aerial reconnaissance of the Barren Fork Creek streambanks was performed as part of a different project funded by the Oklahoma Water Resources Board and Oklahoma Conservation Commission. This video survey was performed by flying a helicopter to video streambanks throughout the Barren Fork Creek watershed (both banks). The average percent reach failing (i.e., unprotected banks) of left and right banks (over two kilometer increments) was estimated for the 55 km of stream (110 km total streambank length) in the watershed. The WSP_{avg}/m of failing and unprotected banks was used with this estimated length to compare water soluble phosphorus loads from streambanks with estimated dissolved phosphorus loads from recently calibrated Soil and Water Assessment Tool (SWAT) simulations for the Barren Fork Creek watershed (Mittelstet, A., personal communication, November 8, 2012).

III. PRINCIPLE FINDINGS AND SIGNIFICANCE

Streambank soil pH values were fairly consistent and on average ranged from 5.5 to 7.0. Soil electrical conductivity (EC) measurements had a wider range of values and were typically between 10 and 100 μS . The P spatial distribution assisted in determining if P was originating from high P events in the streamflow or from upland activities. Higher WSP levels were present on the soil surface at Unprotected Site A and Protected Site B, which was likely due to nearby agricultural activity including historical fertilizer (litter) applications (Figures 5 and 6). Unprotected Site D and Protected Site B had high WSP in the silt loam layer just above the gravel subsoil. This was hypothesized as due to WSP-rich stream water moving into the floodplain gravel, allowing P to sorb to the silt loam.

Unprotected sites eroded on average 45.5 m over the period 2003-2010, with the greatest erosion at Site C, while the protected sites eroded on average 7.8 m over the same period (Table 1, Figures 5 and 6). Of course, streambank erosion depends on multiple factors beyond simply the presence of riparian vegetation, including the bank height, the soil's resistance to fluvial erosion and geotechnical failure, and the applied stress by the streamflow. One important factor related to the applied stress is the curvature or radius of curvature of the streambank (Heeren et al., 2012; Midgley et al., 2012). It is well known that additional stress is created as water flows around a bend in a stream. An important question is whether curvature was a more important factor than riparian vegetation in the results. More specifically, were the unprotected banks located on bends with a tighter (smaller) radius of curvature? Using the aerial images, the radius of curvature was estimated at each time of image acquisition from 2003 to 2010. On average, the radius of curvature of the unprotected banks was approximately 300 m and the corresponding value for protected banks was approximately 750 m. However, the ranges overlapped considerably, suggesting that curvature effects and riparian vegetation were both important factors. A more detailed analysis will need to be performed using a streambank erosion and stability model to more completely understand the role of each of these factors.

Table 1. Total water-soluble phosphorous (WSP), streambank retreat, and quantified erosion for each site.

Site	A	A	B	C	C	D
Protected (P) or Unprotected (UP)	UP	P	P	UP	P	UP
Average WSP (mg P/kg soil)	7.2	3.9	3.2	1.2	2.4	1.4
Reach Length (m)	190	233	138	185	182	146
Average Retreat from 2003-2010 (m)	33.7	8.0	7.3	68.3	8.0	34.6
Topsoil Depth from Cross-Section Surveys (m)	1.6	0.9	2.5	0.9	1.1	1.2
Total Soil Volume Eroded (m ³)	1.02 x 10 ⁴	1.68 x 10 ³	2.52 x 10 ³	1.14 x 10 ⁴	1.60 x 10 ³	6.06 x 10 ³
Total Soil Mass Eroded (kg)	1.54 x 10 ⁷	2.52 x 10 ⁶	3.78 x 10 ⁶	1.71 x 10 ⁷	2.40 x 10 ⁶	9.09 x 10 ⁶
Total Contributed WSP (kg P)	110	10	12	21	6	13

Over the seven year study period a total of 180 kg of WSP for all six sites was contributed to the Barren Fork Creek. Across the sites, the average WSP-load was 30 kg in seven years or 4.3 kg WSP/yr (Table 2). The WSP-load was dominated by erosion at the unprotected sites where the average over the seven years was 50.1 kg or 7.2 kg WSP/yr. In contrast, the protected sites had an average WSP contribution of 9.9 kg in seven years or 1.4 kg WSP/yr (Table 2). The average contributed WSP across all sites was 0.022 kg WSP per year per m of bank. The average for unprotected sites was 0.037 kg WSP per year per m of bank while that for protected sites was 0.008 kg WSP per year per m of bank. These numbers are dependent on how representative the sampled streambanks are relative to the rest of the watershed. More data should be collected to verify these initial findings.

Percent reach failing of left and right banks as collected from the video survey is shown in Figure 7. Total WSP loading from the Barren Fork from unprotected and failing streambanks was estimated at approximately 1540 kg per year when using an estimated 0.037 kg WSP per yr per m as derived in this research. Using an estimated dissolved phosphorus load from SWAT modeling on the Barren Fork Creek watershed, approximately 10% of the total dissolved P load each year originates from streambanks.

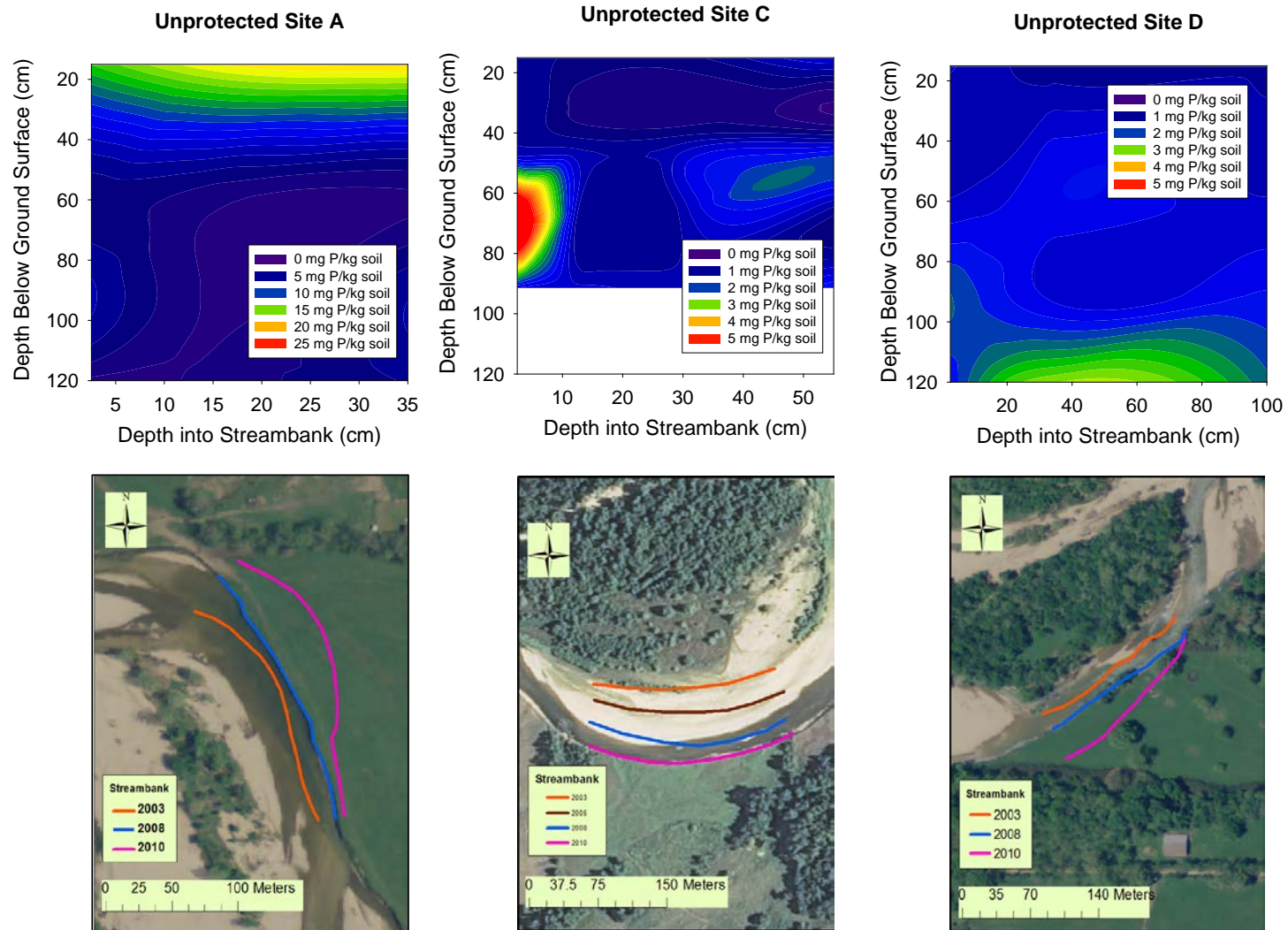


Figure 5. Water-soluble phosphorous (WSP) contour plots and NAIP aerial photographs for unprotected sites. Note that different scales were used in the contour plots to highlight P distributions.

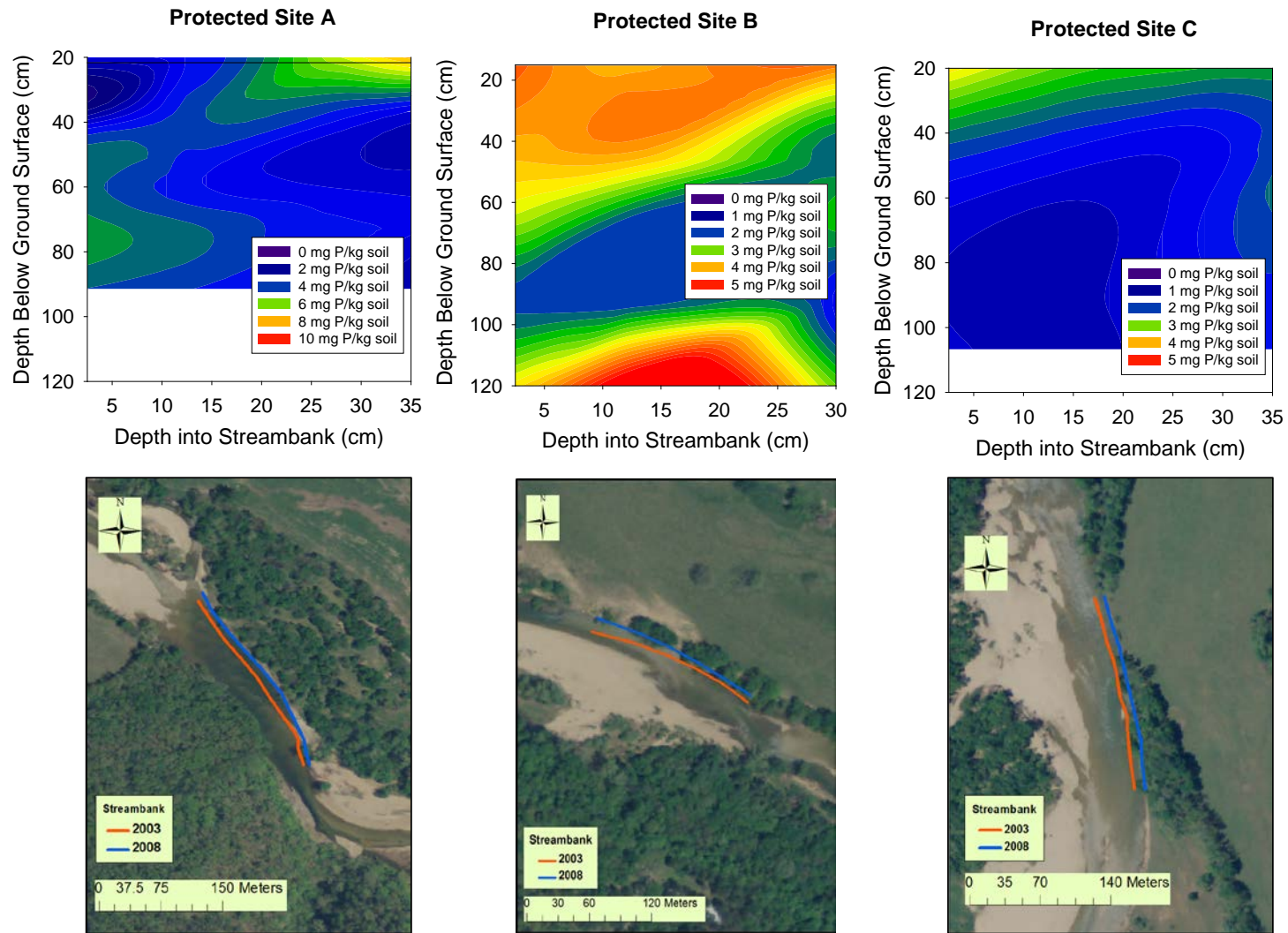


Figure 6. Water-soluble phosphorous (WSP) and NAIP aerial photographs for protected sites. Note that different scales were used in the contour plots to highlight P distributions.

Table 2. Length-averaged water-soluble phosphorus (WSP) per year per length of streambank.

Site	A	A	B	C	C	D
Protected (P) or Unprotected (UP)	UP	P	P	UP	P	UP
Contributed WSP per yr per m of bank (kg P/yr/m)	0.087	0.006	0.015	0.016	0.005	0.013

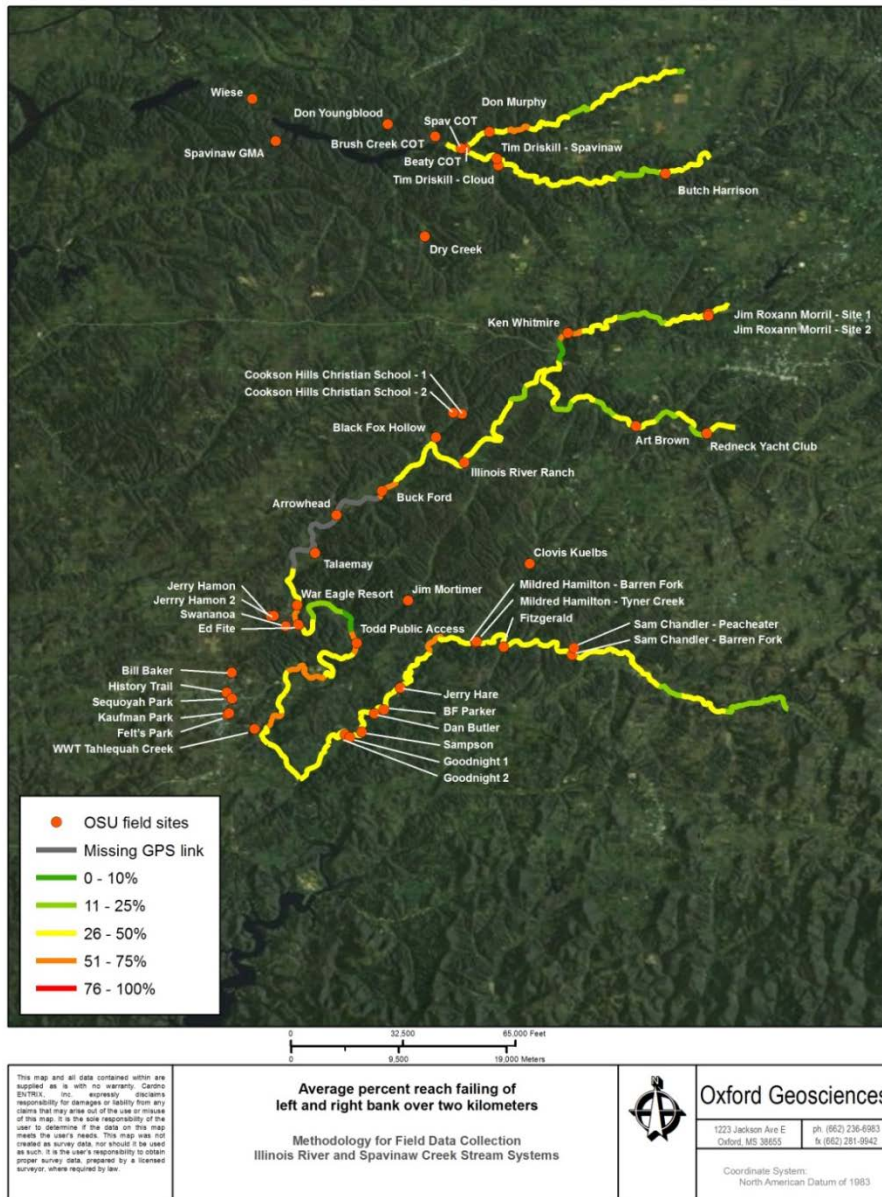


Figure 7. Percent reach failing of left and right streambanks along the Barren Fork Creek watershed (bottom line) and several other streams in eastern Oklahoma.

IV. CONCLUSIONS AND FUTURE WORK

Areas protected by riparian vegetation in the Barren Fork Creek watershed experienced at least four times less bank retreat over a seven year period (2003-2010). While dependent on the presence of riparian protection, this reduction was also due to the fact that unprotected banks were more prevalent on actively eroding meander bends. There was a five times reduction in kg of contributed WSP per year per m of bank with riparian protection. These results show that riparian vegetation is effective in reducing the volume of WSP that is entering the stream due to streambank erosion and failure. Riparian vegetation may help limit streambank erosion along a stream reach and slow the rate of lateral migration even when positioned at a meander bend. Total water soluble phosphorus from streambanks on the Barren Fork Creek from unprotected and failing banks is approximately 1540 kg per year, which represents approximately 10% of the total dissolved phosphorus load. These results can be used directly by conservation agencies to demonstrate and emphasize the importance of riparian best management practices to protect this scenic river.

Future work will involve modeling the specific streambank sites using the Bank Stability and Toe Erosion Model (BSTEM). The modeling will allow us to determine streambank and phosphorus loading rates across a range of hydraulic stresses and near-streambank groundwater conditions. Also, future soil chemistry measurements are planned.

V. ACKNOWLEDGEMENTS

This material is based upon work supported by a FY 2012 Oklahoma Water Resources Research Institute (OWRRI) and the Oklahoma Water Resources Board (OWRB) grant under the U.S. Geological Survey 104b program.

VI. REFERENCES

- Bernhardt, E.S., M.A. Palmer, J.D. Allan, G. Alexander, K. Barnas, S. Brooks, J. Carr, S. Clayton, C. Dahm, J. Follstad-Shah, D. Galat, S. Gloss, P. Goodwin, D. Hart, B. Hassett, R. Jenkinson, S. Katz, G.M. Kondolf, P.S. Lake, R. Lave, J.L. Meyer, T.K. O'Donnell, L. Pagano, B. Powell, and E. Sudduth. 2005. Synthesizing U.S. river restoration efforts. *Science* 308: 636-637, DOI:10.1126/science.1109769.
- Brabander, J.J., R.E. Mastersand, and R.M. Short. 1985. Bottomland Hardwoods of Easter Oklahoma. Oklahoma Dept. of Wildlife Conservation.
- Fuchs, J.W., G.A. Fox, D.E. Storm, C. Penn, and G.O. Brown. 2009. Subsurface transport of phosphorus in riparian floodplains: Influence of preferential flow paths. *J. Environ. Qual.* 38(2): 473-484.
- Fuhrman J. K., H. Zhang, J. L. Schroder, and R. L. Davis. 2005. Water-soluble phosphorus as affected by soil to extractant ratios, extraction times, and electrolyte. *Communications in Soil Science and Plant Analysis* 36: 925-935.

- Heeren, D.M., G.A. Fox, R.B. Miller, D.E. Storm, A.K. Fox, C.J. Penn, T. Halihan, and A.R. Mittelstet. 2011. Stage-dependent transient storage of phosphorus in alluvial floodplains. *Hydrol. Proc.* 25(20): 3230-3243, DOI: 10.1002/hyp.8054.
- Heeren, D.M., A.R. Mittelstet, G.A. Fox, D.E. Storm, A.-S. Al-Madhhachi, T.L. Midgley, A.F. Stringer, K.B. Stunkel, and R.B. Tejral. 2012. Using rapid geomorphic assessments to assess streambank stability in Oklahoma Ozark streams. *Trans. ASABE* 55(3): 957-968.
- Lavendel, B., 2002. The business of ecological restoration. *Ecol. Res.* 20: 173-178.
- Midgley, T., G.A. Fox, and D.M. Heeren. 2012. Evaluation of the Bank Stability and Toe Erosion Model (BSTEM) for predicting lateral streambank retreat on composite streambanks. *Geomorphology* 145-146: 107-114.
- Miller, R.B., D.M. Heeren, G.A. Fox, D.E. Storm, and T. Halihan. 2011. Design and application of a direct-push in-situ gravel permeameter. *Ground Water* 49(6): 920-925, DOI: 10.1111/j.1745-6584.2010.00796.x.
- Mittelstet, A.R., D.M. Heeren, G.A. Fox, D.E. Storm, M.J. White, and R.B. Miller. 2011. Comparison of subsurface and surface runoff phosphorus transport rates in alluvial floodplains. *Ag. Ecosystems Environ.* 141: 417-425, DOI: 10.1016/j.agee.2011.04.006.
- Murphy, J., and J.R. Riley. 1962. A modified single solution method for the determination of phosphate in natural waters. *Anal. Chim. Acta* 27: 31-36.
- Pote, D.H., T.C. Daniel, A.N. Sharpley, P.A. Moore, Jr., D.R. Edwards, and D.J. Nichols. 1996. Relating extractable soil phosphorus to phosphorus losses in runoff. *Soil Sci. Soc. Am. J.* 60: 855-859.
- Zhang, H., S. Kariuki, J. Schroder, M. Payton, and C. Focht. 2009. Interlaboratory validation of the Mehlich 3 for extraction of plant-available phosphorus. *J. AOAC International* 92(1): 91-102.

USGS Award no. G12AP20104 Utilization of Regional Climate Science Programs in Reservoir and Watershed Impact Assessments

Basic Information

Title:	USGS Award no. G12AP20104 Utilization of Regional Climate Science Programs in Reservoir and Watershed Impact Assessments
Project Number:	2012OK269S
Start Date:	5/14/2012
End Date:	4/15/2013
Funding Source:	Supplemental
Congressional District:	
Research Category:	Climate and Hydrologic Processes
Focus Category:	Climatological Processes, Models, Management and Planning
Descriptors:	
Principal Investigators:	Dave Engle, Yang Hong, Renee McPherson

Publication

1. Lei Qiao, Yang Hong, Renee McPherson, Mark Shafer, Sheng Chen, David Williams, David Gade, and Douglas Lilly, 2013, Climate change and hydrological response in the trans-state Oologah Lake watershed - Evaluating dynamically downscaled NARCCAP and statistically downscaled CMIP3 simulations with VIC model, Water Resources Management (in review)

Project Report for “Utilization of Regional Climate Science Programs in Reservoir and Watershed Impact Assessments”
through the Responses to Climate Change Program, U.S. Army Corps of Engineers

PI: Renee A. McPherson; Co-PIs: Yang Hong and Mark Shafer

Overview

The funded work sought to efficiently and effectively capitalize on information from federal and university climate science programs for reservoir yield analyses, reservoir water quality models, watershed models, and development of future drought contingency plans. Tasks completed were as follows:

- The University of Oklahoma (OU) collected downscaled climate projection datasets, using a variety of global climate models, regional climate models, and statistical downscaling. Data was extracted at or near the pilot location (Lake Oologah and its watershed).
- OU compared data from the historical runs for each climate model run and statistically downscaled dataset to observations from near Lake Oologah to verify that the corresponding climate projections represent feasible future projections.
- OU benchmarked the Variable Infiltration Capacity (VIC) model with an historical dataset for at least a 10-year period.
- OU input historical and projected gridded climate data into the VIC model and provided output from this model to the USACE for incorporation into their modeling efforts and decision tools. Output included time-series hydrographs for a 50-year planning horizon that could be used for reservoir simulation and yield studies.
- OU provided input to reports that would be disseminated USACE-wide and to other stakeholders through the Water Management and Reservoir Reallocation Studies Planning Center of Expertise by USACE.

One of the intents of this pilot study was to leverage climate-related resources available at the National Weather Center at the University of Oklahoma in Norman, OK. At the time the grant was funded, there was no straightforward mechanism to transfer funds between the U.S. Army Corps of Engineers–Tulsa District and OU. We strove for several months to find a pathway that would minimize administrative costs, including trying to transfer funds to the National Oceanic and Atmospheric Administration (NOAA), then to OU via an existing cooperative agreement that funds the Southern Climate Impacts Planning Program, a NOAA Regional Sciences and Assessments (RISA) program. Unfortunately, NOAA projected a 6-12 month process that involved lawyers at USACE and NOAA to transfer funding between these government entities. Finally, USACE was able to transfer funds via a standing agreement with the U.S. Geological Survey’s (USGS) Oklahoma Water Science Center, which had an existing agreement with Oklahoma State University (OSU) for the transfer of funds related to water research (via their Oklahoma Water Resources Research Institute). From OSU, funding could be made available to OU, although additional indirect costs for administering the grant at OSU were taken, reducing the amount available for conducting the science at OU. We recommend that the USACE work with the USGS to allow the transfer of funds for climate-related research to the newly established USGS Climate Science Centers. OU is the host institution (as of March 2012) for the

South Central Climate Science Center and has a cooperative agreement with USGS that should allow for transfer of funds between USACE and OU with minimal additional overhead.

Another intent of this pilot study was to determine if there were additional opportunities for collaborative work, especially as related to future climate challenges faced by USACE. Related work in the Red River Basin has been proposed through the annual science supplemental funding process of the USGS for the Climate Science Centers, and we intend to work with USACE on other studies of interest to them for important basins within the Tulsa District. In all, this project has been successful at establishing dialogue and collaborative research between USACE and the National Weather Center, especially its climate science and climate impacts programs. These opportunities are critical for USACE to access experts in cutting-edge science in the university environments as well as for OU to help serve Oklahoma and the south-central region in actionable science.

Study Results

Simulated historical and projected climate data from the North American Regional Climate Change Assessment Program (NARCCAP) and Bias-Corrected and Spatially Downscaled – Coupled Model Intercomparison Phase 3 (BCSD-CMIP3) forced the hydrologic model. In North America, the North American Regional Climate Change Assessment Program (NARCCAP) is currently the most comprehensive regional climate-modeling project for climate change impact studies [Mearns *et al.* 2009; Mearns *et al.* 2012]. The NARCCAP ensemble comprises a set of regional climate models (RCMs) driven by a set of atmosphere-ocean general circulation models (GCMs) over a domain covering the conterminous United States and most of Canada. The GCMs have been forced with the Special Report on ~~the~~ ^{(SR15) A2 Scenario} scenario for the 21st century; hence, the global average CO₂ is projected to reach 850 ppm by 2100 [IPCC 2000]. The RCMs were nested within the GCMs for the period 1971-2000 and for the future period 2041-2070. For comparison of hydrological responses driven by different downscaled climate projections, the bias-corrected and spatially downscaled Coupled Model Intercomparison Phase 3 dataset (BCSD-CMIP3) was also incorporated (using the LLNL-Reclamation-SCU downscaled climate projections data derived from the World Climate Research Program's CMIP3 multi-model dataset that is stored and served at the LLNL Green Data Oasis). This multi-model dataset includes 112 World Climate Research Program CMIP3 members with the CO₂ emission scenarios of A1b, A2, and B1, and each climate projection was bias-corrected and spatially downscaled [Maurer *et al.* 2007; Wood *et al.* 2002]. The A1b and B1 scenarios in BCSD-CMIP3 were not considered for direct comparison with NARCCAP because only the A2 emission scenario is available from NARCCAP.

The VIC model of Liang *et al.* [1994, 1996, and 1999] was implemented for the Oologah Lake watershed (Figure 1). It is a semi-distributed, grid-based hydrological model that simulates land surface-atmosphere hydrometeorological processes with both the water and energy budgets. In our application, version 4.1.2.c was used with three soil layers defined according to the STASTGO dataset. Land use and cover was leveraged from the Land Data Assimilation System project (<http://ldas.gsfc.nasa.gov/nldas/NLDASnews.php>), originally derived from the University of Maryland's 13-land-cover-type scheme (Figure 1). Upscaling of routing phase parameters (e.g., flow direction) was conducted from the Hydro-1k digital elevation model using an algorithm provided by VIC developing group (<http://www.hydro.washington.edu>). The VIC model was first driven by atmospheric forcing from the University of Washington's gridded

dataset [Maurer et al., 2002]. The model was calibrated with the SP-UCI (shuffled complexes with principal component analysis) algorithm [Chu et al. 2010; Chu et al. 2011].

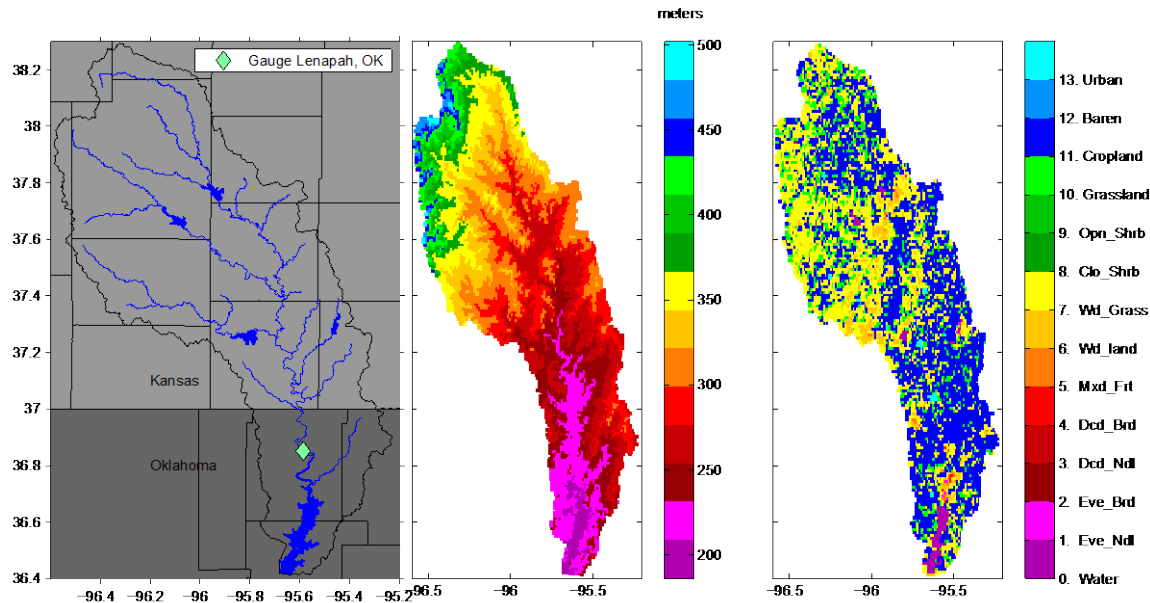


Figure 1. Study area with features of river, lakes, and political boundaries (left), elevation (middle), and land use and cover from the University of Maryland’s 13-land-cover-type scheme (right).

Evaluation and comparison of the results shows the following: (1) From the hydrologic point-of-view, the dynamically downscaled NARCCAP projection performed better, most likely in capturing a larger portion of mesoscale-driven convective rainfall than the statistically downscaled CMIP3 projections; hence, the VIC model generated higher seasonal streamflow amplitudes that are closer to observations. (2) Future water availability (precipitation, runoff, and base flow) in the watershed would increase annually by 3-4%, suggested by both NARCCAP and BCSD-CMIP3. Temperature increases (2.5-3°C) are more consistent between the two types of climate projections both seasonally and annually. However, NARCCAP suggested 2-3 times higher seasonal variability of precipitation and other water fluxes than the BCSD-CMIP3 models. (3) The hydrologic performance could be used as a potential metric to comparatively differentiate climate models, since the land surface and atmosphere processes are considered integrally.

Detailed results of the study are provided in the companion journal article, submitted to Water Resources Research in March 2013 by Lei Qiao, Yang Hong, Renee McPherson, Mark Shafer, Sheng Chen, David Williams, David Gade, and Douglas Lilly.

Financial Update

As of April 15, 2013, the following expenses were incurred:

<u>Item</u>	<u>Budgeted</u>	<u>Actual Expenses</u>
PI and Co-PI salaries	\$4,796	\$XXX
Post-doctoral associate salary	\$18,000	\$20,000
Fringe benefits	\$6,104	\$XXX
University of Oklahoma indirect costs	\$14,450	\$XXX
Oklahoma State indirect costs	\$10,515	\$10,515

Expenses for Oklahoma State University were solely a result of the inability to transfer funding directly from the U.S. Army Corps of Engineers–Tulsa District to the University of Oklahoma.

References

- Chu, W., X. Gao, and S. Sorooshian, 2010: Improving the shuffled complex evolution scheme for optimization of complex nonlinear hydrological systems: Application to the calibration of the Sacramento soil-moisture accounting model. *Water Resour. Res.*, **46**, W09530.
- Chu, W., X. Gao, and S. Sorooshian, 2011: A Solution to the Crucial Problem of Population Degeneration in High-Dimensional Evolutionary Optimization. *Systems Journal, IEEE*, **5**, 362-373.
- Intergovernmental Panel on Climate Change (IPCC), 2000: Special Report on Emissions Scenarios, Cambridge Univ. Press, Cambridge, U. K.
- Liang, X., E. F. Wood, and D. P. Lettenmaier, 1996: Surface soil moisture parameterization of the VIC-2L model: Evaluation and modification. *Global and Planetary Change*, **13**, 195-206.
- Liang, X., E. F. Wood, and D. P. Lettenmaier, 1999: Modeling ground heat flux in land surface parameterization schemes. *J. Geophys. Res.*, **104**, 9581-9600.
- Liang, X., D. P. Lettenmaier, E. F. Wood, and S. J. Burges, 1994: A simple hydrologically based model of land surface water and energy fluxes for general circulation models. *J. Geophys. Res.*, **99**, 14415-14428.
- Maurer, E. P., A. W. Wood, J. C. Adam, D. P. Lettenmaier, and B. Nijssen, 2002: A long-term hydrologically based dataset of land surface fluxes and states for the conterminous United States, *Journal of Climate*. **15**, 3237-3251.
- Mearns, L. O., W. Gutowski, R. Jones, R. Leung, S. McGinnis, A. Nunes, and Y. Qian, 2009: A Regional Climate Change Assessment Program for North America. *EOS, Transactions of the American Geophysical Union*, **90**, 311.
- Mearns, L. O., and Coauthors, 2012: The North American Regional Climate Change Assessment Program: Overview of Phase I Results. *Bulletin of the American Meteorological Society*, **93**, 1337-1362.

Information Transfer Program Introduction

Activities for the efficient transfer and retrieval of information are an important part of the OWRRRI program. The Institute maintains a website that provides information on the OWRRRI and supported research, grant opportunities, and upcoming events. Abstracts of technical reports and other publications generated by OWRRRI projects are updated regularly and are accessible on the website (water.okstate.edu).

OWRRI Information Transfer

Basic Information

Title:	OWRRI Information Transfer
Project Number:	2012OK258B
Start Date:	3/1/2012
End Date:	3/1/2013
Funding Source:	104B
Congressional District:	OK003
Research Category:	Not Applicable
Focus Category:	None, None, None
Descriptors:	None
Principal Investigators:	Dave Engle, Leslie Elmore, Mike Langston

Publications

There are no publications.

An essential part of the mission of the OWRRRI is the transfer of knowledge gathered through university research to appropriate research consumers for application to real-world problems in a manner that is readily understood. To do this in 2012, OWRRRI undertook five efforts: (1) publication of a newsletter, (2) meetings with agency personnel, (3) maintenance of an up-to-date website, (4) making presentations to Extension personnel and the general public, and (5) holding a Water Research Symposium.

Newsletter: The OWRRRI's newsletter is the Aquahoman. With a distribution list of 860, the Aquahoman not only provides a means of getting information to the general public, but also informs researchers throughout the state about water research activities. In 2012, The Aquahoman was produced twice: March and October. The Aquahoman is distributed to state and federal legislators; to water managers throughout Oklahoma; to state, federal, and tribal agency personnel; to water researchers at every university in the State, to members of our Water Research Advisory Board, and to anyone who requests one. It is also available through the OWRRRI website.

Meetings with Agency Personnel:

Water Research Advisory Board - The WRAB consists of 22 water professionals representing state agencies, federal agencies, tribes, and non-governmental organizations. This advisory board was formed in 2006 to assist the OWRRRI by setting funding priorities, recommending proposals for funding, and providing general advice on the direction of the Institute. The Board members have found that they also benefit from their involvement in at least two ways. First, they profit from the opportunity to discuss water issues with other professionals. Second, the semiannual meetings afford them the opportunity to stay informed about water research and water resource planning in Oklahoma. This is accomplished, in part, by having the investigators of the previous year's projects return and present their findings to the Board.

Thus, the WRAB is an important part of the OWRRRI's efforts to disseminate research findings to state agencies for use in problem solving. In 2012, the WRAB met twice. The January meeting included presentations by the five finalists in our research grant competition, selection of three of these finalists for funding, and an update on the State's water plan. The July meeting included presentations on the results of the 2011 OWRRRI-funded projects, and the selection of preproposals to continue in the 2013 grants completion. The funding priorities are distributed as part of the RFP for the annual competition.

Oklahoma Water Quantity Forum – Also in 2012, The Water Center partnered with the Oklahoma Water Survey at the University of Oklahoma to co-host a series of meetings to discuss water quantity issues. The meetings included personnel from universities, state and federal agencies, and tribal governments. The Forum was initiated because although meetings centered on water quality are common, water quantity experts do

Website: The OWRRRI continues to maintain an up-to-date website to convey news and research findings to anyone interested. Site visitors can obtain interim and final reports from any research project sponsored by the OWRRRI (reports from 1965-1999 are available via email; reports from 2000-present are available for immediate download). All OWRRRI project reports (1965 to present) are available through a website maintained

by the OSU Edmon Low Library. This makes them more readily available to the public and more easily located using web search engines. Also available are newsletters beginning in 2005, information about the annual grants competition including the RFP and guidelines for applying, and details about the OWRRI's effort to gather public input for the state's revision of the State's comprehensive water plan. The website is also a major source of information about our annual Research Symposium.

In 2011, the Water Resources Center began production of a series of videos intended to assist landowners and agriculture producers in coping with drought. We established a You Tube Channel that allows all of these videos to be viewed from any media platform with internet access. A total of fifteen videos have been completed and posted there. These videos have been viewed a combined total of 1,455 times.

Training: In 2012, the OWRRI also provided updates on the State's Water Planning effort to staff of the Oklahoma Cooperative Extension Service. Extension staff are located in county offices throughout the State and regularly answer questions from the public about water related issues. OWRRI also traveled to county extension offices to make presentations on hydraulic fracturing and its potential impact on water resources.

Research Symposium: The OWRRI has held an annual Water Research Symposium since 2002. The purpose of this event is to bring together water researchers and water professionals from across the state to discuss their projects and network with others. Again this year, the Symposium was combined with the Oklahoma Water Resources Board's annual Governor's Water Conference. The keynote address was delivered by Dayton Duncan, principal writer of *The Dust Bowl* a documentary film. The OWRRI also brought in Cynthia Barnett to speak on her new book *The Blue Revolution*. The two-day event drew over 450 water professionals, agency staff, politicians, members of the press, researchers, participants in the water planning effort, and interested citizens. This combination of events provides a unique opportunity for interchange between those interested in water policy (who traditionally attend the Governor's Water Conference) and those interested in water research (who traditionally attend the Research Symposium).

The Symposium includes a student poster contest which involves not only staff time, resources, and supplies, but also \$1500 used as prize money (provided by gifts from the Chickasaw, Cherokee, Miami, and Kaw Nations). At the 2012 Symposium, 25 students from three universities presented posters. Each student received feedback on improving the quality of his/her poster from a panel of four judges.

USGS Summer Intern Program

None.

Student Support					
Category	Section 104 Base Grant	Section 104 NCGP Award	NIWR-USGS Internship	Supplemental Awards	Total
Undergraduate	7	5	0	0	12
Masters	5	4	0	0	9
Ph.D.	1	1	0	0	2
Post-Doc.	2	0	0	0	2
Total	15	10	0	0	25

Notable Awards and Achievements

The long-term drought in Oklahoma is a significant threat to our agricultural production. Oklahoma Water Resources Center recognizes this and is working to give farmers and homeowners the tools they need to use water resources responsibly. Thus, in 2010 and 2011 we funded Dr. Tyson Ochsner assistant professor in OSU's Dept. of Plant and Soil Sciences to develop a statewide system of maps that display portion of the water in the soil that is actually available to plant roots (known as plant available water).

Oklahoma is in a unique position to do this. It has an existing state-wide network of 120 weather and environment monitoring stations known as the Oklahoma Mesonet (<http://www.mesonet.org/>). At each of these, soil moisture is measured numerous times daily at three depths (4, 16, and 32 inches). However, soils differ in how tightly they hold water, so Dr. Ochsner's team began by analyzing the soils at each of the Mesonet sites. The daily soil moisture measurements are combined with soil data to produce a measurement of plant available water.

A truly remarkable aspect of the Mesonet is its sophisticated website allowing immediate access to real-time data from anywhere in the world, even a field in western Oklahoma via a mobile phone. Thus, these plant available water maps are already helping agricultural producers and homeowners know when it is time to water and when the soil still has sufficient water to support their plants.

Publications from Prior Years

1. 2008OK104B ("Evaluation of Water Use Monitoring by Remote Sensing ET Estimation Methods") - Articles in Refereed Scientific Journals - Liu, W., Y. Hong, S. I. Khan, M. Huang, B. Vieux, S. Caliskan and T. Grout, 2010: Actual evapotranspiration estimation for different land use and land cover in urban regions using Landsat 5 data. *Journal of Applied Remote Sensing*, 4 (1), 041873-041873. doi:10.1117/1.3525566.
2. 2008OK104B ("Evaluation of Water Use Monitoring by Remote Sensing ET Estimation Methods") - Conference Proceedings - Yang Hong, S. Khan, and B. Vieux (2008), Integrating Remotely Sensed and hydrological Modeled ET for Better Water Resources Management in Oklahoma, *Eos Trans. AGU*, 89(53), Fall Meet. Suppl., Abstract H32B-08, SF, CA, 2008
3. 2008OK104B ("Evaluation of Water Use Monitoring by Remote Sensing ET Estimation Methods") - Articles in Refereed Scientific Journals - Khan, S. I., Y. Hong, B. Vieux, and W. Liu (2010), Development evaluation of an actual evapotranspiration estimation algorithm using satellite remote sensing meteorological observational network in Oklahoma, *International Journal of Remote Sensing*, 31(14), 3799-3819, doi: 10.1080/01431161.2010.483487.
4. 2008OK104B ("Evaluation of Water Use Monitoring by Remote Sensing ET Estimation Methods") - Articles in Refereed Scientific Journals - Liu, W., Y. Hong, S.I. Khan, M. Huang, T. Grout, and P. Adhikari, 2011: Evaluation of Global Daily Reference ET Using Oklahoma's Environmental Monitoring Network-MESONET. *Water Resources Management*, 25, 1601-1613, doi: 10.1007/s11269-010-9763-0
5. 2008OK104B ("Evaluation of Water Use Monitoring by Remote Sensing ET Estimation Methods") - Articles in Refereed Scientific Journals - Liu, W., Y. Hong, S.I. Khan, M. Huang, T. Grout, and P. Adhikari, 2011: Evaluation of Global Daily Reference ET Using Oklahoma's Environmental Monitoring Network-MESONET. *Water Resources Management*, 25, 1601-1613, doi: 10.1007/s11269-010-9763-0
6. 2008OK105B ("Decision Support Model for Evaluating Alternative Water Supply Infrastructure Scenarios") - Dissertations - Lea, Mike. 2009. M.S. Thesis. Use of hydraulic simulation software to evaluate future infrastructure upgrades for a municipal water distribution system in Beggs, OK. Dept. of Civil and Environmental Engineering, Oklahoma State University, Stillwater, OK. 130 pages.
7. 2008OK105B ("Decision Support Model for Evaluating Alternative Water Supply Infrastructure Scenarios") - Dissertations - Bhadbhade, Neha, (2009), Performance evaluation of a drinking water distribution system using hydraulic simulation software for the City of Oilton, Oklahoma, Dept. of Civil and Environmental Engineering, Oklahoma State University, Stillwater, OK., 115 pages.
8. 2008OK105B ("Decision Support Model for Evaluating Alternative Water Supply Infrastructure Scenarios") - Dissertations - Senyondo, Sara, 2009. Using EPANET to optimize operation of the rural water distribution system at Braggs, Oklahoma. Dept. of Civil and Environmental Engineering, Oklahoma State University, Stillwater, OK, 82 pages.
9. 2008OK105B ("Decision Support Model for Evaluating Alternative Water Supply Infrastructure Scenarios") - Dissertations - Atta-Asiamah, Ernest, 2009. Estimation of the cost of building a water treatment plant and related facilities for Kaw City, Oklahoma, Dept. of Agricultural Economics, Oklahoma State University, OK, 141 pages.
10. 2009OK114B ("Alternative Water Conservation Policy Tools for Oklahoma Water Systems") - Articles in Refereed Scientific Journals - Boyer, C.N., D.C. Adams, and J. Lucero. Rural Coverage Bias in Online Surveys?: Evidence from Oklahoma Water Managers. *Journal of Extension*, forthcoming.
11. 2009OK114B ("Alternative Water Conservation Policy Tools for Oklahoma Water Systems") - Conference Proceedings - Adams, D.C., C.N. Boyer, and T. Borisova. 2009. Barriers to Water Conservation by Rural and Municipal Water Systems. *Proceedings of the Southern Region Water*

- Policy & Economics Conference, Gainesville, FL, October 13, 2009. Pp. 36-41.
12. 2009OK114B ("Alternative Water Conservation Policy Tools for Oklahoma Water Systems") - Articles in Refereed Scientific Journals - Boyer, C.N., D.C. Adams, and J. Lucero, Rural Coverage Bias in Online Surveys?: Evidence from Oklahoma Water Managers. *Journal of Extension* [online] 48(3)(2010):3TOT5. Available at: <http://www.joe.org/joe/2010june/tt5.php>.
 13. 2009OK114B ("Alternative Water Conservation Policy Tools for Oklahoma Water Systems") - Conference Proceedings - Adams, D.C., C.N. Boyer, T. Borisova, and M.D. Smolen, Water conservation strategies by rural and municipal water systems. *Proceedings of the USDA/NIFA National Water Program*. Hilton Head, SC, February 20, 2010.
 14. 2009OK114B ("Alternative Water Conservation Policy Tools for Oklahoma Water Systems") - Articles in Refereed Scientific Journals - Boyer, C.N., D.C. Adams, T. Borisova, and C. Clark. 2012. Factors Driving Water Utility Rate Structure Choice: Evidence from Four Southern U.S. States. *Water Resources Management* 26(10):2747-2760.
 15. 2009OK114B ("Alternative Water Conservation Policy Tools for Oklahoma Water Systems") - Articles in Refereed Scientific Journals - Boyer, C.N., Adams, D.C., and Borisova, T. Drivers of Price- and Non-Price Conservation: An Application of Predictive Models to the Southern US. In review at *Journal of Agricultural and Applied Economics*.
 16. 2009OK119B ("Stream Depletion by Ground Water Pumping: A Stream Depletion Factor for the State of Oklahoma") - Conference Proceedings - Fox, G.A., D.M. Heeren, and M.A. Kizer. 2010. Evaluation of alluvial well depletion analytical solutions from a stream-aquifer analysis test along the North Canadian River in Oklahoma. In *Proceedings of the American Society of Civil Engineers, Environmental Water Resources Institute Annual Meeting*, Reston, VA, 10 pages (CD-ROM).
 17. 2009OK119B ("Stream Depletion by Ground Water Pumping: A Stream Depletion Factor for the State of Oklahoma") - Articles in Refereed Scientific Journals - Fox, G.A., D.M. Heeren, and M.A. Kizer. 2011. Evaluation of a stream-aquifer analysis test for deriving reach-scale streambed conductance. *Transactions of the ASABE* 54(2): 473-479.
 18. 2009OK141G ("Eastern redcedar encroachment and water cycle in tallgrass prairie ") - Articles in Refereed Scientific Journals - Zou Chris, Peter Folliott, Michael Wine. 2010. Streamflow responses to vegetation manipulations along a gradient of precipitation in the Colorado River Basin. *Forest Ecology and Management* 259:1268-1276.
 19. 2010OK180B ("Water conservation in Oklahoma urban and suburban watersheds through modification of irrigation practices.") - Conference Proceedings - Martin, Dennis, Santanu Thapa, Steve Batten, Justin Moss, Greg Bell, Jeff Anderson, Yanqi Wu, and Kemin Su. 2010. Evapotranspiration rates of Riviera and U-3 bermudagrasses under non-limiting soil moisture conditions. In: 2010 Agronomy abstracts. ASA, Madison, WI.
 20. 2010OK180B ("Water conservation in Oklahoma urban and suburban watersheds through modification of irrigation practices.") - Conference Proceedings - Moss, Justin, Dennis Martin, Yanqi Wu, Kemin Su, and Bishow Poudel. 2010. Development and selection of bermudagrasses for water conservation in urban landscapes. In: *Proceedings of the 2010 USDA National Water Conference*, Hilton Head, SC.
 21. 2010OK181B ("A Fluvial Geomorphic and Sediment Transport Study of the Little River Upstream of Lake Thunderbird Using an Acoustic Doppler Current Profiler (ADCP)") - Other Publications - Dutnell, Russell, Hollis Henson, Robert Nairn, Randall Kolar, Baxter Vieux, and Jason Julian, 2010, Preliminary Findings of a Fluvial Geomorphic and Sediment Transport Study of the Little River Upstream of Lake Thunderbird Using an Acoustic Doppler Current Profiler (ADCP), in 2010 Governor's Water Conference and Oklahoma Water Research Symposium, Norman, OK. (Poster)
 22. 2009OK114B ("Alternative Water Conservation Policy Tools for Oklahoma Water Systems") - Other Publications - Adams, D.C., C.N. Boyer, and M.D. Smolen. 2009. Water Rate Structure: a Tool for Water Conservation in Oklahoma. Oklahoma Cooperative Extension Service, AGEC-1017.
 23. 2009OK114B ("Alternative Water Conservation Policy Tools for Oklahoma Water Systems") - Articles in Refereed Scientific Journals - Adams, D.C. and Padgett, M. Adoption of Water

- Conservation Tools: Water Users Receptivity to Conservation. In preparation.
24. 2009OK114B ("Alternative Water Conservation Policy Tools for Oklahoma Water Systems") - Conference Proceedings - Adams, D.C., C. Boyer, T. Borisova, M. Smolen, and L. Sanders. Adoption of Water Conservation Tools in the Southern US: Findings of a Study of Water Managers. Southern Regional Water Policy and Economics Meeting, Gainesville, FL, April 27, 2011.
 25. 2010OK180B ("Water conservation in Oklahoma urban and suburban watersheds through modification of irrigation practices.") - Articles in Refereed Scientific Journals - Moss, J.Q., J.E. Haase, J.R. Vogel, T.A. Boyer, and D.L. Martin. 2013. Simple lawn irrigation measurement training for Master Gardeners and homeowners. *Journal of Extension* (In Press).